

May 2020

## Inflammatory disease diagnosis and methods of treatment using down-regulators of lipopolysaccharide-responsive beige-like anchor

Jia-Wang Wang

Richard F. Lockey

Follow this and additional works at: [https://digitalcommons.usf.edu/usf\\_patents](https://digitalcommons.usf.edu/usf_patents)

---

### Recommended Citation

Wang, Jia-Wang and Lockey, Richard F., "Inflammatory disease diagnosis and methods of treatment using down-regulators of lipopolysaccharide-responsive beige-like anchor" (2020). *USF Patents*. 1165.  
[https://digitalcommons.usf.edu/usf\\_patents/1165](https://digitalcommons.usf.edu/usf_patents/1165)

This Article is brought to you for free and open access by Digital Commons @ University of South Florida. It has been accepted for inclusion in USF Patents by an authorized administrator of Digital Commons @ University of South Florida. For more information, please contact [digitalcommons@usf.edu](mailto:digitalcommons@usf.edu).



US010654918B2

(12) **United States Patent**  
**Wang et al.**

(10) **Patent No.:** **US 10,654,918 B2**

(45) **Date of Patent:** **May 19, 2020**

(54) **INFLAMMATORY DISEASE DIAGNOSIS  
 AND METHODS OF TREATMENT USING  
 DOWN-REGULATORS OF  
 LIPOPOLYSACCHARIDE-RESPONSIVE  
 BEIGE-LIKE ANCHOR**

14/4702 (2013.01); C07K 14/4713 (2013.01);  
 C07K 2317/76 (2013.01); C12N 2310/14  
 (2013.01); C12N 2310/141 (2013.01); C12N  
 2310/531 (2013.01); C12N 2330/10 (2013.01);  
 C12N 2330/50 (2013.01)

(71) Applicants: **Jia-Wang Wang**, Tampa, FL (US);  
**Richard F. Lockey**, Tampa, FL (US)

(58) **Field of Classification Search**

None

See application file for complete search history.

(72) Inventors: **Jia-Wang Wang**, Tampa, FL (US);  
**Richard F. Lockey**, Tampa, FL (US)

(56)

#### References Cited

#### U.S. PATENT DOCUMENTS

7,704,963 B2 \* 4/2010 Kerr ..... C07K 14/47  
 435/455

(73) Assignee: **University of South Florida**, Tampa,  
 FL (US)

(\*) Notice: Subject to any disclaimer, the term of this  
 patent is extended or adjusted under 35  
 U.S.C. 154(b) by 110 days.

#### OTHER PUBLICATIONS

Lam et al, 2015. Am J Neurodegener Dis. 4(2): 28-39.\*  
 Webb, 2014. Biochemical Pharmacology. 87: 121-130.\*

(21) Appl. No.: **15/661,784**

\* cited by examiner

(22) Filed: **Jul. 27, 2017**

Primary Examiner — Zachary C Howard

(65) **Prior Publication Data**

US 2018/0002413 A1 Jan. 4, 2018

(74) Attorney, Agent, or Firm — Michele L. Lawson;  
 Smith & Hopen, P.A.

#### Related U.S. Application Data

(57)

#### ABSTRACT

(62) Division of application No. 14/223,490, filed on Mar.  
 24, 2014, now Pat. No. 9,738,706.

(60) Provisional application No. 61/804,451, filed on Mar.  
 22, 2013.

(51) **Int. Cl.**

**A61P 11/06** (2006.01)

**A61K 38/17** (2006.01)

**A61K 31/7105** (2006.01)

**C12N 15/113** (2010.01)

**C07K 16/18** (2006.01)

**A61K 35/16** (2015.01)

**A61K 31/69** (2006.01)

**A61K 45/06** (2006.01)

**A61K 31/713** (2006.01)

**C07K 14/47** (2006.01)

**A61K 39/00** (2006.01)

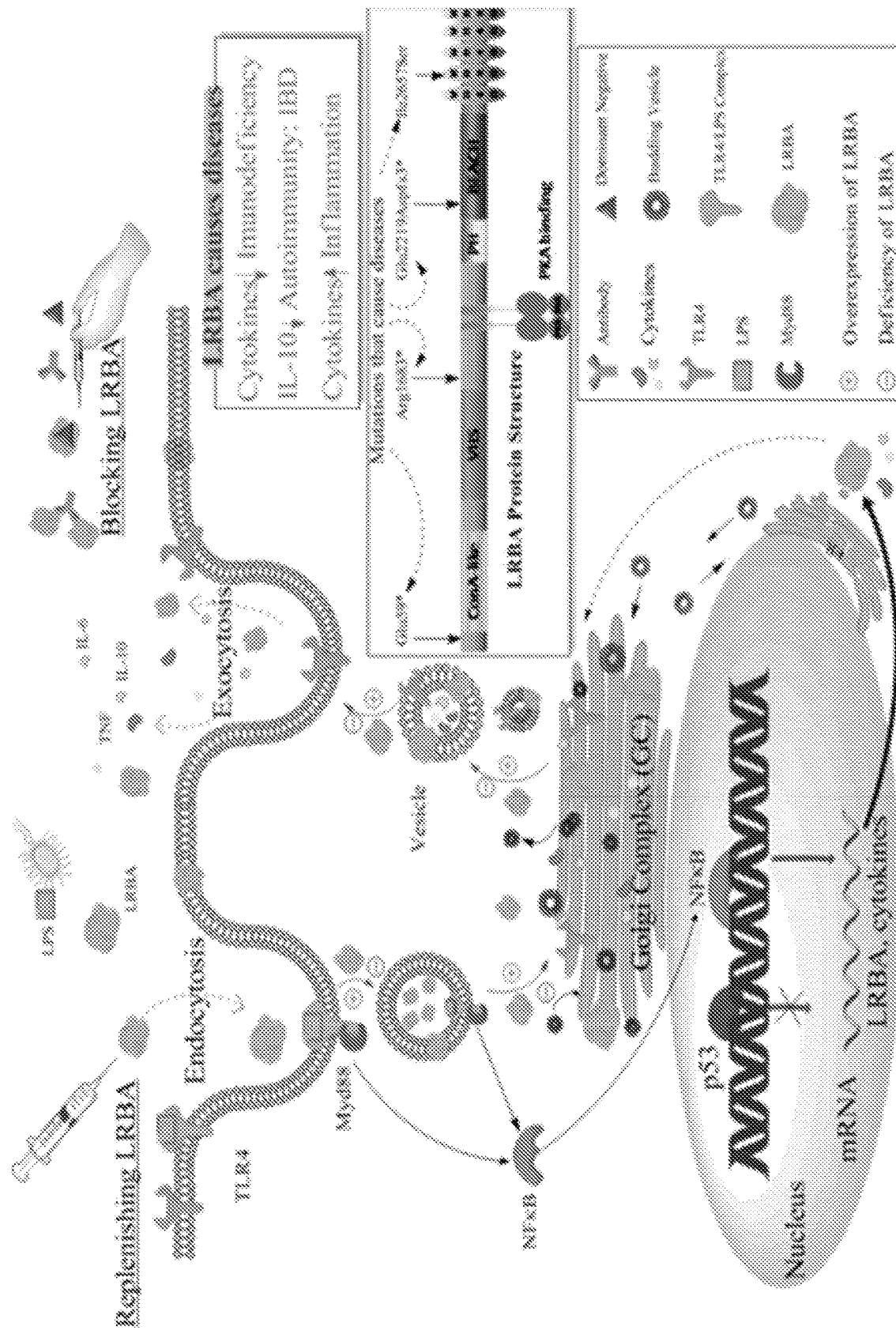
(52) **U.S. Cl.**

CPC ..... **C07K 16/18** (2013.01); **A61K 31/69**  
 (2013.01); **A61K 31/713** (2013.01); **A61K**  
**35/16** (2013.01); **A61K 38/1709** (2013.01);  
**A61K 45/06** (2013.01); **C12N 15/113**  
 (2013.01); **A61K 2039/505** (2013.01); **C07K**

Anti-cytokine therapy has revolutionized immunological  
 disease treatment, but is not always effective and subject to  
 treatment resistance as the cytokine cascade is highly redun-  
 dant and multiple cytokines are involved in inflammation.  
 Targeting a critical common regulator of inflammatory  
 effectors is desirable. Lipopolysaccharide (LPS)-responsive  
 beige-like anchor (LRBA) is a master regulator of multiple  
 genes important for inflammation. Subcellular localization  
 shows that LRBA translocated to the nucleus upon LPS  
 stimulation and colocalized with multiple proteins associ-  
 ated with the endosome membrane system, indicating a  
 critical role in membrane/vesicle trafficking essential for  
 deposition, secretion and signal transduction of immune  
 effectors. Deregulation, deficiency, down-regulation and  
 overexpression of LRBA causes defective trafficking and  
 signaling of immune effector molecules, resulting in immu-  
 nodeficiency and autoimmunity diseases associated with a  
 broader spectrum of severe symptoms when compared to  
 other CVID genes. Modulating LRBA through antibodies,  
 dominant negative mutants, or small interference RNA can  
 be used to treat inflammatory diseases.

**7 Claims, 82 Drawing Sheets**

**Specification includes a Sequence Listing.**



**W**  
**G**  
**H**  
**F**

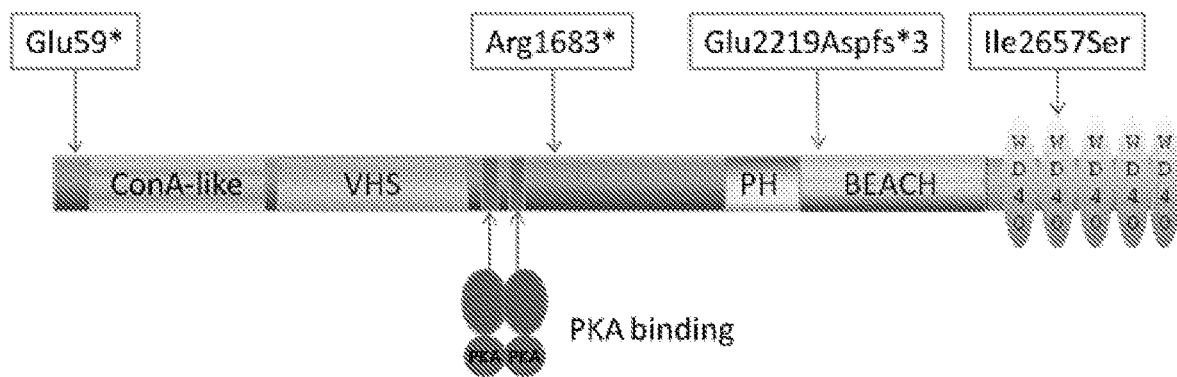


FIG. 2

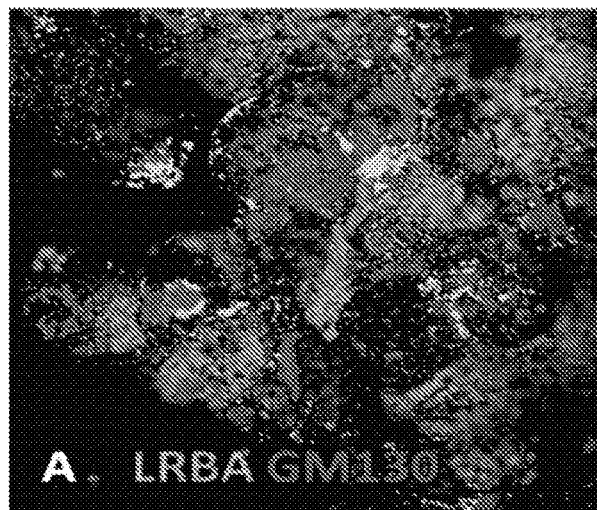


FIG. 3A





FIG. 3B

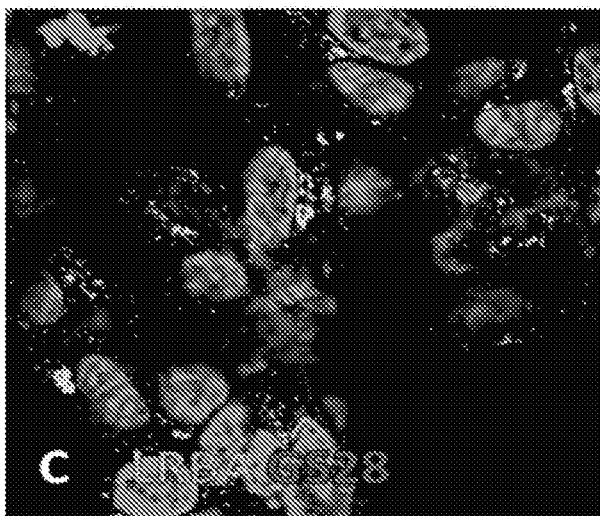


FIG. 3C



FIG. 3D

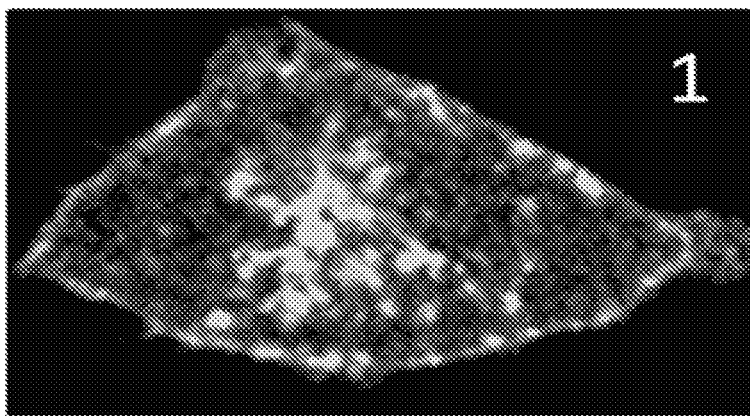


FIG. 3E

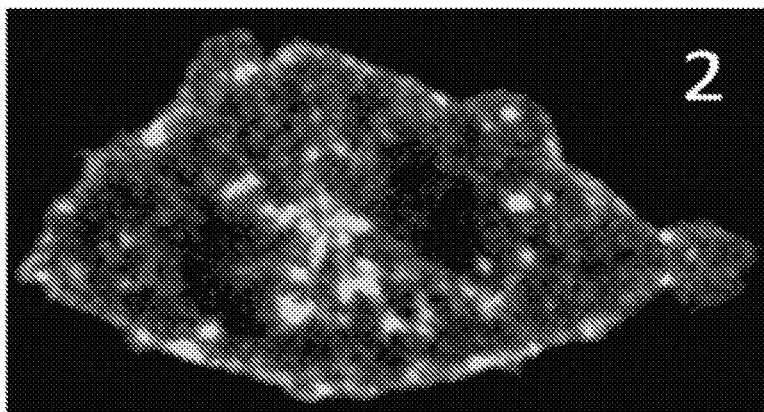


FIG. 3F

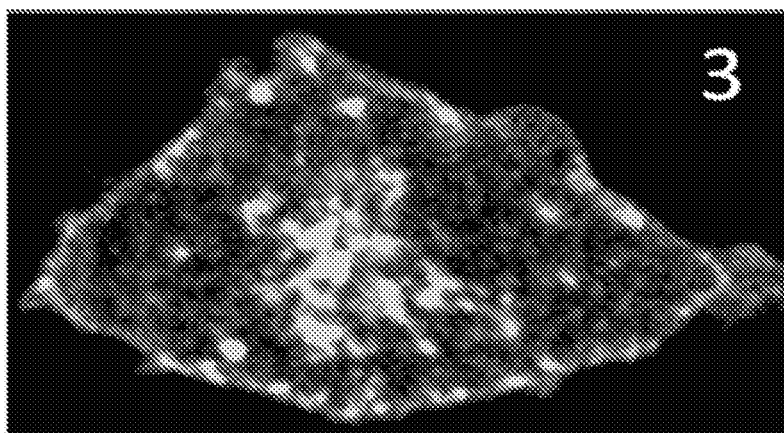


FIG. 3G

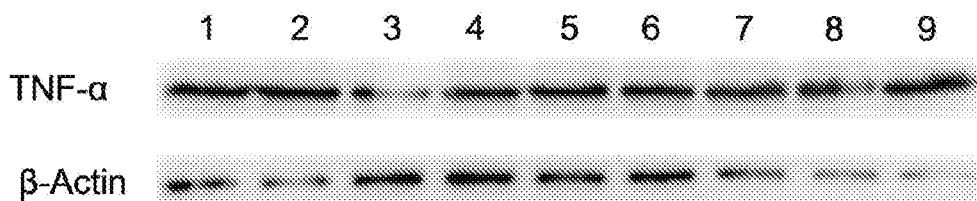


FIG. 4A

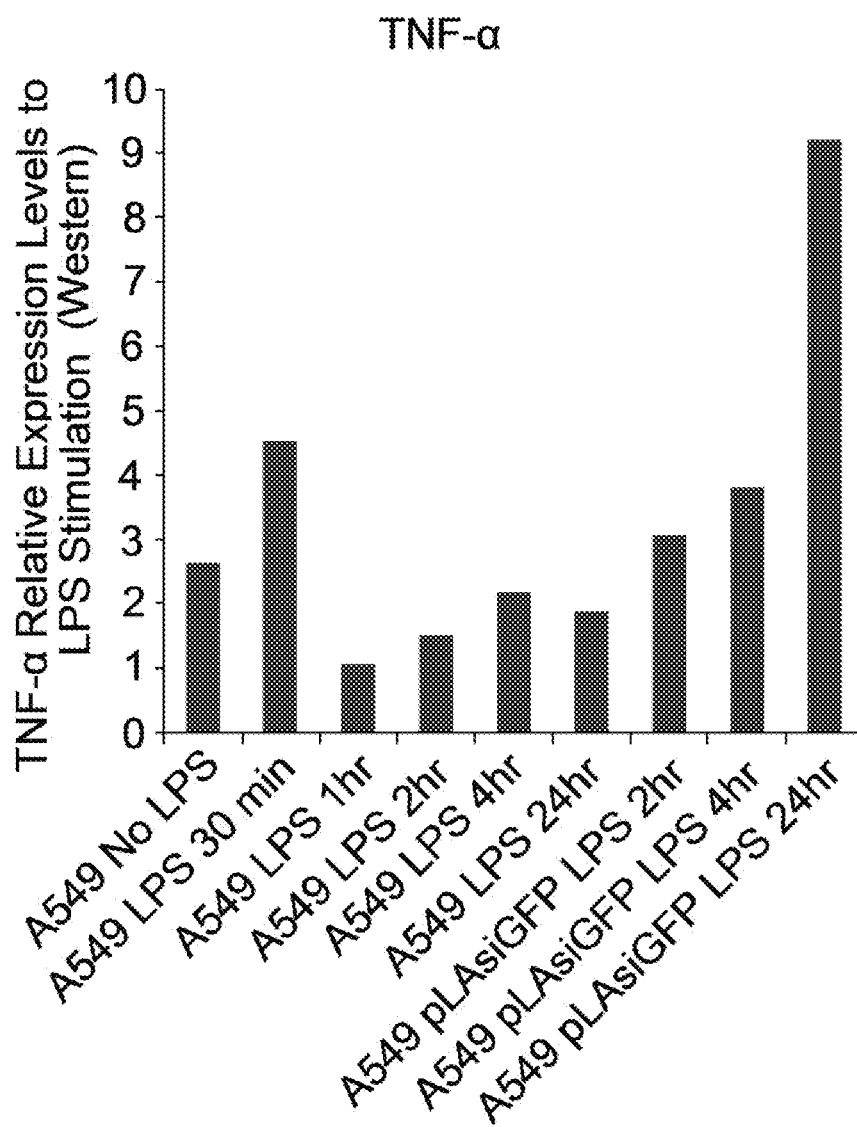


FIG. 4B

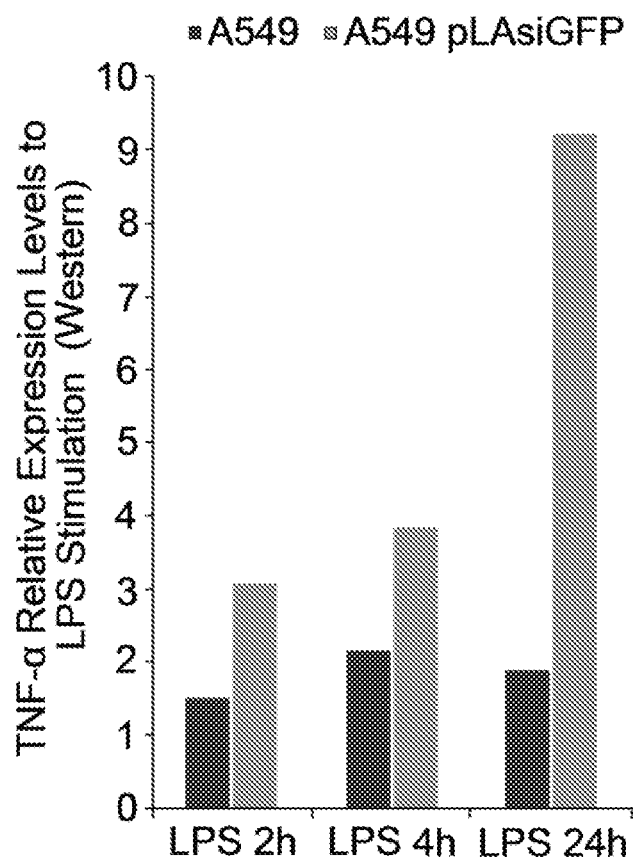


FIG. 4C

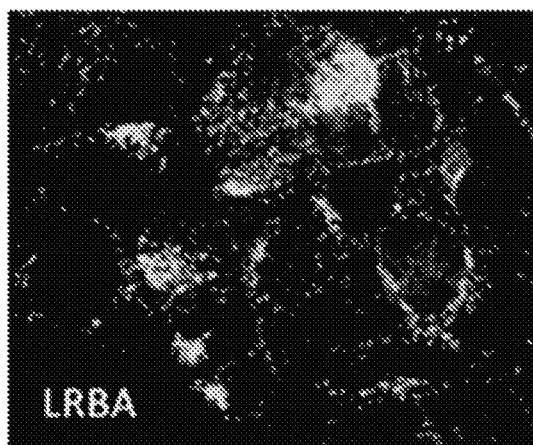


FIG. 5A

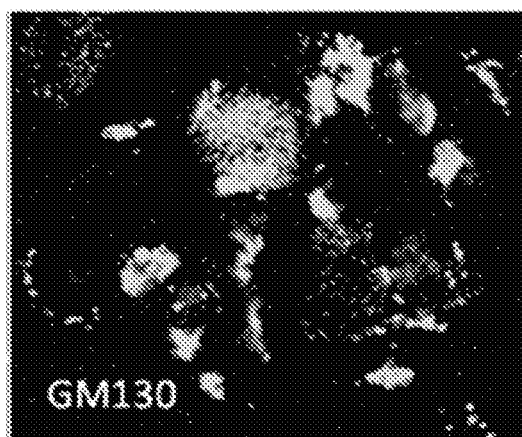


FIG. 5B

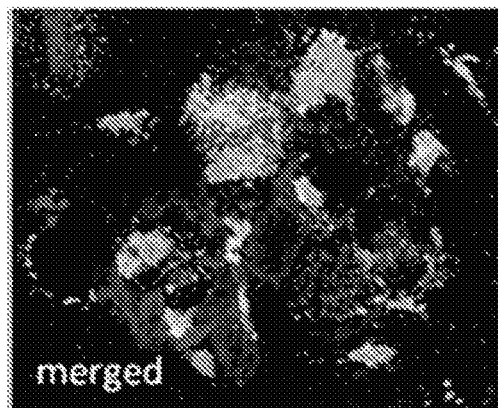


FIG. 5C

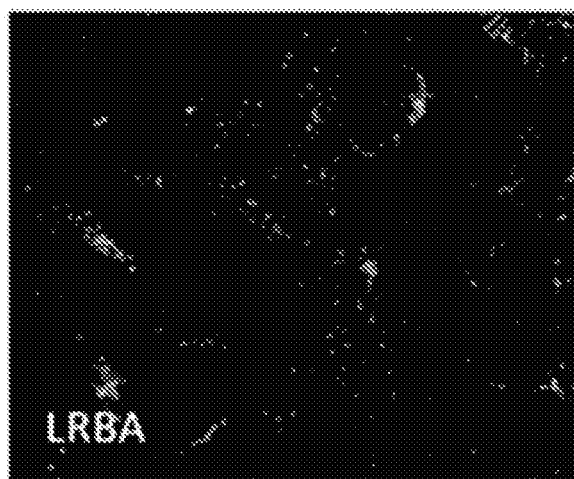


FIG. 5D

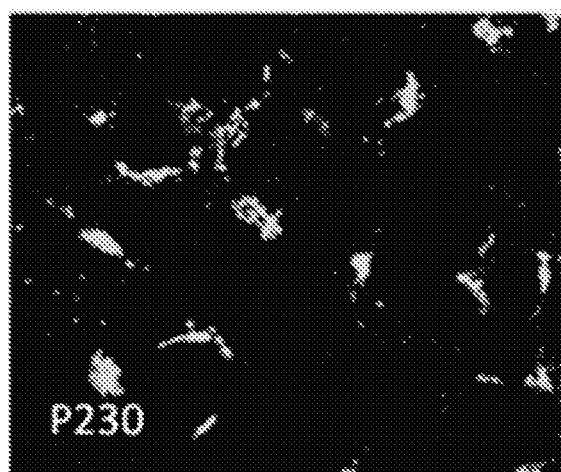


FIG. 5E

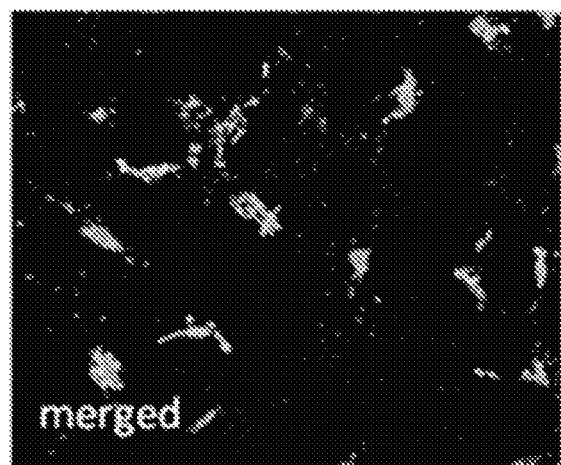


FIG. 5F



FIG. 5G



FIG. 5H



FIG. 5I



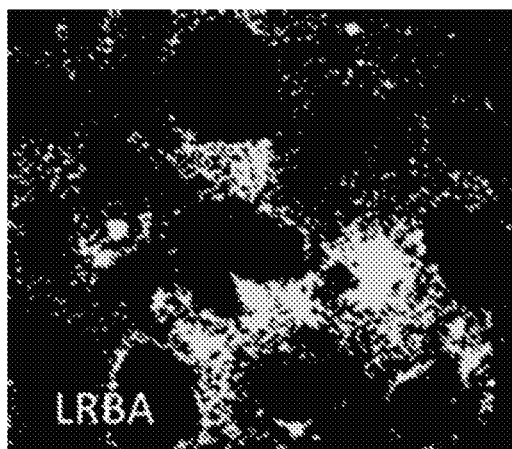


FIG. 6A

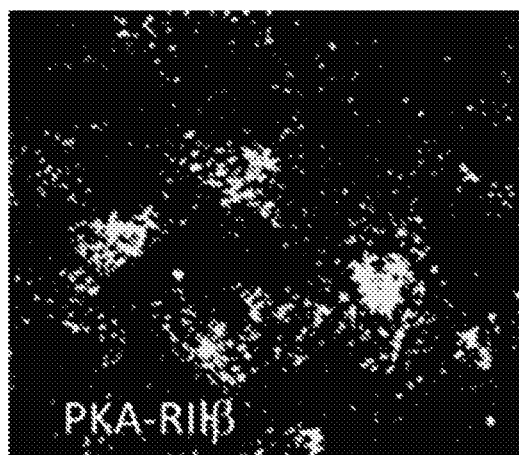


FIG. 6B

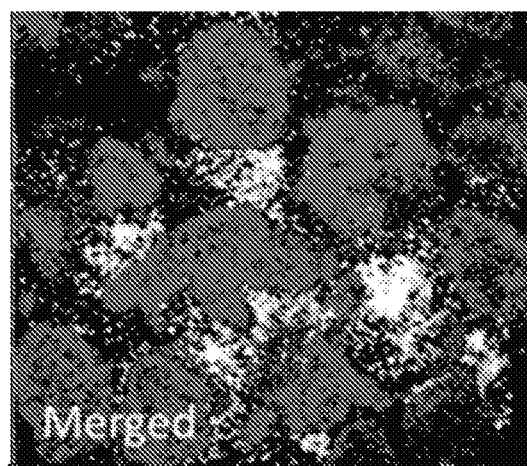


FIG. 6C

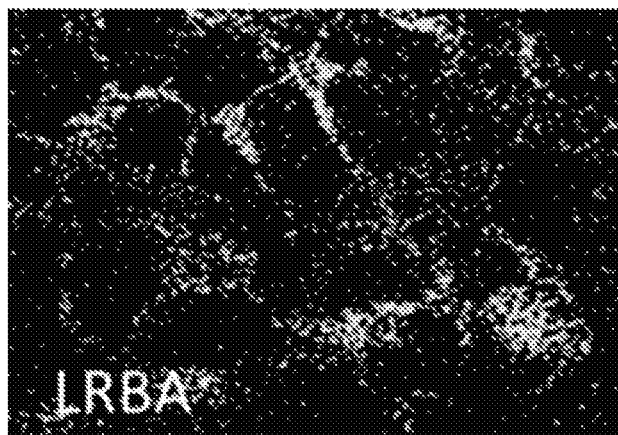


FIG. 7A

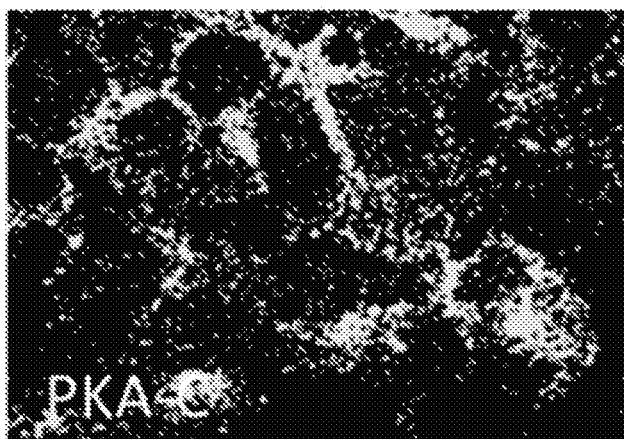


FIG. 7B

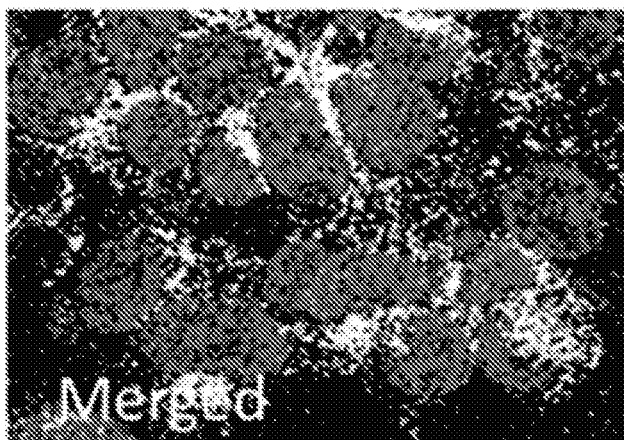


FIG. 7C

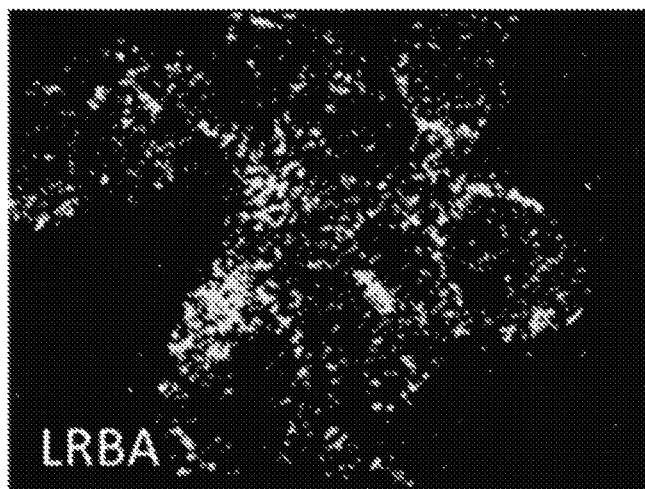


FIG. 8A

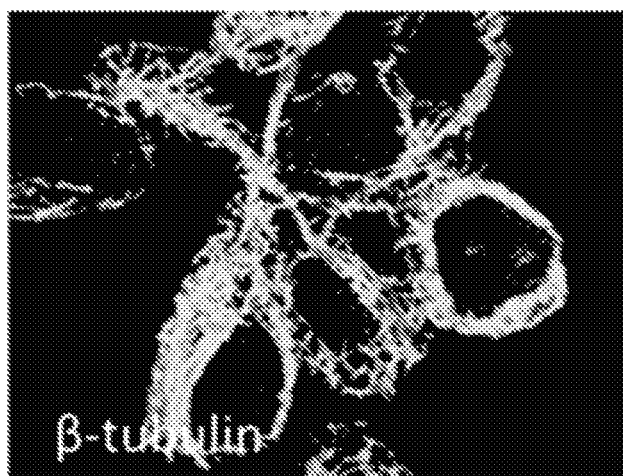


FIG. 8B



FIG. 8C



FIG. 9A



FIG. 9B

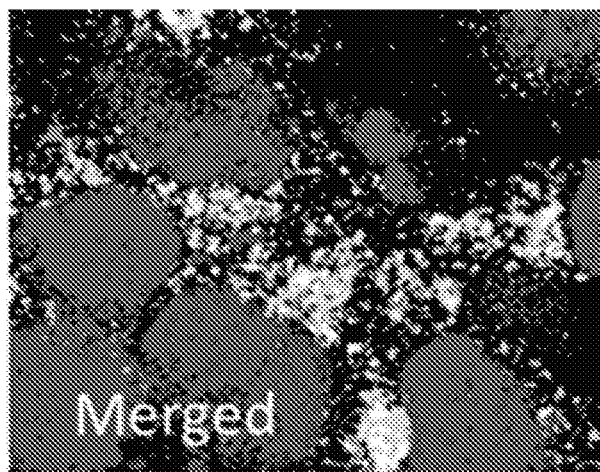


FIG. 9C

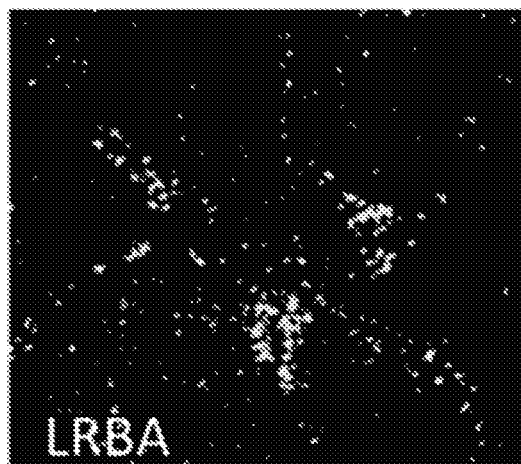


FIG. 10A

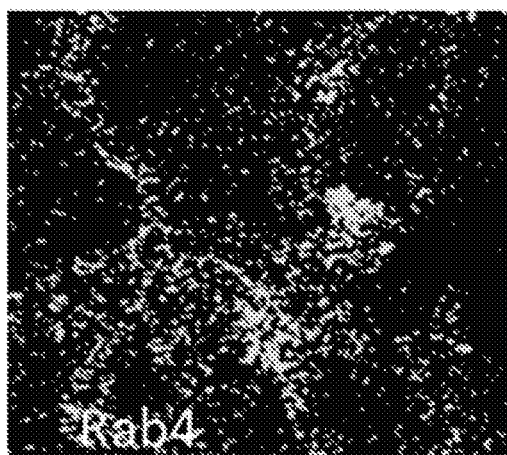


FIG. 10B

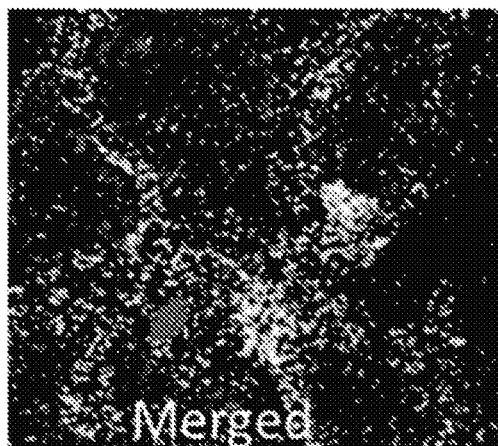


FIG. 10C

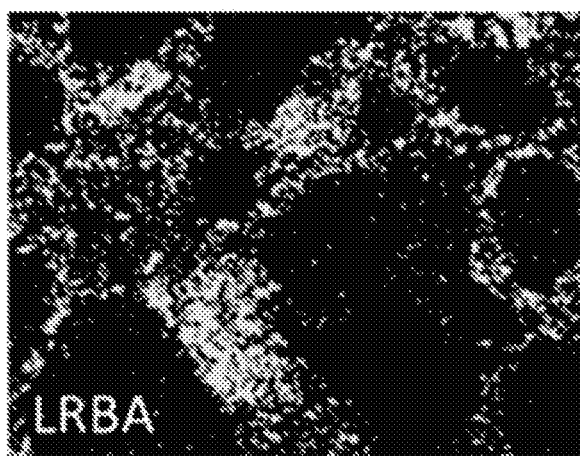


FIG. 11A

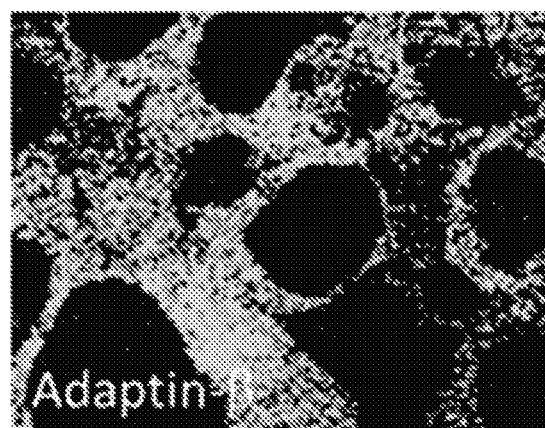


FIG. 11B

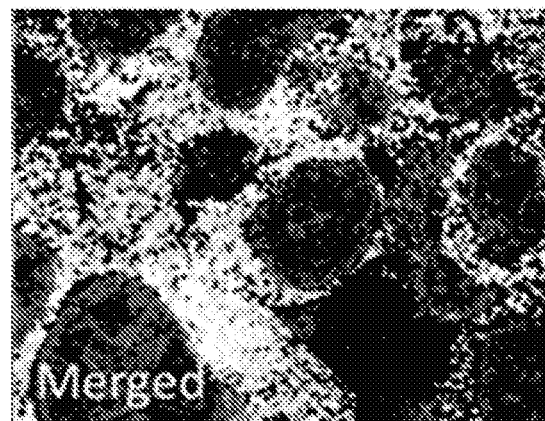


FIG. 11C



FIG. 12A

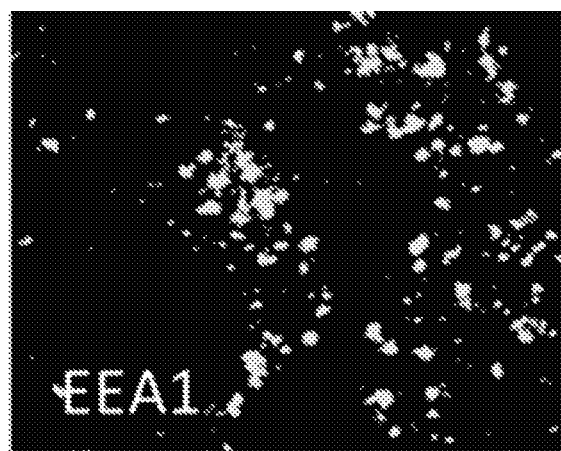


FIG. 12B

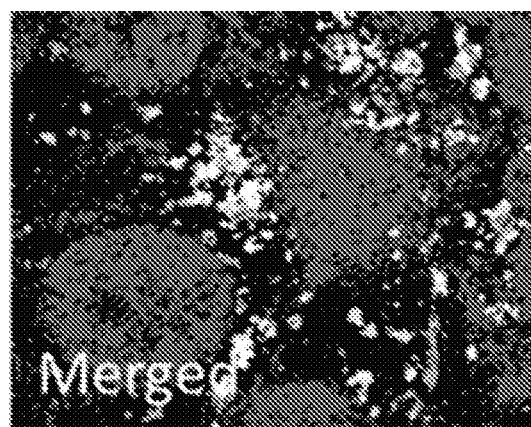


FIG. 12C

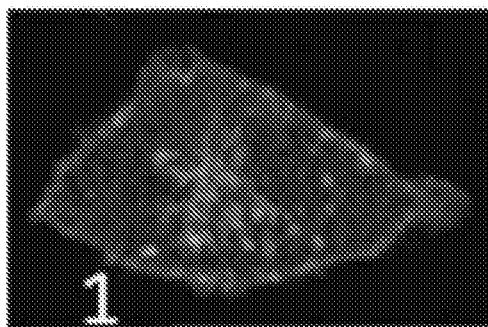


FIG. 13A

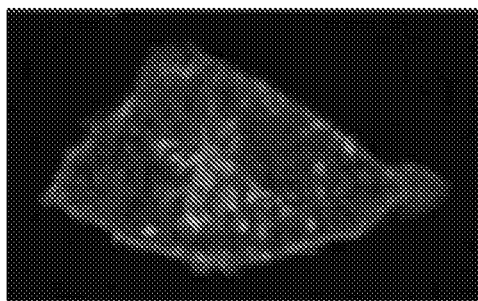


FIG. 13B

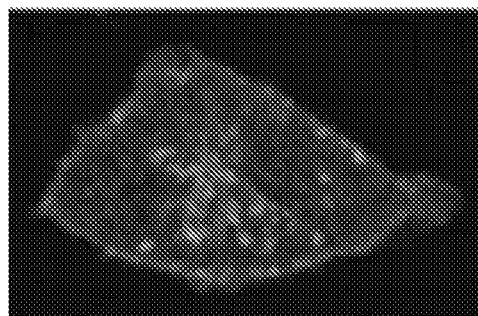


FIG. 13C

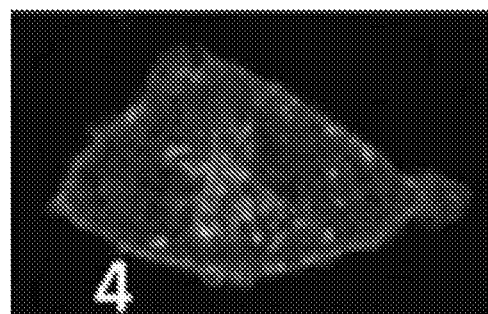


FIG. 13D



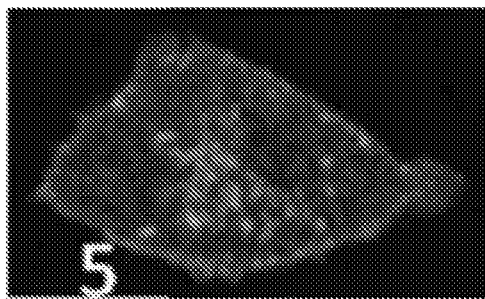


FIG. 13E

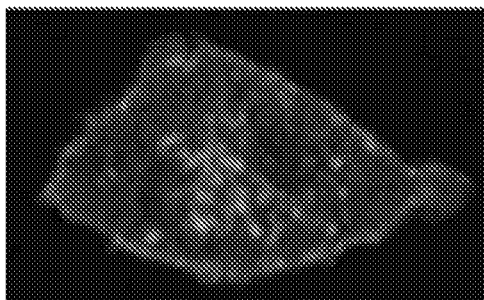


FIG. 13F

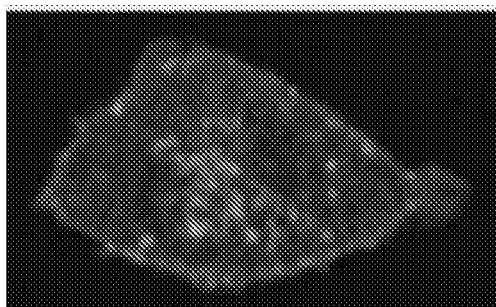


FIG. 13G

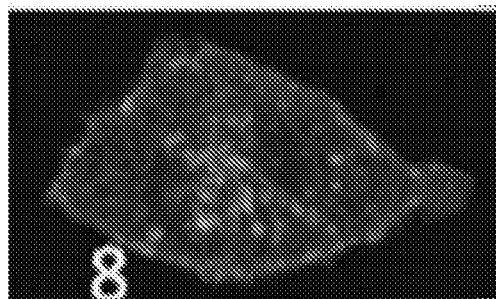


FIG. 13H

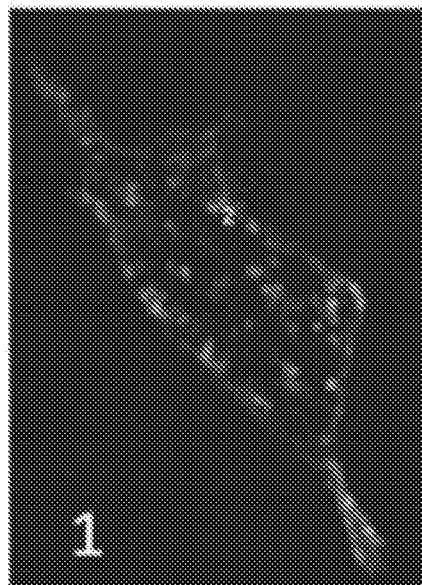


FIG. 13I

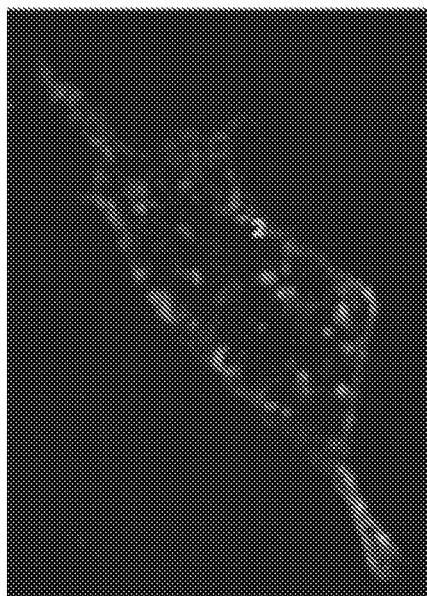


FIG. 13J

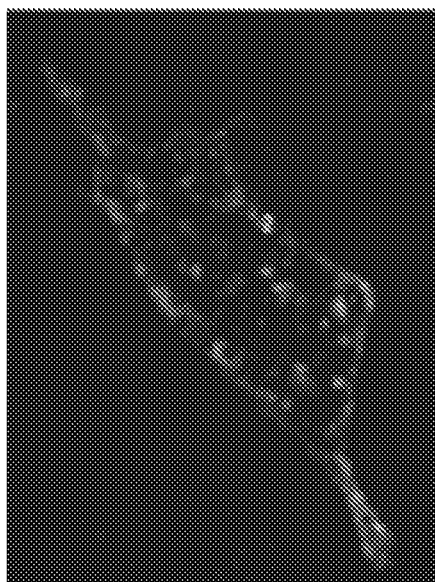


FIG. 13K

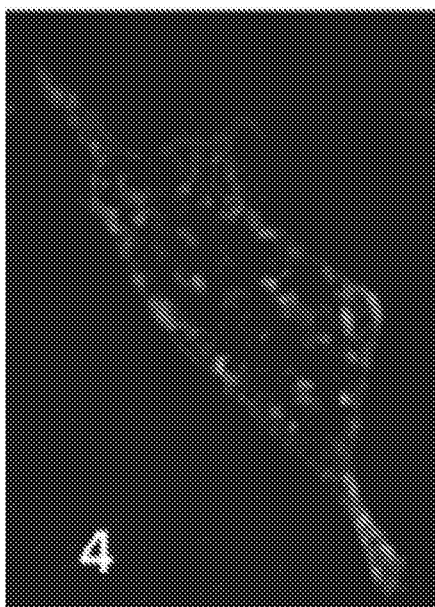


FIG. 13L

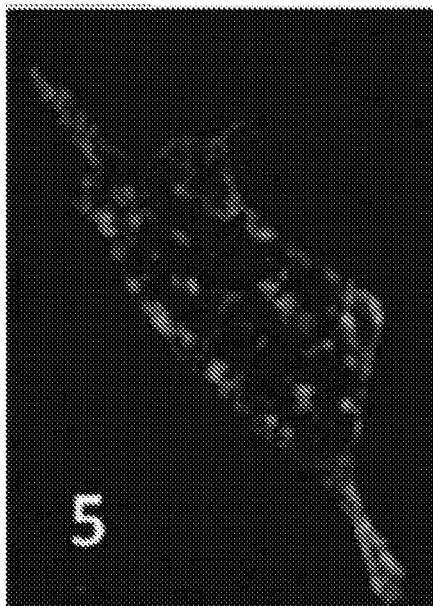


FIG. 13M

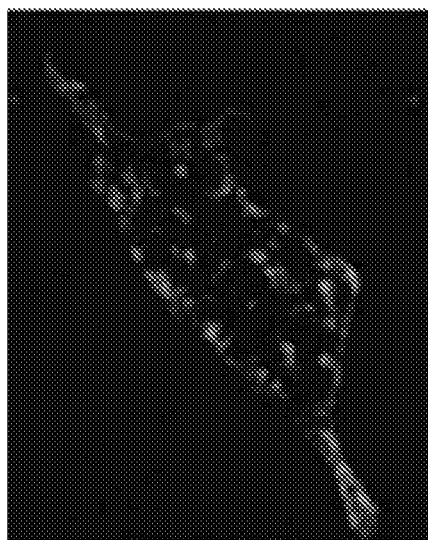


FIG. 13N

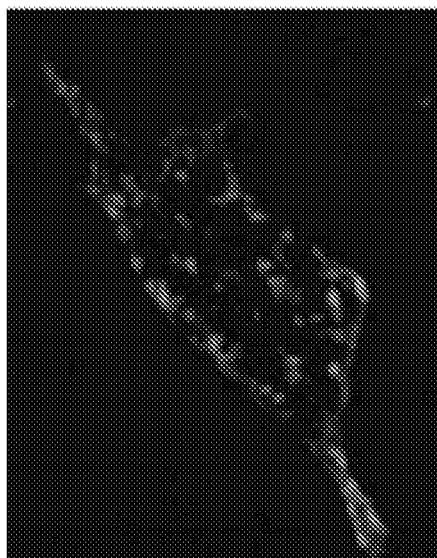


FIG. 13O

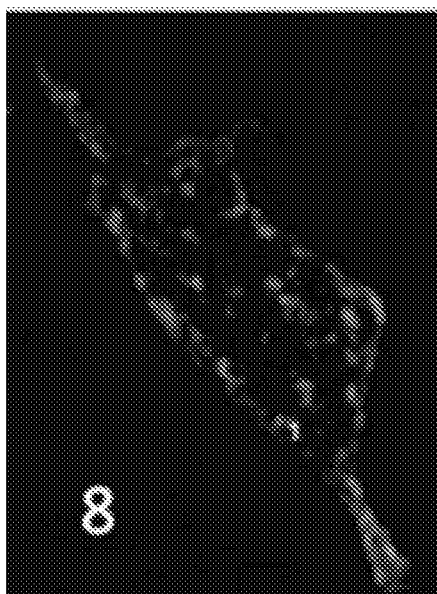


FIG. 13P

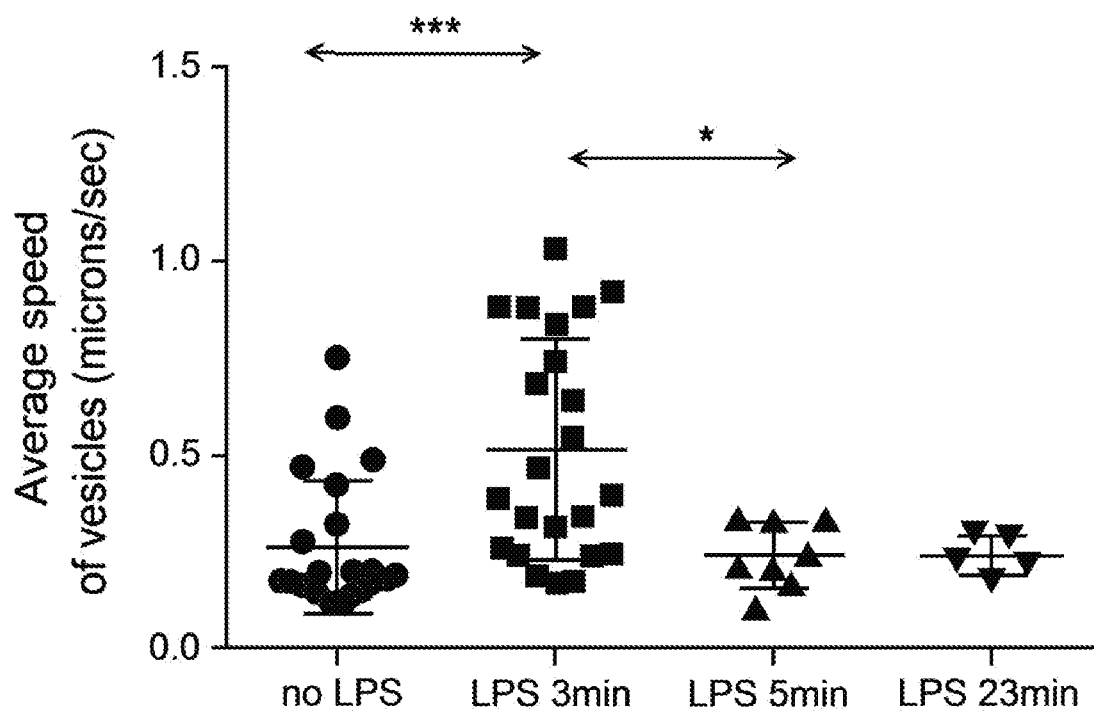


FIG. 14A

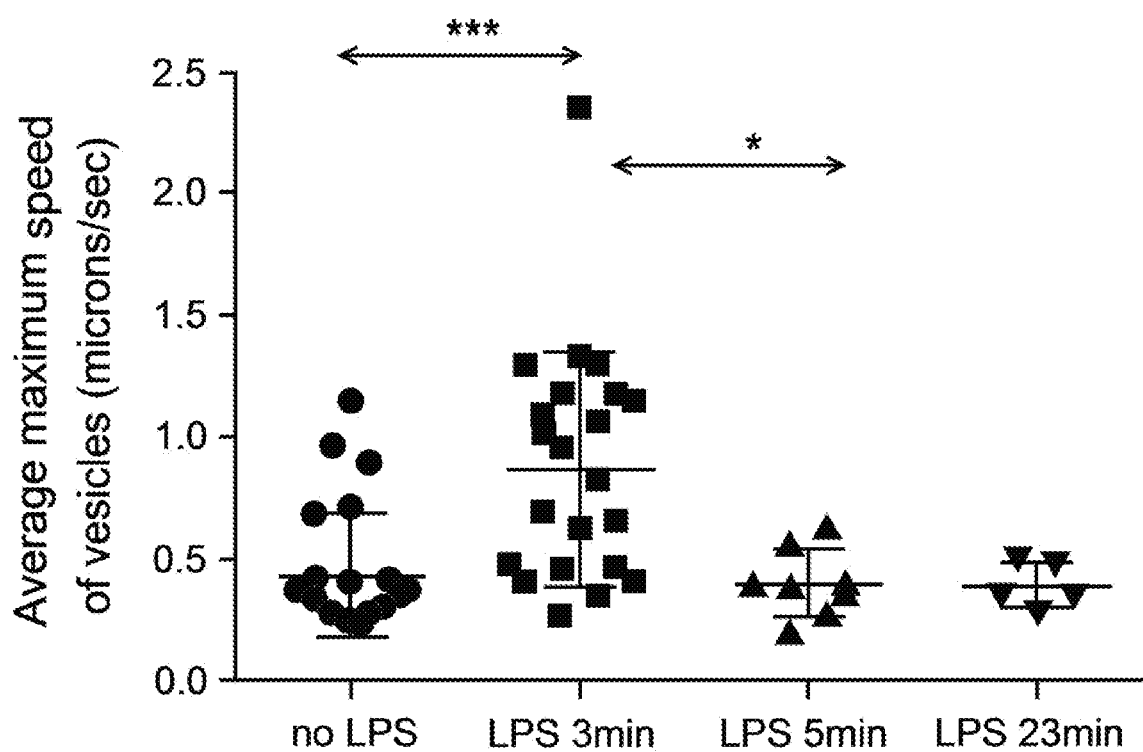


FIG. 14B

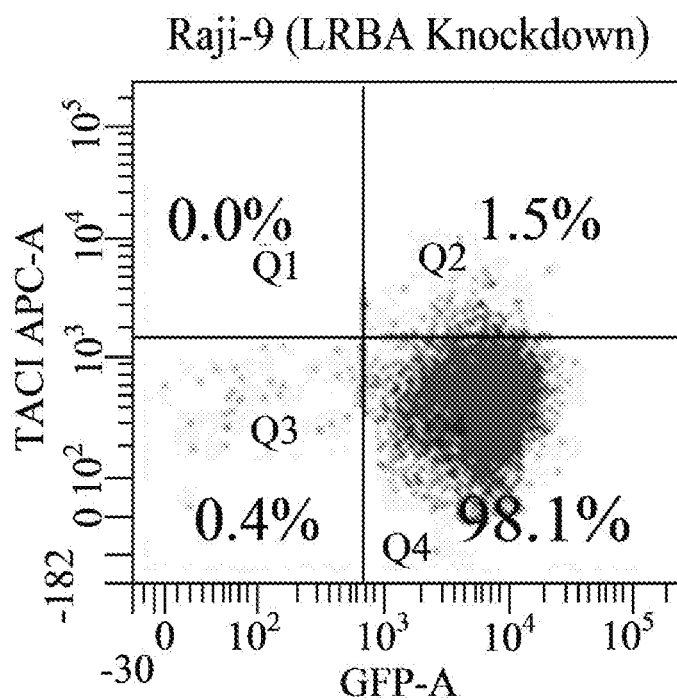


FIG. 15A

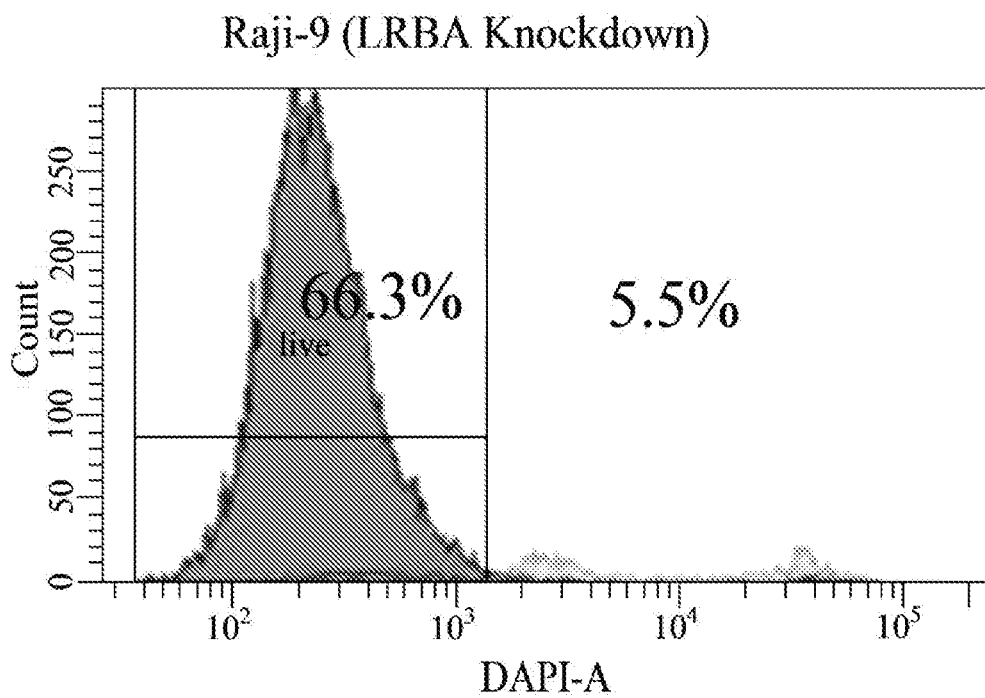


FIG. 15B

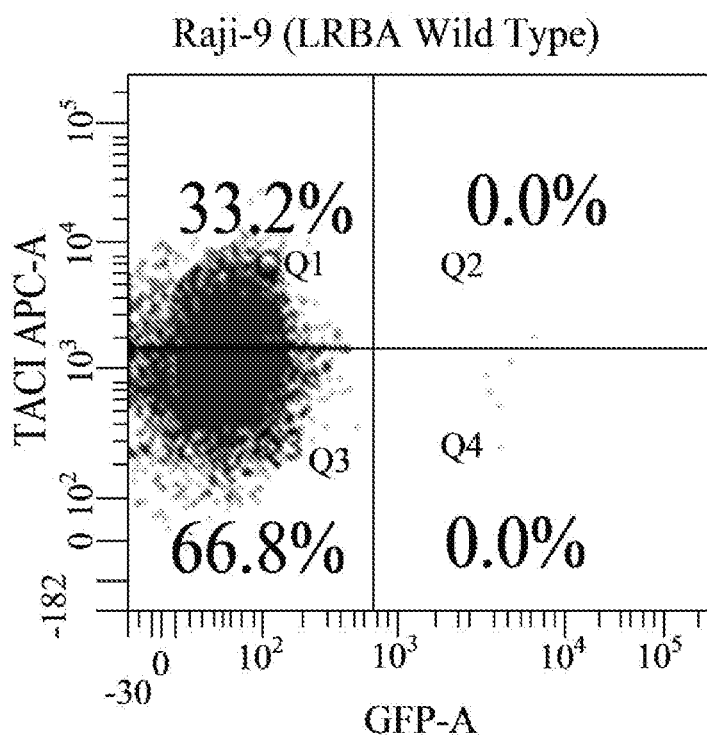


FIG. 15C

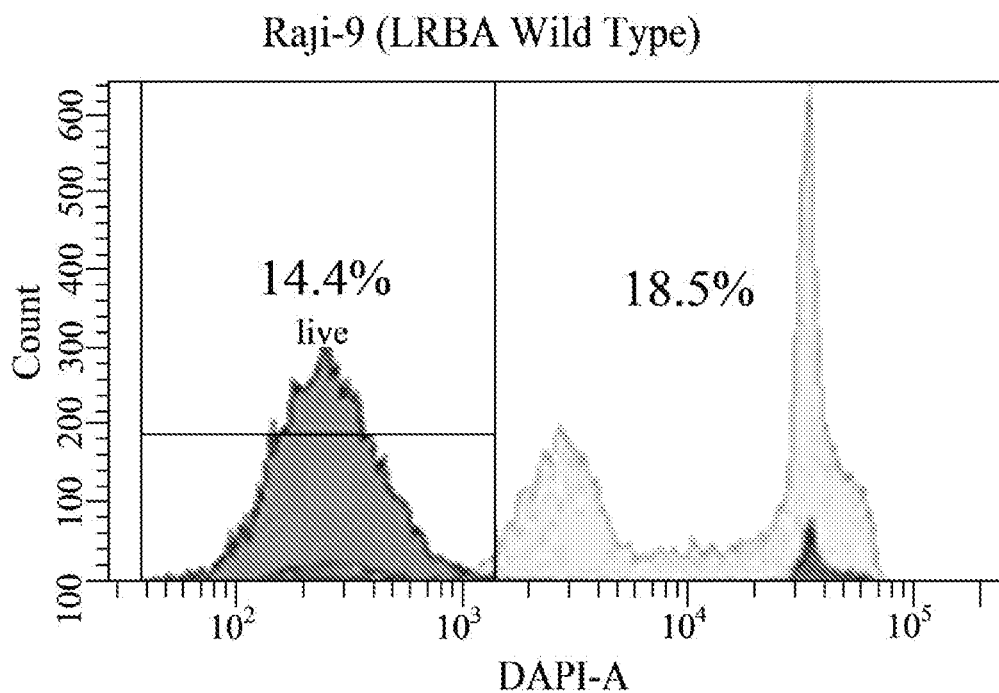


FIG. 15D



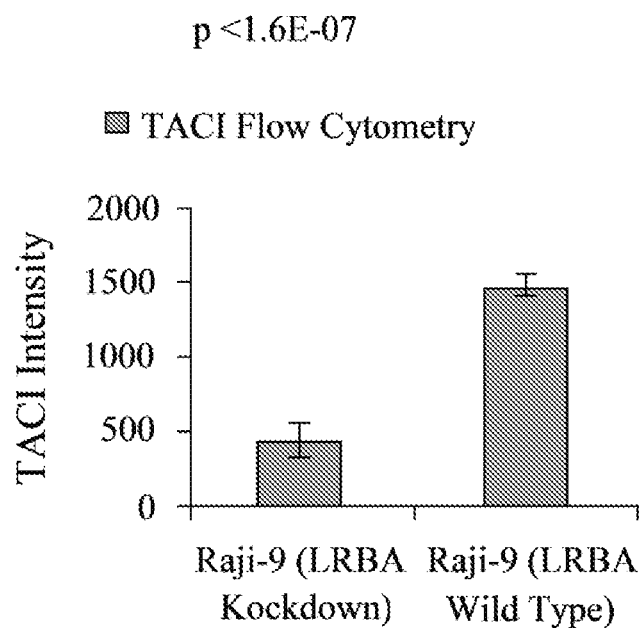


FIG. 15E

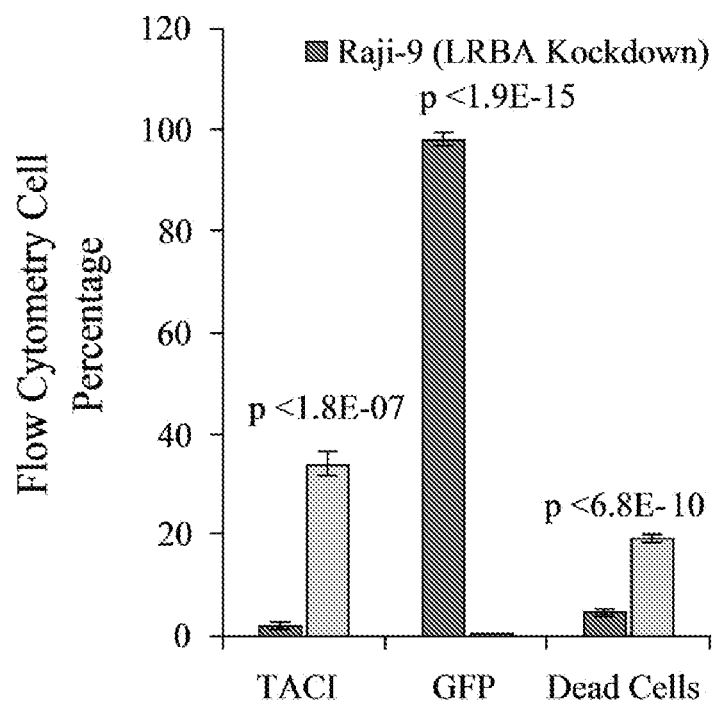


FIG. 15F

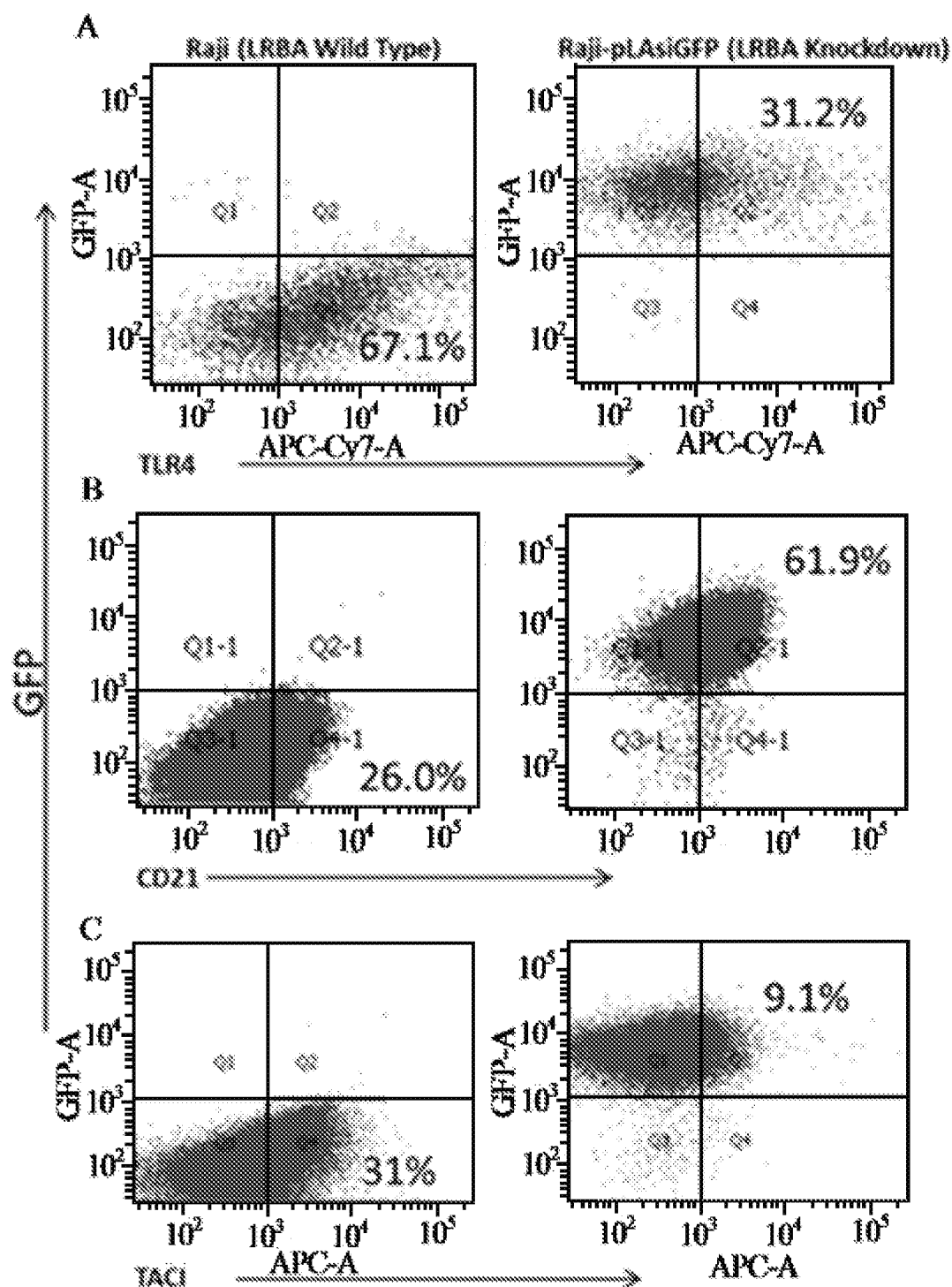


FIG 16A-C

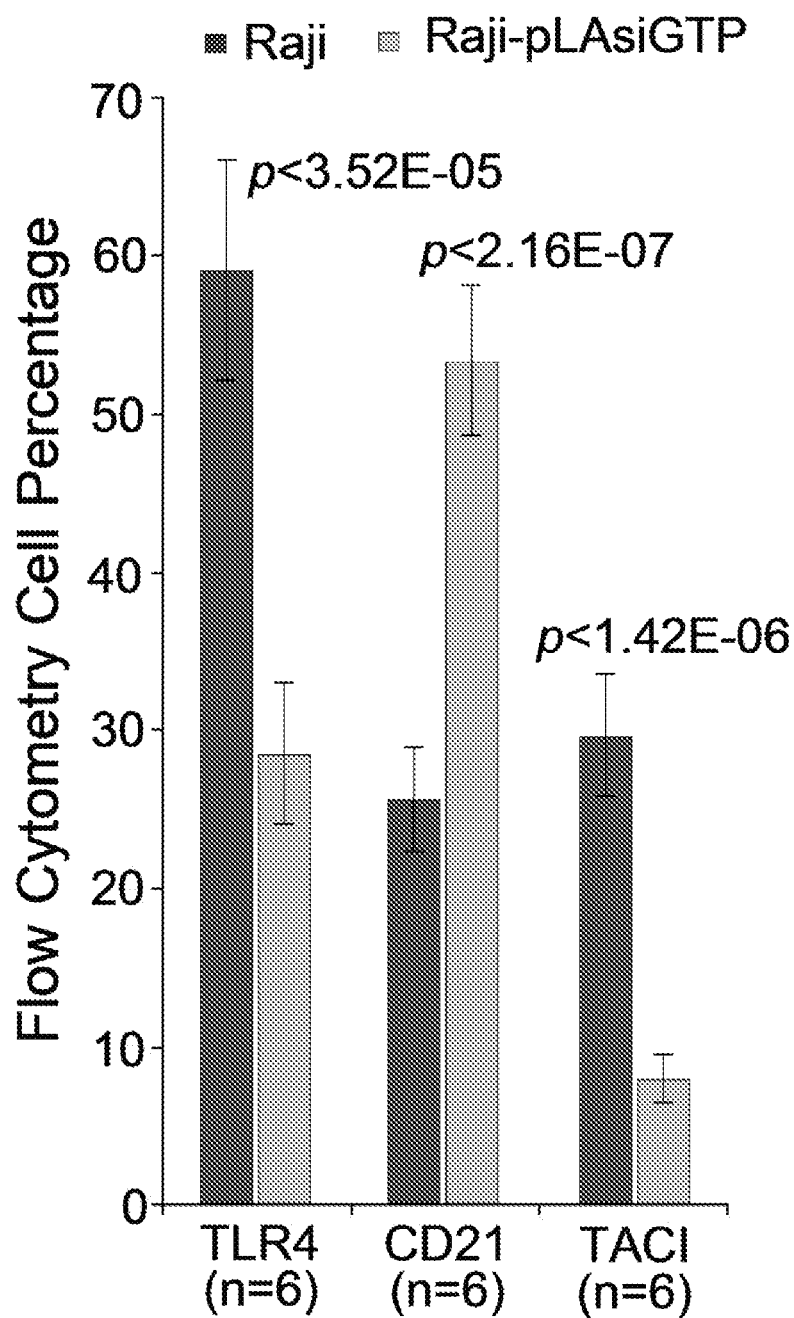


FIG. 16D

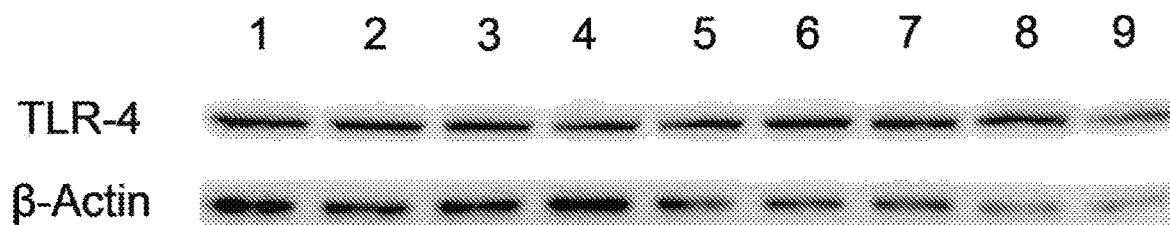


FIG. 17A

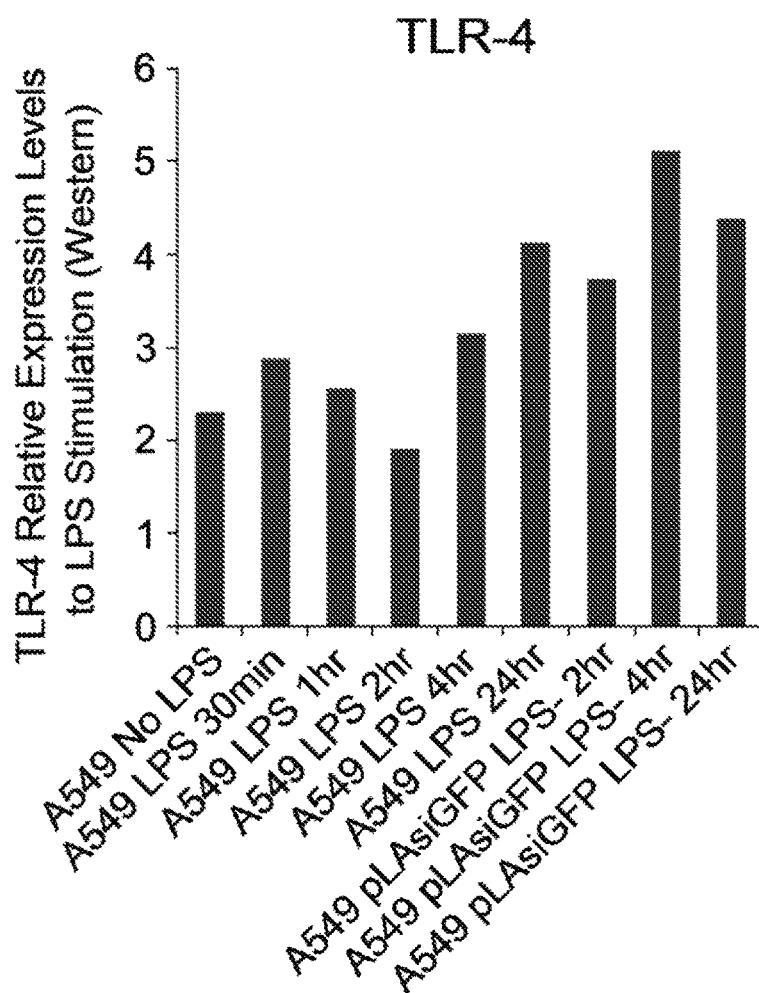


FIG. 17B

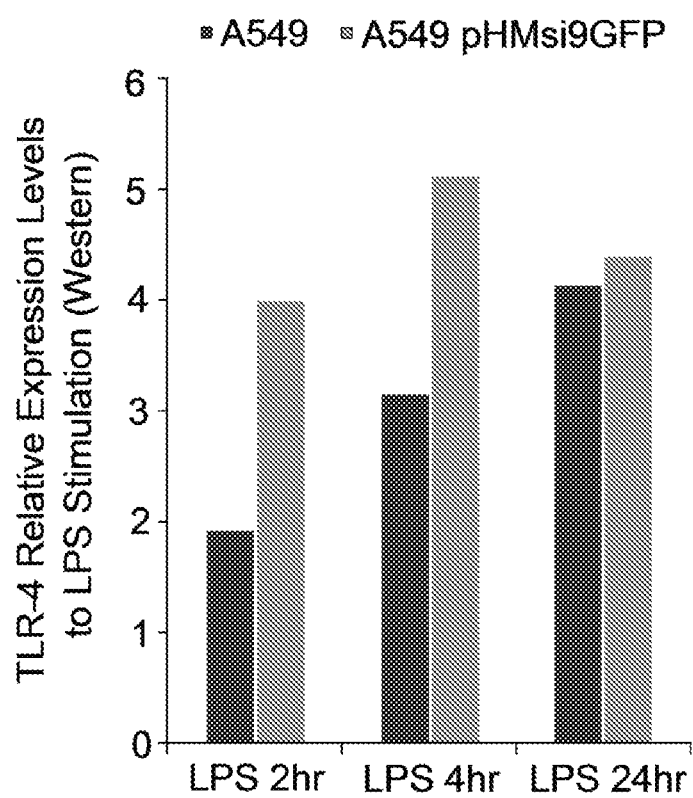


FIG. 17C

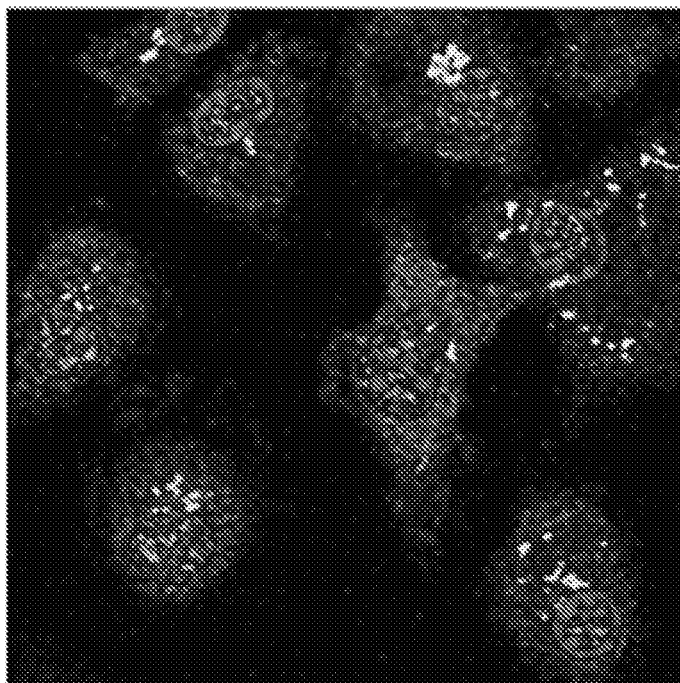


FIG. 18A

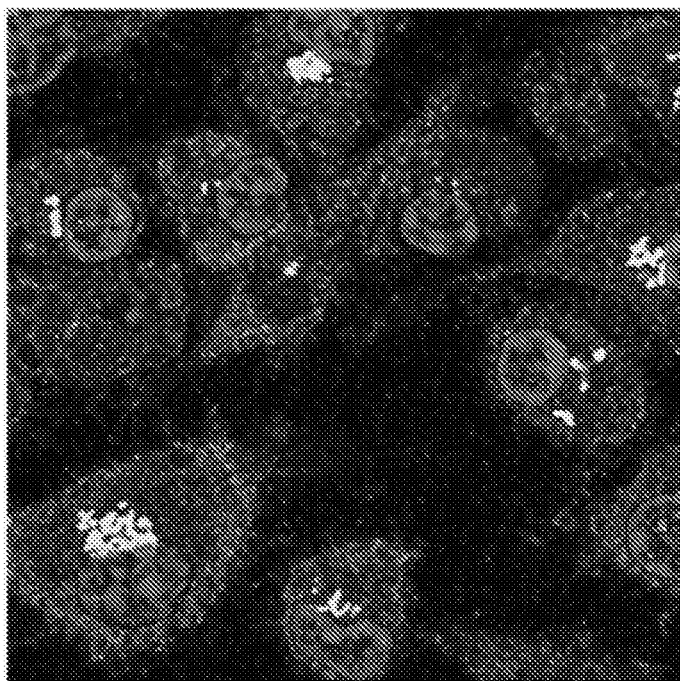


FIG. 18B

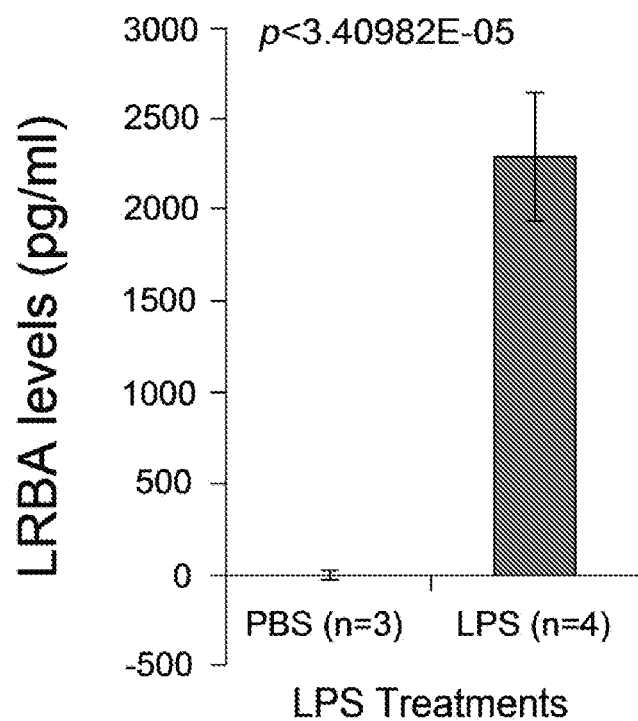


FIG. 19A

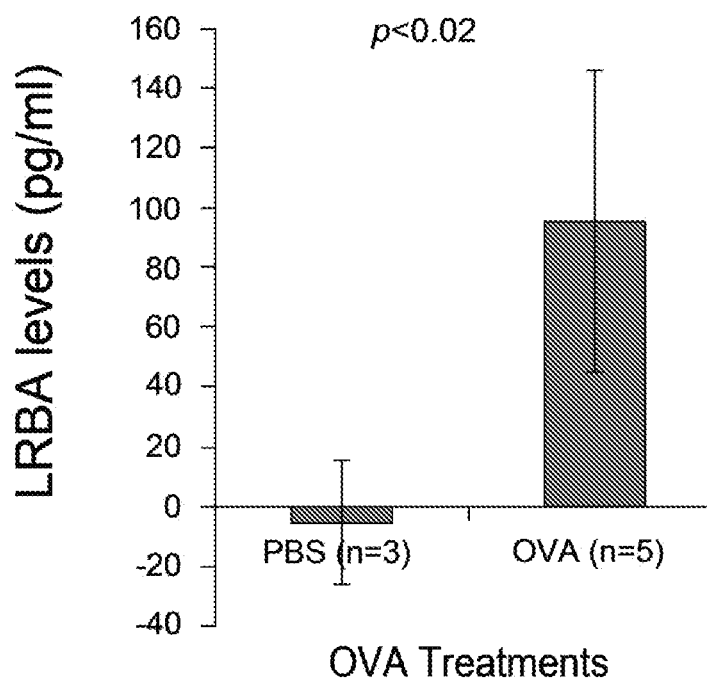


FIG. 19B

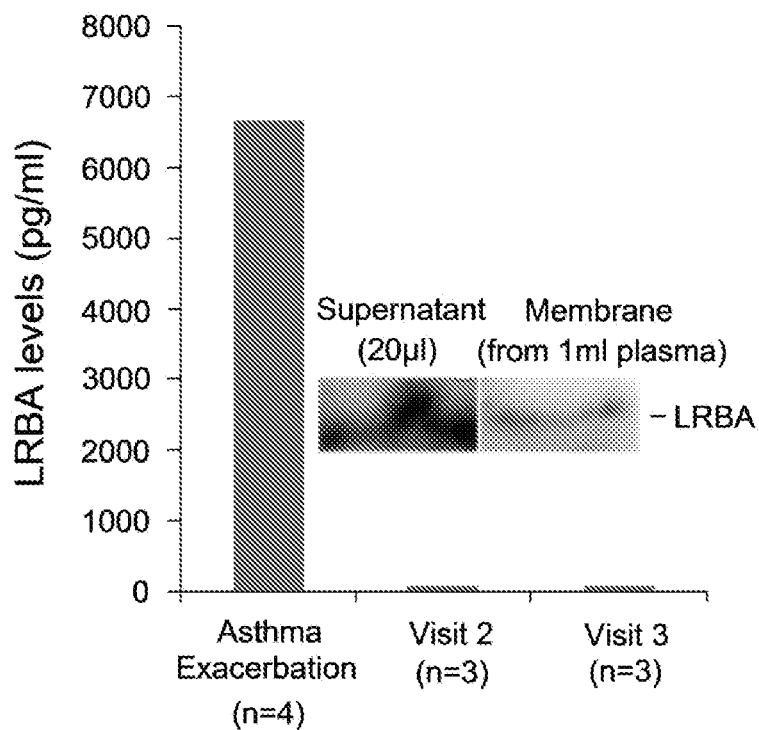


FIG. 19C

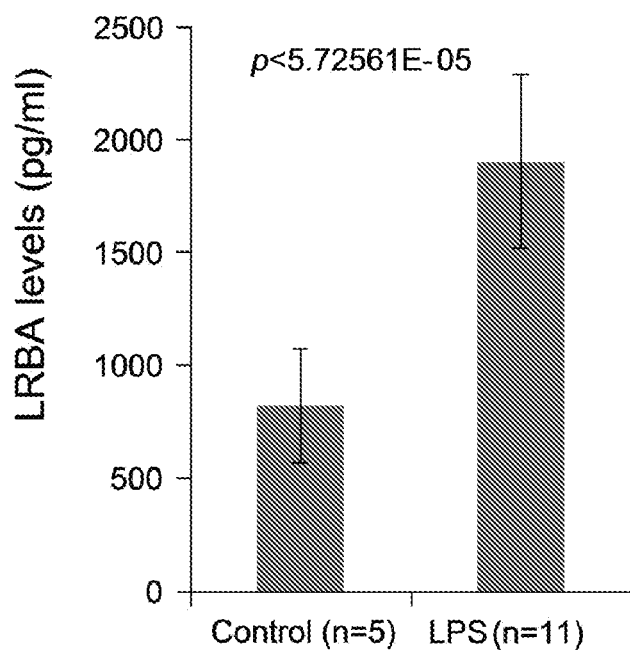


FIG. 19D



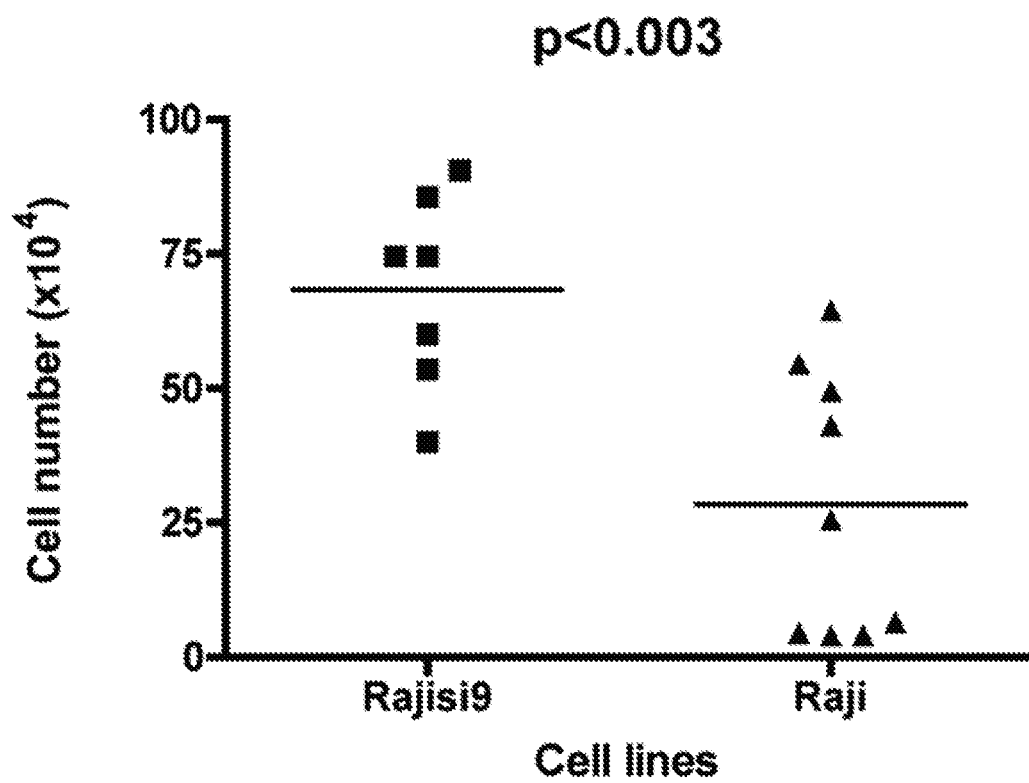


FIG. 20

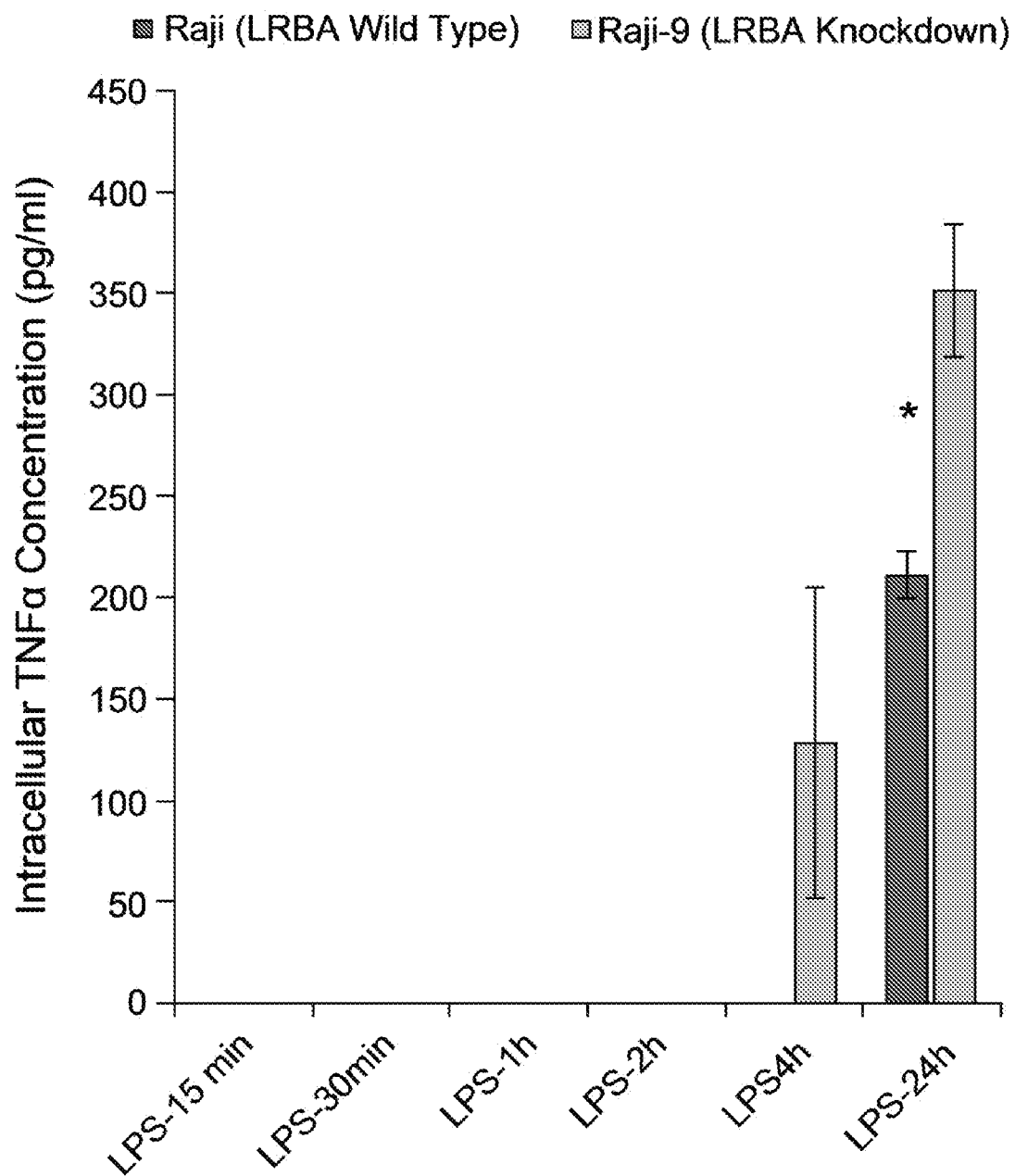


FIG. 21

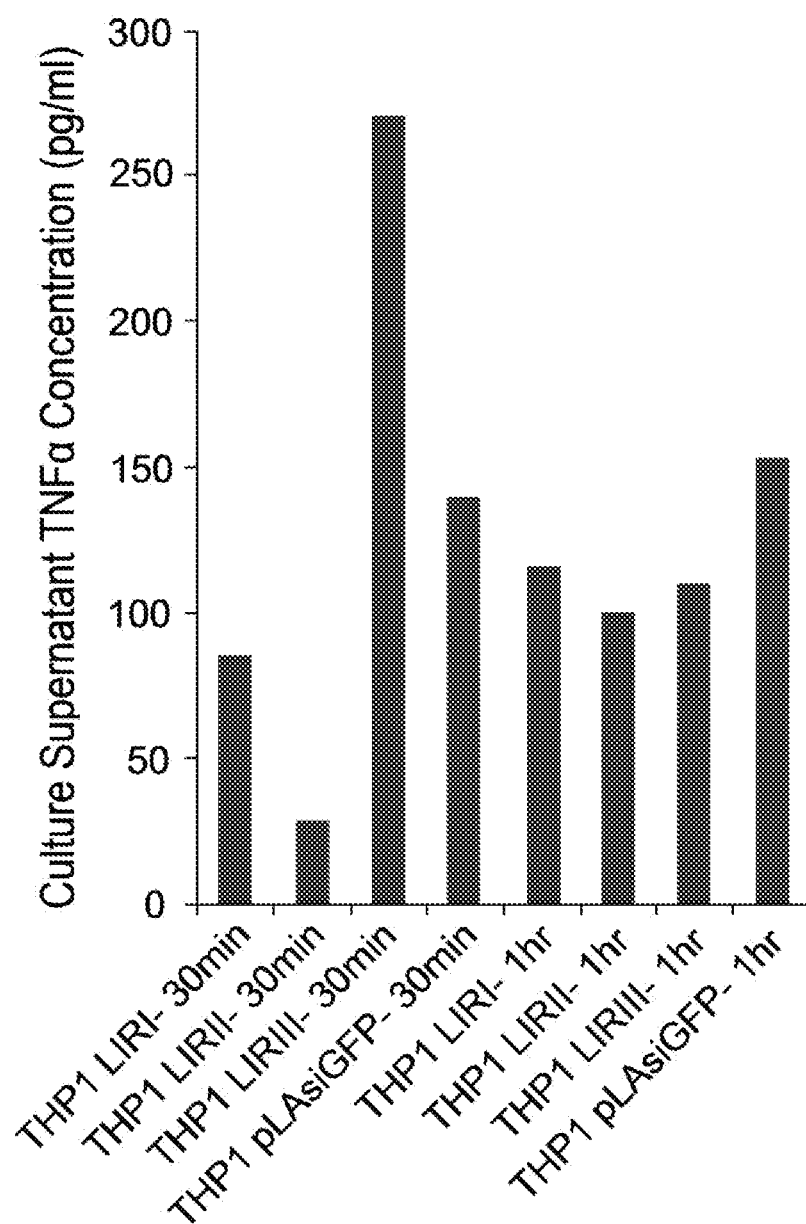


FIG. 22

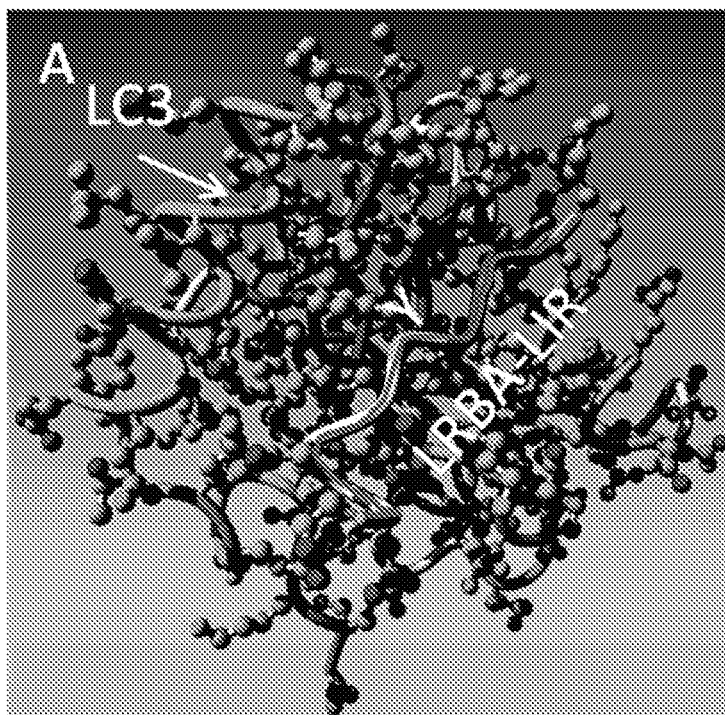


FIG. 23A

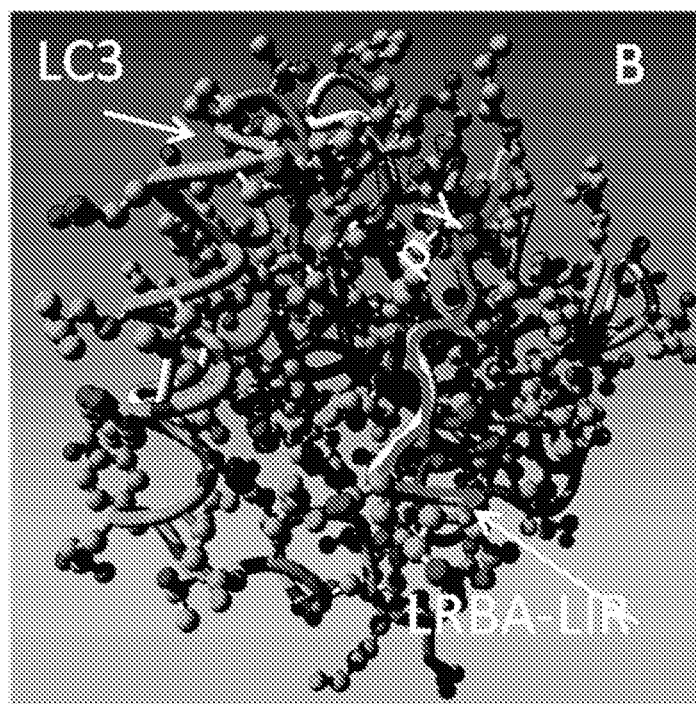


FIG. 23B

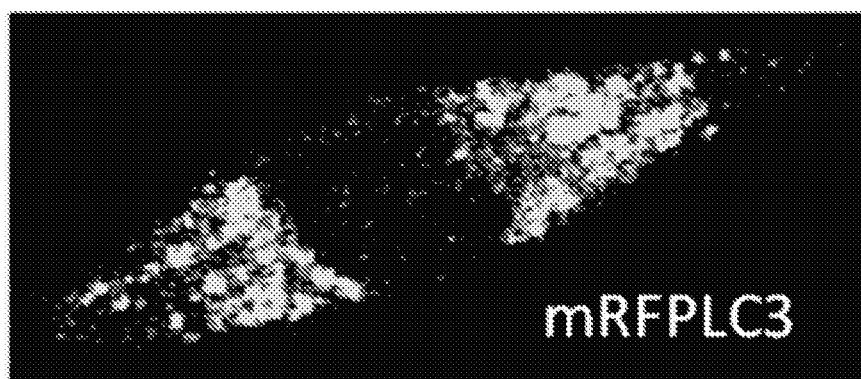


FIG. 23C

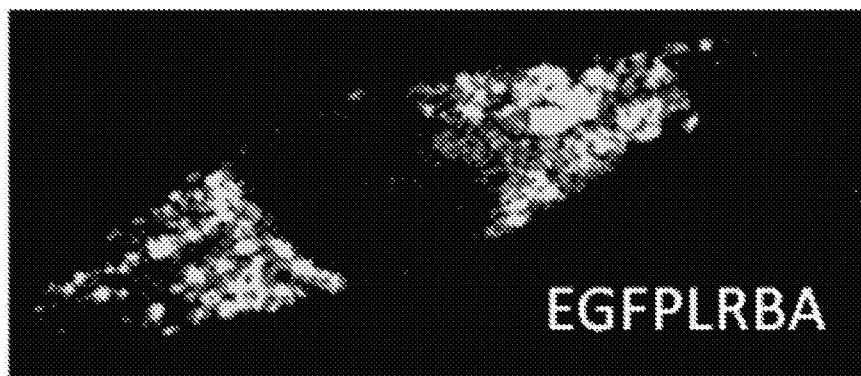


FIG. 23D

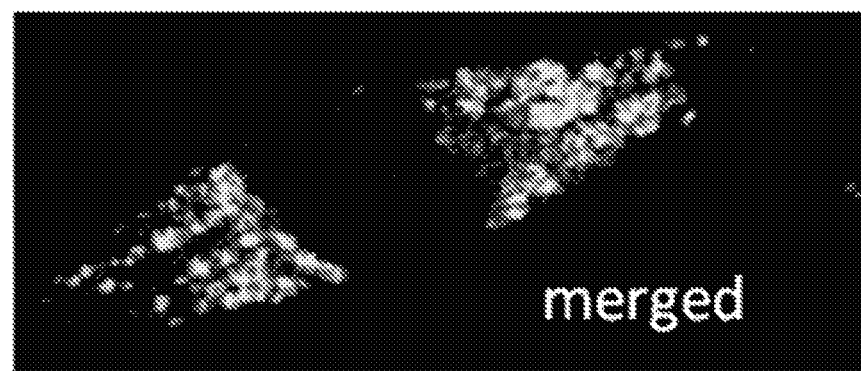


FIG. 23E

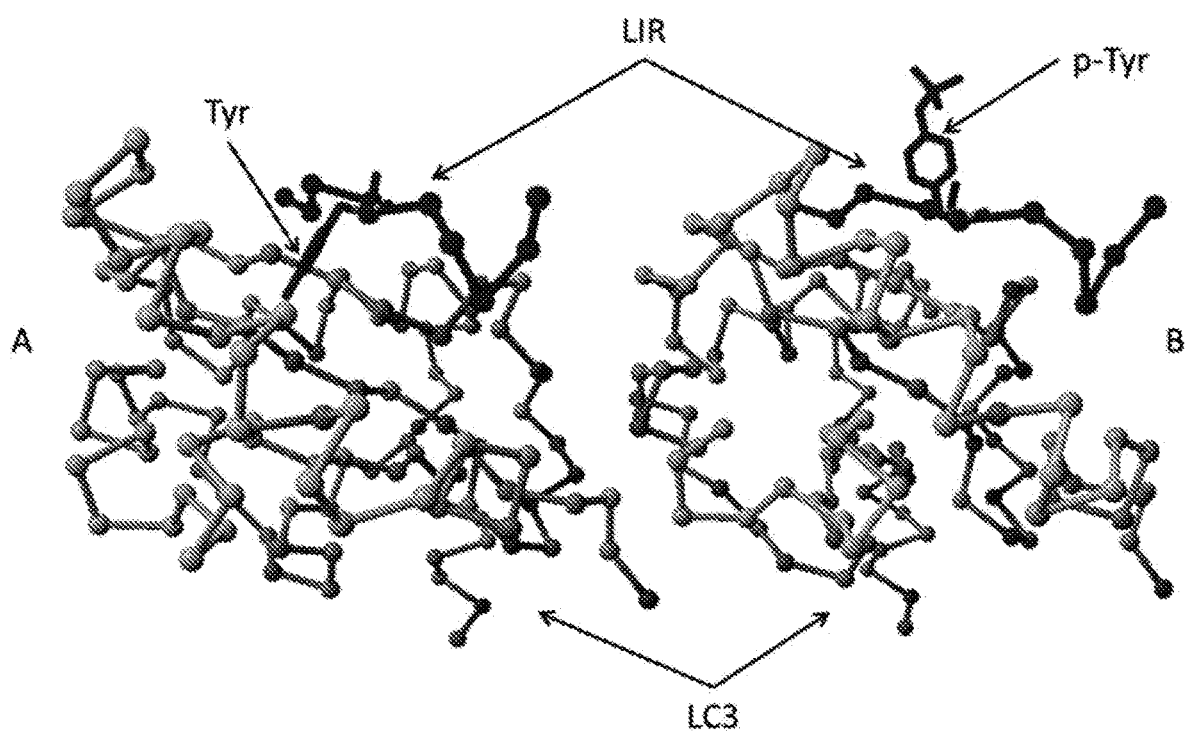


FIG. 24 A-B

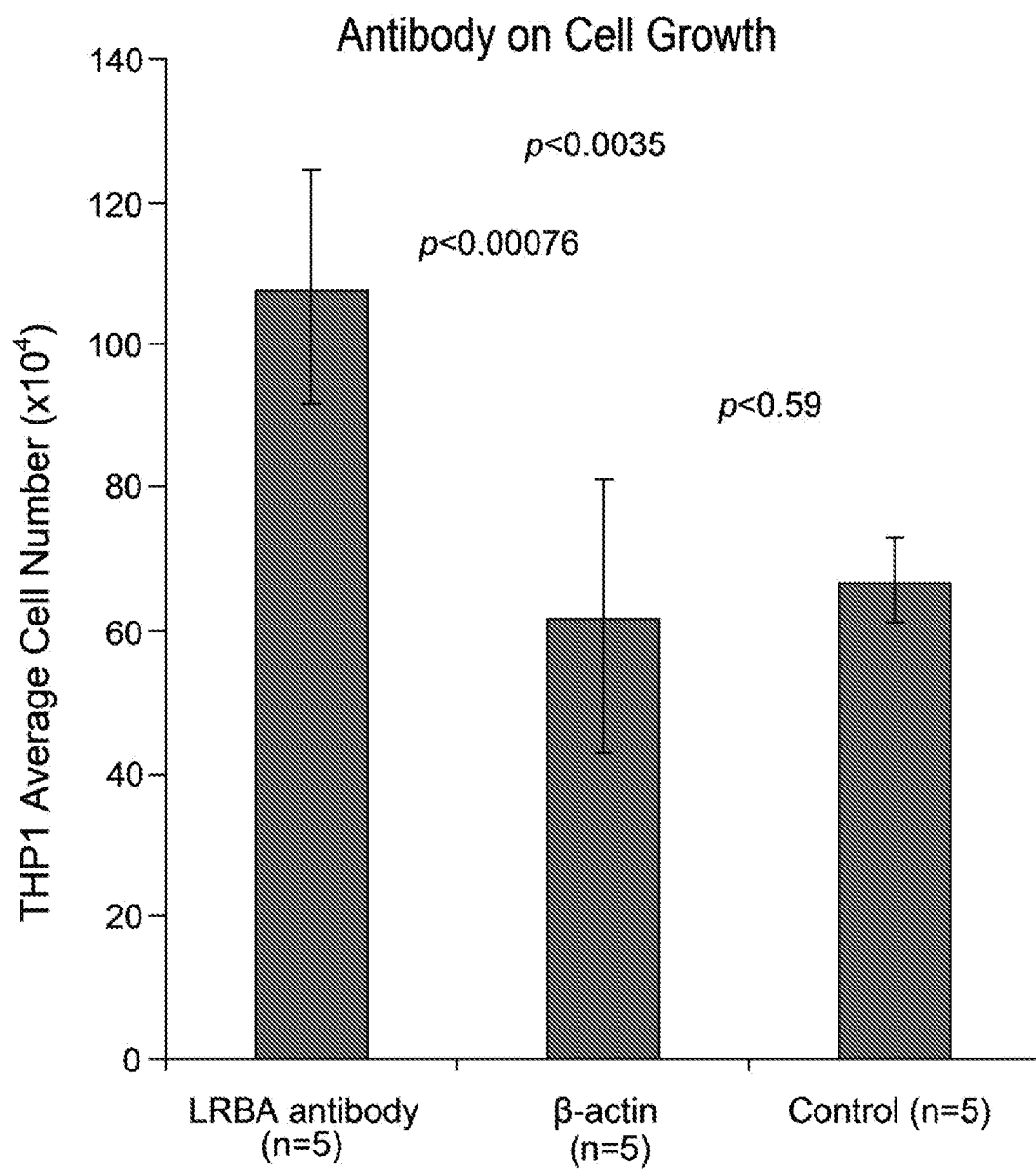


FIG. 25

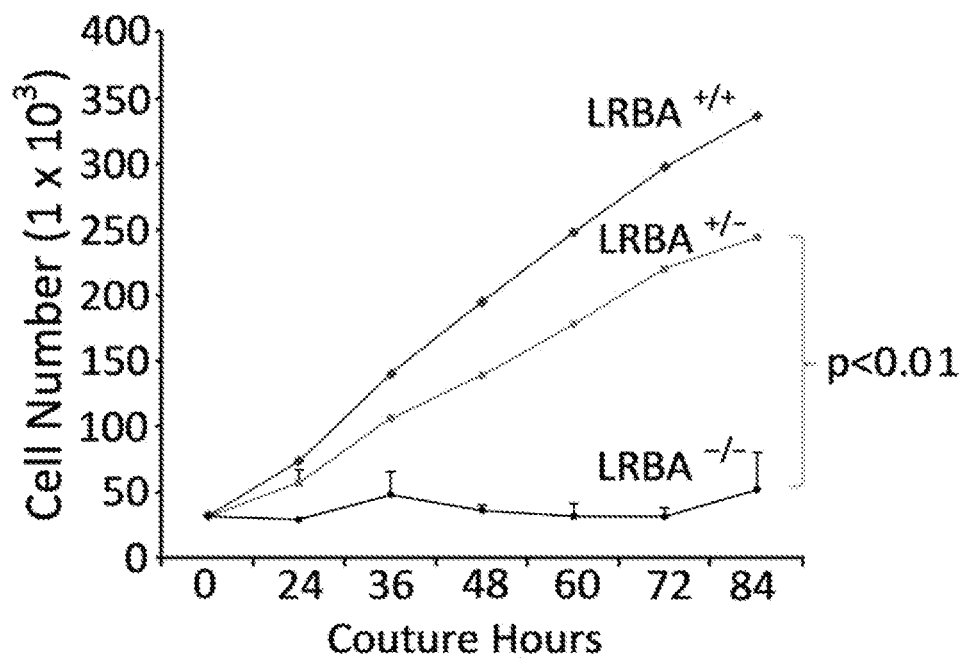


FIG. 26A

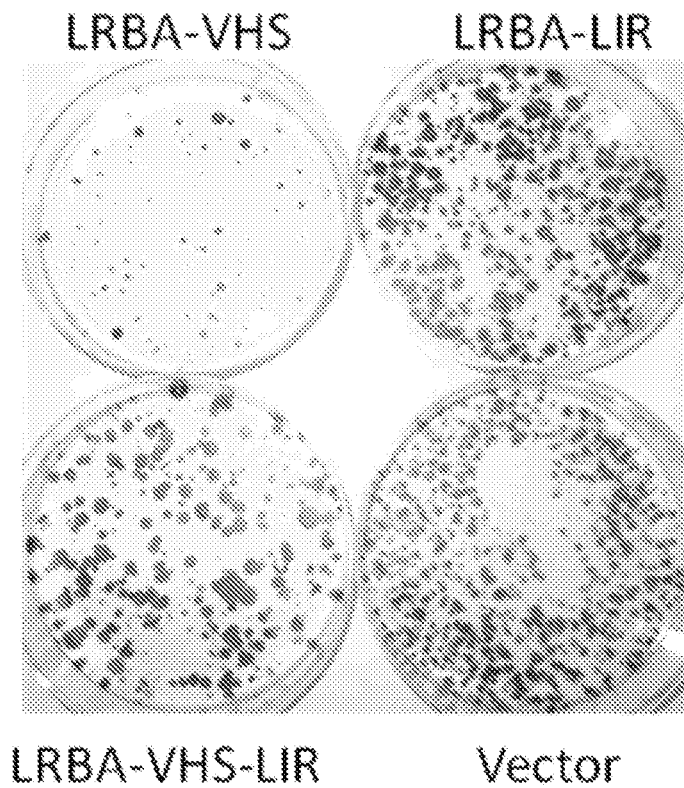


FIG. 26B



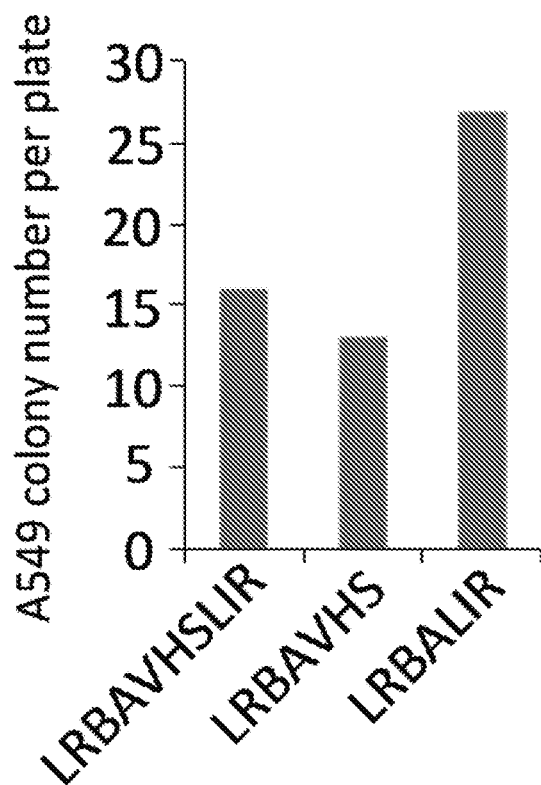


FIG. 26C

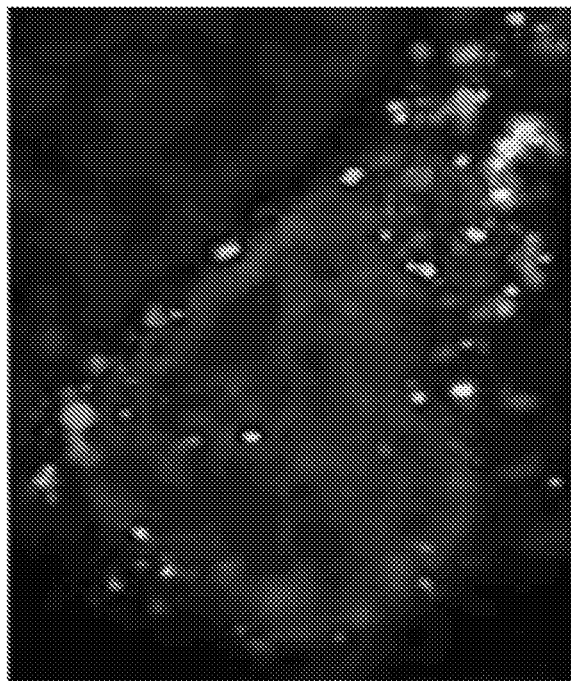


FIG. 26D

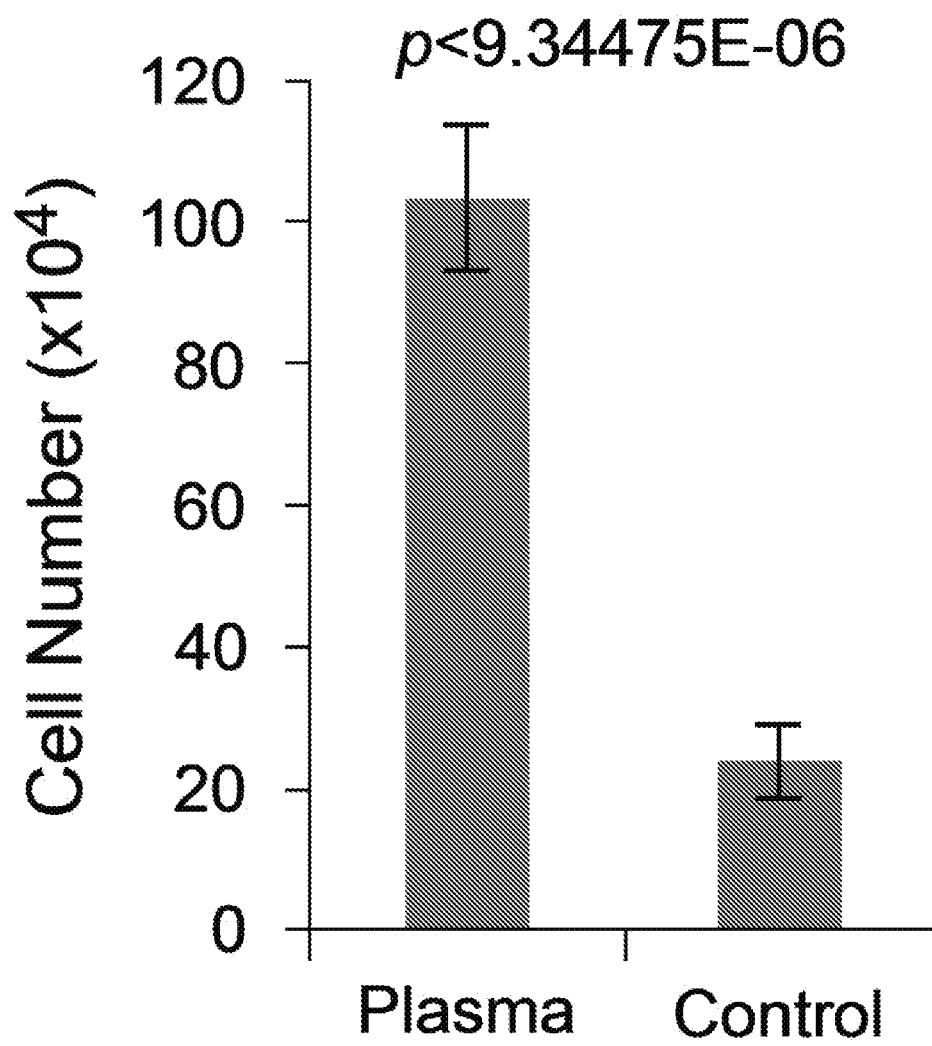


FIG. 26E

FIG. 27

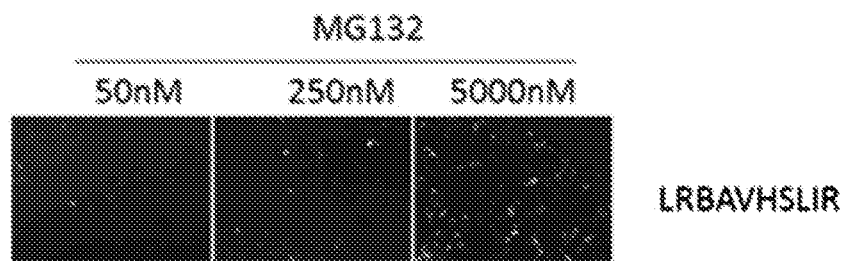


FIG. 28A

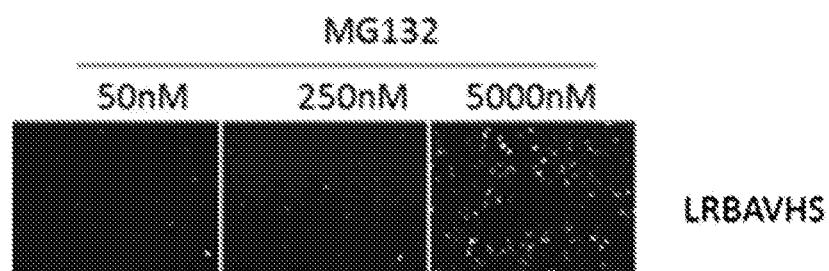


FIG. 28B

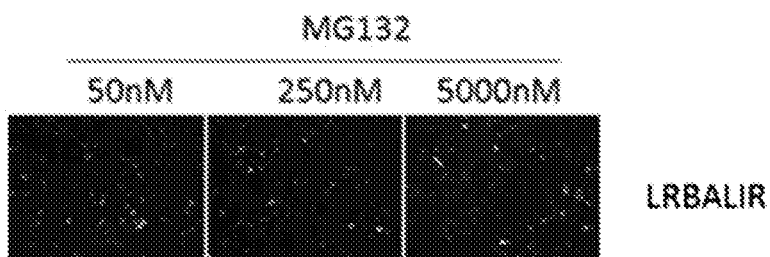


FIG. 28C

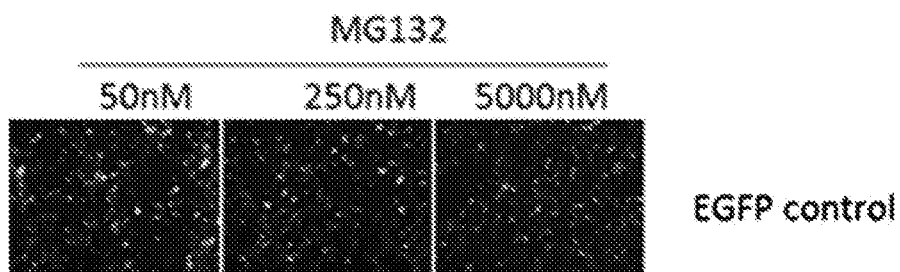


FIG. 28D

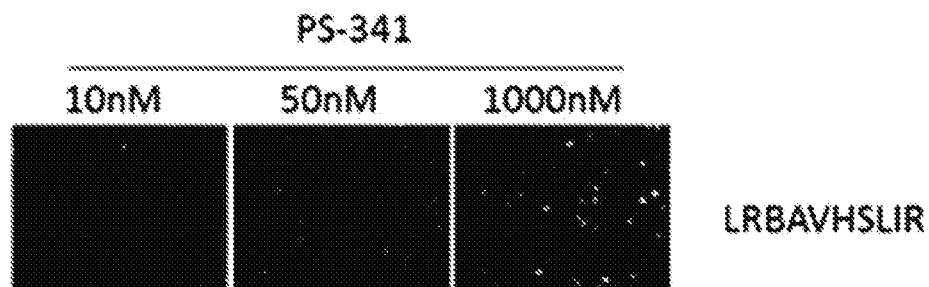


FIG. 28E

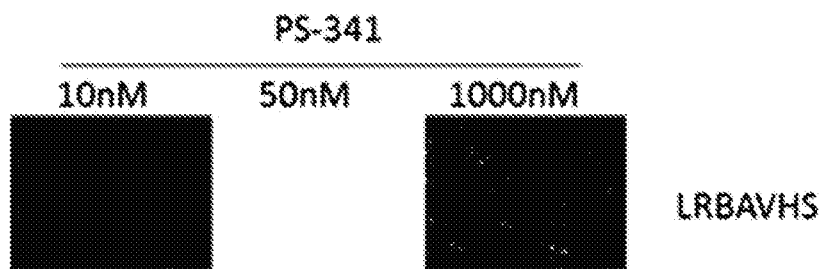


FIG. 28F

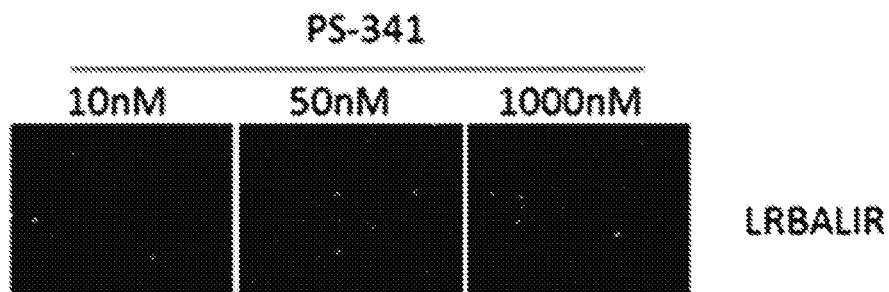


FIG. 28G

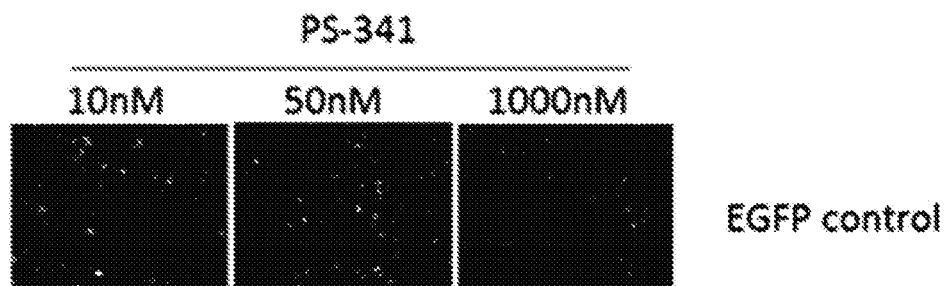


FIG. 28H

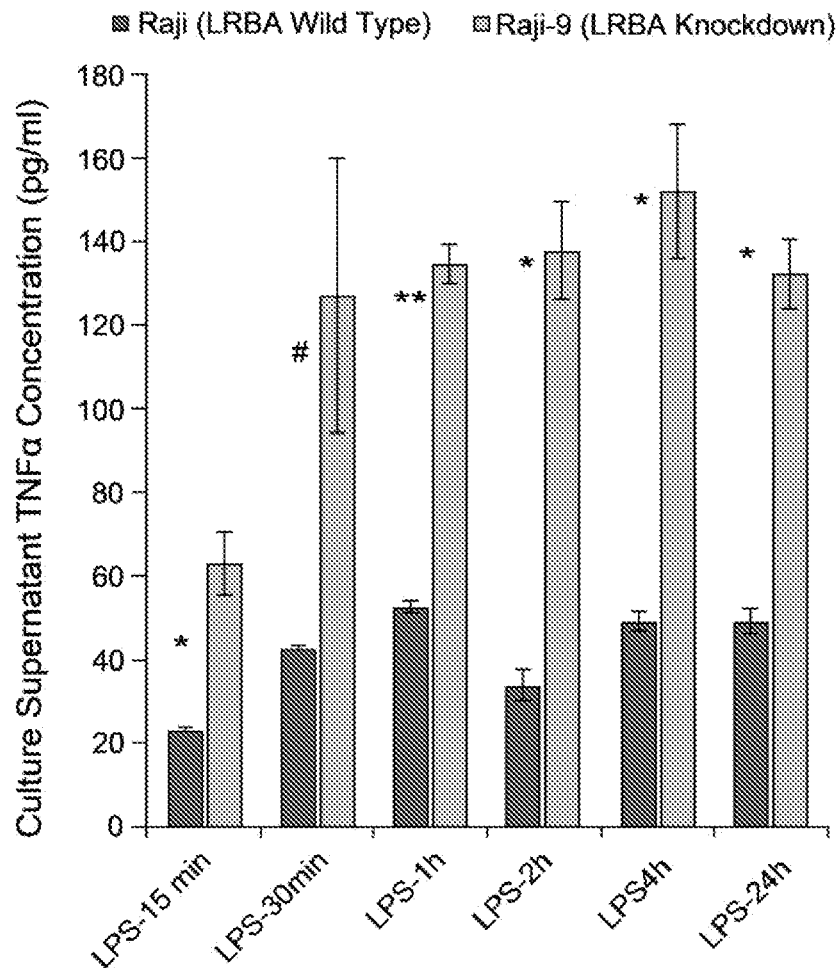


FIG. 29A

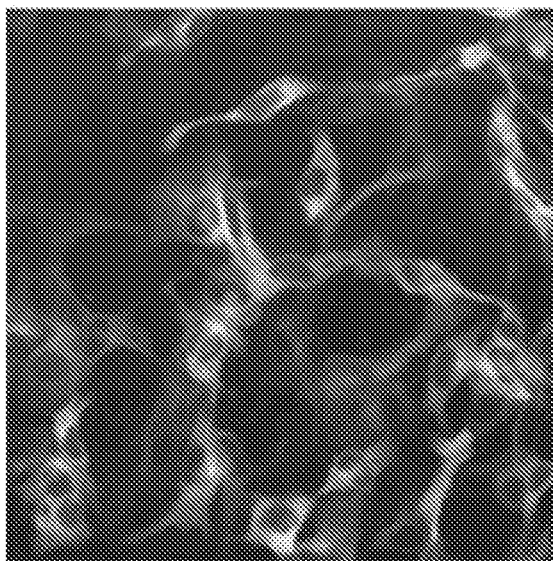


FIG. 29B

Seq ID No.	
23.	T T T T G G T T G A C A T G T T G G G A G T Human LRBA 
24.	G T G A C C A T G T T C C C A A C C T C T miR-150 
25.	A T C T C G T T G A C A T G T T G G G A G T Mouse LRBA

FIG. 30A

Seq ID No.		miRNA-181																											
		7 0										8 0										9 0							
23.	Hsa	Z	-	-	-	C	A	C	A	U	C	U	G	A	A	U	G	U	A	A	C	U	U	A	A	A	U	U	
24.	Ptr	Z	-	-	-	C	A	C	A	U	C	U	G	A	A	U	G	U	A	A	C	U	U	A	A	A	U	U	
25.	Mml	Z	-	-	-	C	A	C	A	U	C	U	G	A	A	U	G	U	A	A	C	U	U	A	A	A	U	U	
---	Oga	-	-	-	-	-	-	-	-	-	-	-	-	-	-	-	-	-	-	-	-	-	-	-	-	-	-		
---	The	-	-	-	-	-	-	-	-	-	-	-	-	-	-	-	-	-	-	-	-	-	-	-	-	-	-		
26.	Mmu	J	-	-	-	C	A	C	A	U	C	U	G	A	A	U	G	U	A	A	C	U	U	A	A	A	U	U	
27.	Rno	J	-	-	-	C	A	C	A	U	C	U	G	A	A	U	G	U	A	A	C	U	U	A	A	A	U	U	
---	Cpo	-	-	-	-	-	-	-	-	-	-	-	-	-	-	-	-	-	-	-	-	-	-	-	-	-	-		
28.	Ocu	J	-	-	-	C	A	C	A	U	C	U	G	A	A	U	G	U	A	A	C	U	G	A	A	A	U	U	
29.	Sar	J	-	-	-	C	C	C	A	U	C	U	G	A	A	U	G	U	A	A	C	U	U	A	A	A	G	U	
30.	Eeu	J	-	-	-	C	C	C	A	U	C	U	G	A	A	U	G	U	A	A	C	U	U	A	A	A	U	G	
31.	Cfa	J	-	-	-	C	A	C	A	U	C	U	G	A	A	U	G	U	A	A	C	U	U	A	A	A	U	U	
32.	Fca	J	-	-	-	C	A	C	A	U	C	U	G	A	A	U	G	U	A	A	C	U	U	A	A	A	U	U	
33.	Eca	J	-	-	-	C	A	C	A	U	C	U	G	A	A	U	G	U	A	A	C	U	U	A	A	A	U	U	
34.	Bta	J	-	-	-	C	A	C	A	U	C	C	G	A	A	U	G	U	A	A	C	U	U	A	A	A	U	U	
35.	Dno	J	-	-	-	U	A	C	A	U	C	U	G	A	A	U	G	U	A	A	C	U	U	A	G	A	U	U	
36.	Laf	J	-	-	-	U	A	C	A	U	C	U	G	A	A	U	G	U	A	A	C	U	U	C	A	A	U	U	
37.	Ete	J	-	-	-	U	A	C	A	U	C	U	G	A	A	U	G	U	A	A	C	U	U	A	A	A	U	U	
38.	Mdo	J	-	-	-	U	A	C	A	U	C	U	G	A	A	U	G	U	A	A	C	U	U	A	A	A	U	U	
39.	Oan	J	A	A	U	U	A	C	A	U	C	U	G	A	A	U	G	U	A	A	C	U	U	A	A	A	U	U	
40.	Aca	J	-	-	-	A	A	C	A	U	C	U	G	A	A	U	G	U	A	A	C	U	U	A	A	A	C	U	
41.	Gca	J	-	-	-	C	C	U	A	U	C	U	G	A	A	U	G	U	A	A	C	U	U	A	A	A	U	U	
42.	Xtr	J	-	-	-	U	A	C	A	U	C	U	G	A	A	U	G	U	A	A	U	U	U	A	A	A	U	G	

FIG. 30B



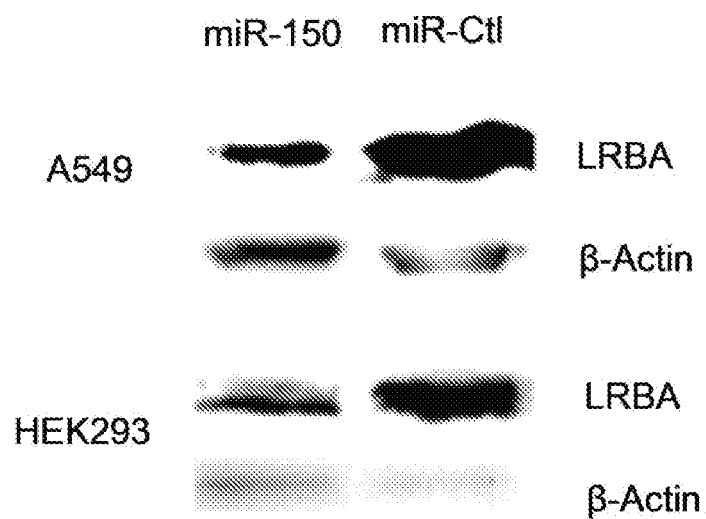


FIG. 30C

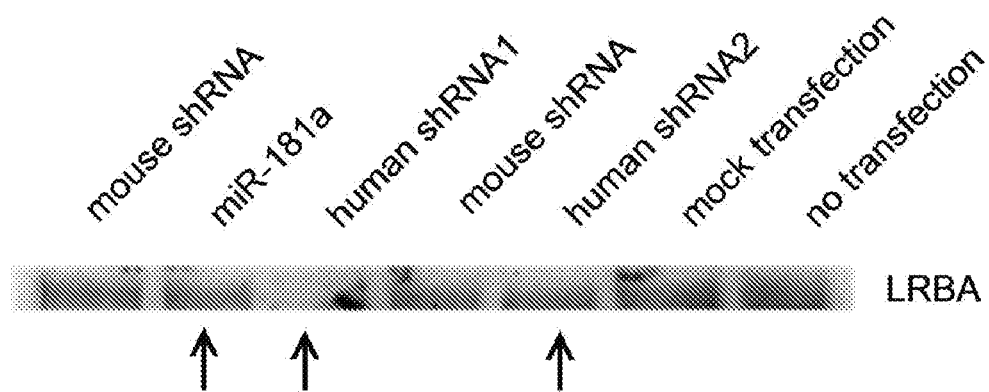


FIG. 30D

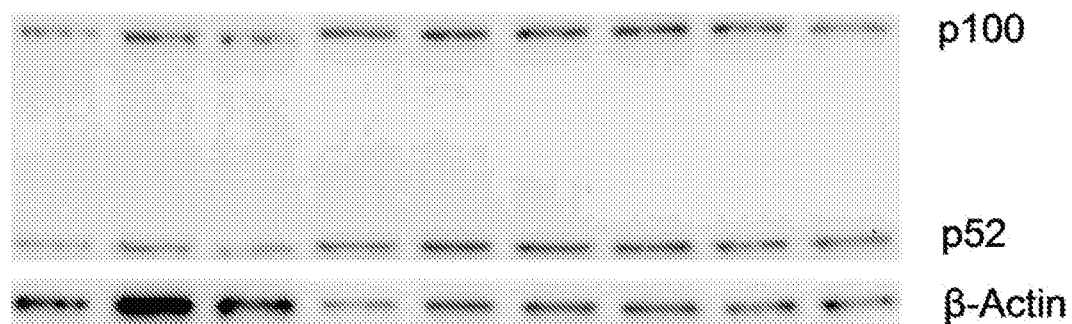


FIG. 31A

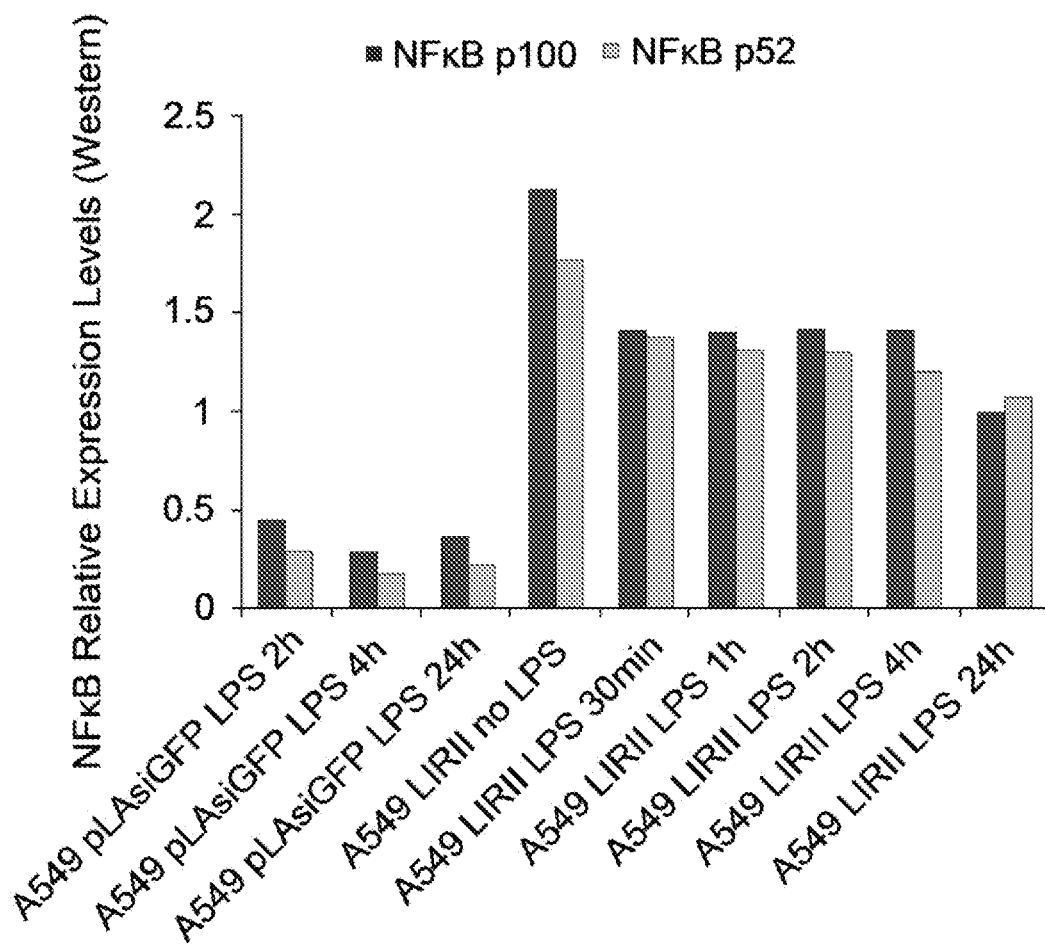


FIG. 31B

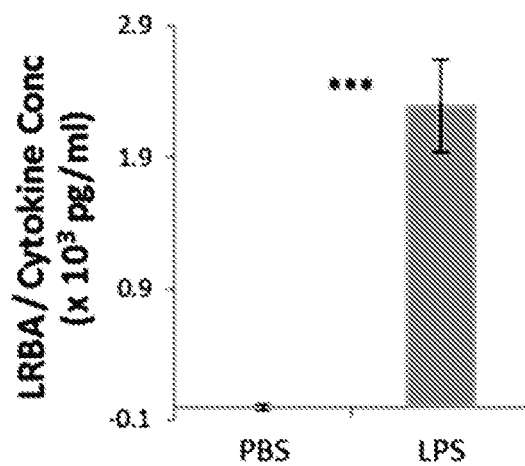


FIG. 32A

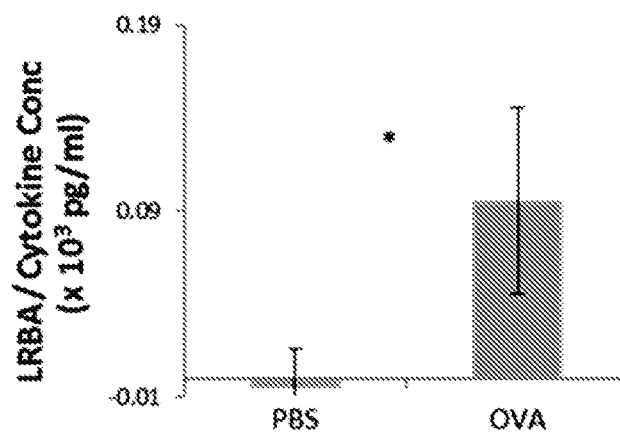


FIG. 32B

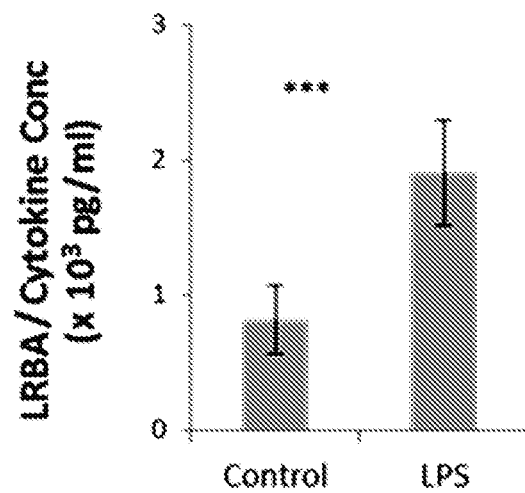


FIG. 32C

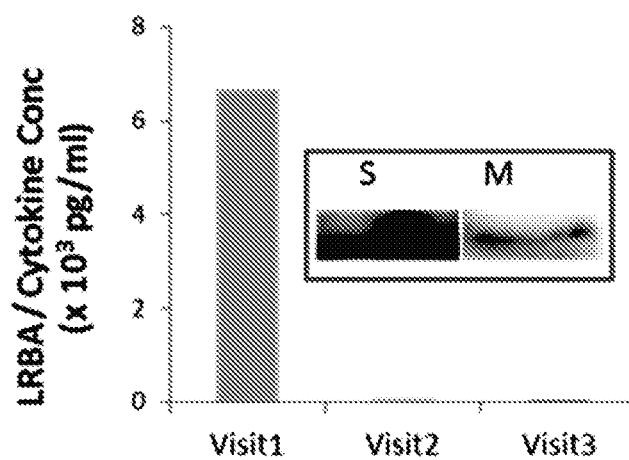


FIG. 32D

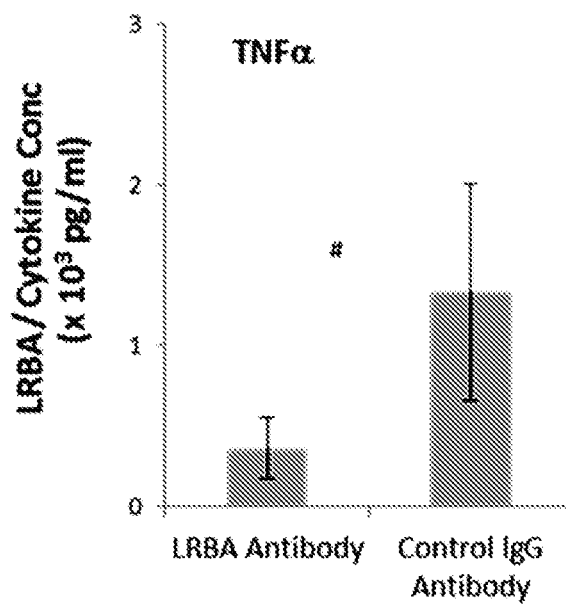


FIG. 32E

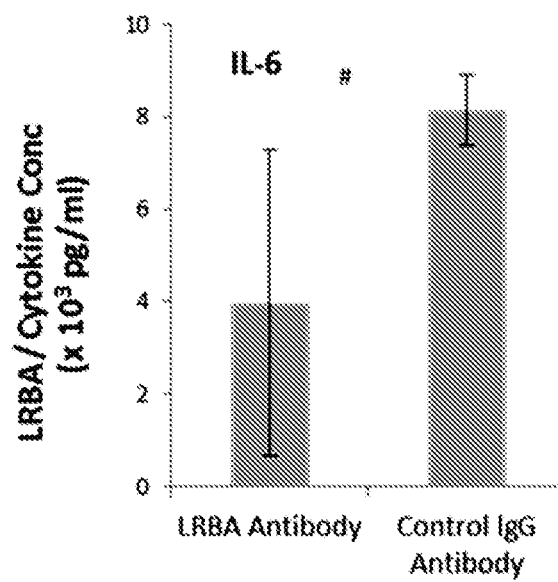


FIG. 32F

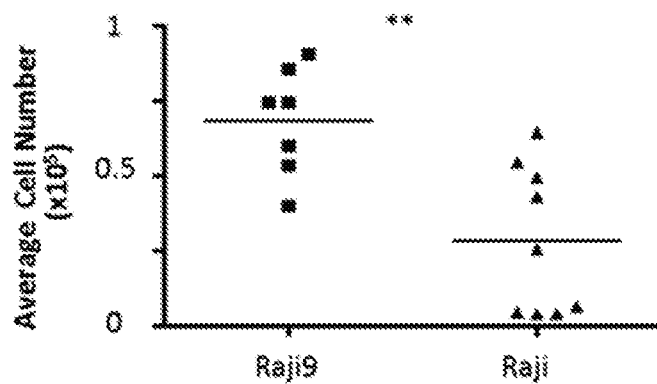


FIG. 33A

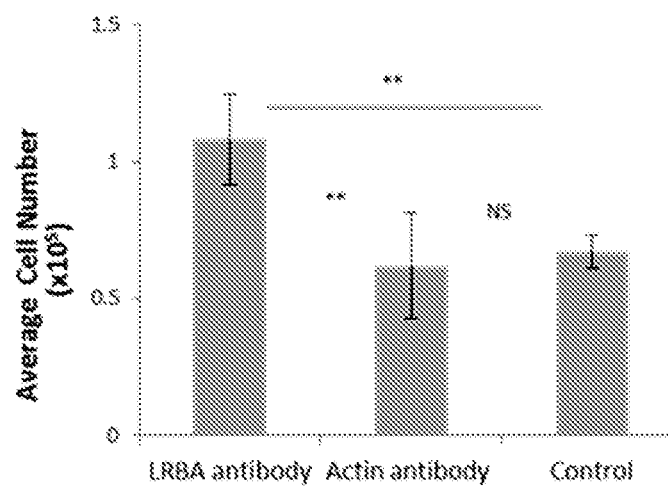


FIG. 33B

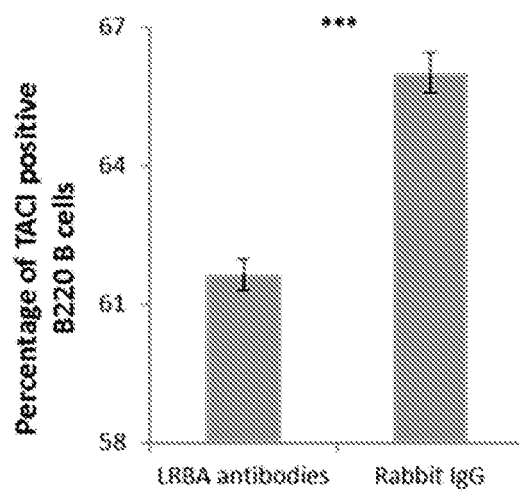


FIG. 33C

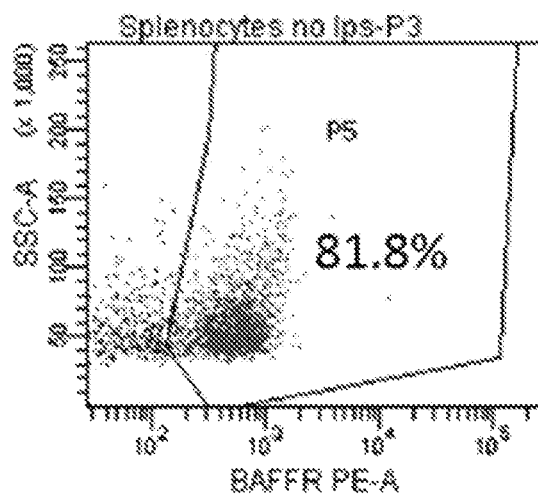


FIG. 34A

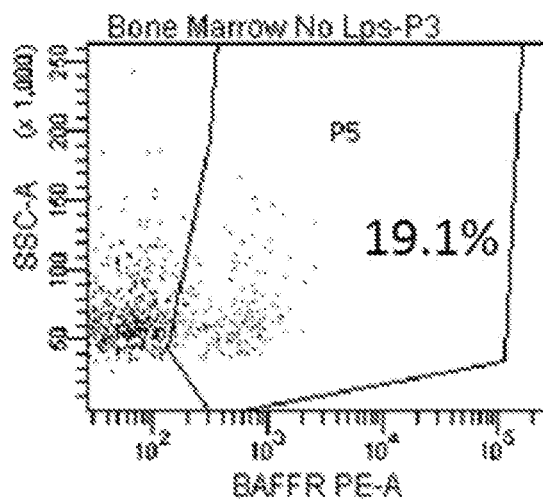


FIG. 34B

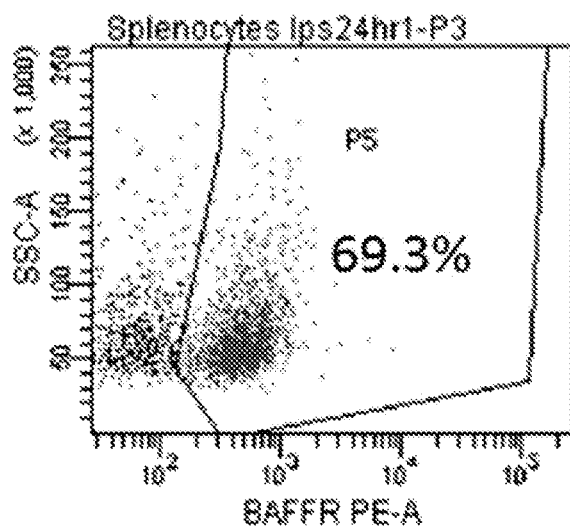


FIG. 34C

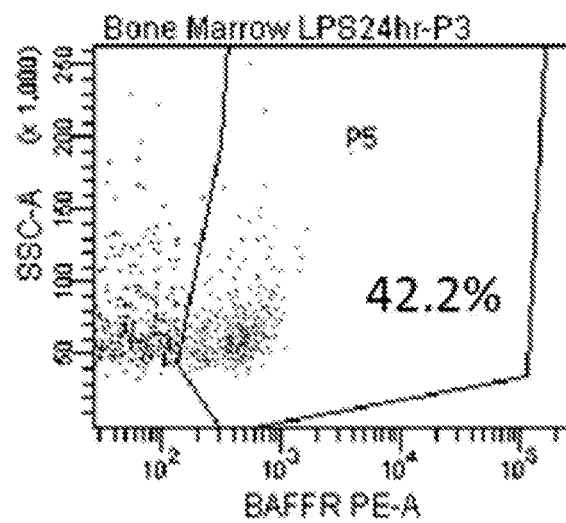


FIG. 34D



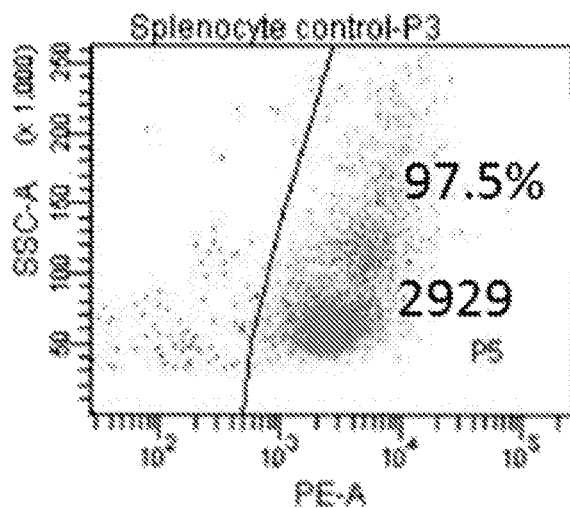


FIG. 34E

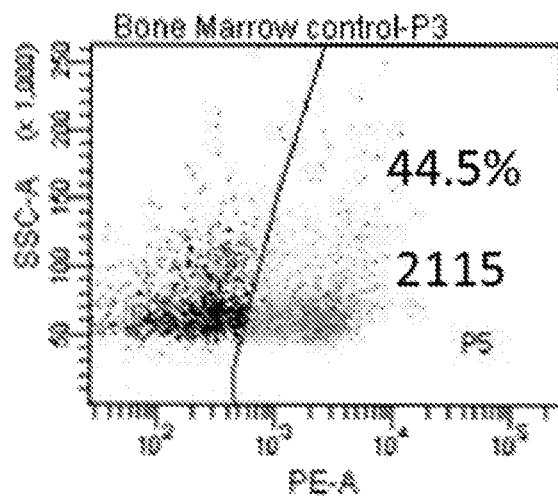


FIG. 34F

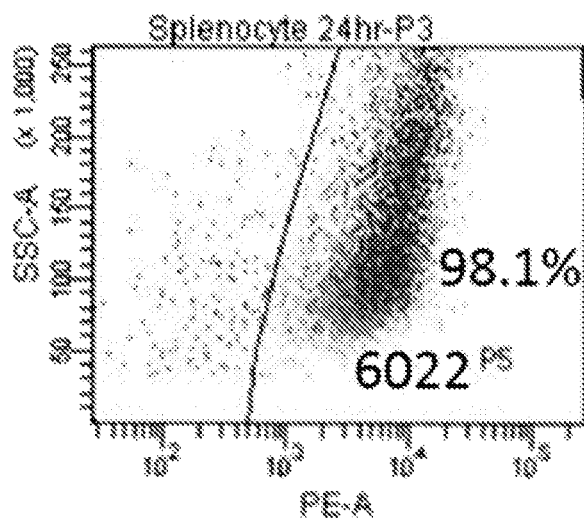


FIG. 34G

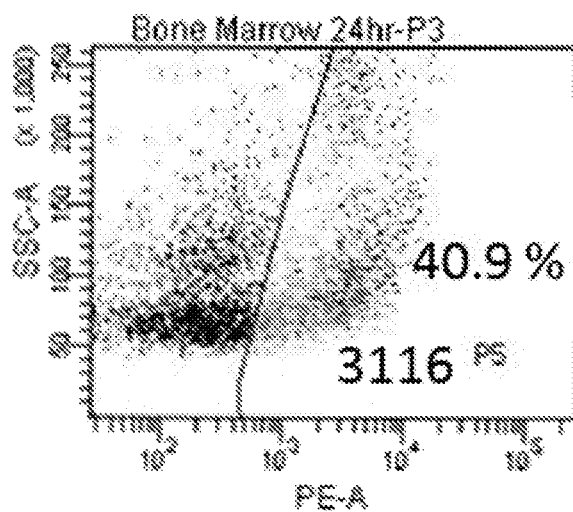


FIG. 34H

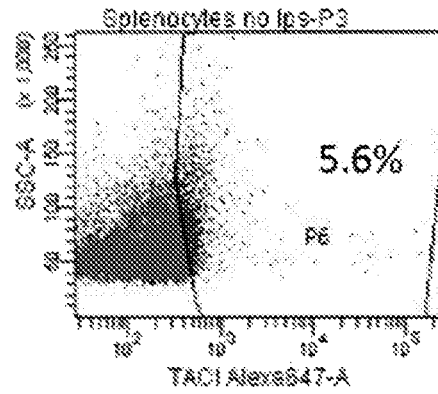


FIG. 35A

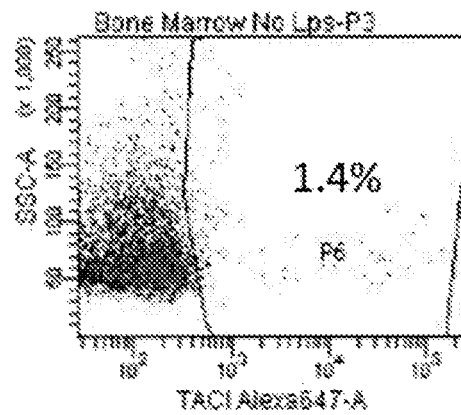


FIG. 35B

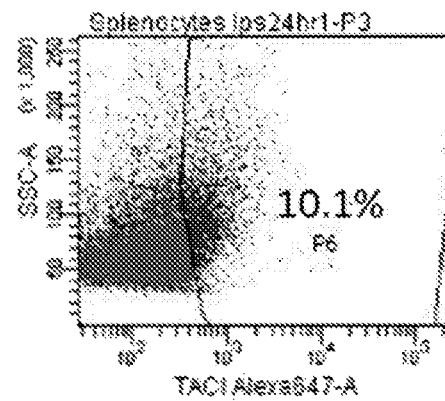


FIG. 35C

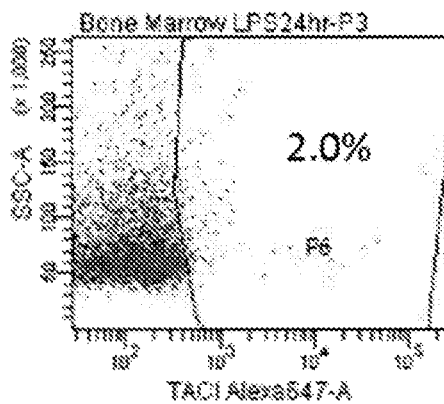


FIG. 35D

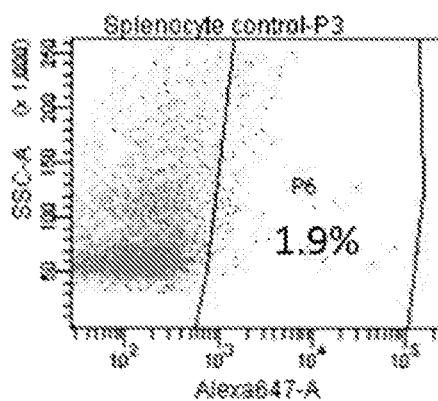


FIG. 35E

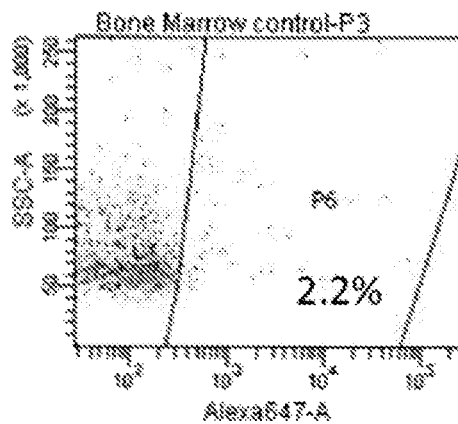


FIG. 35F

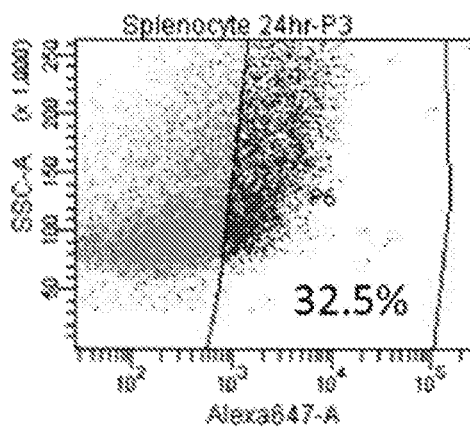


FIG. 35G

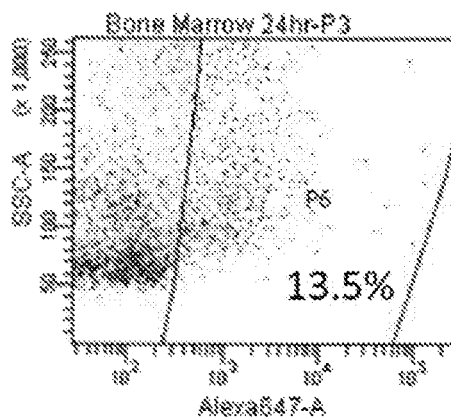


FIG. 35H

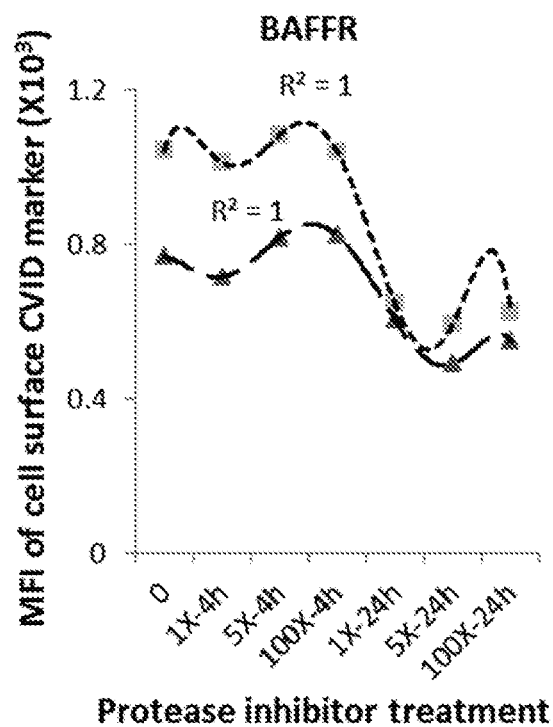


FIG. 36A

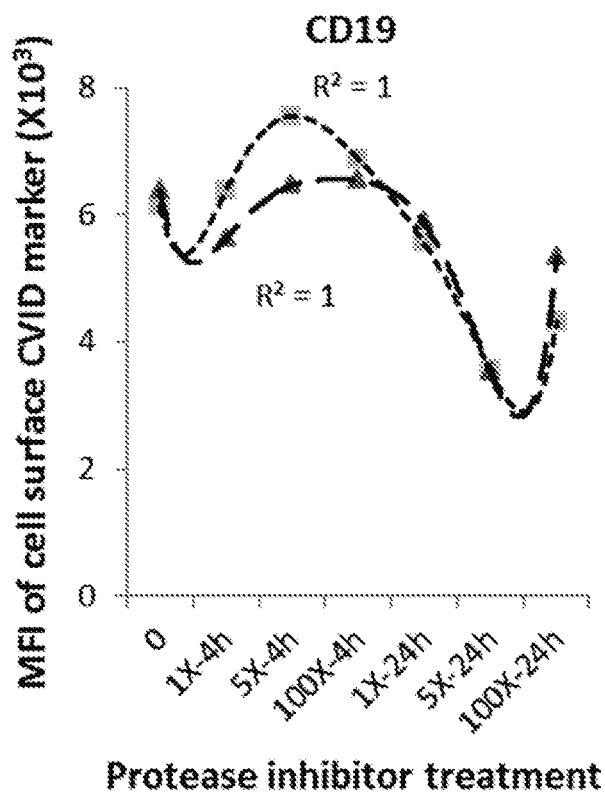


FIG. 36B

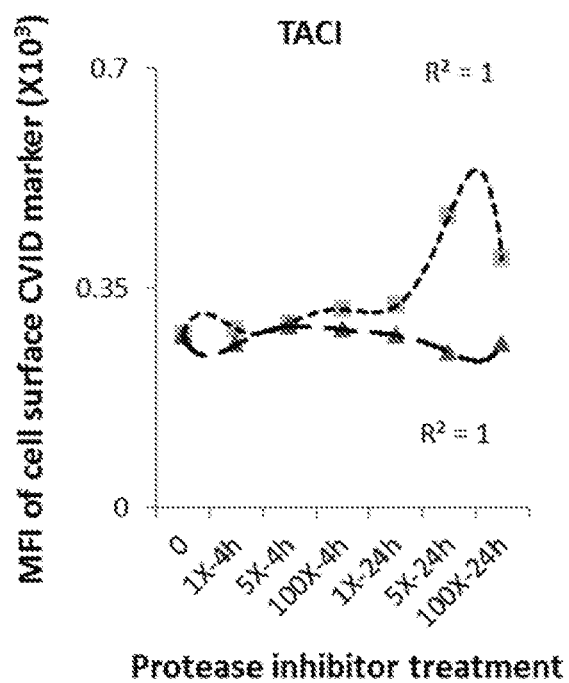


FIG. 36C

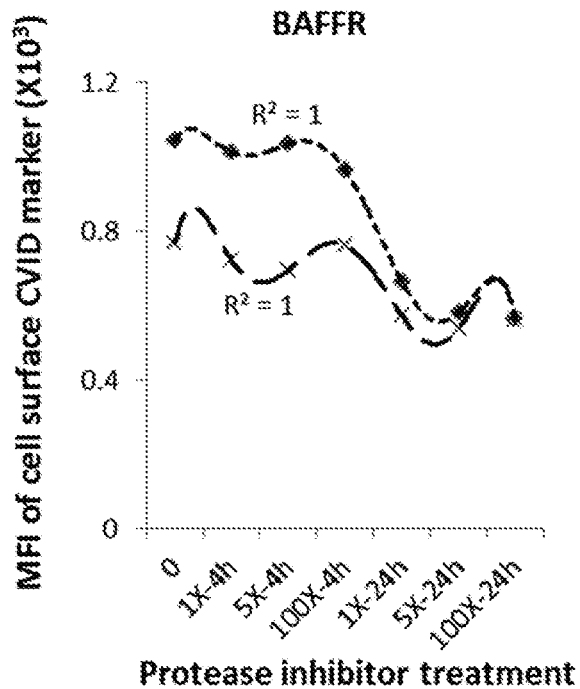


FIG. 37A

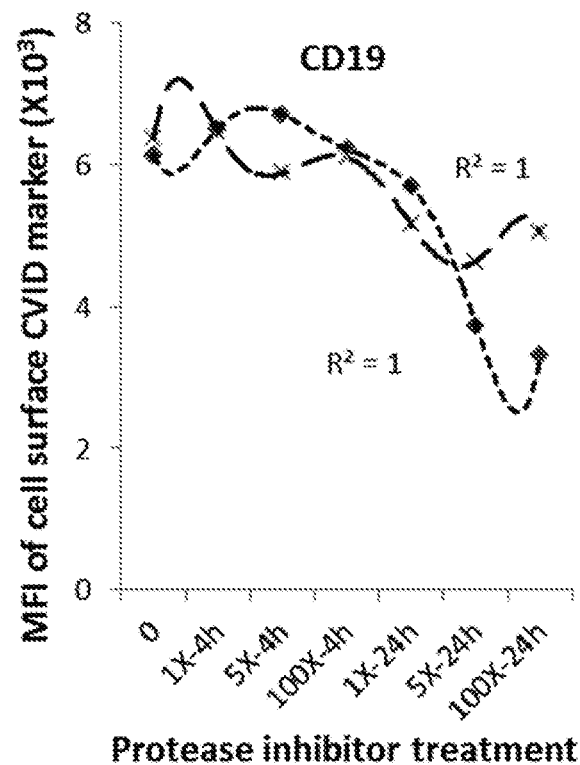


FIG. 37B



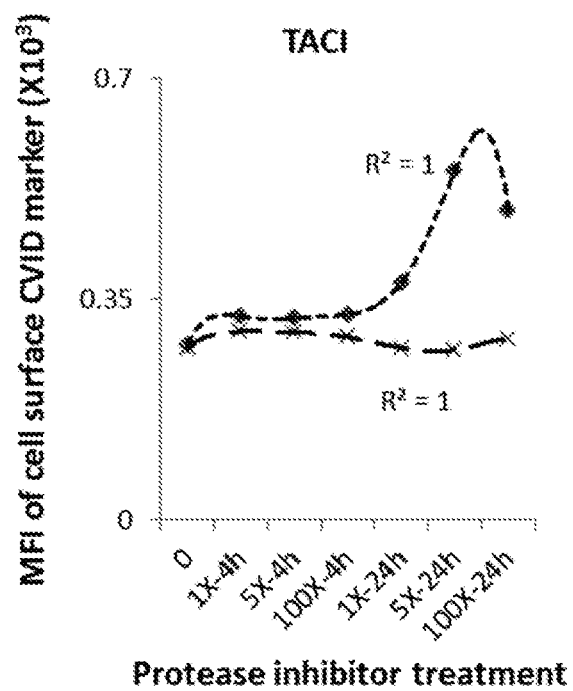


FIG. 37C)

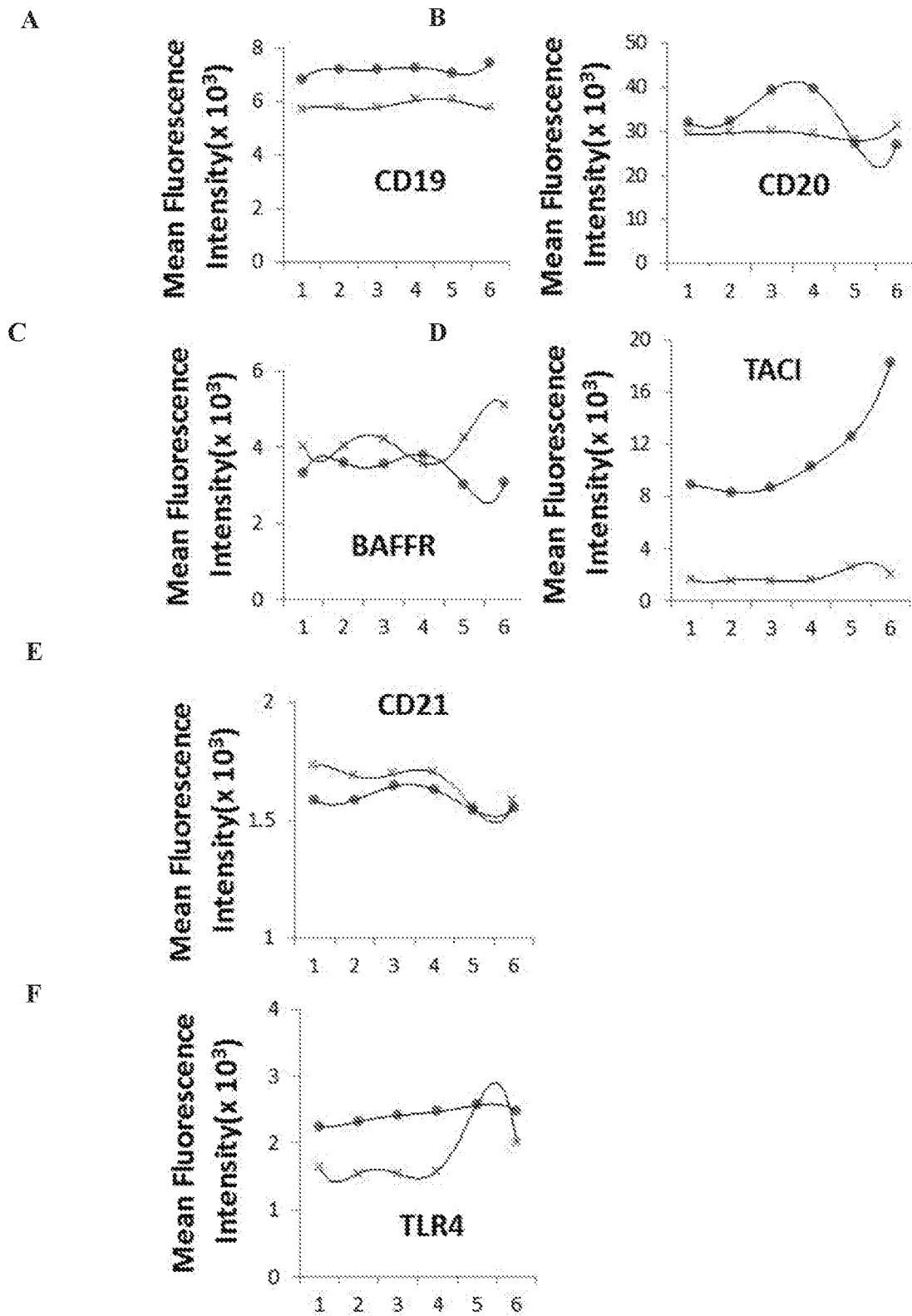


FIG. 38A-F

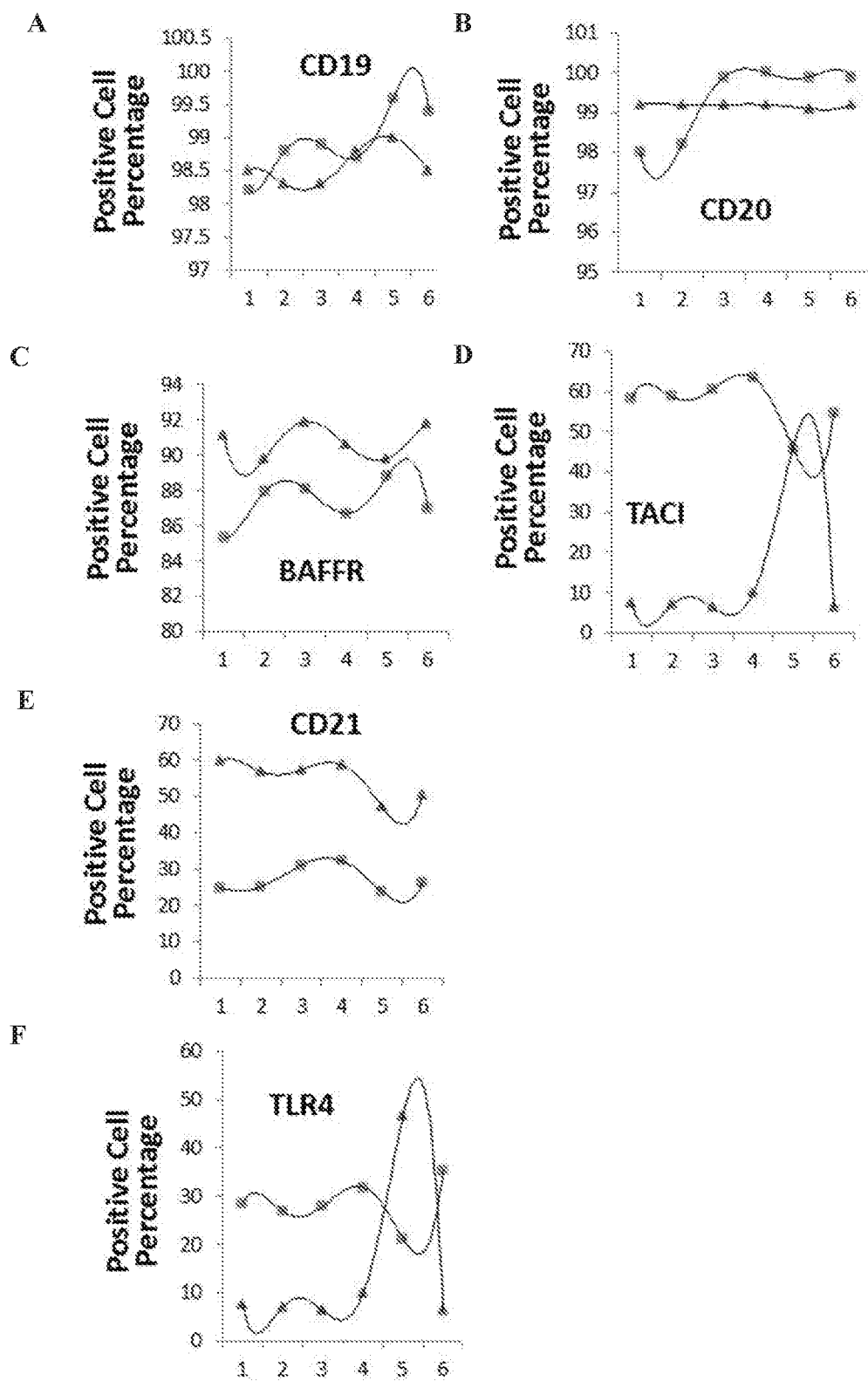


FIG. 39A-F

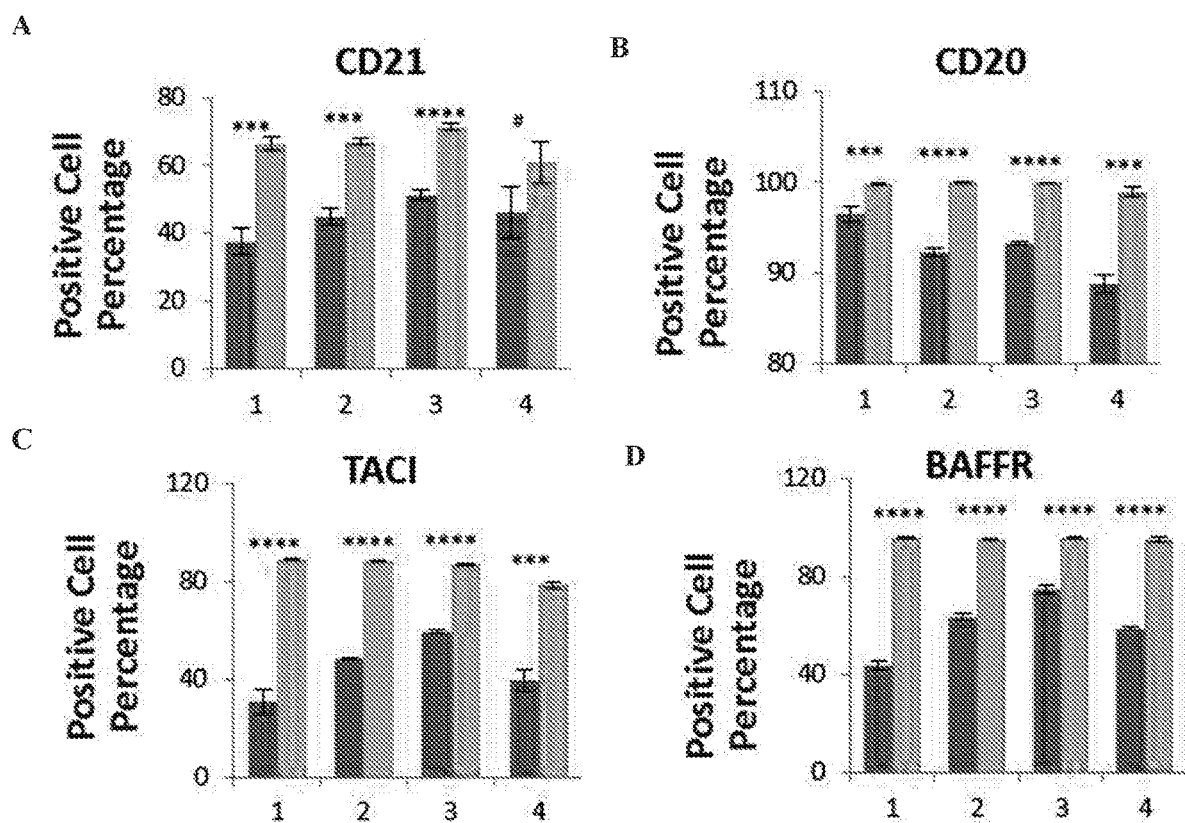


FIG. 40A-D

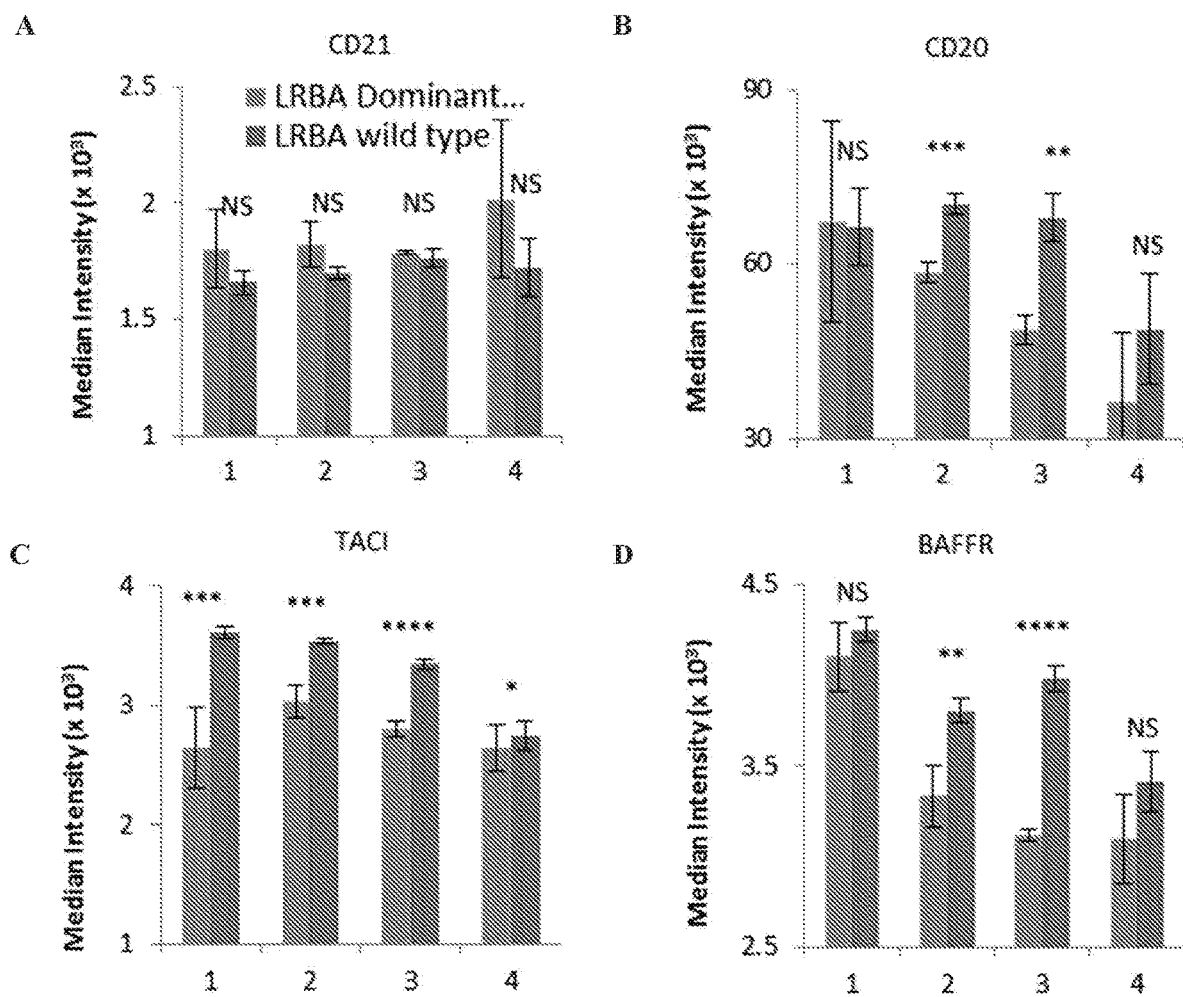


FIG. 41A-D

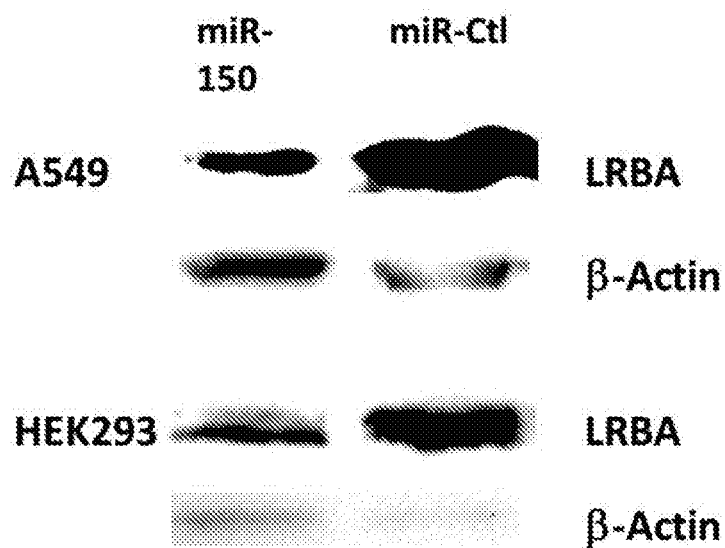


FIG. 42A

```
TTTTGGTTGACATGTTGGGAGT Human LRBA
  |||| | |||||
GTGACCATGTTCCCAACCCTCT miR-150
  || | |||||
ATCTCGTTGACATGTTGGGAGT Mouse Lrba
```

FIG. 42B

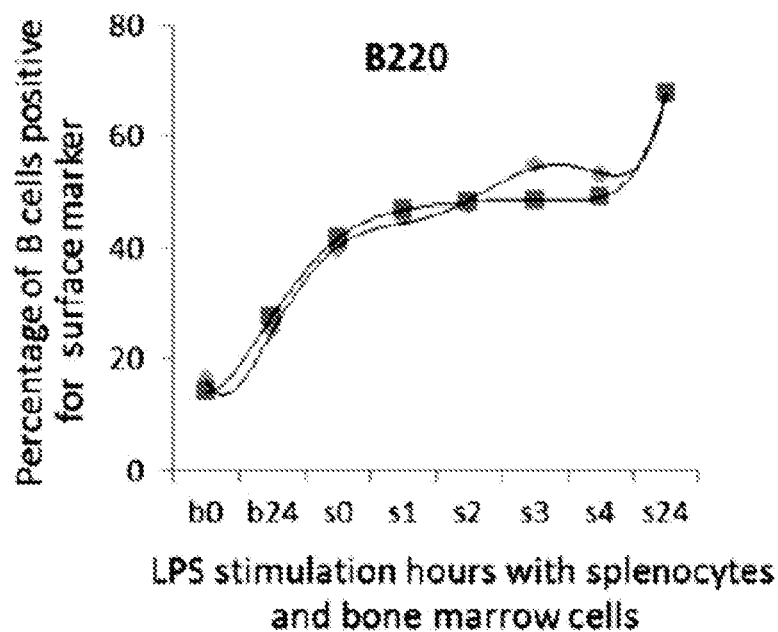


FIG. 43A

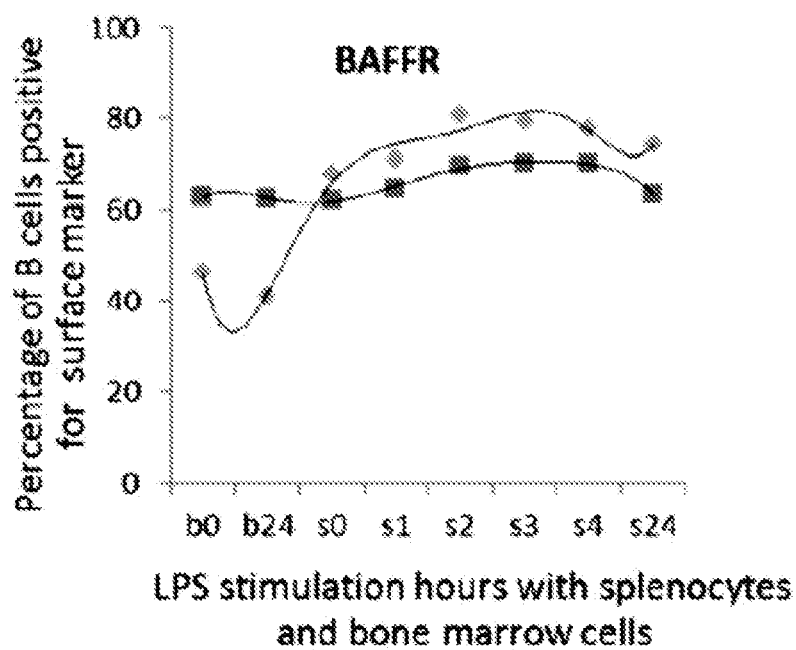


FIG. 43B

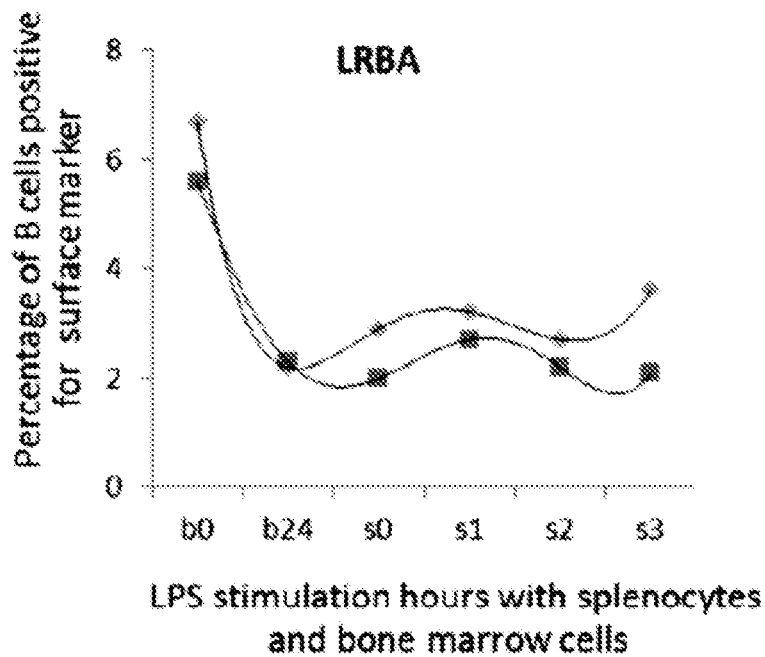


FIG. 43C

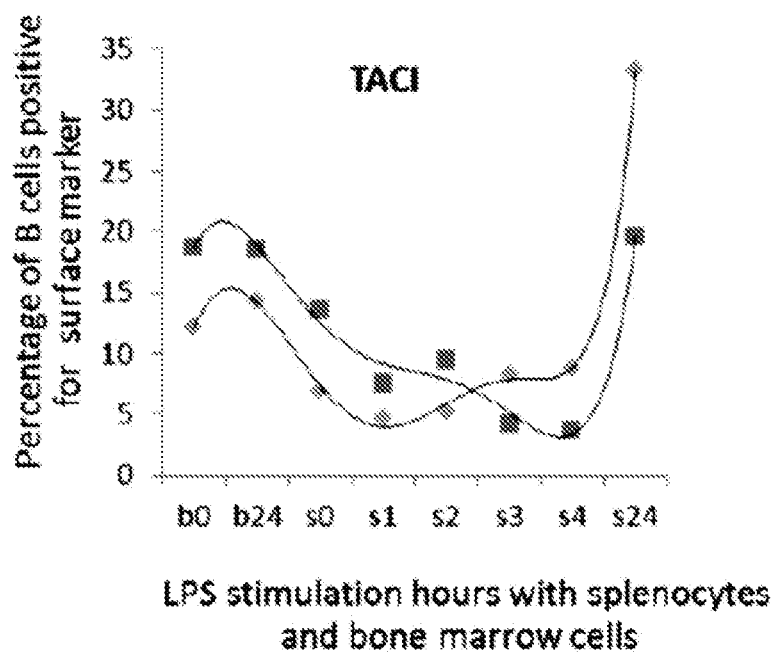


FIG. 43D



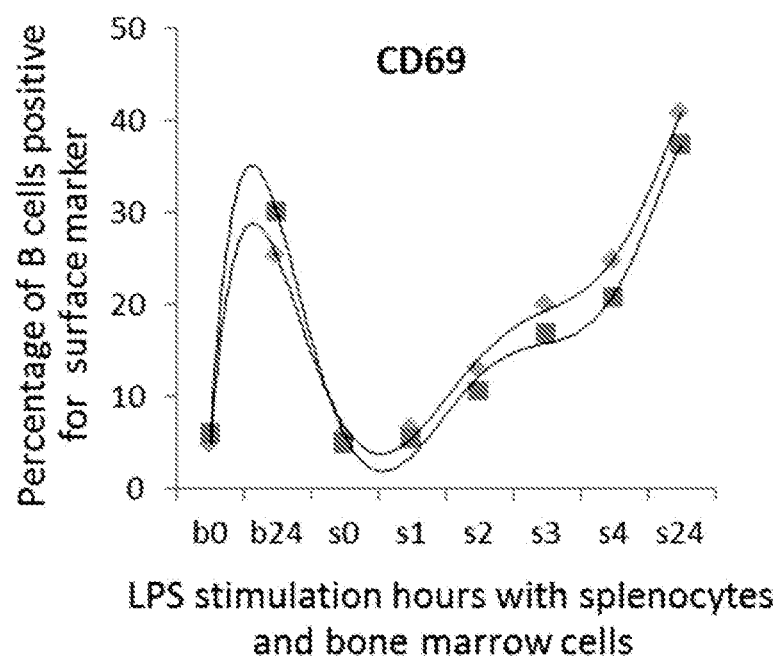


FIG. 44A

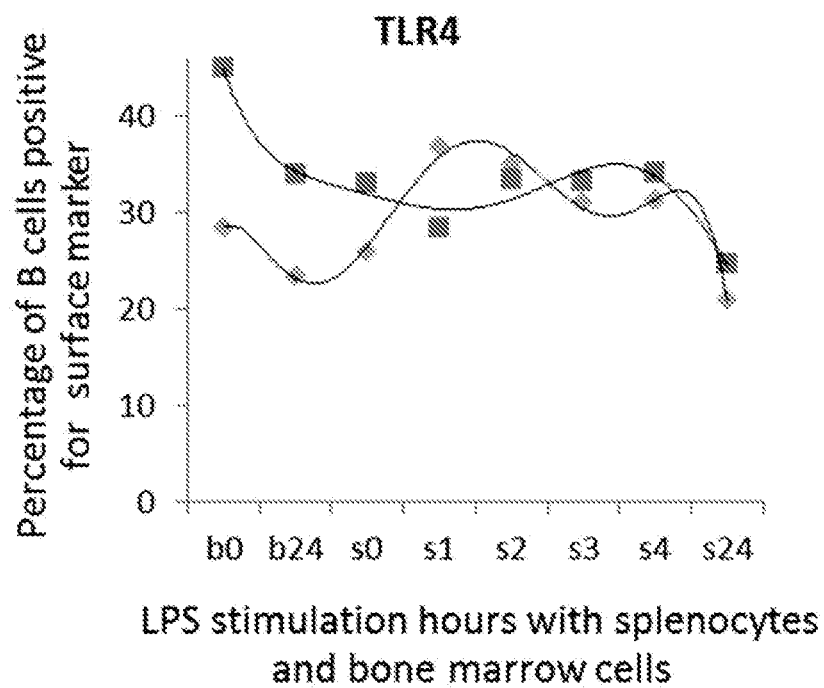


FIG. 44B)

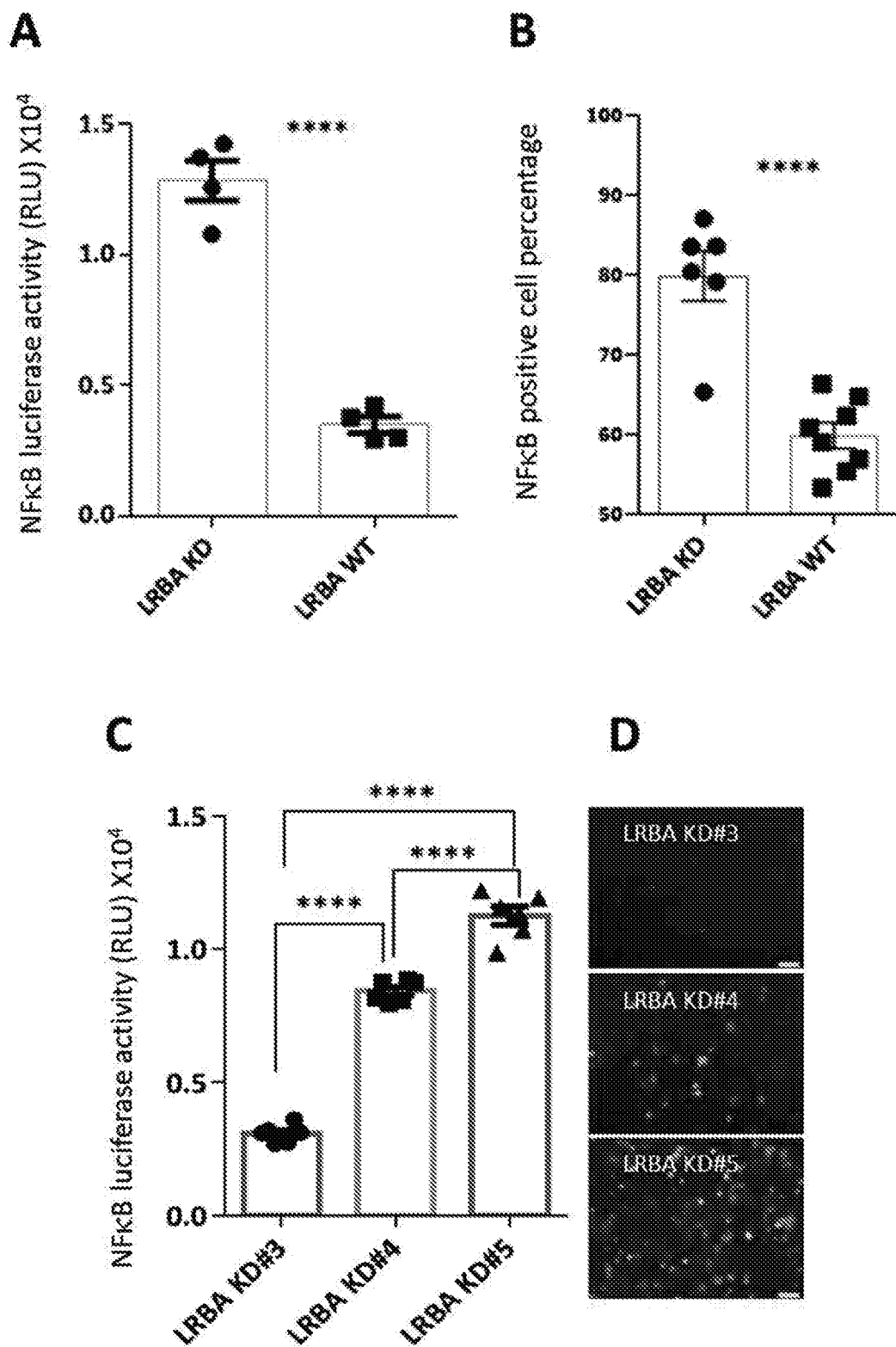
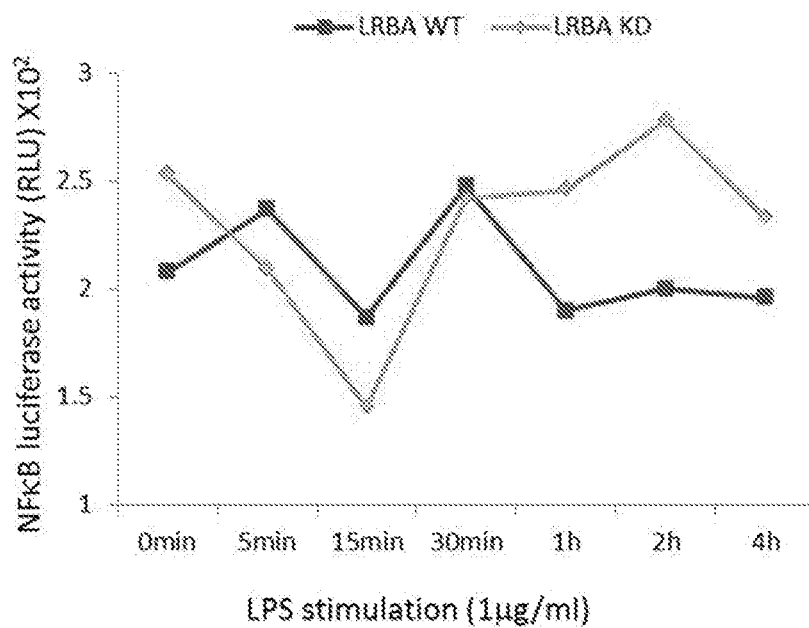


FIG. 45A-D

A



B

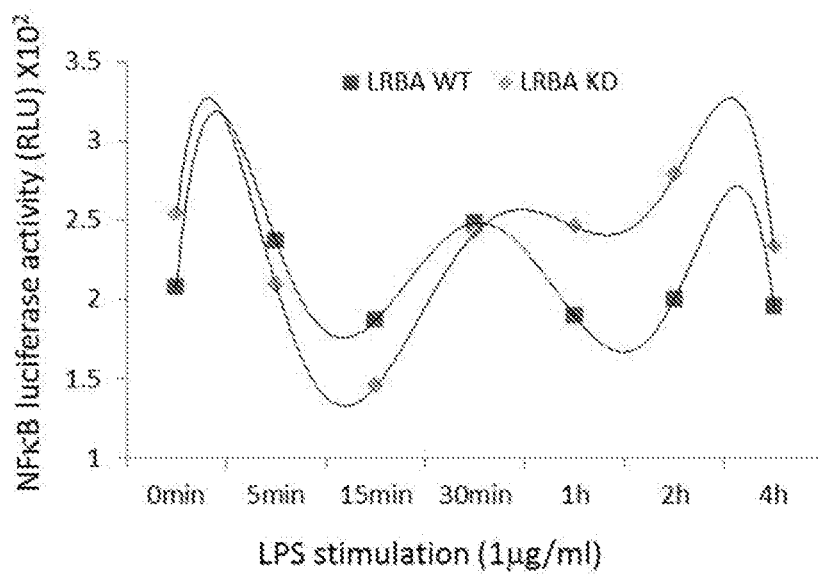


FIG. 46A-B

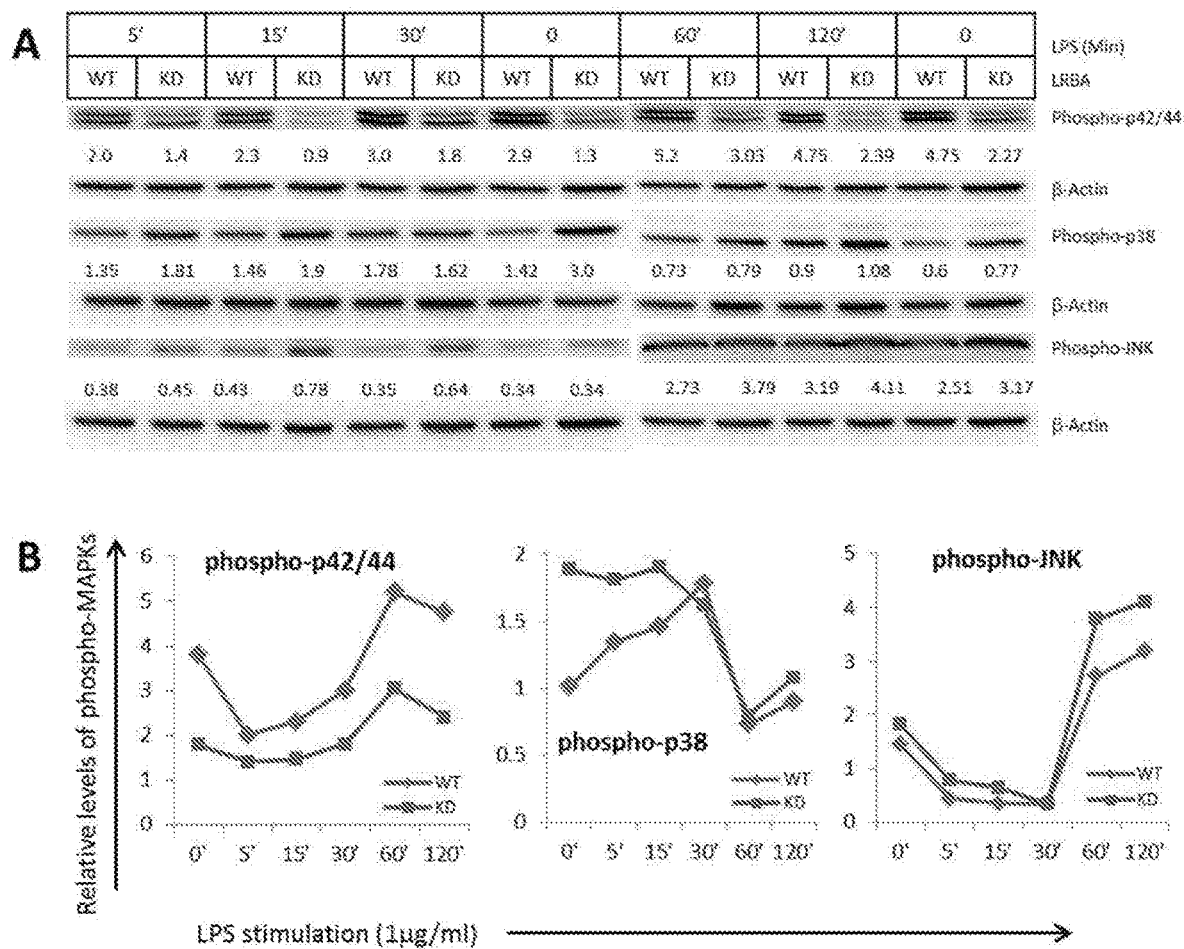


FIG. 47A-B

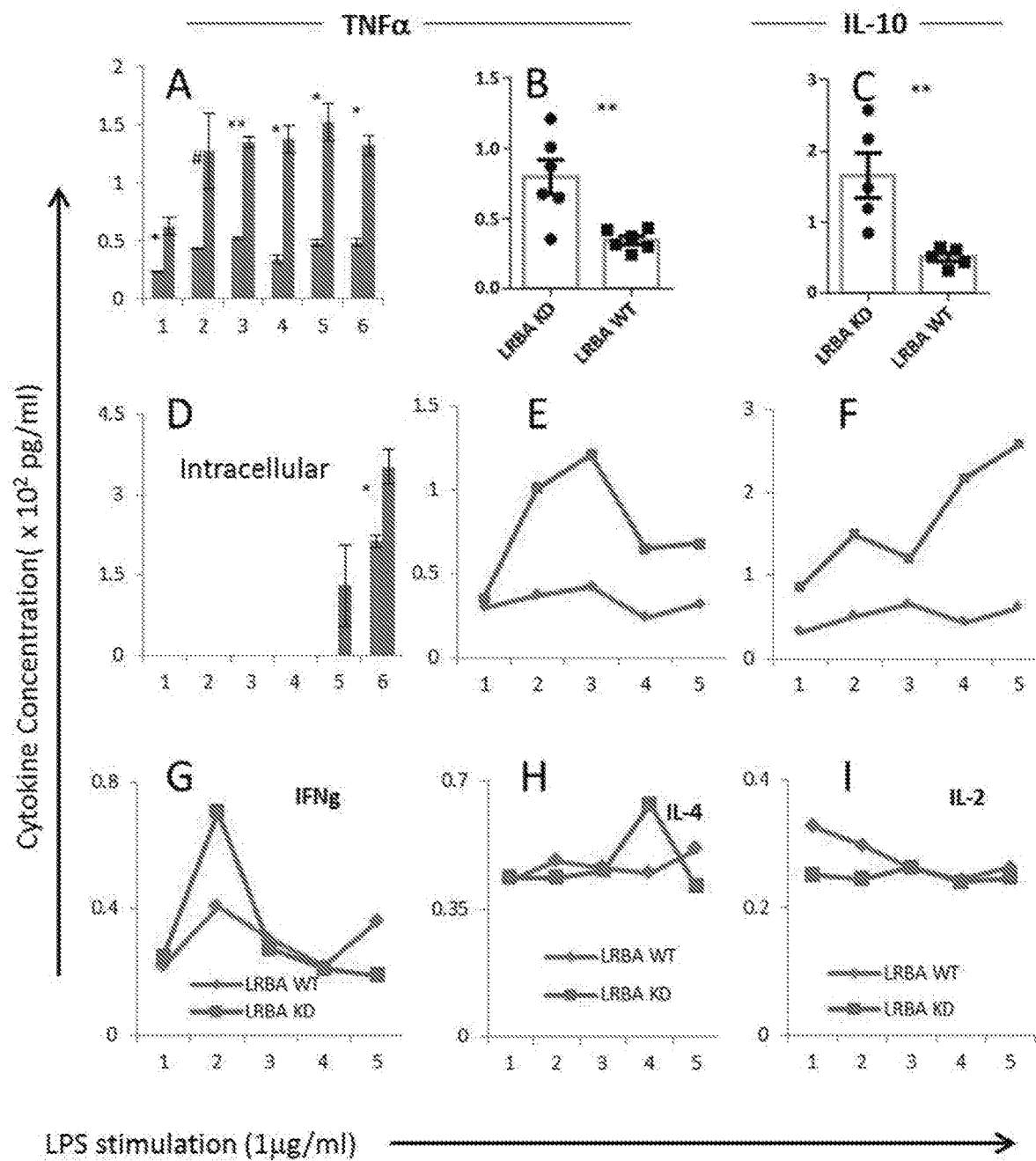


FIG. 48A-I

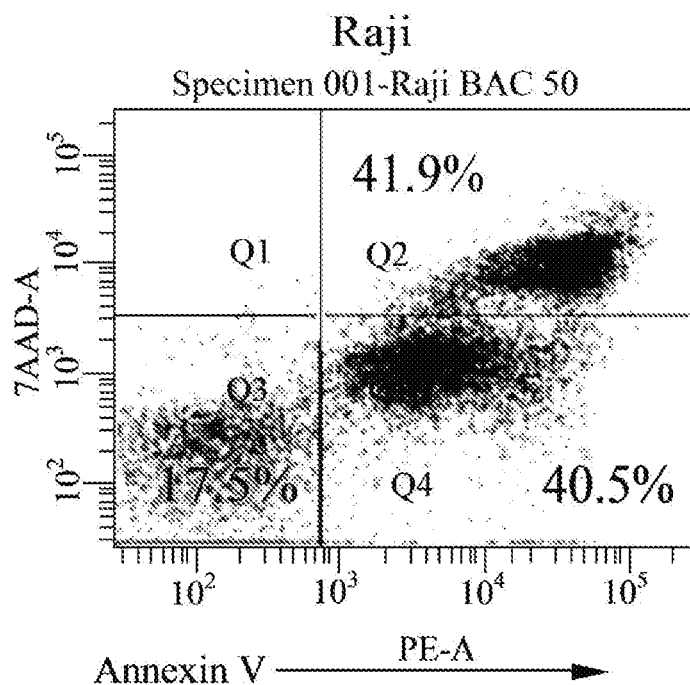


FIG. 49A

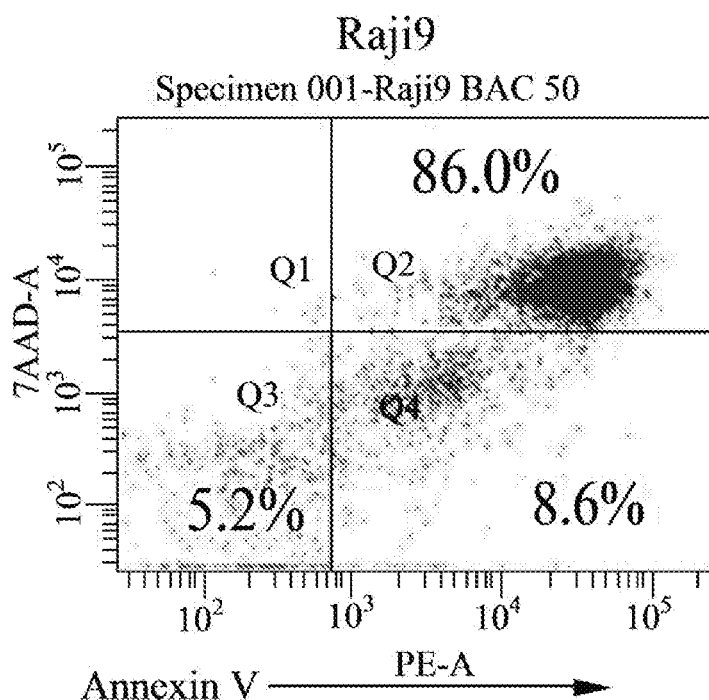


FIG. 49B

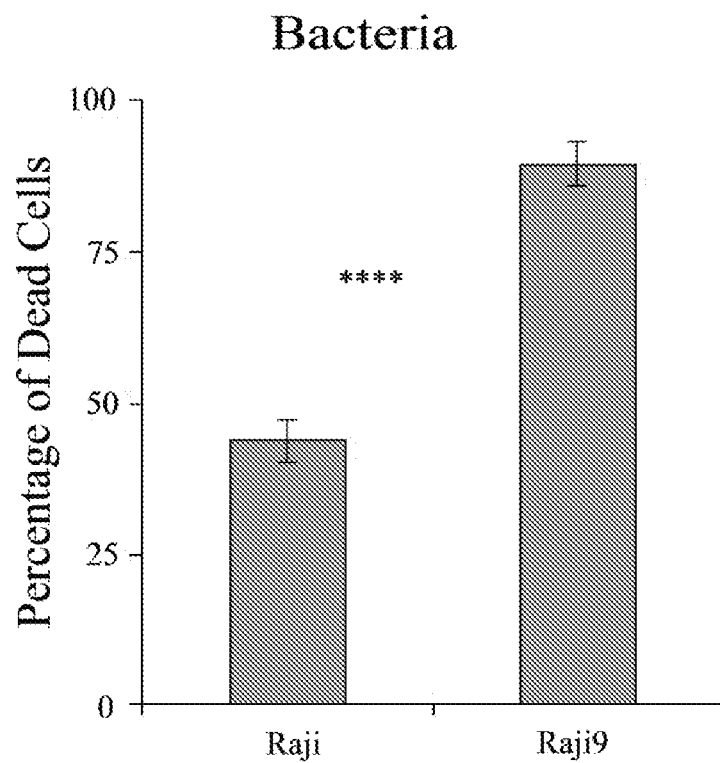


FIG. 49C

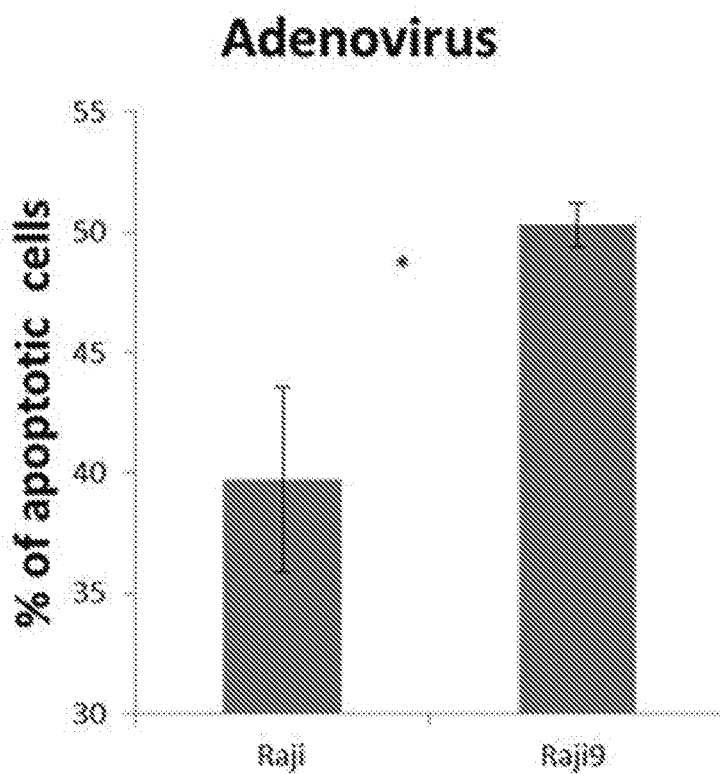


FIG. 49D

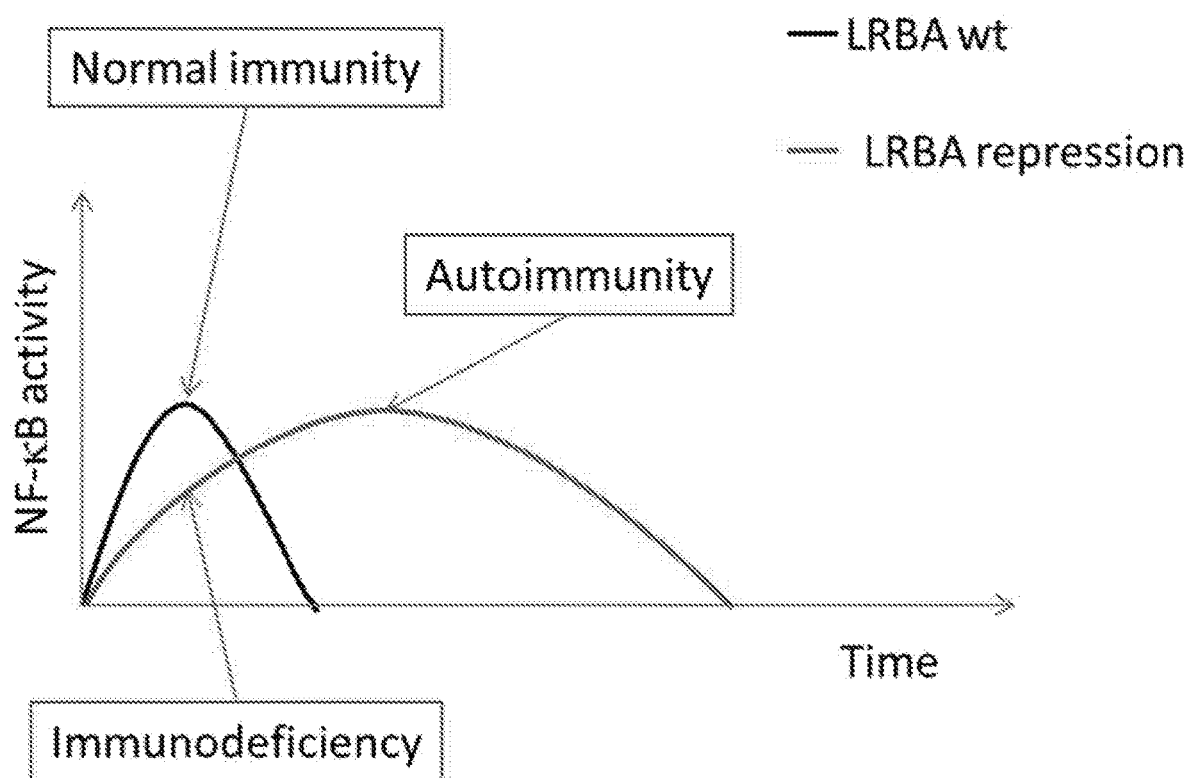


FIG. 50



1

# INFLAMMATORY DISEASE DIAGNOSIS AND METHODS OF TREATMENT USING DOWN-REGULATORS OF LIPOPOLYSACCHARIDE-RESPONSIVE BEIGE-LIKE ANCHOR

## CROSS REFERENCE TO RELATED APPLICATIONS

This application is a divisional, and claims priority to, U.S. Nonprovisional patent application Ser. No. 14/223,490, entitled, "Inflammatory Disease Diagnosis and Methods of Treatment using Lipopolysaccharide-Responsive Beige-Like Anchor", filed Mar. 24, 2014, which claims priority to U.S. Provisional Patent Application 61/804,451, entitled, "Inflammatory Disease Diagnosis and Methods of Treatment using Lipopolysaccharide-Responsive Beige-Like Anchor", filed Mar. 22, 2013, the contents of which are herein incorporated by reference.

## FIELD OF INVENTION

This invention relates to inflammation as part of chronic diseases. Specifically, the invention addresses treating inflammatory diseases through modulation of lipopolysaccharide-responsive beige-like anchor (LRBA).

## BACKGROUND OF THE INVENTION

Lipopolysaccharide (LPS)-responsive beige-like anchor (LRBA) was initially identified as an LPS-upregulated gene, encoding a 2863-amino acid, multiple-protein, as seen in FIG. 1 (Kerr, W. G., Heller, M. & Herzenberg, L. A. Analysis of lipopolysaccharide-response genes in B-lineage cells demonstrates that they can have differentiation stage-restricted expression and contain SH2 domains. *Proc Natl Acad Sci USA* 93, 3947-52 (1996); Wang, J. W., Howson, J., Haller, E. & Kerr, W. G. Identification of a novel lipopolysaccharide-inducible gene with key features of both A kinase anchor proteins and chs1/beige proteins. *J Immunol* 166, 4586-95 (2001)). Human LRBA and murine Lrba proteins are 90% identical (2587/2859) with 94% positive (2690/2859) amino acid homology. Three murine Lrba isoforms with differences at the C-terminal were identified (Wang, et al. Identification of a novel lipopolysaccharide-inducible gene with key features of both A kinase anchor proteins and chs1/beige proteins. 2001. *J Immunol* 166, 4586-95), while the human LRBA has two major isoforms (Wang, et al., Identification of a novel lipopolysaccharide-inducible gene with key features of both A kinase anchor proteins and chs1/beige proteins. 2001. *J Immunol* 166, 4586-95; Lopez-Herrera, et al., Deleterious Mutations in LRBA Are Associated with a Syndrome of Immune Deficiency and Autoimmunity. 2012. *Am J Hum Genet* 90, 986-1001).

LRBA is mainly localized to Golgi complex (GC), but also found in cell membrane, endosomes and vesicles. This is similar to neurobeachin (Nbea) (Wang, J. W. et al. Deregulated expression of LRBA facilitates cancer cell growth. *Oncogene* 23, 4089-97 (2004); Wang, X. et al. Neurobeachin: A protein kinase A-anchoring, beige/Chediak-higashi protein homolog implicated in neuronal membrane traffic. 2000. *J Neurosci* 20, 8551-65), an autism candidate gene and isoform of LRBA, has very similar localizations to that of LRBA and is implicated in post-Golgi membrane traffic and regulatory secretion pathway of large dense-core vesicles containing growth factors and hormones (Volders, et al., *Drosophila rugose* is a functional homolog

2

of mammalian Neurobeachin and affects synaptic architecture, brain morphology, and associative learning. 2012. *J Neurosci* 32, 15193-204; Castermans, et al., SCAMPS, NBEA and AMISYN: three candidate genes for autism involved in secretion of large dense-core vesicles. 2010. *Hum Mol Genet* 19, 1368-78), isoform, Neurobeachin (Wang, et al., Deregulated expression of LRBA facilitates cancer cell growth. 2004. *Oncogene* 23, 4089-97; Wang, et al., Neurobeachin: A protein kinase A-anchoring, beige/Chediak-higashi protein homolog implicated in neuronal membrane traffic. 2000. *J Neurosci* 20, 8551-65).

The exact function of LRBA is unknown. LRBA has structural similarity to lysosomal trafficking regulator (LYST) and potentially is an A-kinase anchoring protein (AKAP)(1). It belongs to the WDL-BEACH-WD40 (WBW) gene family containing the WBW super domain. The WBW proteins appear to function as scaffolding proteins in vesicle trafficking (Wang, et al., Identification of a novel lipopolysaccharide-inducible gene with key features of both A kinase anchor proteins and chs1/beige proteins. 2001. *J Immunol* 166, 4586-95; Lopez-Herrera, et al., Deleterious Mutations in LRBA Are Associated with a Syndrome of Immune Deficiency and Autoimmunity 2012. *Am J Hum Genet* 90, 986-1001; Wang, et al., Deregulated expression of LRBA facilitates cancer cell growth. 2004. *Oncogene* 23, 4089-97) and are important in human diseases (Cullinane, A. R., Schaffer, A. A. & Huizing, M. The BEACH Is Hot: A LYST of Emerging Roles for BEACH-Domain Containing Proteins in Human Disease. 2013. *Traffic* 14(7):749-66). There are nine WBW human family members, which all appear to function as scaffolding proteins in vesicle trafficking regulation, involved in lysosome size regulation; LRBA, lysosomal trafficking regulator (LYST), neutral sphingomyelinase activation associated factor (NSMAF), WD and FYVE zinc finger domain containing protein 3 (WDFY3), WDFY4, neurobeachin-like 1 (NBEAL1), neurobeachin-like 2 (NBEAL2), neurobeachin (NBEA), WD repeat domain 81 (WDR81). They appear to be involved in vesicle trafficking as scaffolding proteins and regulating lysosome size (LYST and NSMAF), apoptosis (NSMAF, LRBA), autophagy (LYST, WD and WDFY3, LRBA), granule size (LYST, NBEAL2, and NBEA), or synapse formation (NBEA).

These family members are important in human diseases. For example, mutations of four WBW genes (LYST, LRBA, NBEAL2 and WDFY4) cause recessive Mendelian diseases and NBEA is a current candidate for autism (Cullinane, A. R., Schaffer, A. A. & Huizing, M. The BEACH Is Hot: A LYST of Emerging Roles for BEACH-Domain Containing Proteins in Human Disease. 2013. *Traffic*; 14(7):749-66)). The WD and FYVE zinc finger domain containing protein 4 (WDFY4) is strongly associated with SLE in Asian populations. NSMAF is a TNF adaptor protein which is required for the TNF-induced expression of cytokines, such as IL-6 and CXCL-2 (Adam-Klages, et al., FAN, a novel WD-repeat protein, couples the p55 TNF-receptor to neutral sphingomyelinase. 1996. *Cell* 86, 937-47; Montfort, et al., FAN stimulates TNF(alpha)-induced gene expression, leukocyte recruitment, and humoral response. 2009. *J Immunol* 183, 5369-78).

Accordingly, LRBA is extensively associated with the endomembrane system and vesicle trafficking. Vesicle trafficking is essential for deposition and signal transduction of membrane proteins and protein secretions, which also controls proper functioning of the immune system.

NBEA, which has 75% of protein homology with LRBA, is an isoform of LRBA linked to autism, platelet development, obesity, and multiple myeloma in humans (O'Neal, et

al., Neurobeachin (NBEA) is a target of recurrent interstitial deletions at 13q13 in patients with MGUS and multiple myeloma. 2009. *Exp Hematol* 37, 234-44) and body length, synaptic spine patterns of neurons, and obesity in mice (Cullinane, et al., The BEACH Is Hot: A LYST of Emerging Roles for BEACH-Domain Containing Proteins in Human Disease. 2013. *Traffic*; 14(7):749-66). It has very similar subcellular localizations to that of LRBA and is implicated in post-Golgi membrane traffic and the regulatory secretion pathway of large dense-core vesicles containing growth factors and hormones (Wang, J. W. et al. Deregu-  
lated expression of LRBA facilitates cancer cell growth. 2004. *Oncogene* 23, 4089-97; Volders, et al., *Drosophila rugose* is a functional homolog of mammalian Neurobeachin and affects synaptic architecture, brain morphology, and asso-  
ciative learning. 2012. *J Neurosci* 32, 15193-204; Castermans, et al., SCAMPS, NBEA and AMISYN: three candi-  
date genes for autism involved in secretion of large dense-core vesicles. 2010. *Hum Mol Genet* 19, 1368-78; Wang, et al., Neurobeachin: A protein kinase A-anchoring, beige/  
Chediak-higashi protein homolog implicated in neuronal membrane traffic. 2000. *J Neurosci* 20, 8551-65). NBEA binds to an important signaling complex, protein kinase A, and acts as a negative regulator of vesicle secretion, as does LRBA ortholog Beige Protein Homolog 1 (Bph1) in yeast. NBEA homozygous knockout mice died perinatally due to the lack of synaptic transmissions (Su, et al., Neurobeachin is essential for neuromuscular synaptic transmission. 2004. *J Neurosci* 24, 3627-36; Medrihan, et al., Neurobeachin, a protein implicated in membrane protein traffic and autism, is required for the formation and functioning of central syn-  
apses. 2009. *Journal of Physiology-London* 587, 5095-5106), suggesting the protein is important in trafficking cargo proteins to pre- and post-synaptic compartments (Niesmann, K. et al. Dendritic spine formation and synaptic function require neurobeachin. 2011. *Nat Commun* 2:557).

LRBA orthologues Bph1 and rugose (rg) (*Drosophila*) are not essential and is both cytosolic and membrane peripherally bound. Deletion of Bph1 increases secretion of carboxypeptidase Y in *Saccharomyces cerevisiae* and misrouting of alkaline phosphatase. The vacuole morphology is not affected by disruption or overexpression of Bph1. The growth of the delta Bph1 strain is impaired by low pH, potassium acetate or calcofluor white, a fluorescent stain that binds strongly to the cell wall which contains cellulose and chitin, probably due to a defect on trafficking from the GC. Genetically, Bph1 interacts with VPS9, FLO1, FLO9, BTS1, OKP1, VPS9, BTS1 and OKP1. These data suggest that Bph1 is involved in protein sorting and cell wall formation (Shiflett, et al., Bph1p, the *Saccharomyces cerevisiae* homologue of CHS1/Beige, functions in cell wall formation and protein sorting. 2004. *Traffic* 5, 700-710). Mutations of rg in *Drosophila* are embryonic semi-lethal, exhibiting a reduced lifespan of the organism and severe rough eye phenotype, caused by cell type-specific apoptosis with increased Jun N-terminal kinase activity and decreased EGFR signaling activity (Wech & Nagel, Mutations in rugose promote cell type-specific apoptosis in the *Drosophila* eye. 2005. *Cell Death Differ* 12, 145-52). Genetically, rg interacts with 14 genes, including multiple components of EGFR, Notch, RAS and MAPK pathways (Schreiber, et al., Genetic screen for modifiers of the rough eye phenotype resulting from overexpression of the Notch antagonist hairless in *Drosophila*. 2002. *Genesis* 33, 141-52; Shamloula, et al., rugose (rg), a *Drosophila* A kinase Anchor Protein, Is Required for Retinal Pattern Formation and Interacts Genetically With Multiple Signaling Pathways. 2002. *Genetics* 161, 693-710).

Similarly, LRBA appears to interact with multiple important signal transduction pathways, including EGFR, Notch, PKA, Ras, E2F1, p53, MAPK, NF- $\kappa$ B, cytokines, immunoglobulins (IgG, IgA, IgE and IgM etc.), CVID receptors and TLRs (Wang, et al., Deregu-  
lated expression of LRBA facilitates cancer cell growth. 2004. *Oncogene* 23, 4089-97; de Souza, et al., SEL-2, the *C. elegans* neurobeachin/LRBA homolog, is a negative regulator of lin-12/Notch activity and affects endosomal traffic in polarized epithelial cells. 2007. *Development* 134, 691-702; Schreiber, et al., Genetic screen for modifiers of the rough eye phenotype resulting from overexpression of the Notch antagonist hairless in *Drosophila*. 2002. *Genesis* 33, 141-52; Shamloula, et al., rugose (rg), a *Drosophila* A kinase Anchor Protein, Is Required for Retinal Pattern Formation and Interacts Genetically With Multiple Signaling Pathways. 2002. *Genetics* 161, 693-710).

LRBA orthologue in *Dictyostelium* is essential for cytokinesis (Kwak, et al., LvsA, a protein related to the mouse beige protein, is required for cytokinesis in *Dictyostelium*. 1999. *Mol Biol Cell* 10, 4429-39). LRBA orthologue, sel-2, also called F10F2.1, in *Caenorhabditis elegans*, is a negative regulator of lin-12/Notch activity in the vulval precursor cells, which are polarized epithelial cells maintained through regulated activity of the basolateral LET-23/EGF receptor and apical LIN-12/Notch. Loss of sel-2 activity causes basolateral mislocalization and increased accumulation of LIN-12/Notch and basolateral LET-23/EGF, indicating that SEL-2 is involved in endosomal traffic and may be involved in the efficient delivery of cell surface proteins to the lysosome (de Souza, et al., SEL-2, the *C. elegans* neurobeachin/LRBA homolog, is a negative regulator of lin-12/Notch activity and affects endosomal traffic in polarized epithelial cells. 2007. *Development* 134, 691-702). Two RII binding motifs were predicted for sel-2, both human and murine LRBA, by aligning with the known B1 and B2 PKA RII tethering sites in rg2.

Mutations of LRBA cause common variable immunodeficiency and autoimmunity, resulting in LRBA's synonym name, common variable immune deficiency-8 (CVID8). Six germ lines of LRBA mutations reported to date cause common variable immunodeficiency (CVID) with autoimmunity, manifested as hypogammaglobulinemia, antibody deficiency, defective B-cell differentiation, recurrent bacterial infections, particularly respiratory infections, and variable autoimmune disorders including idiopathic thrombocytopenic purpura, autoimmune hemolytic anemia, and inflammatory bowel disease (Spickett, et al., Common variable immunodeficiency: how many diseases? 1997. *Immunol Today* 18, 325-8). Other CVID gene mutations include members of the B cell coreceptor complex (CD1919, CD2120 and CD8121), CD2022, transmembrane activator and calcium modulator and cyclophilin ligand interactor (TACI; Salzer, et al. Mutations in TNFRSF13B encoding TACI are associated with common variable immunodeficiency in humans. 2005. *Nat Genet* 37, 820-8) and B cell-activating factor receptor (BAFFR; Warnatz, K. et al. B-cell activating factor receptor deficiency is associated with an adult-onset antibody deficiency syndrome in humans 2009. *Proc Natl Acad Sci USA* 106, 13945-50), and inducible costimulator (ICOS; Grimbacher, et al. Homozygous loss of ICOS is associated with adult-onset common variable immunodeficiency. 2003. *Nat Immunol* 4, 261-8). The discoveries of CVID-causing mutations of these genes show that a monogenic defect may produce the whole spectrum of CVID, and that it is possible to unravel the genetic causes underlying most human diseases thought to be polygenic (Yong, et al., The role of costimulation in antibody defi-

ciencies: ICOS and common variable immunodeficiency. 2009. *Immunol Rev* 229, 101-13).

It is caused by defective B cell differentiation and impaired secretion of immunoglobulins (Saiki, et al., Three distinct stages of B-cell defects in common varied immunodeficiency. 1982. *Proc Natl Acad Sci USA* 79, 6008-12; Bryant, et al., Classification of patients with common variable immunodeficiency by B cell secretion of IgM and IgG in response to anti-IgM and interleukin-2. 1990. *Clin Immunol Immunopathol* 56, 239-48). CVID is a diagnosis of exclusion and is highly heterogeneous, genetically, immunologically and clinically (Gathmann, et al., The European internet-based patient and research database for primary immunodeficiencies: update 2011. 2012. *Clin Exp Immunol* 167, 479-91; Eibel, et al., Common variable immunodeficiency at the end of a prospering decade: towards novel gene defects and beyond. 2010. *Curr Opin Allergy Clin Immunol* 10, 526-33; Park, et al., Common variable immunodeficiency: a new look at an old disease. 2008. *Lancet* 372, 489-502). About two-third of CVID subjects have an autoimmune problem<sup>17</sup>, most commonly autoimmune hemolytic anemia (AHA), autoimmune thrombocytopenia, rheumatoid arthritis, and pernicious anemia (Cunningham-Rundles & Bodian, Common variable immunodeficiency: clinical and immunological features of 248 patients. 1999. *Clin Immunol* 92, 34-48). The etiology of about 80% of CVID remains unknown<sup>18</sup>, although over the past ten years, significant progress has been made in elucidating genetic mechanisms that result in a CVID phenotype.

Unlike the other seven CVID proteins, which are usually small (~27 kD) and localized on the cell membrane, LRBA is a 319 kD multiple-domain protein (Kerr, et al., Analysis of lipopolysaccharide-response genes in B-lineage cells demonstrates that they can have differentiation stage-restricted expression and contain SH2 domains. 1996. *Proc Natl Acad Sci USA* 93, 3947-52; Wang, et al., Identification of a novel lipopolysaccharide-inducible gene with key features of both A kinase anchor proteins and chs1/beige proteins. 2001. *J Immunol* 166, 4586-95) and A kinase anchor protein (AKAP), which could serve as a scaffold to interact with multiple proteins. Additionally, most CVID genes are B cell membrane receptors, except for ICOS which is on T cells, while LRBA is ubiquitously expressed as a vesicle trafficking regulator, required for homeostasis and activation of plasma membrane receptors (Wang, et al., Identification of a novel lipopolysaccharide-inducible gene with key features of both A kinase anchor proteins and chs1/beige proteins. 2001. *J Immunol* 166, 4586-95; Cullinane, et al., The BEACH Is Hot: A LYST of Emerging Roles for BEACH-Domain Containing Proteins in Human Disease. 2013. *Traffic*; 14(7):749-66). Thus, LRBA may regulate other CVID genes, for example, CD19, CD20 and BAFFR, because their levels are low when LRBA is absent

(Lopez-Herrera, et al., Deleterious Mutations in LRBA Are Associated with a Syndrome of Immune Deficiency and Autoimmunity. 2012. *Am J Hum Genet* 90, 986-1001). Further, LRBA deficiency causes both immunodeficiency and autoimmunity (Lopez-Herrera, et al., Deleterious Mutations in LRBA Are Associated with a Syndrome of Immune Deficiency and Autoimmunity 2012. *Am J Hum Genet* 90, 986-1001; Burns, et al., LRBA gene deletion in a patient presenting with autoimmunity without hypogammaglobulinemia. 2012. *J Allergy Clin Immunol* 130, 1428-32; Parvaneh, et al., Primary immunodeficiencies: a rapidly evolving story. 2013. *J Allergy Clin Immunol* 131, 314-23). All 11 LRBA deficient CVID subjects identified thus far have autoimmune diseases, as seen in Table 1. TACI mutations also are associated with autoimmunity but to a lesser degree (36% vs. 23% of patients with wild-type TACI) (Salzer, et al., Relevance of biallelic versus monoallelic TNFRSF13B mutations in distinguishing disease-causing from risk-increasing TNFRSF13B variants in antibody deficiency syndromes. 2009. *Blood* 113, 1967-76). LRBA is the only CVID protein that is a protein kinase A anchor and thus can function as protein kinase A (PKA) to regulate protein activity by phosphorylation. In addition to these above unique features, LRBA also is unique in regulating autophagy, apoptosis, membrane dynamics and receptor signaling, all of which are important for inflammation (Kerr, et al., Analysis of lipopolysaccharide-response genes in B-lineage cells demonstrates that they can have differentiation stage-restricted expression and contain SH2 domains. 1996. *Proc Natl Acad Sci USA* 93, 3947-52; Wang, et al., Identification of a novel lipopolysaccharide-inducible gene with key features of both A kinase anchor proteins and chs1/beige proteins. 2001. *J Immunol* 166, 4586-95). The average age of symptom onset is three years, earlier than the mean age of 26.3 years for most CVID. In addition to immunological disorders, LRBA-deficient patients have an array of other medical problems which include: retarded growth, failure to thrive, growth hormone deficiency, asthma, monoarthritis, seizure disorders, granulomatous infiltration, finger clubbing, hepatosplenomegaly, allergic dermatitis, and nephrotic syndrome (Lopez-Herrera, et al., Deleterious Mutations in LRBA Are Associated with a Syndrome of Immune Deficiency and Autoimmunity 2012. *Am J Hum Genet* 90, 986-1001; Burns, et al., LRBA gene deletion in a patient presenting with autoimmunity without hypogammaglobulinemia. 2012. *J Allergy Clin Immunol* 130, 1428-32; Alangari, et al., LPS-responsive beige-like anchor (LRBA) gene mutation in a family with inflammatory bowel disease and combined immunodeficiency. 2012. *J Allergy Clin Immunol* 130, 481-8 e2; Cunningham-Rundles & Bodian, Common variable immunodeficiency: clinical and immunological features of 248 patients. 1999. *Clin Immunol* 92, 34-48).

TABLE 1

Clinical features of LRBA-deficient patients	
Clinical conditions	Manifestations
Patient 1-5 from the study <sup>1</sup>	
Patient 1	
Autoimmune	Idiopathic thrombocytopenic purpura (ITP).
Treatment	Intravenous immunoglobulin (IVIG) replacement
Immunologic investigations	low immunoglobulin levels

TABLE 1-continued

Clinical features of LRBA-deficient patients	
Clinical conditions	Manifestations
Non-immunological disorders	Severely retarded growth, significant clubbing, strabismus as a result of abducens nerve palsy along with hemiplegia, cerebral mass.
Recurrent infections	Lymphoid interstitial pneumonia (LIP). Pleuropneumonia, chronic lung disease, bilateral bronchiectasis.
Patient 2	
Autoimmune	Self-limiting ITP; Asthma satisfactorily treated with inhaled steroids. Reactive monoarthritis responded well to local steroid injections.
Immunologic investigations	Low immunoglobulin levels.
Non-immunological disorders	Growth retarded (both weight and height were below the fifth percentile since the age of 2).
Recurrent infections	Serous otitis media, massive pneumonia along with loculated empyema, chronic lung disease with bilateral bronchiectasis.
Patient 3	
Chronic diarrhea	Severe diarrhea with no detectable bacterial or parasitic infection.
Autoimmune	ITP, lymphadenopathy, autoimmune haemolytic anemia (AIHA), atrophic gastritis with autoantibodies against intrinsic factor, and a submaxillary abscess, granulomatous infiltration with T cells, plasma cells, and macrophages but showed low B cell numbers.
Immunologic investigations	A moderate IgG hypogammaglobulinemia and complete IgA deficiency but a normal neutrophil count; intermittently elevated IgM; swelling of hilar and mediastinal lymph nodes with a mixed lymphoid follicular hyperplasia with the absence of the follicular mantle zone.
Recurrent infections	Perineal molluscum contagiosum, recurrent warts, recurrent mild respiratory infections, severe recurrent pneumonias, including several interstitial pneumonias, a lymphoid interstitial pneumonia and bronchiectasis.
Treatment	The interstitial lung disease was treated with methylprednisolone. Attempts to taper steroids were frequently associated with relapses, and long-term treatment with infliximab was initiated and allowed the discontinuation of methylprednisolone. Infliximab had little improvement of the chronic diarrhea. IVIG replacement.
Patient 4	
Chronic diarrhea and autoimmune	ITP, AIHA and autoimmune enteropathy (which can be classified as Crohn disease)
Non-immunological disorders	Failure to thrive.
Immunologic investigations	Low immunoglobulin levels.
Treatment	IVIG replacement and antibiotic prophylaxis
Recurrent infections	Recurrent upper-respiratory-tract infections, several episodes of pneumonia recurrent respiratory and gastrointestinal infections, severe lower respiratory-tract infections along with finger clubbing, hepatosplenomegaly an obstruction of the small airways and bronchiectasis, recurrent conjunctivitis and urticaria and a cor pulmonale with consecutive right-heart failure.
Treatment	Antibacterials, antifungals, and IVIG.
Patient 5	
Chronic diarrhea and autoimmune	Recurrent chronic diarrhea, autoimmune phenomena, hypothyroidism, and or AIHA allergic dermatitis, intestinal inflammation and subtotal villous atrophy, autoimmune phenomena, hypothyroidism, and myasthenia gravis. no signs of ITP or AIHA, bronchiectasis; Died at the age of 19 after respiratory failure
Non-immunological disorders	Retarded growth
Immunologic investigations	Selective IgA and IgG2 deficiency, IgG and IgM levels declined gradually.
Recurrent infections	Recurrent upper-respiratory-tract infections, including sinusitis and otitis media, pneumonia.
Patient 6-10 from the study <sup>2</sup>	
Patient 6	
Immunologic investigations	Normal serum IgG, IgA, IgM, and IgE levels and normal numbers of CD3+ T lymphocytes, CD4 <sup>+</sup> and CD8 <sup>+</sup> T-cell subsets, B cells, and natural killer (NK) cells. Normal T-cell proliferation to the mitogens PHA and ConA and a normal increase in antibody titers

TABLE 1-continued

Clinical features of LRBA-deficient patients	
Clinical conditions	Manifestations
Recurrent infections	after vaccination with tetanus toxoid, diphtheria, toxoid and <i>Haemophilus influenzae</i> capsular antigens.
Treatment	no history of recurrent infections Responded to intravenous immunoglobulin (IVIG) replacement therapy and a short course of prednisone.
Patient 7	
Chronic diarrhea and autoimmune	Nephrotic syndrome; mucous non-bloody stools; lymphocytic infiltration of the lamina propria; villous atrophy and marked inflammation.
Treatment	Prednisone and azathioprine with poor compliance; monthly intramuscular vitamin B12 injections; human growth hormone replacement.
Immunologic investigations	Normal serum IgG, IgA, IgM, and IgE levels and normal numbers of CD3 <sup>+</sup> T lymphocytes, CD4 <sup>+</sup> and CD8 <sup>+</sup> T-cell subsets, B lymphocytes, and NK cells, normal T-cell proliferation to the mitogens PHA and ConA and a normal increase in antibody titers after vaccination with pneumococcal vaccine.
Non-immunological disorders	Clubbing; growth hormone deficiency.
Recurrent infections	No history of recurrent infections.
Anemia	Megaloblastic anemia.
Patient 8	
Chronic diarrhea and autoimmune	Non-mucous and non-bloody chronic diarrhea; mucosal inflammation with lymphocytic infiltration but no granulomas or ulcerations; recurrent arthritis in the large joints, mainly the knees with inflammation.
Treatment	Chronic diarrhea improved on oral prednisone.
Immunologic investigations	Low serum IgG and IgA levels and decreased B-cell numbers but normal numbers of T cells, T-cell subsets, and NK cells; markedly reduced T-cell proliferation in response to PHA and anti-CD3 mAb.
Recurrent infections	Recurrent otitis media and pneumonia; bilateral bronchiectasis and finger clubbing.
Patient 9	
Chronic diarrhea and autoimmune	Chronic non-bloody and non-mucous diarrhea; duodenal villous atrophy; autoimmune thrombocytopenia and autoimmune hemolytic anemia both of which responded to treatment with steroids and rituximab.
Immunologic investigations	Low serum IgG and IgA levels and decreased B-cell numbers but normal numbers of T cells, T-cell subsets, and NK cells; markedly reduced T-cell proliferation in response to PHA and anti-CD3 mAb.
Recurrent infections	no history of recurrent infections
Patient 10	
Chronic diarrhea	Chronic diarrhea with no blood or mucus.
Immunologic investigations	Low serum IgG and IgA levels and normal numbers of T cells, T-cell subsets, B cells, and NK cells; markedly reduced T-cell proliferation in response to PHA and anti-CD3 mAb.
Recurrent infections	no history of recurrent infections or autoimmune hematologic manifestations.
Patient 11 the study 8	
Chronic diarrhea and autoimmune	Chronic diarrhea associated with an autoimmune enteropathy, duodenal villous atrophy and large bowel lymphocytic infiltration; erythema nodosum, transient arthritis of both feet, and recurrent hemolytic anemia; extensive lung infiltration of a mixture of CD3 <sup>+</sup> T and CD20 <sup>+</sup> B cells.
Immunologic investigations	Raised IgG levels, raised inflammatory markers, and a low number of natural killer cells; normal lymphocyte subsets, double-negative T cells, T-cell proliferation assays, IgA, IgM, tetanus vaccine responses, and a nitroblue tetrazolium test; lymphadenopathy, splenomegaly, neutropenia, and thrombocytopenia, antineutrophil antibodies; normal CD 19 <sup>+</sup> B cells and IgG level, a new-onset antibody deficiency with absent vaccine responses.
Treatment	Several courses of steroids, rituximab (with prophylactic immunoglobulin replacement), and mycophenolate mofetil.
Non-immunological disorders	Growth failure.
Recurrent infections	No significant history of infections except for a psoas abscess associated with chronic neutropenia; five years after initial

TABLE 1-continued

Clinical features of LRBA-deficient patients	
Clinical conditions	Manifestations
	presentation, after multiple courses of rituximab, developed recurrent infections, after withdrawal of immunoglobulin therapy.

<sup>1</sup>Lopez-Herrera, et al., Deleterious Mutations in LRBA Are Associated with a Syndrome of Immune Deficiency and Autoimmunity. 2012. *Am J Hum Genet* 90, 986-1001.

<sup>2</sup>Alangari, et al., LPS-responsive beige-like anchor (LRBA) gene mutation in a family with inflammatory bowel disease and combined immunodeficiency. 2012. *J Allergy Clin Immunol* 130, 481-8 e2.

As LRBA is structurally conserved throughout the eukaryotic kingdom, it may be involved in pathways similar to its orthologues and paralogues. Mutations in lysosomal trafficking regulator (LYST), which is a paralogue gene of LRBA, causes Chediak-Higashi syndrome (CHS), and A-kinase anchoring proteins (Kerr, et al., Analysis of lipopolysaccharide-response genes in B-lineage cells demonstrates that they can have differentiation stage-restricted expression and contain SH2 domains. 1996. *Proc Natl Acad Sci USA* 93, 3947-52; Wang, et al., Identification of a novel lipopolysaccharide-inducible gene with key features of both A kinase anchor proteins and chs1/beige proteins. 2001. *J Immunol* 166, 4586-95). CHS is characterized by severe immunodeficiency and premature mortality (Faigle, et al., Deficient peptide loading and MHC class II endosomal sorting in a human genetic immunodeficiency disease: the Chediak-Higashi syndrome. 1998. *J Cell Biol* 141, 1121-34; Barrat, et al., Defective CTLA-4 cycling pathway in Chediak-Higashi syndrome: a possible mechanism for deregulation of T lymphocyte activation. 1999. *Proc Natl Acad Sci USA* 96, 8645-50). LRBA and LYST may have similar functions, as they have high similarity of protein structure. Three independent papers show that absence of LRBA, resulting from homozygous mutations or deletions, causes autosomal recessive diseases of severe immunodeficiency (defective B-cell differentiation, hypogammaglobulinemia, recurrent infections), autoimmunity (idiopathic thrombocytopenic purpura (ITP), autoimmune hemolytic anemia and inflammatory bowel disease) (Lopez-Herrera, et al., Deleterious mutations in LRBA are associated with a syndrome of immune deficiency and autoimmunity 2012. *Am J Hum Genet* 90, 986-1001; Burns, et al., LRBA gene deletion in a patient presenting with autoimmunity without hypogammaglobulinemia. 2012. *J Allergy Clin Immunol* 130, 1428-32; Alangari, et al., LPS-responsive beige-like anchor (LRBA) gene mutation in a family with inflammatory bowel disease and combined immunodeficiency. 2012. *J Allergy Clin Immunol* 130, 481-8 e2), and inflammatory cell infiltration (Lopez-Herrera, et al., Deleterious mutations in LRBA are associated with a syndrome of immune deficiency and autoimmunity 2012. *Am J Hum Genet* 90, 986-1001; Burns, et al., LRBA gene deletion in a patient presenting with autoimmunity without hypogammaglobulinemia. 2012. *J Allergy Clin Immunol* 130, 1428-32; Alangari, et al., LPS-responsive beige-like anchor (LRBA) gene mutation in a family with inflammatory bowel disease and combined immunodeficiency. 2012. *J Allergy Clin Immunol* 130, 481-8 e2; Faigle, et al., Deficient peptide loading and MHC class II endosomal sorting in a human genetic immunodeficiency disease: the Chediak-Higashi syndrome. 1998. *J Cell Biol* 141, 1121-34; Barrat, et al., Defective CTLA-4 cycling pathway in Chediak-Higashi syndrome: a possible mechanism for deregulation of T lymphocyte activation. 1999. *Proc Natl Acad Sci USA* 96, 8645-50; Alangari, et al., LPS-responsive beige-like anchor (LRBA) gene mutation in

a family with inflammatory bowel disease and combined immunodeficiency. 2012. *J Allergy Clin Immunol* 130, 481-8 e2). Another analogue, rg interacts with 14 genes, including multiple components of EGFR, Notch, RAS and MAPK pathways (Shamloula, et al., rugose (rg), a *Drosophila* A kinase Anchor Protein, Is Required for Retinal Pattern Formation and Interacts Genetically With Multiple Signaling Pathways. 2002. *Genetics* 161, 693-710). LRBA interacts with the EGFR pathway (Wang, et al., Deregulated expression of LRBA facilitates cancer cell growth. 2004. *Oncogene* 23, 4089-97).

The GC is now viewed as headquarters for signal transduction and cell-fate decisions, in addition to its "classic role" of cargo sorting/processing and metabolism (Wilson, C. et al. The Golgi apparatus: an organelle with multiple complex functions. *Biochem J* 433, 1-9; Wilson, C. et al. The Golgi apparatus: an organelle with multiple complex functions. *Biochem J* 433, 1-9). For example, internalized LPS and Toll-like receptor-4 (TLR-4) are found in GC (Hornef, M. W., Frisan, T., Vandewalle, A., Normark, S. & Richter-Dahlfors, A. Toll-like receptor 4 resides in the Golgi apparatus and colocalizes with internalized lipopolysaccharide in intestinal epithelial cells. *J Exp Med* 195, 559-70 (2002)). Activation of the proto-oncogene Ras on the Golgi can lead to cell transformation (Bivona, T. G. et al. Phospholipase Cgamma activates Ras on the Golgi apparatus by means of RasGRP1. *Nature* 424, 694-8 (2003); Tracey, K. J. et al. Anti-cachectin/TNF monoclonal antibodies prevent septic shock during lethal bacteraemia. *Nature* 330, 662-4 (1987)). The proto-oncogenes Ras and Src are activated on the GC (Pulvirenti, et al., A traffic-activated Golgi-based signalling circuit coordinates the secretory pathway. *Nat Cell Biol* 10, 912-22 (2008); Bivona, T. G. et al. Phospholipase Cgamma activates Ras on the Golgi apparatus by means of RasGRP1. *Nature* 424, 694-8 (2003); Pulvirenti, et al., A traffic-activated Golgi-based signalling circuit coordinates the secretory pathway. *Nat Cell Biol* 10, 912-22 (2008)). Membrane trafficking is crucial in transducing signals to GC and other cellular locations (Kholodenko, Four-dimensional organization of protein kinase signaling cascades: the roles of diffusion, endocytosis and molecular motors. *J Exp Biol* 206, 2073-82 (2003)), as simple diffusion has a limited role in intracellular transport of signaling complexes (Kholodenko, Four-dimensional organization of protein kinase signaling cascades: the roles of diffusion, endocytosis and molecular motors. *J Exp Biol* 206, 2073-82 (2003)). Thus the endomembrane system has critical role in signal transduction, which is not yet appreciated enough. LRBA may be important in GC's function, as LRBA is extensively co-localized with GC proteins and an abnormally high number of GCs is found in LRBA deficient B cells (Lopez-Herrera, et al., Deleterious mutations in LRBA are associated with a syndrome of immune deficiency and autoimmunity. *Am J Hum Genet* 90, 986-1001 (2012)). It is extensively associated with the endomembrane system and

vesicle trafficking. Vesicle trafficking is essential for deposition, secretion and signal transduction of immune effectors.

Taken together, LRBA appears to be critical in vesicle trafficking involving deposition of membrane proteins, endocytosis of signal transduction complex and protein secretion, and thus a crucial regulator of these proteins including the other CVID proteins, TLRs and antibodies, involved in multiple pathways and cellular processes such as growth, apoptosis, autophagy, membrane dynamics, receptor signaling, and cell differentiation (Wang, et al., Identification of a novel lipopolysaccharide-inducible gene with key features of both A kinase anchor proteins and chs1/beige proteins. 2001. *J Immunol* 166, 4586-95). Deficiency of LRBA may cause vesicle trafficking defects and affect many membrane or secreted immune effectors, resulting in broader and severer problems, even death (Lopez-Herrera, et al., Deleterious mutations in LRBA are associated with a syndrome of immune deficiency and autoimmunity. 2012. *Am J Hum Genet* 90, 986-1001; Burns, et al., LRBA gene deletion in a patient presenting with autoimmunity without hypogammaglobulinemia. 2012. *J Allergy Clin Immunol* 130, 1428-32; Alangari, et al., LPS-responsive beige-like anchor (LRBA) gene mutation in a family with inflammatory bowel disease and combined immunodeficiency. 2012. *J Allergy Clin Immunol* 130, 481-8 e2).

A well characterized LRBA polyclonal antibody and organelle-specific antibodies were used in the present study to detect endogenous proteins and study their co-localizations. The results show that LRBA is extensively associated with the endomembrane system, including the Golgi complex, endosomes, lysosomes, plasma membranes, nucleus, pseudopodia and microtubules, and vesicle trafficking, which is responsive to TUB stimulation. These results suggest that LRBA plays a role in vesicle trafficking and signal transduction essential for the immune system (Burns, et al., LRBA gene deletion in a patient presenting with autoimmunity without hypogammaglobulinemia. 2012. *J Allergy Clin Immunol* 130, 1428-32).

It is proposed that LRBA functions as a converging node for multiple pathways through vesicle trafficking and plays a fundamental role in the immune system. This concept is supported by data showing LRBA may interact with multiple important signal transduction pathways (Shamloula, et al. rugose (rg), a *Drosophila* A kinase Anchor Protein, Is Required for Retinal Pattern Formation and Interacts Genetically With Multiple Signaling Pathways. 2002. *Genetics* 161, 693-710); mutations of LRBA cause severe immunodeficiency and autoimmunity (Lopez-Herrera, et al., Deleterious mutations in LRBA are associated with a syndrome of immune deficiency and autoimmunity. 2012. *Am J Hum Genet* 90, 986-1001; Burns, et al., LRBA gene deletion in a patient presenting with autoimmunity without hypogammaglobulinemia. 2012. *J Allergy Clin Immunol* 130, 1428-32; Alangari, et al., LPS-responsive beige-like anchor (LRBA) gene mutation in a family with inflammatory bowel disease and combined immunodeficiency. 2012. *J Allergy Clin Immunol* 130, 481-8 e2); depletion of LRBA results in significant cell growth inhibition, and sensitizes cells to apoptosis (Lopez-Herrera, et al., Deleterious mutations in LRBA are associated with a syndrome of immune deficiency and autoimmunity 2012. *Am J Hum Genet* 90, 986-1001; Wang, et al., Deregulated expression of LRBA facilitates cancer cell growth. 2004. *Oncogene* 23, 4089-97); LRBA is important for cell proliferation, apoptosis and autophagy (Lopez-Herrera, et al., Deleterious mutations in LRBA are associated with a syndrome of immune deficiency and

autoimmunity. 2012. *Am J Hum Genet* 90, 986-1001; Wang, et al., Deregulated expression of LRBA facilitates cancer cell growth. 2004. *Oncogene* 23, 4089-97); and deficiency of LRBA results in fewer cells positive for three CVID proteins: CD19, CD20 and B cell-activating factor receptor (BAFFR). This suggests that it may regulate these genes, and may cause immunodeficiency at least partially through these genes (Lopez-Herrera, et al., Deleterious mutations in LRBA are associated with a syndrome of immune deficiency and autoimmunity. 2012. *Am J Hum Genet* 90, 986-1001).

LRBA appears to regulate cytokines. LRBA-deficient patients have immunodeficiency, and defective cytokines are known to cause immunodeficiency (Leonard, Cytokines and immunodeficiency diseases. 2001. *Nat Rev Immunol* 1, 200-8). LRBA paralogue, FAN (Factor associated with neutral sphingomyelinase activation) is a TNF adaptor protein and is required for the TNF-induced expression of cytokines, such as IL-6 and CXCL-2 (Adam-Klages, et al., FAN, a novel WD-repeat protein, couples the p55 TNF-receptor to neutral sphingomyelinase. 1996. *Cell* 86, 937-47; Montfort, et al., FAN stimulates TNF(alpha)-induced gene expression, leukocyte recruitment, and humoral response. 2009. *J Immunol* 183, 5369-78). LYST is required for LPS induction of inflammatory cytokines (Cheng, et al., Novel functions of a regulator of lysosomal trafficking, LYST in TLR4 signal transduction. 2012. *Immunology* 137, 299-300).

These findings demonstrate that LRBA is essential for proper functioning of the immune system. However, the underlying cellular and molecular mechanisms are most unknown. LRBA may be an effective therapeutic target for inflammatory diseases. For example, RA is a severe, often destructive, chronic inflammatory disease of peripheral joints. Anti-TNF therapy has revolutionized the treatment of RA and other inflammatory diseases (Tracey, et al., Tumor necrosis factor antagonist mechanisms of action: a comprehensive review. 2008. *Pharmacol Ther* 117, 244-79). However, anti-TNF therapy is not effective in about one-third of RA patients and most of other inflammatory diseases, and patients may become refractory to the treatment. It may have severe side effects, and can also cause or increase heart failure (Ambrosi, & Lafforgue, [The cardiologist and immunosuppressive therapy]. 2012. *Presse Med* 41, 655-61; Nicola, et al., The risk of congestive heart failure in rheumatoid arthritis: a population-based study over 46 years. 2005. *Arthritis Rheum* 52, 412-20). New therapeutic strategies, based on a large number of cytokines, for these patients unresponsive to anti-TNF therapy have been explored, but the results are disappointing in most cases. The trials using IL-5 antagonists are disappointing (Commins, et al., Immunologic messenger molecules: cytokines, interferons, and chemokines. 2010. *J Allergy Clin Immunol* 125, S53-72). This may reflect that the cytokine cascade is highly redundant, and an inflammatory disease is often a complex disease, multiple cytokines may be involved in the inflammation (Holgate, S. T. Novel targets of therapy in asthma. *Curr Opin Pulm Med* 15, 63-71 (2009)). Inhibition of a single cytokine may not be sufficient, whereas blocking many cytokines with multiple agents would be impractical. Targeting a crucial gene that regulates multiple cytokines is desirable. LRBA may be one of such genes, as it may be a crucial regulator of multiple immune effectors including secreted cytokines through vesicle trafficking.

LRBA appears to regulate TLR4, as TLR4/LPS complex rapidly cycles between the cell membrane, the GC and endosomes (Latz, et al., Lipopolysaccharide rapidly traffics to and from the Golgi apparatus with the toll-like receptor

4-MD-2-CD14 complex in a process that is distinct from the initiation of signal transduction. 2002. *J Biol Chem* 277, 47834-43; Thieblemont & Wright, Transport of bacterial lipopolysaccharide to the golgi apparatus. 1999. *J Exp Med* 190, 523-34), and can activate signaling pathways at endo-lysosome (Cheng, et al., Novel functions of a regulator of lysosomal trafficking, LYST in TLR4 signal transduction. 2012. *Immunology* 137, 299-300), indicating vesicle-mediated localization and trafficking of TLR4 are required for its activation. Lyst deficient cells exhibit defective TLR signaling, specifically in TLR4 pathways (Cheng, et al., Novel functions of a regulator of lysosomal trafficking, LYST in TLR4 signal transduction. 2012. *Immunology* 137, 299-300). Recurrent bacterial infections in LRBA-deficient patients indicates impaired TLR4/LPS pathway. In summary, LRBA may interact with multiple important signal transduction pathways, including epidermal growth factor receptor (EGFR), Notch, PKA, Ras, E2F1, p53, MAPK, NF- $\kappa$ B LPS, cytokines and TLRs (Schreiber, et al., Genetic screen for modifiers of the rough eye phenotype resulting from overexpression of the Notch antagonist hairless in *Drosophila*. 2002. *Genesis* 33, 141-52; Shamloula, et al., rugose (rg), a *Drosophila* A kinase Anchor Protein, Is Required for Retinal Pattern Formation and Interacts Genetically With Multiple Signaling Pathways. 2002. *Genetics* 161, 693-710; de Souza, et al., SEL-2, the *C. elegans* neurobeachin/LRBA homolog, is a negative regulator of lin-12/Notch activity and affects endosomal traffic in polarized epithelial cells. 2007. *Development* 134, 691-702; Wang, et al., Deregulated expression of LRBA facilitates cancer cell growth. 2004. *Oncogene* 23, 4089-97). This concept is supported by information showing LRBA is highly conserved throughout the eukaryotic kingdom; LRBA interacts with multiple important signal transduction pathways, including those of epidermal growth factor receptor (EGFR), Notch, PKA, Ras, E2F1, p53 and NF- $\kappa$ B (Schreiber, et al., Genetic screen for modifiers of the rough eye phenotype resulting from overexpression of the Notch antagonist hairless in *Drosophila*. 2002. *Genesis* 33, 141-52; Shamloula, et al., rugose (rg), a *Drosophila* A kinase Anchor Protein, Is Required for Retinal Pattern Formation and Interacts Genetically With Multiple Signaling Pathways. 2002. *Genetics* 161, 693-710; de Souza, et al., SEL-2, the *C. elegans* neurobeachin/LRBA homolog, is a negative regulator of lin-12/Notch activity and affects endosomal traffic in polarized epithelial cells. 2007. *Development* 134, 691-702; Wang, et al., Deregulated expression of LRBA facilitates cancer cell growth. 2004. *Oncogene* 23, 4089-97); mutations of LRBA cause severe immunodeficiency and autoimmunity (Lopez-Herrera, et al., Deleterious mutations in LRBA are associated with a syndrome of immune deficiency and autoimmunity. 2012. *Am J Hum Genet* 90, 986-1001; Burns, et al., LRBA gene deletion in a patient presenting with autoimmunity without hypogammaglobulinemia. 2012. *J Allergy Clin Immunol* 130, 1428-32; Alangari, A. et al. LPS-responsive beige-like anchor (LRBA) gene mutation in a family with inflammatory bowel disease and combined immunodeficiency. 2012. *J Allergy Clin Immunol* 130, 481-8 e2); depletion of LRBA results in significant cell growth inhibition, and sensitizes cells to apoptosis (Wang, et al., Deregulated expression of LRBA facilitates cancer cell growth. 2004. *Oncogene* 23, 4089-97; Lopez-Herrera, et al., Deleterious mutations in LRBA are associated with a syndrome of immune deficiency and autoimmunity. 2012. *Am J Hum Genet* 90, 986-1001); LRBA is important for cell proliferation, apoptosis and autophagy (Wang, et al., Deregulated expression of LRBA facilitates cancer cell

growth. 2004. *Oncogene* 23, 4089-97; Lopez-Herrera, et al., Deleterious mutations in LRBA are associated with a syndrome of immune deficiency and autoimmunity. 2012. *Am J Hum Genet* 90, 986-1001) and deficiency of LRBA causes less cells positive for at least three CVID proteins: CD19, CD20 and BAFFR, suggesting that LRBA may regulate these genes (Lopez-Herrera, et al., Deleterious mutations in LRBA are associated with a syndrome of immune deficiency and autoimmunity. 2012. *Am J Hum Genet* 90, 986-1001).

#### SUMMARY OF THE INVENTION

LRBA is found present in the blood stream (Liu, et al., High dynamic range characterization of the trauma patient plasma proteome. 2006. *Mol Cell Proteomics* 5, 1899-913; Qian, et al., Quantitative proteome analysis of human plasma following in vivo lipopolysaccharide administration using 160/180 labeling and the accurate mass and time tag approach. 2005. *Mol Cell Proteomics* 4, 700-9). It is one of the genes critical for inflammation, which include the inflammatory bottle-neck kinase (NF $\kappa$ B, AKT and MAPK), cytokines (TNF $\alpha$  and IL-10), Toll-like receptor 4 (TLR4), and CVID (common variable immunodeficiency) genes (CD19, CD20, CD21, BAFFR and TACI). The plasma presence of LRBA provides a feasible way to therapeutically modulate LRBA levels. The most potent inducer of TNF is LPS (Tracey, et al., Anti-cachectin/TNF monoclonal antibodies prevent septic shock during lethal bacteraemia. 1987. *Nature* 330, 662-4), which also induces LRBA (this study) (Burns, et al., LRBA gene deletion in a patient presenting with autoimmunity without hypogammaglobulinemia. 2012. *J Allergy Clin Immunol* 130, 1428-32; Kerr, et al., Analysis of lipopolysaccharide-response genes in B-lineage cells demonstrates that they can have differentiation stage-restricted expression and contain SH2 domains. 1996. *Proc Natl Acad Sci USA* 93, 3947-52; Wang, et al., Identification of a novel lipopolysaccharide-inducible gene with key features of both A kinase anchor proteins and chsl/beige proteins. 2001. *J Immunol* 166, 4586-95). TNF is an auto-crine growth factor for normal human B cells (Boussiotis, et al., Tumor necrosis factor alpha is an autocrine growth factor for normal human B cells. *Proc Natl Acad Sci USA* 91, 7007-11 (1994)). Anti-TNF therapy inhibits the immune system, such as inhibition of memory B cells and susceptibility to infections (Anolik, J. H. et al. Cutting edge: anti-tumor necrosis factor therapy in rheumatoid arthritis inhibits memory B lymphocytes via effects on lymphoid germinal centers and follicular dendritic cell networks. *J Immunol* 180, 688-92 (2008)). The same phenotype is present in LRBA deficient patients. LRBA deficient patients have very low levels of memory B cells (Lopez-Herrera, G. et al. Deleterious mutations in LRBA are associated with a syndrome of immune deficiency and autoimmunity. *Am J Hum Genet* 90, 986-1001 (2012)), suggesting that TNF may be repressed due to deficient LRBA. These data suggests that LRBA may be involved in TNF pathway and can be explored as a better therapeutic target for inflammatory diseases.

Moreover, as LRBA is found in the blood, and LRBA levels in healthy controls and patients with controlled symptoms are undetectable or much lower, LRBA can be used as a convenient noninvasive biomarker for inflammatory diseases such as asthma exacerbation, rheumatoid arthritis, ulcerative colitis and sepsis. Deficiency of LRBA causes immunodeficiency and autoimmunity.

As such, LRBA therapies are used to target immunodeficiency and autoimmunity. Most of the current biologics are



based on cytokines. For example, anti-TNF therapy has revolutionized the treatment of RA (Tracey, et al., Tumor necrosis factor antagonist mechanisms of action: a comprehensive review. 2008. *Pharmacol Ther* 117, 244-79). However, anti-TNF therapy is not effective in about one-third of RA subjects and in most other inflammatory diseases, and patients may eventually become refractory to it. New therapeutic strategies, based on a large number of cytokines, for patients unresponsive to anti-TNF, have been explored, in most cases, the results were disappointing (Commins, et al., Immunologic messenger molecules: cytokines, interferons, and chemokines. 2010. *J Allergy Clin Immunol* 125, S53-72). This may indicate that the cytokine cascade is highly redundant, for RA and other immune-based diseases, and an inflammatory disease, more often than not, is a complex one involving multiple cytokines (Holgate, Novel targets of therapy in asthma. 2009. *Curr Opin Pulm Med* 15, 63-71). Inhibition of a single cytokine may not be sufficient, whereas blocking many cytokines with multiple agents is impractical and treatment resistance can develop (Sfikakis, P. P. The first decade of biologic TNF antagonists in clinical practice: lessons learned, unresolved issues and future directions. *Curr Dir Autoimmun* 11, 180-210 (2010)). Targeting a vital gene that regulates multiple cytokines is desirable. Targeting a master regulator that is a crucial connection node for multiple inflammatory pathways will lead to a more effective therapy. However, until the present invention, no such gene(s) have been identified.

Anti-LRBA therapy was tested for safety and efficacy using model mice. LRBA is present in the blood stream (Liu, et al., High dynamic range characterization of the trauma patient plasma proteome. 2006. *Mol Cell Proteomics* 5, 1899-913; Qian, et al., Quantitative proteome analysis of human plasma following in vivo lipopolysaccharide administration using 160/180 labeling and the accurate mass and time tag approach. 2005. *Mol Cell Proteomics* 4, 700-9), providing a feasible way for therapeutic modulation. The absence of LRBA in humans is not lethal (Lopez-Herrera, et al., Deleterious mutations in LRBA are associated with a syndrome of immune deficiency and autoimmunity. 2012. *Am J Hum Genet* 90, 986-1001; Burns, et al., LRBA gene deletion in a patient presenting with autoimmunity without hypogammaglobulinemia. 2012. *J Allergy Clin Immunol* 130, 1428-32; Alangari, et al., LPS-responsive beige-like anchor (LRBA) gene mutation in a family with inflammatory bowel disease and combined immunodeficiency. 2012. *J Allergy Clin Immunol* 130, 481-8 e2), suggesting that temporarily blocking it will not cause significant toxicity. This parallels with anti-TNF therapy, which is well tolerated (Grijalva, et al., Initiation of tumor necrosis factor-alpha antagonists and the risk of hospitalization for infection in patients with autoimmune diseases. 2011. *JAMA* 306, 2331-9). The development in TNF knockout mice is normal (Pasparakis, et al., Immune and inflammatory responses in TNF alpha-deficient mice: a critical requirement for TNF alpha in the formation of primary B cell follicles, follicular dendritic cell networks and germinal centers, and in the maturation of the humoral immune response. 1996. *J Exp Med* 184, 1397-411), and anti-TNF therapy is well tolerated (Grijalva, et al., Initiation of tumor necrosis factor-alpha antagonists and the risk of hospitalization for infection in patients with autoimmune diseases. 2011. *JAMA* 306, 2331-9). The LRBA knockout mice are also viable, and absence of LRBA in humans is not lethal (Lopez-Herrera, et al., Deleterious mutations in LRBA are associated with a syndrome of immune deficiency and autoimmunity. 2012. *Am J Hum Genet* 90, 986-1001; Burns, et al., LRBA gene deletion

in a patient presenting with autoimmunity without hypogammaglobulinemia. 2012. *J Allergy Clin Immunol* 130, 1428-32; Alangari, et al., LPS-responsive beige-like anchor (LRBA) gene mutation in a family with inflammatory bowel disease and combined immunodeficiency. 2012. *J Allergy Clin Immunol* 130, 481-8 e2). This mirrors the anti-TNF therapy and suggests that temporarily blocking LRBA may not cause intolerable toxicity.

Cardiovascular disease (CVD) is a complex chronic inflammatory disease (Ross, Atherosclerosis—an inflammatory disease. 1999. *N Engl J Med* 340, 115-26), and pro-inflammatory cytokines play a key role in its pathophysiology (Charalambous, et al., Role of bacterial endotoxin in chronic heart failure: the gut of the matter. 2007. *Shock* 28, 15-23). Heart failure was reported in a LRBA deficient patient (Lopez-Herrera, et al., Deleterious mutations in LRBA are associated with a syndrome of immune deficiency and autoimmunity. 2012. *Am J Hum Genet* 90, 986-1001). LRBA may be directly involved in CVD inflammation, and an effective CVD therapeutic target. As noted above, most current biologics are based on cytokines. LRBA is implied to be a master regulator of inflammatory effectors including pro-inflammatory cytokines through vesicle trafficking. Mutations of LRBA cause immunodeficiency and autoimmunity inflammation. Heart failure was observed in an LRBA deficient patient (Lopez-Herrera, G. et al. Deleterious mutations in LRBA are associated with a syndrome of immune deficiency and autoimmunity. *Am J Hum Genet* 90, 986-1001 (2012)). LRBA is highly expressed in the heart: its levels rank at above 90% percentile in all genes examined (Dufour, C. R. et al. Genome-wide orchestration of cardiac functions by the orphan nuclear receptors ERRalpha and gamma. *Cell Metab* 5, 345-56 (2007)). Those data show that LRBA and CVD may be closely related. Moreover, LRBA can be secreted into plasma at high levels (up to 6.7 µg/L) upon LPS stimulation and high in asthmatic inflammation. LRBA may be directly involved in CVD inflammation, and an effective CVD therapeutic target.

LRBA can be used as a therapeutic through intravenous injection of protein LRBA or genome-editing technology to replenish or correct LRBA deficiency or mutation in the patients who lack functional LRBA, or mutations of LRBA can be corrected through genome-editing technology. On another hand, when LRBA is overexpressed in the patients and contribute to the pathogenesis, we may use LRBA antibody or LRBA dominant negative mutants (DNM) to block LRBA function, or other technologies such as siRNA and shRNA knockdown technologies to knockdown LRBA.

#### BRIEF DESCRIPTION OF THE DRAWINGS

For a fuller understanding of the invention, reference should be made to the following detailed description, taken in connection with the accompanying drawings, in which:

FIG. 1 is an image showing LRBA is a crucial regulator for cytokine secretion and TLR4 activation. Overexpression of LRBA enhances cytokine secretion and TLR4 activation, while depletion of LRBA inhibits these two processes. The plasma presence of LRBA provides a way to feasibly modulate LRBA: intravenously, LRBA can be replenished when down-regulated or blocked with antibody or dominant negative mutants (DNMs) when over-expressed to treat inflammatory diseases. A remote, functional conserved domain related to VHS<sup>64</sup> (Vps-27, Hrs and STAM) domain was identified in LRBA.<sup>63</sup> \* = stop codon; fs\*3 = 3 frame-shift codons then stop codon. For more details, please see the text.

FIG. 2 is an illustration showing LRBA protein structure. The LRBA peptide has a highly conserved WBW [WDL (WD-like)-BEACH-WD40] multi-domain structure at the C-terminal end, two PKA binding sites, a VHS domain that may bind ubiquitin domains, and a ConA-like domain, which generally bind oligosaccharides. The mutations that cause diseases are shown in the boxes. \*=stop codon; fs\*3=3 frame-shift codons then stop codon.

FIG. 3A is an image showing LRBA is co-localized with GC protein, dynamically involved in vesicle trafficking. HEK293 cells cultured on glass cover slips were fixed, permeabilized, and stained following the immuno-fluorescence staining protocol from the Human Protein Atlas Project (Sigma). The LRBA Prestige antibodies and three Golgi protein primary antibodies from BD biosciences were used at 1:500 (volume to volume dilution). The anti-mouse IgG-Alexa Fluor® 555, and anti-rabbit IgG-Alexa Fluor® 488 (Invitrogen) secondary antibodies were used at 1:400. The images were acquired with an Olympus FV1000 scanning confocal microscope with 0.5  $\mu$ m of per slice by sequential scanning.

FIGS. 3B-C are a series of images depicting LRBA is co-localized with GC proteins, dynamically involved in vesicle trafficking. HEK293 cells cultured on glass cover slips were fixed, permeabilized, and stained following the immuno-fluorescence staining protocol from the Human Protein Atlas Project (Sigma). The LRBA Prestige antibodies and three Golgi protein primary antibodies from BD biosciences were used at 1:500 (volume to volume dilution). The anti-mouse IgG-Alexa Fluor® 555, and anti-rabbit IgG-Alexa Fluor® 488 (Invitrogen) secondary antibodies were used at 1:400. The images were acquired with an Olympus FV1000 scanning confocal microscope with 0.5  $\mu$ m of per slice by sequential scanning.

FIG. 3D is an image depicting LRBA is co-localized with early endosome protein, dynamically involved in vesicle trafficking. HEK293 cells cultured on glass cover slips were fixed, permeabilized, and stained following the immuno-fluorescence staining protocol from the Human Protein Atlas Project (Sigma). The LRBA Prestige antibodies and three Golgi protein primary antibodies from BD biosciences were used at 1:500 (volume to volume dilution). The anti-mouse IgG-Alexa Fluor® 555, and anti-rabbit IgG-Alexa Fluor® 488 (Invitrogen) secondary antibodies were used at 1:400. The images were acquired with an Olympus FV1000 scanning confocal microscope with 0.5  $\mu$ m of per slice by sequential scanning.

FIGS. 3E-G are a series of images depicting three time lapse video representative sequential captures of live RAW264.7 macrophage cells stably transfected with LRBA-GFP, showing cell membrane and Golgi locations, dynamic activities of vesicles moving from Golgi to the membrane, acquired from Leica TCS SP2 laser scanning confocal microscope. LRBA Prestige antibodies and primary antibodies from BD biosciences at a concentration of 1:500 against endogenous proteins.

FIGS. 4A-B are a blot and graph showing knockdown of LRBA increases the TNF $\alpha$  levels in A549 cells (adenocarcinomic human alveolar basal epithelial cells). A549 cells and A549 pLasiGFP cells (stably transfected with shRNA plasmid against LRBA) were treated with LPS (1  $\mu$ g/ml). The TNF $\alpha$  concentrations were detected by Western blot. Cells were cultured in 6-well plates and stimulated with LPS (1  $\mu$ g/ml) for different time as shown, then lysed with RIPA buffer. Western blots were carried out. TNF $\alpha$  antibody (sc-1351. Santa Cruz Biotechnology, Santa Cruz, USA) was used at 1:500 ratio and incubated at 4° C. overnight. BioRad

ChemiDoc XRS and Quantity One software were used to acquire gel image and measure band relative intensity. (A) Western blot. 1. A549 No LPS, 2. A549 LPS 30 min, 3. A549 LPS 1 hr, 4. A549 LPS 2 h, 5. A549 LPS 4 h, 6. A549 LPS 24 h, 7. A549 pLasiGFP LPS 2 h, 8. A549 pLasiGFP LPS 4 h, 9. A549 pLasiGFP LPS 24 h. (B) Band intensity quantification from A.

FIG. 4C is a graph showing knockdown of LRBA increases the TNF $\alpha$  levels in A549 cells (adenocarcinomic human alveolar basal epithelial cells). A549 cells and A549 pLasiGFP cells (stably transfected with shRNA plasmid against LRBA) were treated with LPS (1  $\mu$ g/ml). The TNF $\alpha$  concentrations were detected by Western blot. Cells were cultured in 6-well plates and stimulated with LPS (1  $\mu$ g/ml) for different time as shown, then lysed with RIPA buffer. Western blots were carried out. TNF $\alpha$  antibody (sc-1351. Santa Cruz Biotechnology, Santa Cruz, USA) was used at 1:500 ratio and incubated at 4° C. overnight. BioRad ChemiDoc XRS and Quantity One software were used to acquire gel image and measure band relative intensity. (C) TNF $\alpha$  levels in A549 and A549 pLasiGFP cells were compared side by side.

FIGS. 5A-C are a series of confocal images showing LRBA is co-localized with GC proteins demonstrated by confocal microscopy and JACoP software. HEK293 cells cultured on glass cover slips were fixed, permeabilized, and stained following the immuno-fluorescence staining protocol from the Human Protein Atlas Project (Sigma). The LRBA Prestige antibodies and three Golgi protein primary antibodies from BD Biosciences were used at 1:500 (volume to volume dilution). The anti-mouse IgG-Alexa Fluor® 555, and anti-rabbit IgG-Alexa Fluor® 488 (Invitrogen) secondary antibodies were used at 1:400. The images were acquired with an Olympus FV1000 scanning confocal microscope by sequential scanning with 0.5  $\mu$ m per slice. 1, 2 & 3: Three representative sequential captures from a time-lapse video of live RAW264.7 macrophage cells stably transfected with LRBA-GFP, showing cell membrane and Golgi locations, dynamic activities of vesicles moving from GC to the membrane (Leica TCS SP2 laser scanning confocal microscope). GM130: Pearson's Coefficient:  $r=0.562$  Overlap Coefficient:  $r=0.674$   $r^2=k1 \times k2$ :  $k1=0.71$   $k2=0.639$  Using thresholds (thrA=11 and thrB=26) Overlap Coefficient:  $r=0.782$   $r^2=k1 \times k2$ :  $k1=0.926$   $k2=0.661$  Manders' Coefficients (original):  $M1=0.853$  (fraction of A overlapping B)  $M2=0.968$  (fraction of B overlapping A) Manders' Coefficients (using threshold value of 11 for imgA and 26 for imgB):  $M1=0.674$  (fraction of A overlapping B)  $M2=0.916$  (fraction of B overlapping A) Costes' automatic threshold set to 2 for imgA & 16 for imgB Pearson's Coefficient:  $r=0.385$  (0.0 below thresholds)  $M1=0.999$  &  $M2=0.977$  Van Steensel's Cross-correlation Coefficient between H293LRBAgreenframes.tif and H293GM130redframes.tif: CCF min.: 0.377 (obtained for  $dx=-20$ ) CCF max.: 0.562 (obtained for  $dx=0$ ) Results for fitting CCF on a Gaussian ( $CCF=a+(b-a)\exp(-(xshift-c)^2/(2d^2))$ ): Formula:  $y=a+(b-a)*\exp(-(x-c)/(2*d*d))$  Status: Success Number of completed minimizations: 2 Number of iterations: 93 (max: 4000) Time: 4 ms Sum of residuals squared: 0.0021718 Standard deviation: 0.0073685  $R^2$ : 0.98178 Parameters:  $a=0.38178$   $b=0.55472$   $c=-0.45801$   $d=9.31510$  FWHM=21.935 pixels Cytofluorogram's parameters:  $a$ : 0.612  $b$ : 15.267 Correlation coefficient: 0.562 Li's Intensity correlation coefficient: ICQ: 0.28053263239399306 Costes' randomization based colocalization: Parameters: Nb of randomization rounds: 1000, Resolution (bin width): 0.0010  $r$  (original)=0.56  $r$  (randomized)=0.0 $\pm$ 0.0030 (calculated

## 21

from the fitted data) P-value=100.0% (calculated from the fitted data) Results for fitting the probability density function on a Gaussian (Probability= $a+(b-a)\exp(-(R-c)^2/(2d^2))$ ): Formula:  $y=a+(b-a)\exp(-(x-c)/(2*d*d))$  Status: Success Number of completed minimizations: 2 Number of iterations: 160 (max: 4000) Time: 4 ms Sum of residuals squared: 0.00086502 Standard deviation: 0.0062705 R<sup>2</sup>: 0.97303 Parameters: a=0.0013404 b=0.10599 c=-0.00010744 d=-0.0036972 FWHM=0.0080 Colocalization based on distance between centres of mass Threshold for Image A=11; Image B=26 Particles size between 0 & 245385 Image A: 10 centre(s) colocalizing out of 98 Image B: 12 centre(s) colocalizing out of 168 Colocalization based on centres of mass-particles coincidence Threshold for Image A=11; Image B=26 Particles size between 0 & 245385 Image A: 4 centre(s) colocalizing out of 98 Image B: 1 centre(s) colocalizing out of 168.

FIGS. 5D-F are a series of confocal images showing LRBA is co-localized with GC proteins demonstrated by confocal microscopy and JACoP software. HEK293 cells cultured on glass cover slips were fixed, permeabilized, and stained following the immuno-fluorescence staining protocol from the Human Protein Atlas Project (Sigma). The LRBA Prestige antibodies and three Golgi protein primary antibodies from BD Biosciences were used at 1:500 (volume to volume dilution). The anti-mouse IgG-Alexa Fluor® 555, and anti-rabbit IgG-Alexa Fluor® 488 (Invitrogen) secondary antibodies were used at 1:400. The images were acquired with an Olympus FV1000 scanning confocal microscope by sequential scanning with 0.5 µm per slice. 1, 2 & 3: Three representative sequential captures from a time-lapse video of live RAW264.7 macrophage cells stably transfected with LRBA-GFP, showing cell membrane and Golgi locations, dynamic activities of vesicles moving from GC to the membrane (Leica TCS SP2 laser scanning confocal microscope). P230: Pearson's Coefficient: r=0.443 Overlap Coefficient: r=0.469 r<sup>2</sup>=k1×k2: k1=0.734 k2=0.3 Using thresholds (thrA=74 and thrB=27) Overlap Coefficient: r=0.846 r<sup>2</sup>=k1×k2: k1=0.915 k2=0.782 Manders' Coefficients (original): M1=0.933 (fraction of A overlapping B) M2=0.288 (fraction of B overlapping A) Manders' Coefficients (using threshold value of 74 for imgA and 27 for imgB): M1=0.758 (fraction of A overlapping B) M2=0.29 (fraction of B overlapping A) Costes' automatic threshold set to 2 for imgA & 8 for imgB Pearson's Coefficient: r=0.248 (0.0 below thresholds) M1=0.999 & M2=0.943 Van Steensel's Cross-correlation Coefficient between H293LRBAgreenp230red1Cropped.tif.frames (red) and H293LRBAgreenp230red1Cropped.tif.frames (green): CCF min.: 0.07 (obtained for dx=20) CCF max.: 0.443 (obtained for dx=0) Results for fitting CCF on a Gaussian (CCF= $a+(b-a)\exp(-(xshift-c)^2/(2d^2))$ ): Formula:  $y=a+(b-a)\exp(-(x-c)/(2*d*d))$  Status: Success Number of completed minimizations: 2 Number of iterations: 107 (max: 4000) Time: 4 ms Sum of residuals squared: 0.010757 Standard deviation: 0.016399 R<sup>2</sup>: 0.97905 Parameters: a=0.097205 b=0.41277 c=0.33764 d=6.60137 FWHM=15.545 pixels Cytofluorogram's parameters: a: 0.669 b: 7.406 Correlation coefficient: 0.443 Li's Intensity correlation coefficient: ICQ: 0.33931448608371684 Costes' randomization based colocalization: Parameters: Nb of randomization rounds: 1000, Resolution (bin width): 0.0010 r (original)=0.442 r (randomized)=0.0±0.0020 (calculated from the fitted data) P-value=100.0% (calculated from the fitted data) Results for fitting the probability density function on a Gaussian (Probability= $a+(b-a)\exp(-(R-c)^2/(2d^2))$ ): Formula:  $y=a+(b-a)\exp(-(x-c)/(2*d*d))$  Status:

## 22

Success Number of completed minimizations: 2 Number of iterations: 155 (max: 4000) Time: 4 ms Sum of residuals squared: 0.0019026 Standard deviation: 0.012098 R<sup>2</sup>: 0.96178 Parameters: a=-0.0030523 b=0.16637 c=6.67246E-5 d=0.0024017 FWHM=0.0050.

FIGS. 5G-I are a series of confocal images showing LRBA is co-localized with GC proteins demonstrated by confocal microscopy and JACoP software. HEK293 cells cultured on glass cover slips were fixed, permeabilized, and stained following the immuno-fluorescence staining protocol from the Human Protein Atlas Project (Sigma). The LRBA Prestige antibodies and three Golgi protein primary antibodies from BD Biosciences were used at 1:500 (volume to volume dilution). The anti-mouse IgG-Alexa Fluor® 555, and anti-rabbit IgG-Alexa Fluor® 488 (Invitrogen) secondary antibodies were used at 1:400. The images were acquired with an Olympus FV1000 scanning confocal microscope by sequential scanning with 0.5 µm per slice. 1, 2 & 3: Three representative sequential captures from a time-lapse video of live RAW264.7 macrophage cells stably transfected with LRBA-GFP, showing cell membrane and Golgi locations, dynamic activities of vesicles moving from GC to the membrane (Leica TCS SP2 laser scanning confocal microscope). GS-28: Pearson's Coefficient: r=0.366 Overlap Coefficient: r=0.381 r<sup>2</sup>=k1×k2: k1=0.851 k2=0.17 Using thresholds (thrA=63 and thrB=44) Overlap Coefficient: r=0.883 r<sup>2</sup>=k1×k2: k1=1.084 k2=0.72 Manders' Coefficients (original): M1=0.782 (fraction of A overlapping B) M2=0.259 (fraction of B overlapping A) Manders' Coefficients (using threshold value of 63 for imgA and 44 for imgB): M1=0.676 (fraction of A overlapping B) M2=0.173 (fraction of B overlapping A) Costes' automatic threshold set to 2 for imgA & 7 for imgB Pearson's Coefficient: r=0.176 (0.0 below thresholds) M1=0.999 & M2=0.987 Van Steensel's Cross-correlation Coefficient between H293GS28red(red).tif and H293LRBA(green).tif: CCF min.: 0.0080 (obtained for dx=20) CCF max.: 0.366 (obtained for dx=0) Results for fitting CCF on a Gaussian (CCF= $a+(b-a)\exp(-(xshift-c)^2/(2d^2))$ ): Formula:  $y=a+(b-a)\exp(-(x-c)/(2*d*d))$  Status: Success Number of completed minimizations: 2 Number of iterations: 112 (max: 4000) Time: 4 ms Sum of residuals squared: 0.011774 Standard deviation: 0.017157 R<sup>2</sup>: 0.97313 Parameters: a=0.047265 b=0.34334 c=0.32362 d=4.48046 FWHM=10.55 pixels. Cytofluorogram's parameters: a: 0.802 b: 5.927 Correlation coefficient: 0.366 Li's Intensity correlation coefficient: ICQ: 0.4039760078011444 Costes' randomization based colocalization: Parameters: Nb of randomization rounds: 1000, Resolution (bin width): 0.0010 r (original)=0.367 r (randomized)=0.0±0.0020 (calculated from the fitted data) P-value=100.0% (calculated from the fitted data) Results for fitting the probability density function on a Gaussian (Probability= $a+(b-a)\exp(-(R-c)^2/(2d^2))$ ): Formula:  $y=a+(b-a)\exp(-(x-c)/(2*d*d))$  Status: Success Number of completed minimizations: 2 Number of iterations: 508 (max: 4000) Time: 12 ms Sum of residuals squared: 0.00041598 Standard deviation: 0.0049467 R<sup>2</sup>: 0.99252 Parameters: a=-0.00013085 b=0.15664 c=1.21787E-5 d=-0.0025101 FWHM=0.0050.

FIG. 6(A)-(C) is a series of confocal images showing LRBA is co-localized with PKA RIIβ subunits demonstrated by confocal microscopy and JACoP software. The colocalization was evaluated by the Pearson's Coefficient: r=0.225; Overlap Coefficient: r=0.257; r<sup>2</sup>=k1×k2: k1=0.351; k2=0.189 using thresholds (thrA=12 and thrB=8): Overlap Coefficient: r=0.802; r<sup>2</sup>=k1×k2: k1=0.802; k2=0.802 Manders' Coefficients (original): M1=0.407 (fraction of A over-

lapping B) M2=0.348 (fraction of B overlapping A) Manders' Coefficients (using threshold value of 12 for imgA and 8 for imgB): M1=0.338 (fraction of A overlapping B) M2=0.162 (fraction of B overlapping A) Costes' automatic threshold set to 3 for imgA & 2 for imgB Pearson's Coefficient: r=0.111 (0.0 below thresholds) M1=0.958 & M2=0.99 Van Steensel's Cross-correlation Coefficient between H293LRBAgreenframes.tif and H293PKARIIBredframes.tif: CCF min.: 0.048 (obtained for dx=-20) CCF max.: 0.225 (obtained for dx=0) Results for fitting CCF on a Gaussian ( $CCF=a+(b-a)\exp(-(xshift-c)^2/(2d^2))$ ): Formula:  $y=a+(b-a)*\exp(-(x-c)*(x-c)/(2*d*d))$  Status: Success Number of completed minimizations: 2 Number of iterations: 98 (max: 4000) Time: 3 ms Sum of residuals squared: 0.00081518 Standard deviation: 0.0045144 R<sup>2</sup>: 0.99369 Parameters: a=0.042353 b=0.21464 c=-0.17572 d=8.50897 FWHM=20.037 pixels Cytofluorogram's parameters: a: 0.304 b: 1.322 Correlation coefficient: 0.225 Li's Intensity correlation coefficient: ICQ: 0.3859623903228554 Costes' randomization based colocalization: Parameters: Nb of randomization rounds: 1000, Resolution (bin width): 0.0010 r (original)=0.225 r (randomized)=0.0±0.0 (calculated from the fitted data) P-value=100.0% (calculated from the fitted data) Results for fitting the probability density function on a Gaussian (Probability= $a+(b-a)\exp(-(R-c)^2/(2d^2))$ ): Formula:  $y=a+(b-a)*\exp(-(x-c)*(x-c)/(2*d*d))$  Status: Success Number of completed minimizations: 2 Number of iterations: 178 (max: 4000) Time: 4 ms Sum of residuals squared: 0.00016703 Standard deviation: 0.0057798 R<sup>2</sup>: 0.99891 Parameters: a=0.0048521 b=0.45306 c=-1.33088E-5 d=-0.00077178 FWHM=0.0010.

FIGS. 7(A)-(C) are a series of confocal images showing LRBA is co-localized with PKA catalytic subunits demonstrated by confocal microscopy and JACoP software. Pearson's Coefficient: r=0.197 Overlap Coefficient: r=0.261 r<sup>2</sup>=k1×k2: k1=0.232 k2=0.295 Using thresholds (thrA=44 and thrB=68) Overlap Coefficient: r=0.821 r<sup>2</sup>=k1×k2: k1=1.02 k2=0.66 Manders' Coefficients (original): M1=0.307 (fraction of A overlapping B) M2=0.681 (fraction of B overlapping A) Manders' Coefficients (using threshold value of 44 for imgA and 68 for imgB): M1=0.121 (fraction of A overlapping B) M2=0.243 (fraction of B overlapping A) Costes' automatic threshold set to 2 for imgA & 4 for imgB Pearson's Coefficient: r=0.092 (0.0 below thresholds) M1=0.994 & M2=0.995 Van Steensel's Cross-correlation Coefficient between H293LRBAgreen.tif and H293PKAcred.tif: CCF min.: 0.029 (obtained for dx=-20) CCF max.: 0.197 (obtained for dx=0) Results for fitting CCF on a Gaussian ( $CCF=a+(b-a)\exp(-(xshift-c)^2/(2d^2))$ ): Formula:  $y=a+(b-a)*\exp(-(x-c)*(x-c)/(2*d*d))$  Status: Success Number of completed minimizations: 2 Number of iterations: 99 (max: 4000) Time: 4 ms Sum of residuals squared: 0.0024994 Standard deviation: 0.0079048 R<sup>2</sup>: 0.97523 Parameters: a=0.041320 b=0.18057 c=0.094024 d=6.44875 FWHM=15.185 pixels Cytofluorogram's parameters: a: 0.18 b: 3.989 Correlation coefficient: 0.197 Li's Intensity correlation coefficient: ICQ: 0.2826960483630244 Costes' randomization based colocalization: Parameters: Nb of randomization rounds: 1000, Resolution (bin width): 0.0010 r (original)=0.197 r (randomized)=0.0±0.0010 (calculated from the fitted data) P-value=100.0% (calculated from the fitted data) Results for fitting the probability density function on a Gaussian (Probability= $a+(b-a)\exp(-(R-c)^2/(2d^2))$ ): Formula:  $y=a+(b-a)*\exp(-(x-c)*(x-c)/(2*d*d))$  Status: Success Number of completed minimizations: 2 Number of iterations: 172 (max: 4000) Time: 3 ms

Sum of residuals squared: 0.00063475 Standard deviation: 0.0079671 R<sup>2</sup>: 0.99365 Parameters: a=0.0025887 b=0.27547 c=-9.38343E-5 d=-0.0013731 FWHM=0.0030.

FIGS. 8(A)-(C) are a series of confocal images showing LRBA is co-localized with  $\beta$ -tubulin demonstrated by confocal microscopy and JACoP software. Pearson's Coefficient: r=0.171 Overlap Coefficient: r=0.207 r<sup>2</sup>=k1×k2: k1=0.134 k2=0.32 Using thresholds (thrA=33 and thrB=42) Overlap Coefficient: r=0.753 r<sup>2</sup>=k1×k2: k1=0.945 k2=0.599 Manders' Coefficients (original): M1=0.216 (fraction of A overlapping B) M2=0.713 (fraction of B overlapping A) Manders' Coefficients (using threshold value of 33 for imgA and 42 for imgB): M1=0.089 (fraction of A overlapping B) M2=0.362 (fraction of B overlapping A) Costes' automatic threshold set to 5 for imgA & 2 for imgB Pearson's Coefficient: r=0.044 (0.0 below thresholds) M1=0.986 & M2=0.997 Van Steensel's Cross-correlation Coefficient between H293LRBAgreentubulinred(1) cropped.tif.frames (red) and H293LRBAgreentubulinred(1) cropped.tif.frames (green): CCF min.: 0.043 (obtained for dx=20) CCF max.: 0.171 (obtained for dx=0) Results for fitting CCF on a Gaussian ( $CCF=a+(b-a)\exp(-(xshift-c)^2/(2d^2))$ ): Formula:  $y=a+(b-a)*\exp(-(x-c)*(x-c)/(2*d*d))$  Status: Success Number of completed minimizations: 2 Number of iterations: 104 (max: 4000) Time: 4 ms Sum of residuals squared: 0.0013469 Standard deviation: 0.0058028 R<sup>2</sup>: 0.97500 Parameters: a=0.053279 b=0.15896 c=-0.17761 d=7.69119 FWHM=18.111 pixels Cytofluorogram's parameters: a: 0.115 b: 1.507 Correlation coefficient: 0.171 Li's Intensity correlation coefficient: ICQ: 0.3429955832151942 Costes' randomization based colocalization: Parameters: Nb of randomization rounds: 1000, Resolution (bin width): 0.0010 r (original)=0.17 r (randomized)=0.0±0.0010 (calculated from the fitted data) P-value=100.0% (calculated from the fitted data) Results for fitting the probability density function on a Gaussian (Probability= $a+(b-a)\exp(-(R-c)^2/(2d^2))$ ): Formula:  $y=a+(b-a)*\exp(-(x-c)*(x-c)/(2*d*d))$  Status: Success Number of completed minimizations: 2 Number of iterations: 176 (max: 4000) Time: 2 ms Sum of residuals squared: 0.00020366 Standard deviation: 0.0053939 R<sup>2</sup>: 0.99794 Parameters: a=-0.0024953 b=0.31261 c=-2.90146E-5 d=-0.0012107 FWHM=0.0020.

FIGS. 9(A)-(C) are a series of confocal images showing LRBA is co-localized with Clathrin demonstrated by confocal microscopy and JACoP software. Pearson's Coefficient: r=0.363 Overlap Coefficient: r=0.403 r<sup>2</sup>=k1×k2: k1=0.329 k2=0.495 Using thresholds (thrA=21 and thrB=19) Overlap Coefficient: r=0.704 r<sup>2</sup>=k1×k2: k1=0.696 k2=0.711 Manders' Coefficients (original): M1=0.51 (fraction of A overlapping B) M2=0.799 (fraction of B overlapping A) Manders' Coefficients (using threshold value of 21 for imgA and 19 for imgB): M1=0.402 (fraction of A overlapping B) M2=0.621 (fraction of B overlapping A) Costes' automatic threshold set to 2 for imgA & 3 for imgB Pearson's Coefficient: r=0.151 (0.0 below thresholds) M1=0.998 & M2=0.997 Van Steensel's Cross-correlation Coefficient between H293LRBAgreenframes.tif and H293Clathrinredframes.tif: CCF min.: 0.0050 (obtained for dx=-20) CCF max.: 0.363 (obtained for dx=0) Results for fitting CCF on a Gaussian ( $CCF=a+(b-a)\exp(-(xshift-c)^2/(2d^2))$ ): Formula:  $y=a+(b-a)*\exp(-(x-c)*(x-c)/(2*d*d))$  Status: Success Number of completed minimizations: 2 Number of iterations: 103 (max: 4000) Time: 4 ms Sum of residuals squared: 0.018832 Standard deviation: 0.021698 R<sup>2</sup>: 0.95013 Parameters: a=0.016205 b=0.30867 c=2.92049 d=9.06131 FWHM=21.337 pixels Cytofluoro-

gram's parameters: a: 0.301 b: 2.932 Correlation coefficient: 0.363 Li's Intensity correlation coefficient: ICQ: 0.3826994110012978 Costes' randomization based colocalization: Parameters: Nb of randomization rounds: 1000, Resolution (bin width): 0.0010 r (original)=0.363 r (randomized)=0.0±-0.0050 (calculated from the fitted data) P-value=100.0% (calculated from the fitted data) Results for fitting the probability density function on a Gaussian (Probability= $a+(b-a)\exp(-(R-c)^2/(2d^2))$ ): Formula:  $y=a+(b-a)\exp(-(x-c)*(x-c)/(2*d*d))$  Status: Success Number of completed minimizations: 2 Number of iterations: 165 (max: 4000) Time: 5 ms Sum of residuals squared: 0.00065865 Standard deviation: 0.0048501 R<sup>2</sup>: 0.96764 Parameters: a=-0.0049276 b=0.074079 c=-0.00016016 d=-0.0058440 FWHM=0.013 Colocalization based on distance between centres of mass Threshold for Image A=21; Image B=19 Particles size between 0 & 80136 Image A: 15 centre(s) colocalizing out of 67 Image B: 19 centre(s) colocalizing out of 109 Colocalization based on centres of mass-particles coincidence Threshold for Image A=21; Image B=19 Particles size between 0 & 80136 Image A: 5 centre(s) colocalizing out of 67 Image B: 2 centre(s) colocalizing out of 109.

FIGS. 10(A)-(C) are a series of confocal images showing LRBA is co-localized with Rab4 demonstrated by confocal microscopy and JACoP software. Pearson's Coefficient: r=0.395 Overlap Coefficient: r=0.46 r<sup>2</sup>=k1×k2: k1=0.735 k2=0.288 Using thresholds (thrA=3 and thrB=12) Overlap Coefficient: r=0.596 r<sup>2</sup>=k1×k2: k1=0.954 k2=0.372 Manders' Coefficients (original): M1=0.764 (fraction of A overlapping B) M2=0.806 (fraction of B overlapping A) Manders' Coefficients (using threshold value of 3 for imgA and 12 for imgB): M1=0.638 (fraction of A overlapping B) M2=0.728 (fraction of B overlapping A) Costes' automatic threshold set to 2 for imgA & 7 for imgB Pearson's Coefficient: r=0.172 (0.0 below thresholds) M1=0.988 & M2=0.984 Van Steensel's Cross-correlation Coefficient between H293LRBAgreenframes.tif and H293Rab4red(1) frames.tif: CCF min.: 0.259 (obtained for dx=20) CCF max.: 0.395 (obtained for dx=0) Results for fitting CCF on a Gaussian (CCF= $a+(b-a)\exp(-(xshift-c)^2/(2d^2))$ ): Formula:  $y=a+(b-a)\exp(-(x-c)*(x-c)/(2*d*d))$  Status: Success Number of completed minimizations: 2 Number of iterations: 92 (max: 4000) Time: 1 ms Sum of residuals squared: 0.0051683 Standard deviation: 0.011367 R<sup>2</sup>: 0.90661 Parameters: a=0.26934 b=0.36942 c=0.68039 d=6.78003 FWHM=15.965 pixels Cytofluorogram's parameters: a: 0.627 b: 6.485 Correlation coefficient: 0.395 Li's Intensity correlation coefficient: ICQ: 0.3393714371437143 Costes' randomization based colocalization: Parameters: Nb of randomization rounds: 1000, Resolution (bin width): 0.0010 r (original)=0.395 r (randomized)=0.0±-0.0030 (calculated from the fitted data) P-value=100.0% (calculated from the fitted data) Results for fitting the probability density function on a Gaussian (Probability= $a+(b-a)\exp(-(R-c)^2/(2d^2))$ ): Formula:  $y=a+(b-a)\exp(-(x-c)*(x-c)/(2*d*d))$  Status: Success Number of completed minimizations: 2 Number of iterations: 155 (max: 4000) Time: 1 ms Sum of residuals squared: 0.00064254 Standard deviation: 0.0055315 R<sup>2</sup>: 0.98428 Parameters: a=5.76543E-5 b=0.12117 c=-7.94034E-5 d=-0.0032634 FWHM=0.0070 Colocalization based on distance between centres of mass Threshold for Image A=3; Image B=12 Particles size between 0 & 213312 Image A: 351 centre(s) colocalizing out of 996 Image B: 251 centre(s) colocalizing out of 455 Colocalization based on centres of mass-particles coincidence Threshold for Image A=3; Image B=12 Particles size

between 0 & 213312 Image A: 9 centre(s) colocalizing out of 996 Image B: 5 centre(s) colocalizing out of 455.

FIGS. 11(A)-(C) are a series of confocal images showing LRBA is co-localized with β-Adaptin demonstrated by confocal microscopy and JACoP software. Pearson's Coefficient: r=0.234 Overlap Coefficient: r=0.345 r<sup>2</sup>=k1×k2: k1=0.171 k2=0.694 Using thresholds (thrA=84 and thrB=30) Overlap Coefficient: r=0.798 r<sup>2</sup>=k1×k2: k1=0.492 k2=1.294 Manders' Coefficients (original): M1=0.541 (fraction of A overlapping B) M2=0.693 (fraction of B overlapping A) Manders' Coefficients (using threshold value of 84 for imgA and 30 for imgB): M1=0.226 (fraction of A overlapping B) M2=0.303 (fraction of B overlapping A) Costes' automatic threshold set to 2 for imgA & 5 for imgB Pearson's Coefficient: r=0.061 (0.0 below thresholds) M1=0.999 & M2=0.979 Van Steensel's Cross-correlation Coefficient between H293adaptinb(red).tif and H293LRBA(green).tif: CCF min.: 0.076 (obtained for dx=20) CCF max.: 0.234 (obtained for dx=0) Results for fitting CCF on a Gaussian (CCF= $a+(b-a)\exp(-(xshift-c)^2/(2d^2))$ ): Formula:  $y=a+(b-a)\exp(-(x-c)*(x-c)/(2*d*d))$  Status: Success Number of completed minimizations: 2 Number of iterations: 93 (max: 4000) Time: 1 ms Sum of residuals squared: 0.0050619 Standard deviation: 0.011249 R<sup>2</sup>: 0.92969 Parameters: a=0.074437 b=0.20971 c=-2.50994 d=10.06241 FWHM=23.695 pixels Cytofluorogram's parameters: a: 0.123 b: 5.619 Correlation coefficient: 0.234 Li's Intensity correlation coefficient: ICQ: 0.24554066463945545 Costes' randomization based colocalization: Parameters: Nb of randomization rounds: 1000, Resolution (bin width): 0.0010 r (original)=0.234 r (randomized)=0.0±-0.0010 (calculated from the fitted data) P-value=100.0% (calculated from the fitted data) Results for fitting the probability density function on a Gaussian (Probability= $a+(b-a)\exp(-(R-c)^2/(2d^2))$ ): Formula:  $y=a+(b-a)\exp(-(x-c)*(x-c)/(2*d*d))$  Status: Success Number of completed minimizations: 2 Number of iterations: 214 (max: 4000) Time: 2 ms Sum of residuals squared: 0.00014031 Standard deviation: 0.0041879 R<sup>2</sup>: 0.99885 Parameters: a=-0.0011198 b=0.32906 c=-0.00010102 d=-0.0011592 FWHM=0.0020.

FIGS. 12(A)-(C) are a series of confocal images showing LRBA is co-localized with early endosome protein EEA1 demonstrated by confocal microscopy and JACoP software. Pearson's Coefficient: r=0.153 Overlap Coefficient: r=0.193 r<sup>2</sup>=k1×k2: k1=0.353 k2=0.106 Using thresholds (thrA=10 and thrB=19) Overlap Coefficient: r=0.801 r<sup>2</sup>=k1×k2: k1=1.358 k2=0.472 Manders' Coefficients (original): M1=0.448 (fraction of A overlapping B) M2=0.262 (fraction of B overlapping A) Manders' Coefficients (using threshold value of 10 for imgA and 19 for imgB): M1=0.215 (fraction of A overlapping B) M2=0.185 (fraction of B overlapping A) Costes' automatic threshold set to 2 for imgA & 3 for imgB Pearson's Coefficient: r=0.05 (0.0 below thresholds) M1=0.993 & M2=0.968 Van Steensel's Cross-correlation Coefficient between H293LRBAgreenframes.tif and H293EEA1red1mcropped2frames.tif: CCF min.: 0.048 (obtained for dx=-20) CCF max.: 0.153 (obtained for dx=0) Results for fitting CCF on a Gaussian (CCF= $a+(b-a)\exp(-(xshift-c)^2/(2d^2))$ ): Formula:  $y=a+(b-a)\exp(-(x-c)*(x-c)/(2*d*d))$  Status: Success Number of completed minimizations: 2 Number of iterations: 104 (max: 4000) Time: 4 ms Sum of residuals squared: 0.0030669 Standard deviation: 0.0087563 R<sup>2</sup>: 0.91752 Parameters: a=0.058253 b=0.13982 c=-0.46218 d=5.72505 FWHM=13.481 pixels Cytofluorogram's parameters: a: 0.277 b: 3.149 Correlation coefficient: 0.153 Li's Intensity correlation coefficient: ICQ:

0.36891260097958145 Costes' randomization based colocalization: Parameters: Nb of randomization rounds: 1000, Resolution (bin width): 0.0010 r (original)=0.154 r (randomized)=0.0±0.0010 (calculated from the fitted data) P-value=100.0% (calculated from the fitted data) Results for fitting the probability density function on a Gaussian (Probability=a+(b-a)exp(-(R-c)^2/(2d^2))): Formula: y=a+(b-a)\*exp(-(x-c)\*(x-c)/(2\*d\*d)) Status: Success Number of completed minimizations: 2 Number of iterations: 184 (max: 4000) Time: 3 ms Sum of residuals squared: 0.00045802 Standard deviation: 0.0059357 R^2: 0.99305 Parameters: a=0.0017604 b=0.19444 c=-0.00015210 d=0.0019903 FWHM=0.0040.

FIGS. 13(A)-(D) are montages of time-lapse videos of live macrophage cells. The BEACH-WD domain of mouse Lrba gene was cloned into pEGFP-N1 vector as described previously (Wang, et al., Identification of a novel lipopolysaccharideinducible gene with key features of both A kinase anchor proteins and chs1/beige proteins. 2001. *J Immunol* 166: 4586-4595). RAW264.7 macrophage cells were stably transfected with LRBA (BEACH-WD)-GFP and were stimulated with (top panel) or without LPS (bottom panel). The time-lapse video was taken at one picture per second using the Leica TCS SP2 laser scanning inverted confocal microscope with a mini cell culture chamber at 37° C. and 5% CO<sub>2</sub>. The GFP fluorescence shows cell membrane, Golgi and vesicle locations of LRBA, and the dynamic activities of LRBA associated vesicles moving from GC to the membrane. The pictures were ordered sequentially as the original video and labeled accordingly. The smaller numbers indicate vesicle paths.

FIGS. 13E-H are montages of time-lapse videos of live macrophage cells. The BEACH-WD domain of mouse Lrba gene was cloned into pEGFP-N1 vector as described previously (Wang, et al., Identification of a novel lipopolysaccharideinducible gene with key features of both A kinase anchor proteins and chs1/beige proteins. 2001. *J Immunol* 166: 4586-4595). RAW264.7 macrophage cells were stably transfected with LRBA (BEACH-WD)-GFP and were stimulated with (top panel) or without LPS (bottom panel). The time-lapse video was taken at one picture per second using the Leica TCS SP2 laser scanning inverted confocal microscope with a mini cell culture chamber at 37° C. and 5% CO<sub>2</sub>. The GFP fluorescence shows cell membrane, Golgi and vesicle locations of LRBA, and the dynamic activities of LRBA associated vesicles moving from GC to the membrane. The pictures were ordered sequentially as the original video and labeled accordingly. The smaller numbers indicate vesicle paths.

FIGS. 13I-J are montages of time-lapse videos of live macrophage cells. The BEACH-WD domain of mouse Lrba gene was cloned into pEGFP-N1 vector as described previously (Wang, et al., Identification of a novel lipopolysaccharideinducible gene with key features of both A kinase anchor proteins and chs1/beige proteins. 2001. *J Immunol* 166: 4586-4595). RAW264.7 macrophage cells were stably transfected with LRBA (BEACH-WD)-GFP and were stimulated with (top panel) or without LPS (bottom panel). The time-lapse video was taken at one picture per second using the Leica TCS SP2 laser scanning inverted confocal microscope with a mini cell culture chamber at 37° C. and 5% CO<sub>2</sub>. The GFP fluorescence shows cell membrane, Golgi and vesicle locations of LRBA, and the dynamic activities of LRBA associated vesicles moving from GC to the membrane. The pictures were ordered sequentially as the original video and labeled accordingly. The smaller numbers indicate vesicle paths.

FIGS. 13K-L are montages of time-lapse videos of live macrophage cells. The BEACH-WD domain of mouse Lrba gene was cloned into pEGFP-N1 vector as described previously (Wang, et al., Identification of a novel lipopolysaccharideinducible gene with key features of both A kinase anchor proteins and chs1/beige proteins. 2001. *J Immunol* 166: 4586-4595). RAW264.7 macrophage cells were stably transfected with LRBA (BEACH-WD)-GFP and were stimulated with (top panel) or without LPS (bottom panel). The time-lapse video was taken at one picture per second using the Leica TCS SP2 laser scanning inverted confocal microscope with a mini cell culture chamber at 37° C. and 5% CO<sub>2</sub>. The GFP fluorescence shows cell membrane, Golgi and vesicle locations of LRBA, and the dynamic activities of LRBA associated vesicles moving from GC to the membrane. The pictures were ordered sequentially as the original video and labeled accordingly. The smaller numbers indicate vesicle paths.

FIGS. 13M-N are montages of time-lapse videos of live macrophage cells. The BEACH-WD domain of mouse Lrba gene was cloned into pEGFP-N1 vector as described previously (Wang, et al., Identification of a novel lipopolysaccharideinducible gene with key features of both A kinase anchor proteins and chs1/beige proteins. 2001. *J Immunol* 166: 4586-4595). RAW264.7 macrophage cells were stably transfected with LRBA (BEACH-WD)-GFP and were stimulated with (top panel) or without LPS (bottom panel). The time-lapse video was taken at one picture per second using the Leica TCS SP2 laser scanning inverted confocal microscope with a mini cell culture chamber at 37° C. and 5% CO<sub>2</sub>. The GFP fluorescence shows cell membrane, Golgi and vesicle locations of LRBA, and the dynamic activities of LRBA associated vesicles moving from GC to the membrane. The pictures were ordered sequentially as the original video and labeled accordingly. The smaller numbers indicate vesicle paths.

FIGS. 13O-P are montages of time-lapse videos of live macrophage cells. The BEACH-WD domain of mouse Lrba gene was cloned into pEGFP-N1 vector as described previously (Wang, et al., Identification of a novel lipopolysaccharideinducible gene with key features of both A kinase anchor proteins and chs1/beige proteins. 2001. *J Immunol* 166: 4586-4595). RAW264.7 macrophage cells were stably transfected with LRBA (BEACH-WD)-GFP and were stimulated with (top panel) or without LPS (bottom panel). The time-lapse video was taken at one picture per second using the Leica TCS SP2 laser scanning inverted confocal microscope with a mini cell culture chamber at 37° C. and 5% CO<sub>2</sub>. The GFP fluorescence shows cell membrane, Golgi and vesicle locations of LRBA, and the dynamic activities of LRBA associated vesicles moving from GC to the membrane. The pictures were ordered sequentially as the original video and labeled accordingly. The smaller numbers indicate vesicle paths.

FIGS. 14(A) and (B) are graphs showing LPS stimulates LRBA-positive vesicles movements. RAW264.7 macrophage cells stably transfected with pBWEGFP were cultured in a glass bottom dish and put into the culture chamber. LPS was added at final concentration of 100 ng/ml. The time-lapse video of four living cells was taken at one picture per second using the Leica TCS SP2 laser scanning inverted confocal microscope with a mini cell culture chamber at 37° C. and 5% CO<sub>2</sub>. (A) Average speed of LRBA-associated vesicles; (B) Average maximum speed of LRBA-associated vesicles; The two tails and unpaired T test p values: \*\*\*p<0.001; \*p<0.0138 (A); \*\*\*p<0.0005; \*p<0.0117 (B).

LPS 3 min indicates that the measurements were obtained 3 min after adding LPS into the media.

FIGS. 15(A)-(B) are a series of graphs showing knock-down of LRBA decreases the TACI levels on B cells. Raji B cells and Raji-9 (stably transfected with shRNA plasmid against LRBA) B cells were stained with TACI antibody (Hu CD267 APC 1A1-K21-M22, BD BioSciences) and DAPI for dead/live discrimination. A, B. Raji-9 (LRBA Knock-down);

FIGS. 15C-D are a series of graphs showing knockdown of LRBA decreases the TACI levels on B cells. Raji B cells and Raji-9 (stably transfected with shRNA plasmid against LRBA) B cells were stained with TACI antibody (Hu CD267 APC 1A1-K21-M22, BD BioSciences) and DAPI for dead/live discrimination. C, D. Raji (LRBA Wild Type).

FIGS. 15E-F are a series of graphs showing knockdown of LRBA decreases the TACI levels on B cells. Raji B cells and Raji-9 (stably transfected with shRNA plasmid against LRBA) B cells were stained with TACI antibody (Hu CD267 APC 1A1-K21-M22, BD BioSciences) and DAPI for dead/live discrimination. E, Average expression levels of TACI on B cells. F. Flow Cytometry Cell Percentage.

FIGS. 16(A)-(C) are a series of graphs showing knock-down of LRBA decreases the surface levels of TLR4, CD21 and TACI on B cells. Raji B cells and Raji-9 (stably transfected with shRNA plasmid against LRBA) B cells were stained with TLR4, CD21 and TACI antibody (BD BioSciences) and DAPI or 7AAD for dead/live discrimination.

FIG. 16D is a graph showing knockdown of LRBA decreases the surface levels of TLR4, CD21 and TACI on B cells. Raji B cells and Raji-9 (stably transfected with shRNA plasmid against LRBA) B cells were stained with TLR4, CD21 and TACI antibody (BD BioSciences) and DAPI or 7AAD for dead/live discrimination.

FIG. 17(A)-(B) are a series of graphs showing knock-down of LRBA increases the TLR4 levels in A549 cells. A549 cells and A549 pLasiGFP cells (stably transfected with shRNA plasmid against LRBA) were treated with LPS (1  $\mu$ g/ml). The TLR4 concentrations were detected by Western blot. Cells were cultured in 6-well plates and stimulated with LPS (1  $\mu$ g/ml) for different time as shown, then lysed with RIPA buffer. Western blots were carried out. TLR4 antibody (sc-1351, Santa Cruz Biotechnology, Santa Cruz, USA) was used at 1:500 ratio and incubated at 4° C. overnight. BioRad ChemiDoc XRS and Quantity One software were used to acquire gel image and measure band relative intensity. (A) Western blot. 1. A549 No LPS, 2. A549 LPS 30 min, 3. A549 LPS 1 hr, 4. A549 LPS 2 h, 5. A549 LPS 4 h, 6. A549 LPS 24 h, 7. A549 pLasiGFP LPS 2 h, 8. A549 pLasiGFP LPS 4 h, 9. A549 pLasiGFP LPS 24 h. (B) Band intensity quantification from A.

FIG. 17C is a graph showing knockdown of LRBA increases the TLR4 levels in A549 cells. A549 cells and A549 pLasiGFP cells (stably transfected with shRNA plasmid against LRBA) were treated with LPS (1  $\mu$ g/ml). The TLR4 concentrations were detected by Western blot. Cells were cultured in 6-well plates and stimulated with LPS (1  $\mu$ g/ml) for different time as shown, then lysed with RIPA buffer. Western blots were carried out. TLR4 antibody (sc-1351, Santa Cruz Biotechnology, Santa Cruz, USA) was used at 1:500 ratio and incubated at 4° C. overnight. BioRad ChemiDoc XRS and Quantity One software were used to acquire gel image and measure band relative intensity. (C) TNF $\alpha$  levels in A549 and A549 pLasiGFP cells were compared side by side.

FIGS. 18(A) and (B) are a series of images showing LRBA translocates to the nucleus upon LPS stimulation. Mouse (C57BL/6J) bone marrow stromal cells were cultured on glass cover slips with (A) or without (B) LPS (1  $\mu$ g/ml) stimulation for 3 hours, then fixed, permeabilized, and stained following the immuno-fluorescence staining protocol from the Human Protein Atlas Project (Sigma). The LRBA Prestige antibodies and three Golgi protein primary antibodies from BD Biosciences were used at 1:500 (volume to volume dilution). The anti-mouse IgG-Alexa Fluor® 555, and anti-rabbit IgG-Alexa Fluor 488 (Invitrogen) secondary antibodies were used at 1:400. The images were acquired with an Olympus FV1000 scanning confocal microscope by sequential scanning with 0.5  $\mu$ m per slice. Green=LRBA; Red=GM130; Blue=Nucleus.

FIGS. 19(A)-(B) are graphs showing plasma or extracellular LRBA levels are increased significantly in inflammation. (A) Mice stimulated with LPS (1  $\mu$ g/g body weight) for 6 hours. (B) OVA induced asthma mouse model.

FIGS. 19C-D are graphs showing plasma or extracellular LRBA levels are increased significantly in inflammation. (C) Asthma patients with an exacerbation or controlled symptoms; (D) Human mononuclear leukocytes stimulated with LPS (1  $\mu$ g/ml). LPS was derived from *Escherichia coli* 0111:B4 (Sigma, St. Louis, Mo.). LRBA levels were determined by LRBA ELISA Kit using 100  $\mu$ l of plasma or conditioned media in each well, following the manufacturer's protocol.

FIG. 20 is a graph showing knockdown of LRBA promotes B cell proliferations. Raji B cells and Raji9 B cells (Raji B cells stably transfected with shRNA plasmid against LRBA) were culture on a 96 well plate with 10 cells per well for 11 days. Viable cells were counted by the Trypan blue live/dead discrimination method with a Hemocytometer.

FIG. 21 are graphs showing knockdown of LRBA increases the TNF $\alpha$  levels in Raji B (Burkitt's lymphoma) cells. Raji B cells and Raji-9 (stably transfected with shRNA plasmid against LRBA) B cells were treated with LPS (1  $\mu$ g/ml). The TNF $\alpha$  concentrations were measured by Human TNF $\alpha$  DuoSet ELISA kit (R&D) following the manufacturer's instruction. A. Culture supernatant; B. Cell lysate. #= $p$ <0.07, \*= $p$ <0.05, \*\*= $p$ <0.005.

FIG. 22 is a graph showing dominant negative mutants of LRBA decrease the TNF $\alpha$  levels in THP1 cells (Human acute monocytic leukemia cell line). THP1 cells were transfected with LRBA dominant negative constructs with different domains. LIR1=LRBA-VHSLIR1, LIRII=LRBA-VHS and LIRIII=LRBA-LIR3; PhmsiGFP is the construct that expresses shRNA described in the text. After 24 hrs transfection, cells were stimulated with LPS at 1  $\mu$ g/ml for deferent time periods. TNF $\alpha$  levels in the cell culture supernatant were measured as in FIG. 21.

FIGS. 23(A)-(B) are three-dimensional structure remodeling shows that the LIR can form a complex with LC3 more stable than that of p62, a known LC3 binding protein. Tyrosine is in the hydrophobic pocket (A) and phosphorylation of the tyrosine in the LIR destabilizes the complex (B). Confocal microscopy confirmed the interaction

FIGS. 23C-E are three-dimensional structure remodeling shows that the LIR can form a complex with LC3 more stable than that of p62, a known LC3 binding protein. Tyrosine is in the hydrophobic pocket. (C). Green (GFP) and red (RFP) fluorescent protein genes were fused with LRBA and LC3 genes, respectively, and co-transfected into HeLa cervical cancer, A549 adenocarcinomic alveolar basal epithelial and HEK293 embryonic kidney human cells, and Raw264.7 macrophage tumor mouse cells. Three-dimen-



31

sional structure remodeling, confocal microscopy, and immunofluorescence assays (IFA) were utilized. Representative images of LC3 expression (C), LRBA expression (D), and both LC3 and LRBA (D) were shown.

FIGS. 24(A) and (B) are a three-dimensional structure remodeling of LIR and LC3 interaction. (A) The LIR (dark gray) from LRBA is predicted to form a complex with LC3 (light gray) more stable than that of p62, a known LC3 binding protein. Tyrosine is in a hydrophobic pocket. (B) Phosphorylation of the tyrosine in the LIR destabilizes the complex. Phospho-Tyrosine is hydrophobic. Its side chain is away from the hydrophobic pocket and the LC3.

FIG. 25 is a graph showing blockage of LRBA promotes THP1 cell proliferations. THP1 cells (Human acute monocytic leukemia cell line) were cultured in 100  $\mu$ l of RPMI1640 media with or without human LRBA polyclonal IgG antibody (Novus Biologicals, Littleton, USA. NBP1-90764) at 0.67  $\mu$ g/ml or same amount of human Actin polyclonal IgG antibody (Santa Cruz Biotechnology, Santa Cruz, USA. SC-1616) on a 96 well plate with 10 cells per well for 9 days. Viable cells were counted by the Trypan blue live/dead discrimination method with a Hemocytometer.

FIGS. 26(A)-(B) show LRBA is important for cell growth. A. Knockout of LRBA inhibits cell growth in mouse ES cells. LRBA double knockout (KO) ES cell clones were obtained by culturing LRBA single KO cells with 1 mg/ml G418 for about two weeks and confirmed by PCR genotyping. 4000 cells of LRBA<sup>+/+</sup>, LRBA<sup>+/-</sup> and LRBA<sup>-/-</sup> were plated into each well of a 96-well plate. Cell numbers were counted by Trypan blue staining every 12 hours for 3.5 days using a hemocytometer. Each time point had three wells. B. Colony-forming assay (CFA) of HEK293 cells transfected with LRBA dominant negative constructs with different domains. One million cells were plated and 400  $\mu$ g/ml of G418 was used to select positive clones for about 20 days. Then, the clone numbers were counted.

FIGS. 26C-D show LRBA is important for cell growth. C. The full length of murine LRBA coding sequence was cloned into pEGFP-C1. A positive clone (pmLRBAGFP) was identified by EcoRI and BamHI digestion and sequencing. D. The pmLRBAGFP plasmid DNA was transfected into H293 cells. Stable clones were selected with 500  $\mu$ g/ml of G418 for 25 days.

FIG. 26E shows that LRBA is important for cell growth. E. CFA of A549 was obtained from the same experiments as in B.

FIG. 27 shows LRBA promoter region of -438 to +43 (relative to the translation start codon as boxed). Putative binding sites for NF- $\kappa$ B and p53 factors are shown. The two NF $\kappa$ B binding sites are highly homologous to the B element (GGGACTTTCC) at 90% and 80%, respectively, and conserved in mouse and human. The arrows indicate the mutations are created in reporter constructs. Luciferase gene are fused in-frame with LRBA 5' coding sequence as shown.

FIGS. 28(A)-(D) are a series of images showing LRBA is regulated by Ubiquitin-dependent protein degradation system. HEK293 (Human embryo kidney) cells were seeded in 24 well plates at  $4 \times 10^5$  per well overnight, then transfected with 0.8 ng of the following plasmid DNAs per well with Lipofectamine-2000 following the manufacturer's instruction: (A) MG132-treated cells transfected with pLRBA-VHSLIR, (B) MG132-treated cells transfected with pLRBA-VHS, (C) MG132-treated cells transfected with pLRBA-LIR and (D) MG132-treated cells transfected with cloning vector pEGFP-C3;

FIGS. 28E-H are a series of images showing LRBA is regulated by Ubiquitin-dependent protein degradation sys-

32

tem. HEK293 (Human embryo kidney) cells were seeded in 24 well plates at  $4 \times 10^5$  per well overnight, then transfected with 0.8 ng of the following plasmid DNAs per well with Lipofectamine-2000 following the manufacturer's instruction: (E) PS341-treated cells transfected with pLRBA-VHS-LIR, (F) PS341-treated cells transfected with pLRBA-VHS, (G) PS341-treated cells transfected with pLRBA-LIR and (H) PS341-treated cells transfected with cloning vector pEGFP-C3. After 24 hours, media were changed and cells were treated with MG132 and PS341 at the concentration indicated in the figure and microscopy pictures were taken after overnight.

FIGS. 29(A) and (B) are images showing whole length of LRBA gene is fused with EGFP then transfected into H293 cells. Stable clones were screened with 500  $\mu$ g/ml of G418 for 25 days. The GFP fluorescence pattern of LRBA GFP fusion is similar to that of tubulin. Filaments are seen. The explanation for this that there are many LRBA/GFP associated vesicles traveling along the cytoskeleton filaments.

FIG. 30(A) is an alignment showing LRBA is regulated by microRNAs. (A) Human and mouse LRBA have miR-150 site.

FIG. 30B is an alignment showing LRBA is regulated by microRNAs. (B) Human, mouse and other 21 vertebrate LRBA genes have miR-181 sites.

Hsa	Human	<i>Homo sapiens</i>
Ptr	Chimpanzee	<i>Pan troglodytes</i>
Mnnl	Rhesus	<i>Macaca mulatta</i>
Oga	Bushbaby	<i>Otolemur garnetti</i>
Tbe	Treeshrew	<i>Tupaia belangeri</i>
Mnmu	Mouse	<i>Mus musculus</i>
Rno	Rat	<i>Rattus norvegicus</i>
Cpo	Guinea pig	<i>Cavia porcellus</i>
Ocu	Rabbit	<i>Oryctolagus cuniculus</i>
Sar	Shrew	<i>Sorex araneus</i>
Eeu	Hedgehog	<i>Erinaceus europaeus</i>
Cfa	Dog	<i>Canis familiaris</i>
Fca	Cat	<i>Felis catus</i>
Eca	Horse	<i>Equus caballus</i>
Bta	Cow	<i>Bos taurus</i>
Dno	Armadillo	<i>Dasypus novemcinctus</i>
Laf	Elephant	<i>Loxodonta africana</i>
Ete	Tenrec	<i>Echinops telfairi</i>
Mdo	Opossum	<i>Monodelphis domestica</i>
Oan	Platypus	<i>Ornithorhynchus anatinus</i>
Aca	Lizard	<i>Anolis carolinensis</i>
Gga	Chicken	<i>Gallus gallus</i>
Xtr	Frog	<i>Xenopus tropicalis</i>

FIGS. 30C-D is a series of blots showing LRBA is regulated by microRNAs. (C). Western blot results show LRBA is downregulated by overexpression miR-150. (D) Western blot results show LRBA is downregulated by overexpression miR-181.

FIGS. 31(A) and (B) are a blot and graph showing knockdown of LRBA decreases the total NF $\kappa$ B levels in A549 cells. A549 LIRII cells (stably transfected with pLRBA-VHS) and A549 pLAsiGFP cells (stably transfected with shRNA plasmid against LRBA) were treated with LPS (1  $\mu$ g/ml). The NF $\kappa$ B concentrations were detected by Western blot. Cells were cultured in 6-well plates and stimulated with LPS (1  $\mu$ g/ml) for different time as shown, then lysed with RIPA buffer. Western blots were carried out. NF- $\kappa$ B2 p100/p52 Antibody #4882 (Cell Signaling Technology, Danvers, Mass., USA) was used at 1:500 ratio and incubated at 4° C. overnight. BioRad ChemiDoc XRS and



Quantity One software were used to acquire gel image and measure band relative intensity. A. Western blot. B. Band intensity quantification from A.

FIG. 32(A)-(C) are graphs showing plasma or extracellular LRBA levels are increased significantly in inflammation. LRBA levels are increased significantly in plasma from mice stimulated with LPS (A, n=3, 4) or OVA (B, n=3, 5), in culture media of human mononucleocytes stimulated with LPS (C, n=5,11)

FIG. 32D is a graph showing plasma or extracellular LRBA levels are increased significantly in inflammation. In plasma from subjects at first visit (D, n=4) compared to the second and third (with controlled symptoms, n=2, 2) visits (inset: LRBA Western blot, plasma supernatant (S) & membrane (M) fractions from ultracentrifugation).

FIG. 32E is a graph showing proinflammatory cytokine TNF $\alpha$  levels are decreased in plasma of mice contacted with LRBA antibody as compared to those contacted with control IgG antibody.

FIG. 32F is a graph showing proinflammatory cytokine IL-6 levels are decreased in plasma of mice contacted with LRBA antibody as compared to those contacted with control IgG antibody.

FIGS. 33(A)-(C) are a series of graphs showing a mouse model and LRBA antibodies treatment. Asthma patients with an exacerbation or controlled symptoms. Cell survival is increased by knockdown (A) or antibody blockage (B) seen in THP1 cells (n=5) of LRBA. (C) Two million splenocytes from C57BL/6J mice were culture in 24-well plate with 500  $\mu$ l culture media, with 2  $\mu$ g/ml LRBA antibodies (9415) or anti-rabbit IgG control antibodies for 24 hours under LPS (1  $\mu$ g/ml) stimulation. Anti-mouse TACI antibodies were used to detect TACI.

FIG. 34(A)-(B) are graphs showing LPS regulates BAFFR in vivo and in vitro. C57BL/6J mice of 2-month age were injected intraperitoneally with LPS (5  $\mu$ g/g body weight) or PBS (control). For in vitro LPS stimulation, cells from mouse spleen or bone marrow were cultured with or without LPS (1  $\mu$ g/ml) for 24 hr. Cells were stained with fluorophores-conjugated BAFFR and TACI antibodies and DAPI for dead/live discrimination and analyzed with cytometry. (A) Splenocytes without LPS-P3, (B) bone marrow cells without LPS-P3. Negative gating was based on B220 negative cells, which are negative for BAFFR and TACI. Numbers other than percentage are arbitrary MFI units. All experiments were done in triplicate for in the vitro experiment and data shown is representative of two separate experiments.

FIGS. 34C-D are graphs showing LPS regulates BAFFR in vivo and in vitro. C57BL/6J mice of 2-month age were injected intraperitoneally with LPS (5  $\mu$ g/g body weight) or PBS (control). For in vitro LPS stimulation, cells from mouse spleen or bone marrow were cultured with or without LPS (1  $\mu$ g/ml) for 24 hr. Cells were stained with fluorophores-conjugated BAFFR and TACI antibodies and DAPI for dead/live discrimination and analyzed with cytometry. (C) splenocytes with LPS for 24 hours, (D) bone marrow cells with LPS for 24 hours. Negative gating was based on B220 negative cells, which are negative for BAFFR and TACI. Numbers other than percentage are arbitrary MFI units. All experiments were done in triplicate for in the vitro experiment and data shown is representative of two separate experiments.

FIGS. 34E-F are graphs showing LPS regulates BAFFR in vivo and in vitro. C57BL/6J mice of 2-month age were injected intraperitoneally with LPS (5  $\mu$ g/g body weight) or PBS (control). For in vitro LPS stimulation, cells from

mouse spleen or bone marrow were cultured with or without LPS (1  $\mu$ g/ml) for 24 hr. Cells were stained with fluorophores-conjugated BAFFR and TACI antibodies and DAPI for dead/live discrimination and analyzed with cytometry. (E) splenocytes control, (F) bone marrow cell control. Negative gating was based on B220 negative cells, which are negative for BAFFR and TACI. Numbers other than percentage are arbitrary MFI units. All experiments were done in triplicate for in the vitro experiment and data shown is representative of two separate experiments.

FIGS. 34G-H are graphs showing LPS regulates BAFFR in vivo and in vitro. C57BL/6J mice of 2-month age were injected intraperitoneally with LPS (5  $\mu$ g/g body weight) or PBS (control). For in vitro LPS stimulation, cells from mouse spleen or bone marrow were cultured with or without LPS (1  $\mu$ g/ml) for 24 hr. Cells were stained with fluorophores-conjugated BAFFR and TACI antibodies and DAPI for dead/live discrimination and analyzed with cytometry. (G) splenocyte control at 24 hours in PBS, and (H) bone marrow cell control at 24 hours in PBS. TACI is upregulated by LPS in vivo (n=3 for each group) and in vitro in both tissues. Negative gating was based on B220 negative cells, which are negative for BAFFR and TACI. Numbers other than percentage are arbitrary MFI units. All experiments were done in triplicate for in the vitro experiment and data shown is representative of two separate experiments.

FIG. 35(A)-(C) are graphs showing LPS regulates TACI in vivo and in vitro. C57BL/6J mice of 2 month age were injected intraperitoneally with LPS (5  $\mu$ g/g body weight) or PBS (upper panels). For in vitro LPS stimulation, cells from mouse spleen or bone marrow were cultured with or without LPS (1  $\mu$ g/ml) (lower panels) for 24 hr. Cells were stained with fluorophores-conjugated BAFFR and TACI antibodies and DAPI for dead/live discrimination and analyzed with cytometry. TACI is upregulated by LPS in vivo (n=3 for each group) and in vitro in both tissues. Negative gating was based on B220 negative cells, which are negative for BAFFR and TACI. (A) in vivo splenocytes treated with PBS; (B) in vivo bone marrow cells treated with PBS; (C) in vivo splenocytes treated with LPS; Numbers other than percentage are arbitrary MFI units. All experiments were done in triplicate for in the vitro experiment and data shown is representative of two separate experiments.

FIG. 35D-F are graphs showing LPS regulates TACI in vivo and in vitro. C57BL/6J mice of 2 month age were injected intraperitoneally with LPS (5  $\mu$ g/g body weight) or PBS (upper panels). For in vitro LPS stimulation, cells from mouse spleen or bone marrow were cultured with or without LPS (1  $\mu$ g/ml) (lower panels) for 24 hr. Cells were stained with fluorophores-conjugated BAFFR and TACI antibodies and DAPI for dead/live discrimination and analyzed with cytometry. TACI is upregulated by LPS in vivo (n=3 for each group) and in vitro in both tissues. Negative gating was based on B220 negative cells, which are negative for BAFFR and TACI. (D) in vivo bone marrow cells treated with LPS; (E) in vitro splenocytes treated with PBS; (F) in vitro bone marrow cells treated with PBS; Numbers other than percentage are arbitrary MFI units. All experiments were done in triplicate for in the vitro experiment and data shown is representative of two separate experiments.

FIG. 35G-H are graphs showing LPS regulates TACI in vivo and in vitro. C57BL/6J mice of 2 month age were injected intraperitoneally with LPS (5  $\mu$ g/g body weight) or PBS (upper panels). For in vitro LPS stimulation, cells from mouse spleen or bone marrow were cultured with or without LPS (1  $\mu$ g/ml) (lower panels) for 24 hr. Cells were stained with fluorophores-conjugated BAFFR and TACI antibodies

35

and DAPI for dead/live discrimination and analyzed with cytometry. TACI is upregulated by LPS in vivo (n=3 for each group) and in vitro in both tissues. Negative gating was based on B220 negative cells, which are negative for BAFFR and TACI. (G) in vitro splenocytes treated with LPS; (H) in vitro bone marrow wells treated with LPS. Numbers other than percentage are arbitrary MFI units. All experiments were done in triplicate for in the vitro experiment and data shown is representative of two separate experiments.

FIGS. 36(A)-(B) are graphs showing repression of LRBA by shRNA knockdown influences the levels of TLR4, multiple CVID receptors. Raji B cells were transfected with LRBA shRNA plasmid and control plasmid and stable clones were obtained by G418 selection. Cells were treated with LPS (1  $\mu$ g/ml) for 15 min (1), 30 min (2), 1 h (3), 2 h (4), 4 h (5), 24 h (6). Cells were stained with fluorophores-conjugated Cells were stained for CVID antibodies and DAPI for dead/live discrimination and analyzed with cytometry. CVID antibodies were BAFFR (A), CD19 (B), and TACI (C). A. Median fluorescence intensity (MFI): LRBA WT(●), LRBA KD (x); B. Percentage: LRBA WT (■), LRBA KD (▲). Data are representative of 2 to 3 separate experiments. MG132 was used.

FIG. 36C is a graph showing repression of LRBA by shRNA knockdown influences the levels of TLR4, multiple CVID receptors. Raji B cells were transfected with LRBA shRNA plasmid and control plasmid and stable clones were obtained by G418 selection. Cells were treated with LPS (1  $\mu$ g/ml) for 15 min (1), 30 min (2), 1 h (3), 2 h (4), 4 h (5), 24 h (6). Cells were stained with fluorophores-conjugated Cells were stained for CVID antibodies and DAPI for dead/live discrimination and analyzed with cytometry. CVID antibodies were BAFFR (A), CD19 (B), and TACI (C). A. Median fluorescence intensity (MFI): LRBA WT(●), LRBA KD (x); B. Percentage: LRBA WT (■), LRBA KD (▲). Data are representative of 2 to 3 separate experiments. MG132 was used.

FIGS. 37(A)-(B) are graphs showing repression of LRBA by shRNA knockdown influences the levels of TLR4, multiple CVID receptors. Raji B cells were transfected with LRBA shRNA plasmid and control plasmid and stable clones were obtained by G418 selection. Cells were treated with LPS (1  $\mu$ g/ml) for 15 min (1), 30 min (2), 1 h (3), 2 h (4), 4 h (5), 24 h (6). Cells were stained with fluorophores-conjugated CVID antibodies and DAPI for dead/live discrimination and analyzed with cytometry. CVID antibodies were BAFFR (A), CD19 (B), and TACI (C). A. Median fluorescence intensity (MFI): LRBA WT(●), LRBA KD (x); B. Percentage: LRBA WT (■), LRBA KD (▲). Data are representative of 2 to 3 separate experiments. PS341 was used.

FIG. 37C is a graph showing repression of LRBA by shRNA knockdown influences the levels of TLR4, multiple CVID receptors. Raji B cells were transfected with LRBA shRNA plasmid and control plasmid and stable clones were obtained by G418 selection. Cells were treated with LPS (1  $\mu$ g/ml) for 15 min (1), 30 min (2), 1 h (3), 2 h (4), 4 h (5), 24 h (6). Cells were stained with fluorophores-conjugated CVID antibodies and DAPI for dead/live discrimination and analyzed with cytometry. CVID antibodies were BAFFR (A), CD19 (B), and TACI (C). A. Median fluorescence intensity (MFI): LRBA WT(●), LRBA KD (x); B. Percentage: LRBA WT (■), LRBA KD (▲). Data are representative of 2 to 3 separate experiments. PS341 was used.

FIG. 38(A)-(F) are graphs showing the effects of LRBA knockdown using dominant negative influences the levels of

36

multiple CVID receptors. LRBA WT and LRBA KD Raji cells were stimulated with LPS, and the cell surface levels of CVID receptors and TLR4 were analyzed by flow cytometry. Raji B cells were electroporated with different LRBA DNMs: 1. LRBA-VHSLIR, 2. LRBA-VHS, 3. LRBA-LIR and 4. LRBA-BEACH. Blues: GFP positive; Red: GFP negatives. Cells were stained with fluorophores-conjugated CVID antibodies and DAPI for dead/live discrimination and analyzed with cytometry. A GFP marker was used to distinguish transfected and untransfected Raji cells. Cells were treated with LPS (1  $\mu$ g/ml) for 24 h. CVID probes were CD19 (A), CD20 (B), BAFFR (C), TACI (D), CD21 (E), and TLR4 (F). Median fluorescence intensity (MFI). LRBA DNM: first column in each series. LRBA WT: second column in each series.

FIG. 39(A)-(F). Repression of LRBA with dominant negative influences the levels of multiple CVID receptors. Raji B cells were electroporated with different LRBA DNMs: 1. LRBA-VHSLIR, 2. LRBA-VHS, 3. LRBA-LIR and 4. LRBA-BEACH. Blues: GFP positive; Red: GFP negatives. Cells were stained with fluorophores-conjugated CVID antibodies and DAPI for dead/live discrimination and analyzed with cytometry. A GFP marker was used to distinguish transfected and untransfected Raji cells. Cells were treated with LPS (1  $\mu$ g/ml) for 24 h. CVID probes were CD19 (A), CD20 (B), BAFFR (C), TACI (D), CD21 (E), and TLR4 (F). Percentage of positive cells were measured.

FIG. 40(A)-(D). LRBA potential dominant negative mutants (DNM) fused with green fluorescent protein (GFP) were constructed from BEACH (Beige and Chediak-Higashi), VHS-LIR [VPS (vacuolar protein sorting), Hrs (hepatocyte growth factor-regulated tyrosine kinase substrate) and STAM (signal transducing adaptor molecule), LC3 (light chain 3) Interacting Region], VHS and LIR domains and transfected into Raji cells. CVID and TLR4 receptors were analyzed in the GFP positive and negative populations. CVID probes were CD21 (A), CD20 (B), TACI (C), and BAFFR (D).

FIGS. 41(A)-(D). LRBA potential dominant negative mutants and wild type were transfected into Raji cells. CVID and TLR4 receptors were analyzed in the GFP positive and negative populations. CVID probes were CD21 (A), CD20 (B), TACI (C), and BAFFR (D).

FIGS. 42(A) and (B). (A) Overexpression of miR-150 down-regulates LRBA. A549 and HEK293 cells transfected with the vectors that overexpress miR-150 or a control miRNA. After 48 hours, cell lysates were prepared and subjected to Western blotting with LRBA antibody. (B) a comparison of LRBA is different species compared to miR-150.

FIG. 43(A)-(B). Proteasome inhibitors decrease the levels of BAFFR and CD19 but increased the levels of TACI. Raji and Raji9 cells were treated with NFkB inhibitors MG-132 and PS-341 at different dose (for MG-132 1 $\times$ =50 nM, 5 $\times$ =250, 100 $\times$ =5000 nM; PS-341: 10 nM, 50, 1000 nM). Raji/MG-132(■), Raji/PS-341(◆), Raji9/MG-132(▲) Raji9/PS-341(x). All samples were stimulated with LPS at 1 mg/ml. Trend lines with short dash are for Raji cells, while trend lines with long dash are for Raji9 cells. Probes were conducted for (A) B220, (B) BAFFR.

FIG. 43C-D. Proteasome inhibitors decrease the levels of BAFFR and CD19 but increased the levels of TACI. Raji and Raji9 cells were treated with NFkB inhibitors MG-132 and PS-341 at different dose (for MG-132 1 $\times$ =50 nM, 5 $\times$ =250, 100 $\times$ =5000 nM; PS-341: 10 nM, 50, 1000 nM). Raji/MG-132(■), Raji/PS-341(◆), Raji9/MG-132(▲), Raji9/PS-341(x). All samples were stimulated with LPS at 1

mg/ml. Trend lines with short dash are for Raji cells, while trend lines with long dash are for Raji9 cells. Probes were conducted for (C) LRBA, and (D) TACI.

FIGS. 44(A) and (B). Proteasome inhibitors have minor effect on the levels of CVID CD69 and TLR4. Raji and Raji9 cells were treated with NFκB inhibitors MG-132 and PS-341 at different dose (for MG-132 1x=50 nM, 5x=250, 100x=5000 nM; PS-341: 10 nM, 50, 1000 nM). Raji/MG-132(■), Raji/PS-341(◆), Raji9/MG-132(▲), Raji9/PS-341(x). All samples were stimulated with LPS at 1 mg/ml. Trend lines with short dash are for Raji cells, while trend lines with long dash are for Raji9 cells. Probes were for CD69 (A) and TLR4 (B).

FIG. 45A-D. Knockdown of LRBA deregulates NFκB. (A) Knockdown of LRBA increases NFκB luciferase activity. An NFκB luciferase reporter was used to measure the NFκB transcription activity. The data are shown as scatter with bar graph of mean with standard error of mean (SEM). (B) Knockdown of LRBA increases phospho-NFκB. The Phosflow kit including Cytofix Fixation Buffer, Phosflow Perm Buffer III and Stain Buffer (BD) and phospho-antibodies, NFκB p65 (pS529) PE-Cy7 were used for the intracellular staining following the company's instruction. For each samples, 50,000 cells were recorded for the FACS assay. (C) A549 cells were stably transfected with LRBA shRNA knockdown plasmid and several clones were picked up. Half million of cells were seeded in a well of a 24 well plate and incubated overnight, then stimulated with LPS (10 μg/ml) for certain time. Luciferase assay Biotium. NFκB luciferase activity is inversely dose-dependent on the LRBA levels in A549 cells with different levels of LRBA knockdown judged by the GFP levels of the cells stably transfected with the LRBA shRNA/GFP construct. (D) LRBA KD#3, LRBA KD#4 and LRBA KD#5 clones express different levels of GFP expression from low to high. The GFP expression levels can be an indicator of shRNA expression levels and are inversely related to the levels of LRBA. The trend line equations are  $y = -1.9597x^6 + 47.904x^5 - 462.33x^4 + 2225.6x^3 - 5526.7x^2 + 6530.5x - 2560$  for LRBA KD;  $y = -2.1153x^6 + 51.396x^5 - 492.3x^4 + 2354.3x^3 - 5846.6x^2 + 7013.3x - 2870$  for LRBA WT. All experiments are representative of 2 to 5 separate experiments.

FIGS. 46(A) and (B). Knockdown of LRBA deregulates NFκB. (A) Time course study. 2 million, Raji cells transfected 2 mg Secreted luciferase plasmid nucleofector 4D, put 96 well plate with 0.5 Clontech were stimulated with LPS for time period as indicated. NFκB luciferase activity was measured at each time point for both cell lines as in A. RLU: Relative Light Units. (B) Trend lines obtained by polynomial fitting at order of 6 from E. The R2 values for both curves are 1. The trend line equations are  $y = -1.9597x^6 + 47.904x^5 - 462.33x^4 + 2225.6x^3 - 5526.7x^2 + 6530.5x - 2560$  for LRBA KD;  $y = -2.1153x^6 + 51.396x^5 - 492.3x^4 + 2354.3x^3 - 5846.6x^2 + 7013.3x - 2870$  for LRBA WT. All experiments are representative of 2 to 5 separate experiments

FIGS. 47(A) and (B). Knockdown of LRBA deregulates MAPKs. Knockdown of LRBA upregulates p38 and JNK but downregulates p42/44. Half million of Raji or Raji9 cells were put in a well in a 6 well plate. After 24 hr, cells were treated with or without LPS for the time as indicated. 200 μl RIPA buffer with protease inhibitors and PMSF. (A) Western blot of cells was performed. 30 μl of cell extracts were loaded to each well. Phosphorylated protein levels were normalized to β-Actin shown as the numbers between the two blots. (B) curves based on the Western blots. Quantity One software was used to quantify the levels.

FIGS. 48(A)-(I). Knockdown of LRBA influences the levels of cytokines. A. Raji cells (LRBA WT or KD) were seeded in a 24 well plate wells and stimulated with LPS for 15 min (1), 30 min (2) and 1 hr (3) with 0.26 million cells in each well or for 2 h (4), 4 h (5) and 24 h (6) with 0.2 million cells in each well. 0.2 million of cells were plated in each well. ELISA and CBA assays of TNFα and IL-10. Cells were treated as in A.  $0.2 \times 10^6$  cells, timepoint. 500 uL total volume medium. Duoset ELISA human TNF-α kit protocol was followed for cell culture supernatant. Blues: Raji (◆); Red: Raji9 (■). Data are representative of 2 to 5 separate experiments.

FIGS. 49(A) through (B) are graphs showing cells with LRBA knockdown cannot fight viral and bacterial infections efficiently. Half million of Raji and Raji9 cells were infected with adenoviruses at 100 multiplicity of infection (MOI) or 50 μl of Gram-negative bacteria from overnight culture. After 24 hours of incubation at 37° C., Apoptosis was detected by Annexin V-PE and 7-AAD. Cells that were double negative (left lower quadrant) were viable, Annexin only positive cells (right lower quadrant) were early phase of apoptosis or other cell death, and double positive cells (right upper quadrant) were end stage apoptosis or dead. \*\*\*\*p<9E-05, \*p<0.007.

FIGS. 49(C) through (D) are graphs showing cells with LRBA knockdown cannot fight viral and bacterial infections efficiently. Half million of Raji and Raji9 cells were infected with adenoviruses at 100 multiplicity of infection (MOI) or 50 μl of Gram-negative bacteria from overnight culture. After 24 hours of incubation at 37° C., Apoptosis was detected by Annexin V-PE and 7-AAD. Cells that were double negative (left lower quadrant) were viable, Annexin only positive cells (right lower quadrant) were early phase of apoptosis or other cell death, and double positive cells (right upper quadrant) were end stage apoptosis or dead. \*\*\*\*p<9E-05, \*p<0.007.

FIG. 50 is graph showing the effect of LRBA expression on immune system function, plotted against NF-κβ activity and time.

#### DETAILED DESCRIPTION OF THE PREFERRED EMBODIMENT

LRBA and its paralogues are proposed to be involved in vesicle trafficking (Shamloula, et al., rugose (rg), a *Drosophila* A kinase Anchor Protein, Is Required for Retinal Pattern Formation and Interacts Genetically With Multiple Signaling Pathways. 2002. *Genetics* 161, 693-710; Montfort, et al., FAN stimulates TNF(α)-induced gene expression, leukocyte recruitment, and humoral response. 2009. *J Immunol* 183, 5369-78) in immune cells. This finding permits use of LRBA for diagnostics, such as biomarkers, and as a treatment methodology.

As used herein, "treat", "treatment", "treating", and the like refer to acting upon a condition, such as autoimmune disease or immunotolerance, with an agent, like anti-LRBA antibodies or LRBA protein, depending on the desired effect, to affect the condition by improving or altering it. The improvement or alteration may include an improvement in symptoms or an alteration in the physiologic pathways associated with the condition. "Treatment," as used herein, covers one or more treatments of a condition in a host (e.g., a mammal, typically a human or non-human animal of veterinary interest), and includes: (a) reducing the risk of occurrence of the condition in a subject determined to be predisposed to the condition but not yet diagnosed, (b) impeding the development of the condition, and/or (c)

relieving the condition, e.g., causing regression of the condition and/or relieving one or more condition symptoms (e.g., reduce inflammation).

As used herein, the terms “prophylactically treat” or “prophylactically treating” refers completely or partially preventing (e.g., about 50% or more, about 60% or more, about 70% or more, about 80% or more, about 90% or more, about 95% or more, or about 99% or more) a condition or symptom thereof and/or may be therapeutic in terms of a partial or complete cure or alleviation for a condition and/or adverse effect attributable to the condition.

A “pharmaceutically acceptable excipient,” “pharmaceutically acceptable diluent,” “pharmaceutically acceptable carrier,” or “pharmaceutically acceptable adjuvant” means an excipient, diluent, carrier, and/or adjuvant that are useful in preparing a pharmaceutical composition that are generally safe, non-toxic and neither biologically nor otherwise undesirable, and include an excipient, diluent, carrier, and adjuvant that are acceptable for veterinary use and/or human pharmaceutical use. “A pharmaceutically acceptable excipient, diluent, carrier and/or adjuvant” as used in the specification and claims includes one or more such excipients, diluents, carriers, and adjuvants.

The term “therapeutically effective amount” as used herein describes concentrations or amounts of components such as antibodies or other agents which are effective for producing an intended result, including preventing further autoimmune disease or immunotolerance, or treating an autoimmune disease, such as rheumatoid arthritis and asthma, or immunotolerance, such as cancer. Compositions according to the present invention may be used to effect a favorable change on immune cells, whether that change is an improvement, such as stopping or reversing the immune disease, or relieving to some extent one or more of the symptoms of the condition being treated, and/or that amount that will prevent, to some extent, one or more of the symptoms of the condition that the host being treated has or is at risk of developing, or a complete cure of the disease or condition treated.

The term “administration” refers to introducing an agent of the present disclosure into a patient. One preferred route of administration of the agent is oral administration. Another preferred route is intravenous administration. However, any route of administration, such as topical, subcutaneous, peritoneal, intraarterial, inhalation, vaginal, rectal, nasal, introduction into the cerebrospinal fluid, or instillation into body compartments can be used.

As used herein, the term “subject,” “patient,” or “organism” includes humans and mammals (e.g., mice, rats, pigs, cats, dogs, and horses). Typical patients to which an agent(s) of the present disclosure may be administered will be mammals, particularly primates, especially humans. For veterinary applications, a wide variety of subjects will be suitable, e.g., livestock such as cattle, sheep, goats, cows, swine, and the like; poultry such as chickens, ducks, geese, turkeys, and the like; and domesticated animals particularly pets such as dogs and cats. For diagnostic or research applications, a wide variety of mammals will be suitable subjects, including rodents (e.g., mice, rats, hamsters), rabbits, primates, and swine such as inbred pigs and the like.

Reagents: Monoclonal antibodies against the following proteins were purchased from BD Biosciences (San Jose, Calif., USA): Annexin II, BiP/GRP78, b-Catenin, Caveolin 1, Connexin-43, EEA1, GM130, CD49b (Integrin  $\alpha 2$ ), Lamp-1, MAP2B, Bcl-2, Nucleoporin p62, Paxillin, ZO-1 (Organelle Sampler Kit, 612740, BD Pharmingen™); AKAP79, AKAP95, AKAP149, AKAP220, AKAP-KL,

MAP2B, PKAC, PKARI, PKARIa, PKARIa, PKARIb (PKA Sampler Kit, 611420 BD Transduction Laboratories™); GM130, Golgin-84, GS15, GS27, GS28, p115, p230 trans Golgi, Rab8, Syntaxin 6, Vti1a, Vti1b (Golgi Sampler Kit, 611434, BD Transduction Laboratories™) and Adaptin a, Adaptin b, Adaptin g, Adaptin d, Amphiphysin, AP180, Clathrin Heavy Chain, EEA1, eps15, b-NAP, Rab4 (Coated Vesicle Sampler Kit, 611424, BD Transduction Laboratories™). The LRBA Prestige antibodies (NBP1-90764) were purchased from Novus Biologicals (Littleton, Colo., USA). The Alexa Fluor Conjugated secondary antibodies: anti-mouse IgG-Alexa Fluor® 555, and anti-rabbit IgG-Alexa Fluor® 488 were purchased from Life Technologies (Grand Island, N.Y., USA).

#### Statistical Analysis

Each experiment is repeated at least three times independently, and each sample assayed in at least triplicate wells or plates to provide statistically meaningful data, and to avoid false data introduced by errors during each experiment. The statistical significance of the experimental results are calculated by using a two tailed unpaired T-test at 95% confidence intervals.  $P < 0.05$  will be considered to be statistically significant.

#### Example 1

Human and mouse LRBA genes were cloned and sequenced (Wang, et al., Deregulated expression of LRBA facilitates cancer cell growth. 2004. *Oncogene* 23, 4089-97; Barrat, et al., Defective CTLA-4 cycling pathway in Chediak-Higashi syndrome: a possible mechanism for deregulation of T lymphocyte activation. 1999. *Proc Natl Acad Sci USA* 96, 8645-50), contributing seven LRBA sequences to GenBank, as seen in NM006726, AF216648, AF188507, AF188506, AF187731, AF188505, AF188504.

LRBA (Seq ID No. 1) is composed of multiple domains, as seen in FIG. 2. The Concanavalin A-like (ConA) lectin binding domain (Burgess, et al., A concanavalin A-like lectin domain in the CHS1/LYST protein, shared by members of the BEACH family 2009. *Bioinformatics* 25: 1219-1222), VHS (Bradshaw, et al., HMMer Thread: detecting remote, functional conserved domains in entire genomes by combining relaxed sequence-database searches with fold recognition. 2011. *PloS one* 6: e17568) [VPS (vacuolar protein sorting)] (Fearon, et al., Regulation of B lymphocyte responses to foreign and self-antigens by the CD19/CD21 complex. 2000. *Annu Rev Immunol* 18, 393-422), Hrs (hepatocyte growth factor-regulated tyrosine kinase substrate) domain and STAM (signal transducing adaptor molecule)], RII binding motifs and WBW super domain. The molecular weight of LRBA predicted from the largest open reading frame (ORF) of LRBA cDNA is 319 KD and similar size of protein was detected by Western blot (Lopez-Herrera, et al., Deleterious Mutations in LRBA Are Associated with a Syndrome of Immune Deficiency and Autoimmunity. *Am J Hum Genet* 90, 986-1001 (2012)). The three-dimensional structure of the WDLBEACH of LRBA has been determined (Gebauer, et al., Crystal structure of the PH-BEACH domains of human LRBA/BGL. 2004. *Biochemistry* 43: 14873-14880).

Human LRBA protein sequence (Seq ID No. 1):  
 MASEDNRVSPPTGDDGGGGREETPTGGGSLKPLPIRGIRMKFAV  
 LTGLVEVGVEVSNRDIVETVFNLLVGGQFDLENNFIIQEGESINCMVDLLE

41

-continued

KCDITCQAEVWSMFTAILKKSIRNLQVCTEVGLVEKVLGKIEKVDNMIAD  
 LLVMDLGLVLA SYNLT VRELKLF FSKLQGD KGRWPPHAGKLLSVLKHPQK  
 YGPD A F N F P G K S A A A I A L P P I A K W P Y Q N G F T F H T W L R M D P V N N I N V D K D  
 K P Y L Y C F R T S K G L G Y S A H F V G G C L I V T S I K S K G K G F Q H C V K F D F K P Q K W Y  
 M V T I V H I N R W K N S E L R C Y V N G E L A S Y G E I T W F V N T S D T F D K C F L G S S E T  
 A D A N R V F C G Q M T A V Y L F S E A L N A A Q I F A I Y Q L G L G Y K G T F K F A E S D L F L  
 A E H H K L L L Y D G K L S S A I A F T Y N P R A T D A Q L C L E S S P K D N P S I F V H S P H A L  
 M L Q D V K A V L T H S I Q S A M H S I G G V Q V L F P L F A Q L D Y R Q Y L S D E I D L T I C S T  
 L L A F I M E L L K N S I A M Q E Q M L A C K G F L V I G Y S L E K S S K S H V S R A V L E L C L A  
 F S K Y L S N L Q N G M P L L K Q L C D H V L L N P A I W I H T P A K V Q L M L Y T Y L S T E F I G  
 T V N I Y N T I R R V G T V L L I M H T L K Y Y W A V N P Q D R S G I T P K G L D G P R N Q K E  
 M L S L R A F L L M F I K Q L V M K D S G V K E D E L Q A I L N Y L L T M H E D D N L M D V L Q L L  
 V A L M S E H P N S M I P A F D Q R N G L R V I Y K L L A S K S E G I R V Q A L K A M G Y F L K H L  
 A P K R K A E V M L G H G L F S L L A E R L M L Q T N L I T M T Y N V L F E I L I E Q I G T Q V I  
 H K Q H P D P D S S V K I Q N P Q I L K V I A T L L R N S P Q C P E S M E V R R A F L S D M I K L F  
 N N S R E N R R S L L Q C S V W Q E W M L S L C Y F N P K N S D E Q K I T E M V Y A I F R I L L Y H  
 A V K Y E W G G W R V W D T L S I T H S K V T F E I H K E N L A N I F R E Q Q K G V D E E I G L C  
 S S T S V Q A A S G I R R D I N V S V G S Q Q P D T K D S P V C P H T T N G N E N S S I E K T S S  
 L E S A N I E L Q T T N T S Y E E M K A E Q E N Q E L P D E G T L E E T L T N E T R N A D D L E V  
 S S D I I E A V A I S S N F I T T G K D S M T V S E V T A S I S S P S E E D A S E M P E F L D K S  
 I V E E E E D D D Y V E L K V E G S P T E A N L P T E L Q D N S L S P A A S E A G E K L D M F G N  
 D D K L I F Q E G K P V T E K Q T D T E T Q D S K D S G I Q T M T A S G S S A M P E T T V S Q I A  
 V E S D L G Q M L E E G K K A T N L T R E T K L I N D C H G S V S E A S S E Q K I A K L D V S N V A  
 T D T E R L E L K A S P N V E A P Q P H R H V L E I S R Q H E P Q G G I A P D A V N G Q R R D S R  
 S T V F R I P E F N W S Q M H Q R L L T D L L F S I E T D I Q M W R S H S T K T V M D F V N S S D N  
 V I F V H N T I H I L S Q V M D N M V M A C G G I L P L L S A A T S A T H E L E N I E P T Q G L S I  
 E A S V T F L Q R L I S L V D L I F A S S L G F T E I E A E K S M S S G G I L R Q C L R L V C A V  
 A V R N C L E C Q Q H S Q L K T R G D K A L K P M H S L I P L G K S A A K S P V D I V T G G I S P V  
 R D L D R L L Q D M D I N R L R A V V F R D I E D S K Q A Q F L A L A V V Y F I S V L M V S K Y R D  
 I L E P Q N E R H S Q S C T E T G S E N E N V S L S E I T P A A F S T L T T A S V E S E S T S S A  
 R R R D S G I G E E T A T G L G S H V E V T P H T A P P G V S A G P D A I S E V L S T L S L E V N K  
 S P E T K N D R G N D L D T K A T P S V S V S K N V N K D I L R S L V N I P A D G V T V D P A L L  
 P P A C L G A L G D L S V E Q P V Q R S F D R S V I V A A K S A V S P S T F N T S I P T N A V S  
 V V S S V D S A Q A S D M G G E S P G S R S S N A K L P S V P T V D S V S Q D P V S N M S I T E R L  
 E H A L E K A A P L L R E I F V D F A P F L S R T L L G S H G Q E L L I E G T S L V C M K S S S S V  
 V E L V M L L C S Q E W Q N S I Q K N A G L A F I E L V N E G R L L S Q T M K D H L V R V A N E A E  
 F I L S R Q R A E D I H R H A E F E S L C A Q Y S A D K R E D E K M C D H L I R A A K Y R D H V T A  
 T Q L I Q K I I N I L T D K H G A W G N S A V S R P L E F W R L D Y W E D D L R R R R R F V R N P L  
 G S T H P E A T L K T A V E H V C I F K L R E N S K A T D E D I L A K G K Q S I R S Q A L G N Q N S  
 E N E I L L E G D D D T L S S V D E K D L E N L A G P V S L S T P A Q L V A P S V V V K G T L S V T  
 S S E L Y F E V D E E D P N F K K I D P K I L A Y T E G L H G K W L F T E I R S I F S R R Y L L Q N

42

-continued

TALEIFMANRVAVMFNFPDPATVKKVNYLPRVGVGTSGFLPQTRRISLA  
 SPRQLFKASNMTQRWQHREISNFEYLMFLNTIAGRSYNDLNQYPVPFWVI  
 5 TNYESEELDLTLPTNFRDLSPKIGALNPKRAFFAERYESWEDDQVPKPH  
 YGTHYSTASFLAWLLRIEPFTTYFLNLQGGICPDHADRTFSSISRARN  
 SQRDTSDIKELIPEFYLPPEMFVNFNNYNLGVMDGTVVSDELPPWAKT  
 10 SEEFVHINRLALESEFVSCQLHQWIDLIFGYKQQGPEAVRALNVFYLYTY  
 EGAVNLNSITDPVLEAVEAQIRSFQQTSPQLLIEPHPPRGSAMQVSPLM  
 FTDKAQQDVIMVLKFPSPNSPVTHVAANTQPLATPAVITVTANRLFAVVK  
 15 WHNLPAHQGAVQDQPYQLPVEIDPLIASNTGMHRRQITDLDDQSIQVHSQ  
 CFVITSDNRYILVCGFWDKSFRVYSTDTGRLIQVVFHWDVVTCLARSES  
 YIGGNCYILSGSRDATLLWYWGKCSGIGDNPGSETAAPRAILTGHDIYE  
 20 VTCAAVCAELGLVLSGSQEGPCLIHSMNGDLLRTLEGPENCLPKLIQAS  
 REGHCVIFYENGLFCTFSVNGKLQATMETDDNIRAIQLSRDGQYLLTGDD  
 RGVVVVRQVSDLKQLFAYPGCDAGIRAMALSVDQRCIISGMASGSIVLFY  
 25 NDNFRWHHEYQTRY

The ConA-like lectin domain was proposed to bind oligosaccharide associated with protein traffic and sorting, especially in relation with the vesicle fusion machinery (Burgess, et al., A concanavalin A-like lectin domain in the CHS1/LYST protein, shared by members of the BEACH family 2009. *Bioinformatics* 25: 1219-1222). The ConA domain was predicted in LRBA and other four LRBA paralogues (Burgess, et al., A concanavalin A-like lectin domain in the CHS1/LYST protein, shared by members of the BEACH family 2009. *Bioinformatics* 25, 1219-2).

The VHS domain is considered to have a general membrane targeting/cargo recognition role in vesicular trafficking by binding sorting receptors that move and transfer cargo between the trans-Golgi network and the endosomal compartment (Lohi, et al., VHS domain—a longshoreman of vesicle lines. 2002. *FEBS letters* 513: 19-23; Misra, et al., Structure of the VHS domain of human Tom1 (target of myb 1): insights into interactions with proteins and membranes. 2000. *Biochemistry* 39, 11282-90). LRBA contains two potential RII binding sites for anchoring PKA through the RII subunits (Wang, et al., Identification of a novel lipopolysaccharide-inducible gene with key features of both A kinase anchor proteins and chs1/beige proteins. 2001. *J Immunol* 166, 4586-95; Hou, et al., Prediction of peptides binding to the PKA RIIalpha subunit using a hierarchical strategy. 2011. *Bioinformatics* 27, 1814-21).

The WBW super-domain at the C-terminal is composed of a WDL and BEACH domain and five WD40 repeats. This same super-domain C-terminal architecture is shared by various large proteins which define the WBW family. The WDL is structurally similar to the pleckstrin homology (PH) domain and strongly interacts with the BEACH domains. The interface between WDL and BEACH two domains form a prominent groove which may be used to recruit binding partners (Gebauer, et al., Crystal structure of the PH-BEACH domains of human LRBA/BGL. 2004. *Biochemistry* 43, 14873-14880; Jögl, et al., Crystal structure of the BEACH domain reveals an unusual fold and extensive association with a novel PH domain. 2002. *Embo Journal* 21, 4785-4795). LRBA GFP fusion protein is associated with vesicles, suggesting that BEACH and/or WD40

domains are involved in vesicle-binding or can form a dimer with LRBA or other proteins including WBW proteins (Wang, et al., Identification of a novel lipopolysaccharide-inducible gene with key features of both A kinase anchor proteins and chs1/beige proteins. 2001. *J Immunol* 166, 4586-95).

LRBA also contains a microtubule-associated protein 1 light chain 3 (LC3) interaction region LC3 interaction region (LIR), which is shared in both human and murine LRBA. The LIR consensus sequence is [DE]-[DE]-[DE]-[WFY]-X-X-[LIV] (Birgisdottir, et al., The LIR motif—crucial for selective autophagy. 2013. *J Cell Sci* 126, 3237-47; Seq ID No. 2). The DDDYVEL (Seq ID No. 3) sequence from LRBA has high homology with LIR from TP53INP1 (similarity is 92%) and TP53INP249, as seen in Table 2.

TABLE 2

The potential LIR of LRBA has high homology with two known LIR motifs			
Seq ID No.	Gene	LIR sequence	Length
4	LIR-TP53INP1	EKEDDEWILVDFI	13
2	LIR-LRBA	EEEDDDYVELKVE	13
5	LIR-TP53INP2	EDEVGDWLIIDL	13
	homology	*.* .: : : .	

Three dimensional structure remodeling (YASARA v12.7.16) shows that the LIR forms a complex with LC3 which is more stable than with p62, a known LC3 binding protein, as seen in FIGS. 23(A) and 24.

Interestingly, mutated LRBA proteins cannot be detected in LRBA deficient patients by Western blot (Lopez-Herrera, et al., Deleterious Mutations in LRBA Are Associated with a Syndrome of Immune Deficiency and Autoimmunity. 2012. *Am J Hum Genet* 90, 986-1001; Burns, et al., LRBA gene deletion in a patient presenting with autoimmunity without hypogammaglobulinemia. *J Allergy Clin Immunol* 130, 1428-32 (2012). Alangari, A. et al., LPS-responsive beige-like anchor (LRBA) gene mutation in a family with inflammatory bowel disease and combined immunodeficiency. 2012. *J Allergy Clin Immunol* 130, 481-8 e2).

It was previously suggested that LRBA is involved in vesicle trafficking for polarized secretion and/or membrane deposition of immune effector molecules, as seen by LRBA's subcellular localizations obtained by over-expressing a part of Lrba (the BEACH-WD40 super-domain) fused with the EGFP gene (BWGFP). The BWGFP fusion protein was colocalized with the vesicular system, including the Golgi complex, lysosomes, ER, plasma membrane, and perinuclear ER demonstrated by GFP fluorescence confocal microscopy and Immunoelectron microscopy. (Wang, et al., Identification of a novel lipopolysaccharide-inducible gene with key features of both A kinase anchor proteins and chs1/beige proteins. 2001. *Journal of immunology* (Baltimore, Md.: 1950) 166, 4586-4595) However, as the BWGFP fusion protein can interfere with the function of the endogenous LRBA, (Wang, J. W., Gamsby, J. J., Highfill, S. L., Mora, L. B., Bloom, G. C., Yeatman, T. J., Pan, T. C., Ramne, A. L., Chodosh, L. A., Cress, W. D., et al. (2004). Deregulated expression of LRBA facilitates cancer cell growth. *Oncogene* 23, 4089-4097) and GFP tag also interferes with protein function, (Yewdell, J. W., Lacsina, J. R., Rechsteiner, M. C., and Nicchitta, C. V. (2011). Out with the

old, in with the new? Comparing methods for measuring protein degradation. *Cell biology international* 35, 457-462) and only a part of LRBA gene is used for the colocalization study. Moreover, the organelle-specific antibodies were not used in the previous study. (Wang, J. W., Howson, J., Haller, E., and Kerr, W. G. (2001). Identification of a novel lipopolysaccharide-inducible gene with key features of both A kinase anchor proteins and chs1/beige proteins. *Journal of immunology* (Baltimore, Md.: 1950) 166, 4586-4595). The LysoTracker Red used in the previous study can be photoconverted to a green fluorescent molecule. (Freundt, E. C., Czapiga, M., and Lenardo, M. J. (2007). Photoconversion of LysoTracker Red to a green fluorescent molecule. *Cell research* 17, 956-958). Therefore, it is still not clear whether the subcellular localization of the fusion protein is the same as that of the endogenous LRBA protein.

Subcellular LRBA colocalization was analyzed against known organelle proteins using immunofluorescence staining and confocal microscopy to better understand the cellular and molecular mechanisms by which LRBA functions in the cell.

RAW264.7, A549, and HEK293 cell lines (American Type Culture Collection, Manassas, Va., USA) at concentration of  $5 \times 10^6$ /ml were plated on glass coverslips in Dulbecco's modified minimum essential medium (D-MEM) supplemented with 10% fetal calf serum (Gemini Bio-Products, West Sacramento, Calif.), penicillin and streptomycin, according to ATCC instructions in Dulbecco's modified minimum essential medium (DMEM) or RPMI1640 supplemented with 10% FBS and penicillin-streptomycin (5,000 IU/ml penicillin and 5,000  $\mu$ g/ml streptomycin). BMMs were obtained by the protocol described by Weischenfeldt, et al. (Weischenfeldt & Porse, Bone Marrow-Derived Macrophages (BMM): Isolation and Applications. 2008. *CSH Protoc* 2008, pdb prot5080). Bone marrow cells were obtained by flushing the femurs and tibias from 8-12-week-old C57BL/6 wild type mice and LRBA<sup>-/-</sup> mice, and the bone marrow cells plated in 10-cm bacteriological plastic plates at  $2 \times 10^6$  cells/mL with 10% FCS in RPMI 1640 supplemented with 100 ng/ml of recombinant murine M-CSF. On day 7, BMMs were plated at  $1 \times 10^5$  cells/ml in 24-well plates and cultured with or without 100 ng/ml of LPS for 7 h (Nagai, et al., Essential role of MD-2 in LPS responsiveness and TLR4 distribution. 2002. *Nat Immunol* 3, 667-72).

After 24 h of stimulation, cells were fixed, permeabilized, and stained following the immuno-fluorescence staining protocol from the Human Protein Atlas Project (Sigma). Briefly, growth medium was removed and the cells were washed in 1xPBS, the cells were fixed for 15 minutes in ice cold 4% paraformaldehyde pH 7.2-7.3 in growth medium supplemented with 10% fetal bovine serum (FBS). The cells were permeabilized 3 times for 5 minutes each with 0.1% TRITON® X-100 in PBS. The cells were washed with 1xPBS and incubated overnight at 4° C. with the primary antibodies, disclosed above, in 1xPBS supplemented with 4% FBS. The following day the cells were washed 4 times for 10 minutes each with 1xPBS and incubated for 1.5 hours at room temperature with the secondary antibodies in 1xPBS supplemented with 4% FBS. The cells were counterstained for 4 minutes with the nuclear stain DAPI (0.6  $\mu$ M in 1xPBS). The cells were washed 4 times for 10 minutes with 1xPBS and then mounted in glycerol+10% 10xPBS. The LRBA antibodies and three Golgi protein primary antibodies were used at 1:500 (volume to volume dilution). The anti-mouse IgG-Alexa Fluor® 555, and anti-rabbit IgG-Alexa Fluor® 488 secondary antibodies were used at 1:400. The

confocal imaging was acquired with an Olympus FV1000 MPE multiphoton laser scanning microscope using 60× objective (U Plan APO 1.42 N.A. oil) and sequential scanning with 0.5 µm per slice. Colocalization analysis for dual stained samples was carried out using JACoP and FV10-ASW software.

Colocalization analysis for dual stained samples was carried out using JACoP and FV10-ASW software. JACoP (Just Another Colocalization Plugin) integrates current global statistic methods and a novel object-based approach (Bolte, et al., A guided tour into subcellular colocalization analysis in light microscopy. 2006. *Journal of microscopy* 224: 213-232). All of the following features were used: Calculating a set of commonly used co-localization indicators: Pearson's coefficient, Overlap coefficient, k1 & k2 coefficients, Manders' coefficient, Cytofluorogram for generating commonly used visualizations, Costes' automatic threshold, Costes' randomization, Li's intensity correlation coefficient, and two objects based methods: distances between centers and center-particle coincidence. The calculated P-value of 100% based on the Costes' randomization colocalization in the JACoP suggests that colocalization in the regions masked in white is highly probable (Bolte, et al., A guided tour into subcellular colocalization analysis in light microscopy. 2006. *Journal of microscopy* 224: 213-232).

LRBA is mainly localized to the GC, as demonstrated by the co-localization of LRBA with three Golgi proteins; two golgins (GM-130 and P-230) and another GC protein (GS-28), as seen in FIGS. 7-11. The GC is a central organelle in the endomembrane system, and viewed as the "headquarters" for signal transduction and cell-fate decisions, controlling mitotic entry, cytoskeleton organization and dynamics, calcium homeostasis, and plasma membrane receptor-initiated and organelle-autochthonous signaling events, in addition to its "classic role" of cargo sorting/processing and metabolism (Wilson, et al., The Golgi apparatus: an organelle with multiple complex functions. 2011. *Biochem J* 433: 1-9).

Immunofluorescent confocal microscopy indicated endogenous LRBA colocalized with Golgi proteins (GM-130, P-230, and GS-28) and with EEA1, an early endosome marker. The overlap between LRBA and GM-130 is 62% in one million cells, seen in FIG. 4. GM-130 is a coiled-coil protein associated with the Golgi matrix necessary for tethering events in membrane fusion and has a role in maintaining cis-Golgi structure (Barr, & Short, Golgins in the structure and dynamics of the Golgi apparatus. 2003. *Current opinion in cell biology* 15: 405-413; Nakamura, et al., Characterization of a cis-Golgi matrix protein, GM130. 1995. *The Journal of cell biology* 131: 1715-1726; Puthenveedu, et al., GM130 and GRASP65-dependent lateral cis-terial fusion allows uniform Golgi-enzyme distribution. 2006. *Nature cell biology* 8: 238-248). P-230 is associated with vesicles budding from the trans-Golgi network (Gleeson, et al., p230 is associated with vesicles budding from the trans-Golgi network. 1996. *Journal of cell science* 109 (Pt 12): 2811-2821) and required for the regulated secretion of TNF (Lieu, et al., A trans-Golgi network golgin is required for the regulated secretion of TNF in activated macrophages in vivo. 2008. *Proceedings of the National Academy of Sciences of the United States of America* 105: 3351-3356). GS28 is a 28-kDa membrane protein that plays an essential role in mammalian endoplasmic reticulum (ER)-Golgi or intra-Golgi vesicle transport (Subramaniam, et al., GS28, a 28-kilodalton Golgi SNARE that participates in ER-Golgi transport. 1996. *Science* 272: 1161-1163), found to protect p53 from degradation (Sun, et al., Golgi-SNARE GS28

potentiates cisplatin-induced apoptosis by forming GS28-MDM2-p53 complexes and by preventing the ubiquitination and degradation of p53. 2012. *The Biochemical journal* 444: 303-314).

The immunofluorescence confocal microscopy results show that LRBA also colocalized with EEA1, Clathrin, Rab4 and Adaptin-β, FIGS. 5(A) through (I), 6(A) through (C), 7(A) through (C), 8(A) through (C), 9(A) through (C), 10(A) through (C), 11(A) through (C). EEA1 is an early endosome marker; Clathrin is a vesicle coating protein, shown in FIGS. 12(A) through (C), and Adaptin-β, seen in FIGS. 11(A) through (C), is an adaptor protein that mediates the formation of vesicles by Clathrin-coated pits, through interaction with membrane-bound receptors. Rab4 a member of the RAB family of RAS-related GTP-binding proteins, important regulators of vesicular transport and are located in specific intracellular compartments. Rab4A is a master regulator of receptor recycling from endocytic compartments to the plasma membrane (Goueli, et al., TBC1D16 is a Rab4A GTPase activating protein that regulates receptor recycling and EGF receptor signaling. 2012. *Proceedings of the National Academy of Sciences of the United States of America* 109: 15787-15792). Vesicle trafficking is required for homeostasis (deposition, recycling and degradation) of cell membrane proteins.

Immunofluorescence confocal microscopy results also demonstrated that LRBA colocalized with tubulin in the microtubules, as seen in FIGS. 8(A)-(C). The results also were supported by the H293 cells stably transfected with a plasmid that overexpresses the full length of Lrba tagged with EGFP at the C-terminal. Cell skeleton association of the Lrba/EGFP fusion protein is demonstrated.

LRBA was predicted to have two RII binding motifs (Wang, et al., Identification of a novel lipopolysaccharide-inducible gene with key features of both A kinase anchor proteins and chs1/beige proteins. 2001. *J Immunol* 166: 4586-4595) and its orthologue in *Drosophila rugose* (rg) is an A kinase anchor protein (AKAP) (Han, et al., Molecular characterization of a novel A kinase anchor protein from *Drosophila melanogaster*. 1997. *The Journal of biological chemistry* 272: 26611-26619). PKA, also known as cAMP-dependent protein kinase, functions based on its location or its anchor protein and is involved in various membrane trafficking events including the generation of vesicles at the trans-Golgi network (TGN) for both constitutive and regulated secretion (Ohashi & Huttner, An elevation of cytosolic protein phosphorylation modulates trimeric G-protein regulation of secretory vesicle formation from the trans-Golgi network. 1994. *The Journal of biological chemistry* 269: 24897-24905; Muniz, et al., Protein kinase A activity is required for the budding of constitutive transport vesicles from the trans-Golgi network. 1997. *Proceedings of the National Academy of Sciences of the United States of America* 94: 14461-14466). LRBA contains two potential RII binding motifs for anchoring PKA through the type II regulatory subunits (RII) (Wang, et al., Identification of a novel lipopolysaccharide-inducible gene with key features of both A kinase anchor proteins and chs1/beige proteins. 2001. *J Immunol* 166: 4586-4595). A computer program, which has over 80 percent accuracy to predict RII binding motifs, predicted one of the two potential RII binding motifs (Hou, et al., Prediction of peptides binding to the PKA RIIα subunit using a hierarchical strategy. 2011. *Bioinformatics* 27: 1814-1821). A previous study suggests that LRBA may not bind the RII subunit (Wang, et al., Neurobeachin: A protein kinase A-anchoring, beige/Chediak-higashi protein homolog implicated in neuronal membrane traffic. 2000. *The*

*Journal of neuroscience: the official journal of the Society for Neuroscience* 20: 8551-8565). However, LRBA was found to colocalized with the RII $\beta$ , RII $\alpha$  and RIIc subunits of PKA, as seen in FIGS. 6(A)-(C), contradicting the previous study and indicating it binds to PKA directly.

LRBA also colocalized with nucleus in mouse bone marrow cells, shown in FIGS. 4-11 and colocalized with Lysosome-associated membrane glycoprotein (Lamp) in A549 cells (Data not shown).

Time lapse video was taken for living macrophage cells. RAW264.7 macrophage cells stably transfected with pBWEGFP were cultured in a glass bottom dish and put into the mini cell culture chamber at 37° C. and 5% CO<sub>2</sub> in a Leica TCS SP2 laser scanning inverted confocal microscope. LPS was added at final concentration of 100 ng/ml. The time-lapse video of four living cells was taken at one picture per second using the Avg. timelapse interval: 1000.05 ms (1.0 Hz) (+/-8.9 ms); Initial SAC Position: 1700; Objective: 100 $\times$  (magnification: 100.00 $\times$ ); Mag. changer: EMCCD (magnification: 1.00 $\times$ ); 8 inring: 1 $\times$ 1; Channel 1: c488em at 50 ms. Gain: 3 Intensification: 700 ND: 60 [Independent]. The time-lapse video was taken at one picture per second using the Leica TCS SP2 laser scanning inverted confocal microscope with a mini cell culture chamber at 37° C. and 5% CO<sub>2</sub>.

Snapshots from a time lapse video of a live cell show that LRBA-positive vesicles are budding from Golgi and moving to cell membrane. These processes accelerate within minutes of LPS stimulation, seen in FIGS. 5(A)-(I). These data strongly correlate with previous information (Wang, et al., Identification of a novel lipopolysaccharide-inducible gene with key features of both A kinase anchor proteins and chs1/beige proteins. 2001. *J Immunol* 166: 4586-4595) and the data from Human Protein Atlas Project (Fagerberg, et al., Contribution of Antibody-based Protein Profiling to the Human Chromosome-centric Proteome Project (C-HPP). 2012. *Journal of proteome research* 12(6):2439-48). This indicates that LRBA is dynamically involved in vesicle trafficking.

The RAW 264.7 cells were stably transfected with a plasmid expressing LRBA BEACH-WD/EGFP fusion protein to study the subcellular localizations of LRBA as described (Wang, et al., Identification of a novel lipopolysaccharide-inducible gene with key features of both A kinase anchor proteins and chs1/beige proteins. 2001. *J Immunol* 166: 4586-4595). Confocal time lapse video was used to observe vesicle trafficking. The results show that LRBA-associated vesicles are isolated from Golgi area, traveling along cytoskeleton, towards cell membrane and fused with the cell membrane. LRBA-associated vesicles forming at the cell membrane were also observed, seen in FIGS. 13(A)-(H). The uneven distribution of LRBA-GFP on the cell membrane and vesicles were observed, indicating that LRBA may not be a component of these structures, rather a regulator of these structures, seen in FIGS. 13(I) to (P). The results confirm the data obtained by IF that LRBA is located at the Golgi, vesicle and cell membrane. LRBA associated vesicles are very active in the pseudopodia. The vesicle movements respond to LPS stimulation quickly: the average speed of vesicles doubles 3 min after adding LPS into the media, but slows down to original levels after 5 and 23 min, as seen in FIGS. 14(A) and (B), Table 3.

TABLE 3

Path Movement Statistics of LRBA-Associated Vesicles (Manual Path).					
Path	Average Speed (microns/sec)	Maximum Speed (microns/sec)	Total Displacement (microns)	Path duration (time points)	Path duration (sec)
No LPS					
0	0.1669	0.2947	3.17	20	19
1	0.1794	0.35	3.404	20	19
2	0.7541	0.9724	1.504	3	1.99
3	0.1378	0.2832	5.648	42	41
4	0.1823	0.3607	5.286	30	29
5	0.1947	0.3451	5.841	31	30
6	0.1991	0.412	3.983	21	20
7	0.4725	1.15	1.413	4	2.99
8	0.2055	0.4228	2.875	15	14
9	0.1795	0.34	1.795	11	10
10	0.1755	2.99	1.93	12	11
11	0.2019	0.3402	1.817	10	9
12	0.4894	0.7241	2.44	6	4.98
13	0.1128	0.2282	2.597	24	23
14	0.153	0.2674	4.59	31	30
15	0.2782	0.3785	0.8321	4	2.99
16	0.3228	0.3782	0.6436	3	1.99
17	0.1191	0.2674	2.62	23	22
18	0.1472	0.2282	1.765	13	12
19	0.4228	0.4228	0.4215	2	0.997
20	0.1521	0.299	3.648	25	24
21	0.5979	0.8969	1.192	3	1.99
LPS (100 ng/ml) 3 min					
0	0.838	1.183	1.684	3	2.01
1	0.2647	0.3559	1.056	5	3.99
2	0.8811	1.302	1.757	3	1.99
3	0.2441	0.4091	3.421	15	14
4	0.4695	1.09	3.291	8	7.01
5	0.1914	0.467	2.105	12	11
6	0.9217	1.185	6.46	8	7.01
7	0.314	0.4174	1.888	7	6.01
8	0.1812	0.4847	2.535	15	14
9	0.6408	0.8366	1.917	4	2.99
10	0.1748	0.2694	1.051	7	6.01
11	0.3406	0.4748	1.698	6	4.98
12	0.5446	1.07	2.715	6	4.99
13	0.2439	0.4224	2.439	11	10
14	0.3444	0.7056	2.404	8	6.98
15	0.6841	1.15	3.41	6	4.98
16	0.2469	0.6685	1.977	9	8.01
17	0.8842	1.304	3.553	5	4.02
18	0.3985	0.6356	1.589	5	3.99
19	0.7431	0.9641	1.482	3	1.99
20	1.034	2.365	4.153	5	4.02
21	0.3936	1.017	3.543	10	9
22	0.8833	1.338	3.523	5	3.99
LPS (100 ng/ml) 5 min					
0	0.216	0.3656	1.514	8	7.01
1	0.338	0.5667	4.728	15	14
2	0.2072	0.4058	3.105	16	15
3	0.3326	0.406	2.994	10	9
4	0.3394	0.6398	4.409	14	13
5	0.1072	0.2006	0.855	9	7.98
6	0.2481	0.3905	5.456	23	22
7	0.1717	0.2832	3.263	20	19
LPS (100 ng/ml) 23 min					
0	0.1798	0.36	1.081	7	6.01
1	0.2899	0.4821	3.188	12	11
2	0.2219	0.2832	2.219	11	10
3	0.2321	0.3555	4.179	19	18
4	0.2982	0.5082	4.171	15	14

Membrane trafficking is crucial to the transduction of signaling complexes to the GC and other cellular locations (Kholodenko, Four-dimensional organization of protein kinase signaling cascades: the roles of diffusion, endocytosis and molecular motors. 2003. *The Journal of experimental*



biology 206: 2073-2082). Thus the endomembrane system plays a critical role in signal transduction. Previous data show that LRBA regulates two cell membrane receptors: epidermal growth factor receptor (EGFR) and NOTCH (Wang, et al., Deregulated expression of LRBA facilitates cancer cell growth. 2004. *Oncogene* 23: 4089-4097; Volders, et al., *Drosophila* rugose is a functional homolog of mammalian Neurobeachin and affects synaptic architecture, brain morphology, and associative learning. 2012. *The Journal of neuroscience: the official journal of the Society for Neuroscience* 32: 15193-15204; Yatim, et al., NOTCH1 nuclear interactome reveals key regulators of its transcriptional activity and oncogenic function. 2012. *Molecular cell* 48: 445-45), and regulates CVID receptors (Lopez-Herrera, et al., Mutations in LRBA are Associated with a Syndrome of Immune Deficiency and Autoimmunity. 2012. *Journal of Clinical Immunology* 32: 363-364).

The data show that LRBA is co-localized to several components of PKA: the catalyst unit, RII $\beta$  and RII $\alpha$ , supporting that LRBA is an AKAP and can phosphorylate substrate proteins such as NF $\kappa$ B (Gao, et al., Neddylation of a breast cancer-associated protein recruits a class III histone deacetylase that represses NF $\kappa$ B-dependent transcription. 2006. *Nature cell biology* 8: 1171-1177), which is central to the immune system. The Golgi complex and TGN are major subcellular locations of RII (De Camilli, et al., Heterogeneous distribution of the cAMP receptor protein RII in the nervous system: evidence for its intracellular accumulation on microtubules, microtubule-organizing centers, and in the area of the Golgi complex. 1986. *The Journal of cell biology* 103: 189-203; Griffiths, et al., Ultrastructural localization of the regulatory (RII) subunit of cyclic AMP-dependent protein kinase to subcellular compartments active. 1990. *J Cell Sci.* 96 (Pt 4):691-703).

Well characterized LRBA polyclonal antibody and organelle-specific antibodies were used to detect endogenous proteins and study their co-localizations to LRBA. LRBA appears imperative to the GC's function, as LRBA is highly co-localized with GC proteins and LRBA-deficient B cells show an abnormally high number of GCs (Lopez-Herrera, et al., Deleterious Mutations in LRBA Are Associated with a Syndrome of Immune Deficiency and Autoimmunity. 2012. *American journal of human genetics* 90: 986-1001).

Endogenous LRBA is co-localized with multiple endomembrane proteins including Golgi proteins (GM-130, P-230, and GS-28), EEA1, PKA Rub and RIIc subunits, Tubulin, Clathrin, Rab4 and Adaptin, seen in FIGS. 6(A)-11(C). LRBA appears to be involved in endocytosis based on co-localization staining results. EEA1 is an early endosome marker, Clathrin is a vesicle coating protein, and Adaptin-B is an adaptor protein. Adaptins are proteins that mediate the formation of vesicles by Clathrin-coated pits, through interaction with membrane-bound receptors.

Additionally, Golgi co-localization of LRBA was demonstrated by in primary mouse cultured adherent bone marrow cells, as seen in FIGS. 6(A)-12(C). This shows that LRBA is mainly localized to the GC and dynamically involved in vesicle trafficking. LRBA associated vesicles are very active in the pseudopodia, indicating that LRBA may be involved in forming and growth of pseudopodia membrane.

The data support a two-stimulation model of vesicle trafficking for WBW proteins using LRBA as a prototype, as seen in FIG. 1, which was modified from a previous model (Wang, et al., Identification of a novel lipopolysaccharide-inducible gene with key features of both A kinase anchor proteins and chs1/beige proteins. 2001. *J Immunol* 166:

4586-4595). It suggests that two stimulations are required for LRBA function: the first stimulation is required to recruit LRBA to the membrane structure, such as GC and plasma membrane; while the second stimulation involves cAMP production and is required to activate the PKA anchored by LRBA. After the first stimulation of an immune cell, LRBA binds to the GC, plasma membrane or ER, and is involved in the sorting of cargo proteins, forming vesicles containing proteins for secretion or deposition on the plasma membrane. LRBA also may be involved in vesicle movements along microtubules to the plasma membrane where the PKA anchored by LRBA may be activated by the second messenger cyclic adenosine monophosphate (cAMP). PKA then phosphorylates the intracellular sequences of the membrane receptor/ligand complexes.

The WD domain of LRBA binds to the phosphorylated sequences to mediate the fusion of the vesicles with the membrane to release the cargo proteins or deposit membrane proteins on the plasma membrane of immune cells.

LRBA plays a role in membrane/vesicle trafficking and signal transduction required for the regulation and function of many immune molecules. The co-localization results show that LRBA is extensively associated with the endomembrane/vesicle trafficking system, including Golgi complex, endosome, lysosome and plasma membrane, indicating that LRBA is involved in membrane/vesicle trafficking, and LRBA deficiency may cause defective trafficking and signaling of immune effector molecules, resulting in immunodeficiency and autoimmunity diseases. (Kovanen, P. E., and Leonard, W. J. (2004). Cytokines and immunodeficiency diseases: critical roles of the gamma(c)-dependent cytokines interleukins 2, 4, 7, 9, 15, and 21, and their signaling pathways. *Immunol Rev* 202, 67-83).

## Example 2

Lipopolysaccharide (LPS)-responsive beige-like anchor (LRBA) critical in cell proliferation and survival. LRBA was initially identified as an LPS-upregulated gene, with structural similarity to lysosomal trafficking regulator (LYST in human; beige in mouse) and A-kinase anchoring proteins (AKAPs). (Fagerberg, et al., Contribution of Antibody-based Protein Profiling to the Human Chromosome-centric Proteome Project (C-HPP). 2012. *J proteome res.*; 12(6):2439-48; Freundt, et al., Photoconversion of Lysotracker Red to a green fluorescent molecule. 2007. *Cell research* 17, 956-958). LRBA deficiency, resulting from homozygous deletion or mutations in LRBA gene, causes common variable immunodeficiency (CVID8) and autoimmunity. LRBA-deficient patients have an array of serious symptoms including hypogammaglobulinemia, antibody deficiency, recurrent bacterial infections, defective B-cell differentiation, decreased or absent antibody production, recurrent infections particularly respiratory infections, variable autoimmune disorders (idiopathic thrombocytopenic purpura autoimmune hemolytic anemia, inflammatory bowel disease). Death can occur from complication. The underlying cellular and molecular mechanisms are mostly unknown.

Additionally, knockdown of LRBA resulted in significant growth inhibition in multiple cell lines and sensitized cells to apoptosis; and LRBA upregulation is found in multiple cancer types including breast cancer, cervical cancer, epidermal carcinoma, renal cancer, pancreatic cancer, colorectal cancer, and lung cancer. E2F and p53 transcription factors up- and down-regulate LRBA, respectively.

## 51

Thus far, mutations in 7 genes are associated with or cause CVID (common variable immunodeficiency), as seen in Table 4. LRBA is the 8th gene, the newest gene, mutations of which causes CVID, thus the name CVID8. Deficiency of LRBA results in fewer cells positive for three CVID proteins: CD19, CD20 and B cell-activating factor receptor (BAFFR) (Lopez-Herrera, et al., Deleterious mutations in LRBA are associated with a syndrome of immune deficiency and autoimmunity. 2012. *American journal of human genetics* 90:986-1001). Knockdown of LRBA decreases the TACI (transmembrane activator and calcium modulator and cyclophilin ligand interactor) levels on B cells. TACI controls T cell-independent B cell antibody responses, isotype switching, and B cell homeostasis, as seen in FIGS. 15(A) through (F). LRBA and TLR4 co-localized at GC and endosome or

## 52

cell membrane, providing direct evidence that LRBA is involved in TLR4 activation. Knockdown of LRBA also decreases the surface levels of Toll-like receptor 4 (TLR4) and CD21 on B cells, seen in FIGS. 16(A) through 17.

CD21 is also known as complement component (3d/Epstein Barr virus) receptor 2(CR2), is a protein involved in the complement system. It binds to iC3b (inactive derivative of C3b), C3dg, or C3d. B cells have CR2 receptors on their surfaces, allowing the complement system to play a role in B-cell activation and maturation. These results indicate that LRBA is a master regulator of other CVID genes, and that its deficiency's causing immunodeficiency is at least partially through deregulation of these genes. Thus, deficiency of LRBA causes more severe and broader symptoms in patients due to that LRBA is a master regulator of multiple important genes.

TABLE 4

Comparison of eight CVID genes.				
CVID genes	Molecular weight (kD)	Subcellular localization	Function	Diseases
ICOS: inducible costimulator	27	T Cell Surface	CD28 and CTLA-4 cell-surface receptor family, germinal center formation, isotype class switching, and the development of memory B cells. Cell-cell signaling, immune response, and regulation of cell proliferation.	CVID26
TACI: transmembrane activator and calcium modulator and cyclophilin ligand interactor. Receptor	32	B Cell Surface	Mutations impair the development of IgA- and IgG-secreting plasma cells and promote lymphoproliferation. Antibody class switching autoimmunity. Negative regulator of B-cell. Activation of the transcription factors NFAT, AP1, and NF-κB, humoral immunity by interacting with TNF ligand	Significantly reduced IgA levels mutated in 5%-10% of CVID patients Common variable immunodeficiency and IgA deficiency
CD19	61	B Cell Surface	B cell co-receptor in conjunction with CD21 and CD81.	CVID 19,
BAFFR: B-cell activating factor receptor	19	B Cell Surface	B-lymphocyte survival (BAFF-R deficiency blocks B-cell development at the stage of transitional B cells, The most important B cell survival signals. Major B-cell-activating factor receptor. Regulation of cell development, activation, growth and motility.	An adult-onset antibody deficiency syndrome <sup>24</sup> High levels of BAFF in mice, lead to an autoimmune disease similar to SLE75
CD81	26	B Cell Surface	Receptor for Epstein-Barr virus (EBV) binding on B and T lymphocytes	CVID21
CD21	145	B Cell Surface	Expansion of CD21 <sup>lo</sup> in CVID patients has been clearly associated with a higher incidence of splenomegaly and more recently with autoimmune cytopenia	CVID 20
CD20	35	B Cell Surface	Impaired T cell-independent antibody responses markedly	Impaired T cell-independent antibody

TABLE 4-continued

Comparison of eight CVID genes.				
CVID genes	Molecular weight (kD)	Subcellular localization	Function	Diseases
LRBA	320	Golgi apparatus, nucleus, plasma membrane, and cytoplasm.	augment antigen presentation and the B-cell receptor response to antigen development and differentiation of B-cells into plasma cells Master vesicle trafficking regulator required for other CVID genes.	responses <sup>22</sup> Expansion of CD21 <sup>lo</sup> has been found in patients with SLE <sup>76</sup> and CVID <sup>77</sup> Switched memory B cells are low 4, 8, 38 Disrupting BAFFR signaling causes a dramatic drop in B cell numbers 30 More CD20 positive B cells and respond to anti-CD20 therapy 4, 8, 9

LRBA is co-localized with GC proteins including p230, seen in FIGS. 3(A) through (D), which is required for the regulated secretion of TNF (Lieu, et al., A trans-Golgi network golgin is required for the regulated secretion of TNF in activated macrophages in vivo. 2008. *Proc Natl Acad Sci USA* 105, 3351-6). FAN is required for the TNF-induced expression of cytokines (Adam-Klages, et al. FAN, a novel WD-repeat protein, couples the p55 TNF-receptor to neutral sphingomyelinase. 1996. *Cell* 86, 937-47; Montfort, et al., FAN stimulates TNF(alpha)-induced gene expression, leukocyte recruitment, and humoral response. 2009. *J Immunol* 183, 5369-78). LYST is required for inflammatory cytokine production in response to LPS (Cheng, et al., Novel functions of a regulator of lysosomal trafficking, LYST in TLR4 signal transduction. 2012. *Immunology* 137, 299-300). One of the most common symptoms in LRBA-deficient patients is diarrhea associated with autoimmunity, probably due to a reduction in or absence of IL10 secretion. IL10 knockout mice develop fetal diarrhea (Kuhn, et al., Interleukin-10-deficient mice develop chronic enterocolitis. 1993. *Cell* 75, 263-74). These data along with the subcellular localization of LRBA and the dynamic involvement of LRBA in vesicle trafficking, all point to LRBA being required for cytokine secretion in response to LPS stimulation. Absence of LRBA may inhibit pro-inflammatory cytokine secretion and causes immunodeficiency.

#### Example 3

Testing was undertaken to determine if absence of LRBA inhibit pro-inflammatory cytokine secretion. The immunodeficiency caused by LRBA deficiency may result from defective cytokine signaling pathways (Leonard, Cytokines and immunodeficiency diseases. 2001. *Nat Rev Immunol* 1, 200-8; Kovanen, & Leonard, Cytokines and immunodeficiency diseases: critical roles of the gamma(c)-dependent cytokines interleukins 2, 4, 7, 9, 15, and 21, and their signaling pathways. 2004. *Immunol Rev* 202, 67-83), indicating LRBA is involved in cytokine regulation and TLR activation. Moreover, data show that LRBA is involved in the LPS pathway and most likely serves to facilitate transportation and secretion of cytokines through vesicle trafficking.

Testing has shown LRBA is involved transcription regulation through translocation to the nucleus upon LPS stimulation, as seen in FIG. 18. LRBA is found to bind NOTCH1 in the nucleus (Yatim, A., Benne, C., Sobhian, B., Laurent-Chabalier, S., Deas, O., Judde, J. G., Lelievre, J. D., Levy, Y., and Benkirane, M. (2012). NOTCH1 nuclear interactome reveals key regulators of its transcriptional activity and oncogenic function. *Molecular cell* 48, 445-458). In humans, plasma or extracellular LRBA levels are increased significantly in inflammation induced by LPS, or asthma patients (C) with an exacerbation, as seen in FIGS. 19(A) through (D). LRBA is present in the human plasma in mainly membrane-free fraction, with the presence of LRBA in the plasma confirmed by Western blot. The results show that LRBA is mainly present in vesicle-free plasma. Since LRBA is present in the plasma it can be used as a noninvasive biomarker alone or combined with other genes.

Mouse models and primary cell culture models were tested to determine if LRBA is crucial in LPS-induced inflammation.: LRBA<sup>-/-</sup> patients suffer from recurrent infections (Lopez-Herrera, et al., Deleterious mutations in LRBA are associated with a syndrome of immune deficiency and autoimmunity. 2012. *Am J Hum Genet* 90, 986-1001; Burns, et al., LRBA gene deletion in a patient presenting with autoimmunity without hypogammaglobulinemia. 2012. *J Allergy Clin Immunol* 130, 1428-32; Alangari, et al., LPS-responsive beige-like anchor (LRBA) gene mutation in a family with inflammatory bowel disease and combined immunodeficiency. 2012. *J Allergy Clin Immunol* 130, 481-8 e2), indicating that the LPS pathway is impaired, as an impaired LPS pathway often causes more bacteria infections (Hoshino, et al., Cutting edge: Toll-like receptor 4 (TLR4)-deficient mice are hyporesponsive to lipopolysaccharide: evidence for TLR4 as the Lps gene product. 1999. *J Immunol* 162, 3749-52). LPS/sepsis mouse models were used for in vivo tests. As males develop sepsis more easily than females (Aoyama, et al., Gender difference in granulocyte dynamics and apoptosis and the role of IL-18 during endotoxin-induced systemic inflammation. 2009. *Shock* 32, 401-9), the male C57BL/6J littermates (LRBA<sup>+/+</sup>, LRBA<sup>+/-</sup> and LRBA<sup>-/-</sup>, 6-8 weeks, n=5 each genotype) were intraperitoneally injected with a 200 µl single sub-lethal dose of lipopolysaccharide (LPS) from *E. coli* (1 mg/kg) in sterile

saline or 200 µl saline using a 26 gauge needle (Haziot, et al., Resistance to endotoxin shock and reduced dissemination of gram-negative bacteria in CD14-deficient mice. 1996. *Immunity* 4, 407-14). The induced pro-inflammatory cytokines have the highest levels 2 h after injection (Haziot, et al., Resistance to endotoxin shock and reduced dissemination of gram-negative bacteria in CD14-deficient mice. 1996. *Immunity* 4, 407-14). At that time point, blood samples (150 µl per 20 gram body weight) were collected into BD Microtainer EDTA tubes by submandibular venipuncture procedure, and immediately placed on ice and processed within 1 h. Plasma was centrifuged twice, the first time at 1,000×g for 10 minutes and the second time at 2,000×g for 15 minutes at 4° C., then assayed immediately or stored at -80° C. until assayed. Cytokine assays were conducted as described above.

LRBA plasma levels in the mice challenged with LPS increased dramatically from undetectable levels. LRBA was also detected by mass spectrometry in the plasma from subjects stimulated with LPS. These data suggest that LRBA is involved in LPS induced inflammation *in vivo*. LPS induces three pro-inflammatory cytokines, TNFα, IFNβ, and IL-6, which induce acute phase response and systemic inflammation. The murine endotoxin model has dramatically improved the understanding of the inflammation (Steer, et al., Glucocorticoids suppress tumor necrosis factor-α expression by human monocytic THP-1 cells by suppressing transactivation through adjacent NF-κB and c-Jun-activating transcription factor-2 binding sites in the promoter. 2000. *J Biol Chem* 275, 18432-40; MacRedmond, et al., Respiratory epithelial cells require Toll-like receptor 4 for induction of human beta-defensin 2 by lipopolysaccharide. 2005. *Respir Res* 6, 116). Injecting endotoxin into mice led to the discovery of TNF (Carswell, et al., An endotoxin-induced serum factor that causes necrosis of tumors. 1975. *Proc Natl Acad Sci USA* 72, 3666-70).

#### Example 4

Because LRBA deficiency causes diseases of immunodeficiency and autoimmunity, NFκB was analyzed to determine if it activates LRBA promoter activity upon LPS stimulation. LRBA mRNA levels are 34% lower in the Crohn's group and 45% lower in the ulcerative colitis group compared to healthy controls (McKinley, et al., LPS-responsive beige-like anchor (LRBA): A novel gene with a potential role in the pathophysiology of inflammatory bowel disease. 2008. *Gastroenterology* 134, A461-A461).

Briefly, human LRBA promoter including the two NFκB sites were cloned into a promoterless firefly luciferase vector, seen in FIG. 27, using SLIC technology (Li & Elledge, Harnessing homologous recombination *in vitro* to generate recombinant DNA via SLIC. 2007. *Nat Methods* 4, 251-6). The positive clones were identified by digestion and sequencing, and then transfected into A549 cells, which are LPS responsive. Promoter assay using LPS stimulation was conducted as described (Steer, et al., Glucocorticoids suppress tumor necrosis factor-α expression by human monocytic THP-1 cells by suppressing transactivation through adjacent NF-κB and c-Jun-activating transcription factor-2 binding sites in the promoter. 2000. *J Biol Chem* 275, 18432-40; MacRedmond, et al., Respiratory epithelial cells require Toll-like receptor 4 for induction of human beta-defensin 2 by lipopolysaccharide. 2005. *Respir Res* 6, 116). To determine, whether upregulation of LRBA by LPS is through NFκB, the two potential NFκB binding sites (consensus NFκB binding sequence: gggRNNYYCC

(Seq ID No. 6), R=purine Y=pyrimidine) were mutated to ggTRNNYYAC (Seq ID No. 7) separately or in combination. In all experiments, the NF-κB reporter positive control is used to monitor NF-κB activity.

LRBA is regulated by NF-κB, a pivotal inflammatory transcription factor (Edwards, et al., Targeting the NF-κB pathway in asthma and chronic obstructive pulmonary disease. 2009. *Pharmacol Ther* 121, 1-13), as its promoter has two NFκB binding sites highly homologous to the κB element and is conserved in mouse and human, seen in FIG. 27. The two potential NFκB binding sites in the LRBA sequence are true NFκB binding sites, and the mutations, seen in FIG. 27, abolished NFκB activation, confirming that LRBA is an NFκB downstream gene, and LPS activates NFκB, which, in turn, upregulates LRBA.

EBV immortalized LRBA deficient and LRBA positive control B cell lines were cultured in T25 culture flasks at 10<sup>6</sup> cells/ml for 24 h. Media was changed and 10<sup>5</sup> cells seeded in each well with 100 µl culture media in 96 well plates 2 h before LPS treatment. Serial concentrations of LPS were used (0.1-10 µg) to stimulate B cells. After 0.5 to 18 h, the levels of secreted and intracellular TNF, IL-6 and IFN from 100 µl of culture supernatants and all cell lysates made from 100 µl of RIPA buffer, respectively, were measured using ELISA kits following the manufacturer's protocols. The intracellular cytokine ELISA results was confirmed by Western blots, flow cytometry, immunofluorescence (IF) staining. LRBA levels are significantly increased in inflammation induced by LPS, seen in FIGS. 32(A) & (D), or ovalbumin (OVA), seen in FIG. 32(B), and in asthma patients, seen in FIG. 32(C), with an exacerbation. The presence of LRBA in the plasma was confirmed by Western blots, seen in FIG. 32(C), inset). LRBA in the plasma from subjects stimulated with LPS (Qian, et al., Quantitative proteome analysis of human plasma following *in vivo* lipopolysaccharide administration using 160/180 labeling and the accurate mass and time tag approach. 2005. *Mol Cell Proteomics* 4, 700-9) or from trauma patients was also detected using mass spectrometry (Liu, et al., High dynamic range characterization of the trauma patient plasma proteome. 2006. *Mol Cell Proteomics* 5, 1899-913). Data indicate that plasma LRBA levels are significantly increased in asthma patients with an exacerbation and in mouse asthma models, seen in FIG. 32(C), suggesting that overexpression of LRBA is associated with inflammatory diseases.

#### Example 5

The B cell is one of most affected cell types in LRBA deficient patients, while monocytes are highly responsive to LPS stimulation. Accordingly, these two cell types were used to examine LRBA and test the effectiveness of LRBA treatment. B cells are responsive to LPS stimulation and secrete various cytokines including IL-6 (Dumont, et al., Increased secretion of hyperimmune antibodies following lipopolysaccharide stimulation of CD40-activated human B cells *in vitro*. 2009. *Immunology* 126, 588-95) and TNFα (Boussiotis, et al., Tumor necrosis factor α is an autocrine growth factor for normal human B cells. 1994. *Proc Natl Acad Sci USA* 91, 7007-11; Frasca, et al., A molecular mechanism for TNF-α-mediated downregulation of B cell responses. 2012. *J Immunol* 188, 279-86).

EBV immortalized LRBA-deficient and LRBA-positive control B cell lines were used (Alangari, et al., LPS-responsive beige-like anchor (LRBA) gene mutation in a family with inflammatory bowel disease and combined immunodeficiency. 2012. *J Allergy Clin Immunol* 130, 481-8

57

e2). The LRBA<sup>-/-</sup> B cell lines were obtained from patients with a homozygous deletion or mutations, in LRBA gene (Lopez-Herrera, et al., Deleterious mutations in LRBA are associated with a syndrome of immune deficiency and autoimmunity. 2012. *Am J Hum Genet* 90, 986-1001; Alan-gari, et al., LPS-responsive beige-like anchor (LRBA) gene mutation in a family with inflammatory bowel disease and combined immunodeficiency. 2012. *J Allergy Clin Immunol* 130, 481-8 e2). These cell lines were cultured in T25 culture flasks at 10<sup>6</sup> cells/ml for 24 h. The “loss of function” and “gain of function” strategies are used to determine whether LRBA plays a crucial role in key cytokine production and TLR4 activation induced by LPS in cell culture and mouse models. For “gain of function” strategy, whole length LRBA was successfully overexpressed.

TLRs (TLR4, input signal) and cytokines (TNF, IL6 and IFN output signal) are two of most critical components of inflammation mediated by LPS, thus are examined TLR4 detects lipopolysaccharide from Gram-negative bacteria and is thus important in the activation of the innate immune system. Internalized LPS and TLR4 are found in the GC (Hornef, et al., Toll-like receptor 4 resides in the Golgi apparatus and colocalizes with internalized lipopolysaccharide in intestinal epithelial cells. 2002. *The Journal of experimental medicine* 195: 559-570). Proto-oncogenes Ras and Src are activated on the GC (Bivona, et al., Phospholipase C gamma activates Ras on the Golgi apparatus by means of RasGRP1. 2003. *Nature* 424: 694-698; Pulvirenti, et al., A traffic-activated Golgi-based signaling circuit coordinates the secretory pathway. 2008. *Nature cell biology* 10: 912-922). LRBA deficiency appears to impair TLR4 activation by interfering with TLR4 trafficking between cell membrane and GC.

The shRNA knockdown of LRBA increases the TLR4 levels in A549 cells at 2 h and 4 h after LPS stimulation, when compared to untransfected A549 cells, evidencing that LRBA regulates TLR4 in these cells. TLR4 levels have no difference in the two cell lines at 24 h, seen in FIGS. 17(A) through (C).

Intracellular and secreted TNF, IL-6 and IFN $\beta$  are significantly reduced in the LRBA deficient B cells compared to LRBA positive control B cells, because LRBA is involved in more than the secretion of cytokines, such as signal transductions that are required for de novo production of cytokines started from transcription by NF $\kappa$ B transcription factor. Three Raji B cell lines stably transfected with LRBA shRNA that knockdown LRBA over 90% were generated, along with RAW246.7 mouse cell lines stably transfected with a LRBA DNM.

The DNA sequence used to express DNM was SEQ ID No. 8:

```
AGGCTCATGCTTCAGACAAATTTAATCACAATGACCACATATAATGTGC
TGT TTGAGATTCTTATAGAACAGATTGGTACTCAGTGATACATAAACA
GCATCCAGATCCTGATTCTTCAGTGAAGATACAAACCTCAGATACTA
AAAGTAATTGCGACCCTACTTCGAAATTCTCCCGAGTGCCAGAGAGCA
TGGAGGTTGCGAGAGCCTTTCTTTCTGACATGATTAACTTTTAAATAA
CAGTAGAGAAAACAGGAGGAGCTTGCTACAATGCTCTGTGTGGCAAGAA
TGGATGCTTTCTCTGCTATTTTAACTCCTAAGAATTGAGATGAGCAAA
AGATAACAGAAATGGTATACGCCATATTGAGAACTCTGCTTTAC.
```

58

This sequence was used to produce the LRBA-VHS peptide described in the figures.

Cloning of LRBA Dominant Negative Mutant:

The LRBA dominant negative mutants were amplified using the following primers and cloned into the pEGFP-C3 vector using the Gibson cloning method: (Seq ID No. 9) GFPLRBAF, TGTACAAGTACTCAGATCGGCTCATGCTTCAGACAAATTTAATC; GFPVHSR, (Seq ID No. 10) AGTTATCTAGATCCGGTGGTAAAGCAGGATTCTGAATATG; The GFP gene was fused at the C-terminal of every one of these LRBA fragments and expressed as LRBA GFP fusion proteins. The cloned sequence of the LRBA domain is (Seq ID No. 11)

```
QTNLITMTTYNVLFELIEQIGTQVIHKQHPDPDSSVKIQNPQILKVIAT
LLRNSPQCPESMEVRRRAFLSDMIKLFNNSRENRRSLQC SVWQEWMLSLC
YFNPKN SDEQKITEMVYAI FRIL.
```

LRBA knockdown showed that LRBA regulates both extracellular and intracellular TNF $\alpha$  levels in Raji B cells (Burkitt's lymphoma), A549 cells and THP1 cells. Knockdown of LRBA significantly increased the TNF $\alpha$  levels in Raji B cells in the cell culture supernatants and in cells lysates during LPS stimulation for 15 min to 24 h, when compared to untransfected Raji B cells, seen in FIG. 21. This data agrees with that of Western blot results with A549 cells stably transfected with the same shRNA plasmid against LRBA, seen in FIG. 4. Two LRBA dominant negative mutants (LRBA-VHSLIR1, LRBA-VHS) but not LRBA-LIR3 decrease TNF $\alpha$  levels in the cell culture supernatants, seen in FIG. 22.

```
LRBA-VHS peptide (Seq ID No. 12):
QTNLITMTTYNVLFELIEQIGTQVIHKQHPDPDSSVKIQNPQILKVIATL
LRNSPQCPESMEVRRRAFLSDMIKLFNNSRENRRSLQC SVWQEWMLSLCYF
NPKNSDEQKITEMVYAI FRIL
```

```
LRBA-LIR3 (Seq ID No. 13):
GWRVWVDTLSTHSHKVTPEIHKENLANIFREQQGVDEEIGLCSSTSVQAA
SGIRRDINVSVGSQQPDTKDSVPCPHFTTNGNENSSIEKTSLSLESASNIEL
QTTNTSYEEMKAEQENQELPDEGTLEETLTNETRNADDLEVSSDIIEAVAI
SSNSFITTGKDSMTVSEVTASISSPSEEDASEMPEFLDKSIVEEEEDDDYV
ELKVEGSPTEEANLHRI
```

```
LRBA-VHSLIR1 (Seq ID No. 14):
RLMLQTNLITMTTYNVLI-BILIEQIGTQVIHKQHPDPDSSVKIQNPQILK
VIATLLRNSPQCPESMEVRRRAFLSDMIKLFNNSRENRRSLQC SVWQEWML
SLCYFNPKN SDEQKITEMVYAI FRILLYHAVKYEWGGWRVWVDTLSTHSHK
VTFEIHKENLANIFREQQGVDEEIGLCSSTSVQAA SGIRRDINVSVGSQQ
PDTKDSVPCPHFTTNGNENSSIEKTSLSLESASNIELQTTNTSYEEMKAEQE
NQELPDEGTLEETLTNETRNADDLEVSSDIIEAVAISSNSFITTGKDSMTV
SEVTASISSPSEEDASEMPEFLDKSIVEEEEDDDYVELKVEGSPTEEANLP
TELQDNLSPAASEAGEKLD MFGNDDKLIFQEGKPVTEKQTD TETQDSKDS
GIQTMTASGSSAMSPETTVSQI AVESDLGQMLEEGKATNL TRETKLINDC
```

-continued

HGSVSEASSEQKIAKLDVSNVATDTERLELKASPNVEAPQPHRVLEISRQ  
HEQPGQGIAPDAVNGQRDRSRSTVFRIPEF

The impact on these intracellular cytokines likely represents de novo synthesis. These results confirm that LRBA is crucial in cytokine secretion and signal transduction, which leads to increased cytokine production in inflammation.

## Example 6

LRBA deficiency suppresses autophagy by more than 50% and accumulates more autophagosome and Golgi apparatuses, suggesting that LRBA is critical for autophagy. Autophagy is involved in almost all facets of innate and adaptive immunity. LRBA has a LC3 interaction region (LIR). A microtubule-associated protein 1 light chain 3 (LC3) interaction region LC3 interaction region (LIR) motif in both human and murine LRBA. The LIR consensus sequence is [DE]-[DE]-[DE]-[WFY]-X-X-[LIV]+(Birgis-dottir, et al., The LIR motif—crucial for selective autophagy. 2013. *J Cell Sci* 126, 3237-47; Seq ID No. 2). The DDDYVEL (Seq ID No. 3) sequence from LRBA has high homology with LIR from TP53INP1 (similarity is 92%) and TP53INP249. Three dimensional structure remodeling (YASARA v12.7.16) shows that the LIR forms a complex with LC3 which is more stable than with p62, a known LC3 binding protein, as seen in FIG. 23(A). Tyrosine phosphorylation in the LIR destabilizes this complex, seen in FIG. 23(B).

Co-localization microscopy and LRBA has a potential LC3 interaction region (LIR) and ubiquitin binding domain (UBD). Confocal microscopy and IFA show that LRBA is highly co-localized with LC3, as seen in FIGS. 23(C) through (E), and show LRBA co-localized with autophagosomes. Dominant-negatives containing UBD and/or LIR inhibit and/or LIR inhibit cell growth.

Structural analysis of LRBA indicated that the protein contains an LC3 interaction region (LIR) region and ubiquitin

epidermal carcinoma, renal cancer, pancreatic cancer, colorectal cancer, and lung cancer (Wang, et al., Deregulated expression of LRBA facilitates cancer cell growth. 2004. *Oncogene* 23, 4089-97). LRBA may also contribute to the following cancers: adrenal cancer, anal cancer, Bile Duct Cancer, Bladder Cancer, Bone Cancer, Brain/CNS Tumors In Adults, Brain/CNS Tumors In Children, Breast Cancer In Men, Cancer in Adolescents, Cancer in Children, Cancer in Young Adults, Cancer of Unknown Primary, Castleman Disease, Colon/Rectum Cancer, Endometrial Cancer, Esophagus Cancer, Ewing Family Of Tumors, Eye Cancer, Gallbladder Cancer, Gastrointestinal Carcinoid Tumors, Gastrointestinal Stromal Tumor (GIST), Gestational Trophoblastic Disease, Hodgkin Disease, Kaposi Sarcoma, Kidney Cancer, Laryngeal and Hypopharyngeal Cancer, Leukemia, Leukemia—Acute Lymphocytic (ALL) in Adults, Leukemia—Acute Myeloid (AML), Leukemia—Chronic Lymphocytic (CLL), Leukemia—Chronic Myeloid (CML), Leukemia—Chronic Myelomonocytic (CMML), Leukemia in Children, Liver Cancer, Lung Cancer—Non-Small Cell, Lung Cancer—Small Cell, Lung Carcinoid Tumor, Lymphoma, Lymphoma of the Skin, Malignant Mesothelioma, Multiple Myeloma, Myelodysplastic Syndrome, Nasal Cavity and Paranasal Sinus Cancer, Nasopharyngeal Cancer, Neuroblastoma, Non-Hodgkin Lymphoma, Non-Hodgkin Lymphoma In Children, Oral Cavity and Oropharyngeal Cancer, Osteosarcoma, Ovarian Cancer, Penile Cancer, Pituitary Tumors, Prostate Cancer, Retinoblastoma, Rhabdomyosarcoma, Salivary Gland Cancer, Sarcoma—Adult Soft Tissue Cancer, Skin Cancer, Skin Cancer—Basal and Squamous Cell, Skin Cancer—Melanoma, Skin Cancer—Merkel Cell, Small Intestine Cancer, Stomach Cancer, Testicular Cancer, Thymus Cancer, Thyroid Cancer, Uterine Sarcoma, Vaginal Cancer, Vulvar Cancer, Waldenstrom Macroglobulinemia, Wilms Tumor. Of note, LRBA expression is correlated to that of estrogen receptor (Wang, et al., Deregulated expression of LRBA facilitates cancer cell growth. 2004. *Oncogene* 23, 4089-97). These results provide a molecular mechanism for clinical intervention of autophagy and cell growth related to human diseases.

TABLE 5

Calculated interaction energy between LC3 and LIRs of other proteins using Foldx.						
	LRBA-LIR	p62-LIR	LRBA-LIR-p	TP53INP1-LIR	TP53INP2-LIR	Alanine Scan
Interaction energy with LC3 (kcal/mol)	-15.19	-13.89	-13.22	-18.35	-15.13	-3.76
Interaction	++ predicted	+ experimental	+ predicted	+++ experimental	++ experimental	- predicted

itin binding domain (UBD). The interaction energy between LC3 and LIRs of LRBA and three known LC3 binding proteins, the phosphorylated LIR of LRBA and the alanine scan were calculated using Foldx50, seen in Table 5. These findings demonstrate that LRBA serves as an adaptor for ubiquitinated proteins destined for degradation through association with LC3 and ubiquitin by LIR and UBD respectively during autophagy. Tyrosine phosphorylation may impede LRBA binding with LC3, inhibit autophagy, but favor cell growth, in agreement with the hypothesis that LIR is phosphorylated in several cancer types, such as lung, breast, bladder, kidney, gastric cancers and leukemia. Moreover, overexpression of LRBA has been observed in several types of cancer cells, such as breast cancer, cervical cancer,

In agreement with these findings, blockage of LRBA by antibody against LRBA or using LRBA dominant negative mutants promotes cell proliferations in THP1 cells, as seen in FIG. 25, and RAW264.7 cells (data not shown), and Raji B cells (Burkitt's lymphoma), seen in FIG. 20.

These data suggest that LRBA expression levels are closely related to chronic diseases such as ALS (Lou Gehrig's Disease), Alzheimer's Disease and other Dementias; Arthritis, Asthma, Chronic Obstructive Pulmonary Disease (COPD), Cystic Fibrosis, Diabetes, End Stage Renal Disease, Heart Disease, Obesity and Related Conditions, in addition to cancer, immunodeficiency and autoimmunity,

and must be tightly regulated. The transcription is the first and most important control step for gene expression.

#### Example 7

Overexpression of LRBA has been observed in several types of cancer cells, such as cervical cancer, breast cancer, lung cancer, and epidemral cancer (Wang, et al., *Deregulated expression of LRBA facilitates cancer cell growth*. 2004. *Oncogene* 23, 4089-97). Data show that plasma LRBA levels are significantly increased in asthma patients with an exacerbation and in mouse asthma models, seen in FIG. 32(C), suggesting that overexpression or up-regulation of LRBA facilitates vesicle trafficking of cytokines and is associated with inflammatory diseases. Accordingly, absence or repression of LRBA inhibits cytokine secretion.

Next, blocking of LRBA using dominant negative mutant (DN-VHS) was tested as a therapeutic strategy to treat inflammatory diseases. HEK293, RAW264.7 and A549 cell lines (American Type Culture Collection, Manassas, Va., USA) were maintained according to the ATCC's instructions. Stable cell lines comprising RAW264.7, H293 and A549 cells, transfected with LRBA DNM or shRNA, and tested for impaired growth as discussed above. The mutated or truncated LRBA protein cannot be detected in the cells from LRBA-deficient patients (Lopez-Herrera, et al., *Deleterious mutations in LRBA are associated with a syndrome of immune deficiency and autoimmunity*. 2012. *Am J Hum Genet* 90, 986-1001; Burns, et al., *LRBA gene deletion in a patient presenting with autoimmunity without hypogammaglobulinemia*. 2012. *J Allergy Clin Immunol* 130, 1428-32; Alangari, et al., *LPS-responsive beige-like anchor (LRBA) gene mutation in a family with inflammatory bowel disease and combined immunodeficiency*. 2012. *J Allergy Clin Immunol* 130, 481-8 e2), suggesting that these mutated LRBA proteins could serve as DNMs and are harmful to the body and must be degraded. When over-expressed in the cells, DN-VHS greatly suppresses cell growth, as seen in FIGS. 26(B) & (E), indicating that it can serve as a DMN to inhibit LRBA function. DN-VHS associated vesicles were motionless, data not shown, suggesting that the vesicle trafficking is blocked. This provides direct evidence that LRBA is crucial for vesicle trafficking. Moreover, the VHS domain of LRBA is a small 14 kD peptide, which may be easier to deliver into cells. Taken together, DN-VHS is a promising peptide to be developed into a biologic to treat inflammatory diseases.

HEK293 cell lines (American Type Culture Collection, Manassas, Va., USA) were cultured in Dulbecco's modified minimum essential medium (DMEM) or RPMI1640 supplemented with 10% FBS and penicillin-streptomycin (5,000 IU/ml penicillin and 5,000 µg/ml streptomycin) as provided by ATCC. Three constructs of LRBA fragments fused with EGFP were generated and successfully expressed in HEK293 cells. To explore if LRBA DN-VHS is useful as a biologic to treat inflammatory diseases, its effects on pro-inflammatory cytokine secretion were examined as disclosed above. To this end, the three constructs are transfected into Raw246.7 cells and stable clones selected with G418. The proinflammatory cytokine (TNF and IL-6) production induced by LPS stimulation was compared in the three cell lines: RAW246.7 (Wt control), RAW<sup>LRBA-EGFP</sup> (LRBA-VHS-EGFP, LRBA-LIR-EGFP, LRBA-VHS and LIR-EGFP) and RAW<sup>GFP</sup> (vector control).

The inhibitory effects on the proinflammatory cytokines by the three LRBA DNMs is similar to that of their growth inhibitions, seen in FIGS. 26(B) & (E), i.e. the order of

cytokine inhibitory effects is VHS-EGFP>VHSLIR-EGFP>LIR-EGFP. This suggests that the functions of LRBA on cell growth and cytokine production are related, and VHS domain is a promising target to treat inflammatory diseases.

Both absence of LRBA and defective cytokines can cause immunodeficiency. LRBA<sup>-/-</sup> may first inhibit the production and secretion of cytokines, resulting in defective cytokines, the latter then cause immunodeficiency.

LRBA was tested for its effect on cell growth. For the "loss of function" strategy, EBV immortalized LRBA-deficient B cell lines were generated from LRBA deficient patients, and dominant negative LRBA mutants (DNM) and knockout mouse models. The LRBA sequence targeted by the shRNA used was SEQ ID No. 15;

GGGATATTGTAGAAACTGTCTTT,

which is 100% conserved in mouse and human LRBA. Determination of shRNAs can be performed by those skilled in the art. For example, a possible shRNA is shown in SEQ ID No. 43 for the top strand;

GGGATATTGTAGAAACTGTCTTTTCAAGAGAAAAGACAGTTTCTACAA

TATCCCTTTTTT

and SEQ ID No. 44 for the bottom strand;

CCCTATAACATCTTTGACAGAAAAAGTTCTTTTCTGTCAAAGATGTAA

TAGGGAAAAA

The DNA sequence used to express DNM was SEQ ID No. 8:

AGGCTCATGCTTCAGACAAATTAATCACAATGACCACATATAATGTGC

TGTTTGAGATTCTTATAGAACAGATTGGTACTCAGGTGATACATAAACA

GCATCCAGATCCTGATTCTTCAGTGAAGATACAAAACCTCAGATACTA

AAAGTAATTGCGACCCCTACTTCGAAATTCCTCCAGTCCAGAGAGCA

TGGAGGTTGCGAGAGCCTTTCTTTCTGACATGATTAACTTTTAAATAA

CAGTAGAGAAAAACAGGAGGAGCTTGCTACAATGCTCTGTGTGGCAAGAA

TGGATGCTTTCTCTGCTATTTTAAATCCTAAGAATTCAGATGAGCAAA

AGATAACAGAAATGGTATACGCCATATTCAGAATCCTGCTTTAC.

This sequence was used to produce the LRBA-VHS peptide described in the figures, and shown as SEQ ID No. 11;

QTNLITMTTYNVLFELIEQIGTQVIHKQHPDPDSSVKIQNPQILKVIAT

LLRNSPQCPSMESVRRFLSDMIKLFNNSRENRRSLQCQSVQEWMLSLC

YFNPKNSEQKITEMVYAIIFRIL.

Knockout of LRBA (LRBA<sup>-/-</sup>) greatly suppresses cell growth in mouse embryo stem (ES) cells, as seen in FIG. 26(A). The results from HEK293 cells, seen in FIGS. 26(B), and A549 cells, seen in FIG. 26(C), are very similar, indicating that the data are reliable and LRBA likely plays the same role in different types of cells. The cells transfected with LRBA-VHS, seen in FIG. 2, an LRBA dominant

negative mutation (DNM), produced fewer and smaller colonies, seen in FIG. 26(B). LRBA-VHS is associated with membranous vesicles, as seen in FIG. 26(D). Live cell microscopy shows no movement of LRBA-VHS-EGFP vesicles and some directional movement of mRFP-LC3 vesicles. This suggests that these vesicles have defects caused by the LRBA DNM.

These findings correspond well to the studies showing that LRBA-deficient patients had retarded growth (Lopez-Herrera, et al., Deleterious mutations in LRBA are associated with a syndrome of immune deficiency and autoimmunity. 2012. *Am J Hum Genet* 90, 986-1001; Burns, et al., LRBA gene deletion in a patient presenting with autoimmunity without hypogammaglobulinemia. 2012. *J Allergy Clin Immunol* 130, 1428-32; Alangari, et al., LPS-responsive beige-like anchor (LRBA) gene mutation in a family with inflammatory bowel disease and combined immunodeficiency. 2012. *J Allergy Clin Immunol* 130, 481-8 e2), T-cell proliferation to Phytohaemagglutinin (PHA) and anti-CD3 mAb was markedly reduced in the absence of LRBA (Alangari, et al., LPS-responsive beige-like anchor (LRBA) gene mutation in a family with inflammatory bowel disease and combined immunodeficiency. 2012. *J Allergy Clin Immunol* 130, 481-8 e2). The growth inhibition by a LRBA DNM can be overridden by plasma from mice stimulated with LPS, as seen in FIG. 27(G).

LRBA is regulated by Ubiquitin-dependent protein degradation system. LRBA protein has 11 ubiquitination sites (Oshikawa, K., Matsumoto, M., Oyamada, K., and Nakayama, K. I. (2012). Proteome-wide identification of ubiquitylation sites by conjugation of engineered lysine-less ubiquitin. *Journal of proteome research* 11, 796-807). The EGFP levels of LRBA-EGFP fusion proteins expressed by the plasmids pLRBA-VHSLIR-EGFP and pLRBA-VHS-EGFP are much lower than that expressed by the plasmids pLRBA-LIR and the control pEGFP-C3. LRBA peptides VHSLIR and VHS contain two and one ubiquitination sites respectively. LIR does not contain any ubiquitination site. MG132, a specific, potent, reversible, and cell-permeable proteasome inhibitor, can increase the expression levels of LRBA-EGFP fusion proteins expressed by the plasmids pLRBA-VHSLIR-EGFP and pLRBA-VHS-EGFP, but not that of LRBA-EGFP fusion proteins expressed by the plasmid pLRBA-LIR. The effects of MG132 on the expression levels of LRBA-EGFP fusion proteins are dose dependent, seen in FIG. 18(A). The similar results were obtained with PS341, seen in FIG. 18(B), which is a proteasome inhibitor, FDA-approved medicine for multiple myeloma and mantle cell lymphoma. These data demonstrate that LRBA is regulated by Ubiquitin-dependent protein degradation system, seen in FIGS. 28(A) through (H).

Both absence of LRBA and defective cytokines can cause immunodeficiency. LRBA<sup>-/-</sup> inhibit the production and secretion of cytokines, resulting in defective cytokines, which cannot be recapitulated by transformed primary cell culture models. As such, the primary cultures appear to provide accurate results that are similar to the in vivo settings. The mouse BMM cell culture model is an excellent models to study the LPS pathway.

BMMs were obtained by the protocol described by Weischenfeldt, et al. (Weischenfeldt & Porse, Bone Marrow-Derived Macrophages (BMM): Isolation and Applications. 2008. *CSH Protoc* 2008, pdb prot5080). Bone marrow cells were obtained by flushing the femurs and tibias from 8-12-week-old C57BL/6 wild type mice and LRBA<sup>-/-</sup> mice, and the bone marrow cells plated in 10-cm bacteriological plastic plates at 2×10<sup>6</sup> cells/mL with 10% FCS in RPMI

1640 supplemented with 100 ng/ml of recombinant murine M-CSF. On day 7, BMMs were plated at 1×10<sup>5</sup> cells/ml in 24-well plates and cultured with or without 100 ng/ml of LPS for 7 h (Nagai, et al., Essential role of MD-2 in LPS responsiveness and TLR4 distribution. 2002. *Nat Immunol* 3, 667-72). Culture supernatants were collected for ELISA assay as disclosed in other Examples. While there is a concern BMMs from LRBA<sup>-/-</sup> mice may produce less cytokines compared to wild-type mice, data from transformed cell culture models was used to confirm results on cytokine levels.

It was first examined whether replenishing LRBA cured LRBA-deficient inflammatory diseases. LRBA's presence in plasma may provide a way to easily modulate LRBA to cure the incurable (Burns, et al., LRBA gene deletion in a patient presenting with autoimmunity without hypogammaglobulinemia. 2012. *J Allergy Clin Immunol* 130, 1428-32) LRBA-deficient patients are treated by replenishing LRBA, and to cure LRBA-overexpressing patients by using anti-LRBA reagents to block LRBA. LRBA can be secreted. This can explain why LRBA<sup>-/-</sup> ES cells can be obtained but failed to grow after being thawed from freezer storage.

As pure LRBA proteins are not available, LRBA protein must be expressed in insect cells or mammalian cells for testing. Mice and C57BL/6 mononuclear leukocytes cell cultures in lymphocyte culture media (RPMI 1640, fetal bovine serum 10%, L-glutamine 2 mM, Na pyruvate 1 mM, 0.5 μM 2-mercaptoethanol) were stimulated by injection of LPS, resulting in high levels of LRBA in the plasma or the culture supernatants. Mouse plasma was collected 24 hour after LPS stimulation and 100 μl of the mouse plasma (~250 pg LRBA) applied into 10 ml culture media and observed growth stimulation.

LRBA<sup>-/-</sup> ES cells were selected from LRBA<sup>+/-</sup> ES cells by using a high concentration of G418. The LRBA<sup>-/-</sup> ES cells grow during the selection as the media containing LRBA proteins secreted by the parent cells, but cannot grow without these secreted proteins. Growth was rescued for several types of LRBA-deficient cells, data not shown, by adding conditioned media or plasma from LPS-stimulated mice, which contain high levels of LRBA, seen in FIG. 2(A). The growth defect is manifested by retarded growth (Lopez-Herrera, et al., Deleterious mutations in LRBA are associated with a syndrome of immune deficiency and autoimmunity. 2012. *Am J Hum Genet* 90, 986-1001; Burns, et al., LRBA gene deletion in a patient presenting with autoimmunity without hypogammaglobulinemia. 2012. *J Allergy Clin Immunol* 130, 1428-32; Alangari, et al., LPS-responsive beige-like anchor (LRBA) gene mutation in a family with inflammatory bowel disease and combined immunodeficiency. 2012. *J Allergy Clin Immunol* 130, 481-8 e2), and reduced T-cell proliferation in LRBA-deficient patients (Alangari, et al., LPS-responsive beige-like anchor (LRBA) gene mutation in a family with inflammatory bowel disease and combined immunodeficiency. 2012. *J Allergy Clin Immunol* 130, 481-8 e2).

It is possible that the enhancement of cytokine secretion are dose-dependent, or cell-type dependent. As such, H293 and Raji stable clones that over-express LRBA fused with EGFP were used. To confirm the attachment of EGFP to the LRBA C-Terminus does not affect its function, a sequence and ligation-independent cloning (SLIC) seamless cloning technology, which can insert DNA fragments anywhere in the vector without the limitation of restriction enzyme sites (Li, M. Z. & Elledge, S. J. Harnessing homologous recombination in vitro to generate recombinant DNA via SLIC. *Nat Methods* 4, 251-6 (2007)) was used to remove the EGFP



tag and compare the two versions of LRBA on the cytokine secretion. The expression vector was transfected into RAW246.7 cells, and stable clones obtained by G418 selection, as seen in FIGS. 29(A) and (B). LRBA overexpression was judged by the GFP brightness and Western blots. The control clones that overexpress EGFP (RAW<sup>GFP</sup>) were obtained by the same strategy. The proinflammatory cytokine (TNF, IL-6 and IFN) production induced by LPS stimulation was compared in the three cell lines: RAW246.7, RAW<sup>LRBA-GFP</sup> and RAW<sup>GFP</sup> seen in FIGS. 26(C) & (D). It is likely that higher levels of cytokines in the culture supernatants of the RAW<sup>LRBA-GFP</sup> than RAW<sup>GFP</sup> suggest that overexpression of LRBA enhances cytokine secretion and is associated with inflammatory diseases.

#### Example 8

As LRBA is involved in apoptosis (Wang, et al., *Deregulated expression of LRBA facilitates cancer cell growth*. 2004. *Oncogene* 23, 4089-97), and LRBA-deficient B cells have slower growth and are susceptible to apoptosis (Lopez-Herrera, et al. *Deleterious mutations in LRBA are associated with a syndrome of immune deficiency and autoimmunity* 2012. *Am J Hum Genet* 90, 986-1001), the amount of apoptotic cells induced by serum deprivation was used to judge the rescue effects by replenishing LRBA. Apoptosis assays were conducted (Lopez-Herrera, et al., *Deleterious mutations in LRBA are associated with a syndrome of immune deficiency and autoimmunity* 2012. *Am J Hum Genet* 90, 986-1001) using LRBA<sup>-/-</sup> and LRBA<sup>+/+</sup> B cells (1×10<sup>6</sup> cells/ml) cultured under serum deprivation for 6 h. Each 18 wells are treated with equal amount of protein, i.e. anti-LRBA antibody, anti-actin antibody (A2066, Sigma) or bovine serum albumin (BSA). After six days, the cell number is measured using the CellTiter-Glo® Luminescent Cell Viability Assay (Promega). After starvation, cells were harvested, and apoptosis measured by Annexin V and propidium iodide (PI) staining, with a threshold of 10,000 events as analyzed by flow cytometry, to determine the percentage of cells in early apoptosis (positive for Annexin V and negative for PI). Viability numbers are determined in triplicate using CellTiter-Glo® kit (Promega) seeded in serum deprivation conditions in 96-well plates for 6 hours. Cells were given LRBA protein and collected at 24, 48, 72, 96 and 120 h after.

LRBA<sup>-/-</sup> ES cells do not grow or grow slowly. The ES cells were cultured at 37° C., 5% CO<sub>2</sub>, using mouse ES culture media under the conditions recommended by the company (Emdmillipore). Treatment of the cultures with LRBA plasma or conditioned media resulted in detected LRBA levels in the culture supernatants at up to 2.4 ng/ml, which can rescue LRBA<sup>-/-</sup> ES cells, data not shown. Increased apoptosis and retarded growth of LRBA<sup>-/-</sup> were rescued by adding LRBA to the media, suggesting that LRBA<sup>-/-</sup> patients may be cured by replenishing LRBA. This suggests that LRBA functions as an autocrine growth factor.

Anti-LRBA antibodies were tested as a therapeutic strategy to treat inflammatory diseases. Data show that LRBA levels are significantly increased in plasma from mice stimulated with LPS or OVA, seen in FIGS. 32(A) & (B), from asthma patients with an exacerbation, seen in FIGS. 32(C) & (D), and in the culture supernatants of human mononuclear leukocytes stimulated with LPS, indicating that LRBA is involved in LPS-induced inflammation, and suggesting that overexpression of LRBA may be associated with inflammatory diseases. The presence of LRBA in plasma is also confirmed by Western blots, seen in FIG. 32(D) (inset).

Blocking LRBA in plasma is therefore proposed to inhibit inflammation, and thus be useful to treat inflammatory diseases. TNF is highly expressed in RA patients and anti-TNF is an effective therapeutic. The same strategy used for anti-TNF may apply to anti-LRBA: a monoclonal antibody against LRBA targets LRBA in the plasma to treat inflammatory disease and cancers having overexpression of LRBA (Wang, et al., *Deregulated expression of LRBA facilitates cancer cell growth*. 2004. *Oncogene* 23, 4089-97).

LRBA antibody was used at 400 ng/ml, about four hundred times the molar ratio of antibody to protein, to bind LRBA protein in the supernatant. LRBA antibody eliminated the effects seen by exogenous LRBA, indicating the antibody inhibits LRBA-stimulated cell growth, and that blocking LRBA in the culture supernatant inhibits cell growth. The highest concentration of LRBA detected in the culture supernatants was 2.4 ng/ml. LRBA antibody, was used at 400 ng/ml, about four hundred times the molar ratio of antibody to protein, to bind LRBA protein in the supernatant, to ensure adequate LRBA neutralization.

Anti-LRBA antibody, anti-actin antibody and BSA have no effect on the growth of EBV LRBA<sup>-/-</sup> B cells, as these cells lack LRBA, and actually serve as a control. However, anti-LRBA antibody inhibits the growth of EBV LRBA<sup>+/+</sup> B cells, confirming that extracellular LRBA is required for the growth of the cells and possibly confirming that anti-LRBA antibody can be used as a therapeutic to inflammatory diseases and cancers with overexpression of LRBA.

Testing also showed LRBA is regulated by microRNAs. MicroRNAs (miRs) are ~22 nucleotides long non-coding RNAs that are believed to inhibit most human genes and the spectrum of biological pathways through inhibition of mRNA translation by the base pairing rule at the accuracy of one base. Deregulation of miRs may contribute to various diseases. Overexpression of the miRNAs miR-150 and miR-181 show LRBA is downregulated by overexpression of the miRNA, as seen in FIGS. 30(A) through (D).

#### Example 9

About two-third of CVID patients have autoimmune problems (Cunningham-Rundles & Bodian, *Common variable immunodeficiency: clinical and immunological features* of 248 patients. 1999. *Clinical immunology* 92: 34-48; Podjasek & Abraham, *Autoimmune cytopenias in common variable immunodeficiency*. 2012. *Frontiers in immunology* 3: 189). As opposed to other CVID genes, the immunodeficiency caused by LRBA deficiency is highly associated with autoimmunity. To date, the 11 identified LRBA-deficient CVID patients had autoimmunity (Lopez-Herrera, et al., *Deleterious Mutations in LRBA Are Associated with a Syndrome of Immune Deficiency and Autoimmunity*. 2012. *American journal of human genetics* 90: 986-1001; Sham-loula, et al., *rugose (rg), a Drosophila A kinase anchor protein, is required for retinal pattern formation and interacts genetically with multiple signaling pathways*. 2002. *Genetics* 161: 693-710; Parvaneh, et al., *Primary immunodeficiencies: a rapidly evolving story*. 2013. *The Journal of allergy and clinical immunology* 131: 314-323.). TACI mutations also are associated with autoimmunity but to a lesser degree (36% vs. 23% of patients with wild-type TACI) (Salzer, et al., *Relevance of biallelic versus monoallelic TNFRSF13B mutations in distinguishing disease-causing from risk-increasing TNFRSF13B variants in antibody deficiency syndromes*. 2009. *Blood* 113: 1967-1976).

LRBA deficient patients have low switched memory B cells, low or absent immunoglobulins including IgG, IgA

and IgM (Lopez-Herrera, et al., Deleterious Mutations in LRBA Are Associated with a Syndrome of Immune Deficiency and Autoimmunity. 2012. *American journal of human genetics* 90: 986-1001; Shamloula, et al., rugose (rg), a *Drosophila* A kinase anchor protein, is required for retinal pattern formation and interacts genetically with multiple signaling pathways. 2002. *Genetics* 161: 693-710; Parvaneh, et al., Primary immunodeficiencies: a rapidly evolving story. 2013. *The Journal of allergy and clinical immunology* 131: 314-323). These patients have markedly reduced T-cell proliferation in response to phytohemagglutinin (PHA) and anti-CD3 mAb, and reduced B cell survival. These cellular defects may account for immunodeficiency. However, LRBA deficient patients also have more peripheral T cells, more CD20 positive B cells, lymphocyte infiltration and respond to anti-CD20 therapy (Lopez-Herrera, et al., Deleterious Mutations in LRBA Are Associated with a Syndrome of Immune Deficiency and Autoimmunity 2012. *American journal of human genetics* 90: 986-1001; Shamloula, et al., rugose (rg), a *Drosophila* A kinase anchor protein, is required for retinal pattern formation and interacts genetically with multiple signaling pathways. 2002. *Genetics* 161: 693-710; Alangari, et al., LPS-responsive beige-like anchor (LRBA) gene mutation in a family with inflammatory bowel disease and combined immunodeficiency. 2012. *The Journal of allergy and clinical immunology* 130: 481-488 e482). These cellular defects may contribute to variable autoimmune disorders, such as thrombocytopenic purpura, autoimmune hemolytic anemia, inflammatory bowel disease (IBD).

Mutations in TACI impair the development of IgA- and IgG-secreting plasma cells and promote lymphoproliferation, and are associated with IgA deficiency and autoimmunity (Salzer, U., H. M. Chapel, A. D. Webster, Q. Pan-Hammarstrom, A. Schmitt-Graeff, et al., Mutations in TNFRSF13B encoding TACI are associated with common variable immunodeficiency in humans. 2005. *Nat Genet* 37: 820-828; Castigli, et al., TACI is mutant in common variable immunodeficiency and IgA deficiency. 2005. *Nat Genet* 37: 829-834). TACI is required for antibody class switching and is a negative regulator of B-cells (Seshasayee, et al., Loss of TACI causes fatal lymphoproliferation and autoimmunity, establishing TACI as an inhibitory BlyS receptor. 2003. *Immunity* 18: 279-288; Yan, et al., Activation and accumulation of B cells in TACI-deficient mice. 2001. *Nat Immunol* 2: 638-643).

BAFF-R deficiency blocks B-cell development at the stage of transitional B cells (Barkett & Gilmore, Control of apoptosis by Rel/NF-kappaB transcription factors. 1999. *Oncogene* 18: 6910-6924). High levels of BAFF in mice lead to an autoimmune disease similar to systemic lupus erythematosus (SLE) (Gross, et al., TACI and BCMA are receptors for a TNF homologue implicated in B-cell autoimmune disease. 2000. *Nature* 404: 995-999).

CVID receptors were examined in the cell culture and mouse LPS/sepsis models. LRBA was repressed in Raji B cells by the short hairpin RNA (shRNA) knocked down (KD) technique or LRBA dominant negative mutants (DNMs). A mouse model that has LRBA overexpression was also used. The results demonstrate that LRBA repression deregulates the three parameters (protein levels, response speed and phase) of CVID receptors, while overexpression of LRBA in a mouse model has opposite effects on these receptors, which are responsive to LPS stimulation, as seen in FIGS. 31(A) and (B), and NFkB inhibitors, and have NFkB binding sites. LRBA deficiency may exert its

effects on immunodeficiency and autoimmunity by deregulating these receptors through NFkB.

HEK293 cell line were purchased from the American Type Culture Collection (Manassas, Va., USA) and maintained according to the company's instructions. Raji B cell line (Burkitt's lymphoma) was kindly provided by Dr. George Blanck (University of South Florida Morsani College of Medicine). These cells were cultured in RPMI1640 supplemented with 10% FBS and penicillin-streptomycin (5,000 IU/ml penicillin and 5,000 µg/ml streptomycin). The mouse studies have been reviewed and approved by the Institutional Animal Care and Use Committee (IACUC) at the University of South Florida.

#### Cloning of LRBA Dominant Negative Mutants:

The LRBA dominant negative mutants were amplified using the following primers and cloned into the pEGFP-C3 vector using the Gibson cloning method: (Seq ID No. 9) GFPLRBAF, TGTACAAGTACTCAGATCGGCTCATGCTTCAGACAAATTTAATC; (Seq ID No. 16) GFPLR-BAR, AGTTATCTAGATCCGGTGGAACTCAG-GAATACGAAACACAG; (Se ID No. 10) GFPVHSR, AGTTATCTAGATCCGGTGGTAAAGCAGGATTCT-GAATATG; (Seq ID No. 17) GFPLIRF, TGTACAAGTACTCAGATCGTGGCTGGCGTGTATGGGTAG; (Seq ID No. 18) GFPLIRR, AGTTATCTAGATCCGGTGTAGATTAGCTTCCTCAGTAG. The GFP gene was fused at the C-terminal of every one of these LRBA fragments and expressed as LRBA GFP fusion proteins.

#### Immunofluorescent Confocal Microscopy:

HEK293 cells at concentration of  $5 \times 10^6$ /ml were plated on glass coverslips in Dulbecco's modified minimum essential medium (D-MEM) supplemented with 10% fetal calf serum (Gemini Bio-Products, West Sacramento, Calif.), penicillin and streptomycin. After 24 h, cells were fixed, permeabilized, and stained following the immuno-fluorescence staining protocol from the Human Protein Atlas Project (Sigma). Briefly, growth medium was removed and the cells were washed in 1xPBS, the cells were fixed for 15 minutes in ice cold 4% paraformaldehyde pH 7.2-7.3 in growth medium supplemented with 10% fetal bovine serum (FBS). The cells were permeabilized 3 times for 5 minutes each with 0.1% TRITON® X-100 in PBS. The cells were washed with 1xPBS and incubated overnight at 4° C. with the primary antibodies in 1xPBS supplemented with 4% FBS. The following day the cells were washed 4 times for 10 minutes each with 1xPBS and incubated for 1.5 hours at room temperature with the secondary antibodies in 1xPBS supplemented with 4% FBS. The cells were counterstained for 4 minutes with the nuclear stain DAPI (0.6 µM in 1xPBS). The cells were washed 4 times for 10 minutes with 1xPBS and then mounted in glycerol+10% 10xPBS. The LRBA antibodies and three Golgi protein primary antibodies were used at 1:500 (volume to volume dilution). The anti-mouse IgG-Alexa Fluor® 555 and anti-rabbit IgG-Alexa Fluor® 488 secondary antibodies were used at 1:400. The confocal imaging was acquired with an Olympus FV1000 MPE multiphoton laser scanning microscope using 60x objective (U Plan APO 1.42 N.A. oil) and sequential scanning with 0.5 µm per slice. Colocalization analysis for dual stained samples was carried out using JACoP and FV10-ASW software.

#### Electroporation:

Three million Raji B cells in the exponential phase were mixed with 20 µg of plasmid DNA expressing a specific LRBA dominant negative (LRBA-BEACH, LRBA-VHS-LIR, LRBA-VHS and LRBA-LIR) in 800 µl of culture media and electroporated by a Bio-Rad Gene Pulser at 400

V, 400 Ohms and 500  $\mu$ F. After 24 hours, cells were stained with specific antibodies conjugated with different fluorophores against CVID cell surface proteins and 7AAD for dead/live discrimination. About half a million cells were acquired and analyzed with GFP positive and negative populations. The percentage and intensity of these markers were analyzed in the two populations.

#### Cell Survival Assay and LRBA Antibody Blockage.

Raji B cells and Raji9 B cells (Raji B cells stably transfected with shRNA plasmid against LRBA) were cultured in a 96 well plate with 10 cells per well for 9 days. Blockage of LRBA promotes THP1 cell proliferation. THP1 cells (human acute monocytic leukemia cell line) were cultured in 100  $\mu$ l of RPMI1640 media with or without human LRBA polyclonal IgG antibody at 0.67  $\mu$ g/ml or the same amount of human actin polyclonal IgG antibody on a 96 well plate with 10 cells per well for 9 days. Viable cells were counted by the trypan blue live/dead discrimination method with a hemocytometer.

#### Mouse Model and LRBA Antibodies Treatment:

A) Mice stimulated with LPS (5  $\mu$ g/g body weight) for 6 hours. (B) OVA induced asthma mouse model; (C) Asthma patients with an exacerbation or controlled symptoms; (D) Human mononuclear leukocytes stimulated with LPS (1  $\mu$ g/ml). LRBA levels were determined by LRBA ELISA Kit using 100  $\mu$ l of plasma or conditioned media in each well. C57BL/6J mice were injected intraperitoneally with 500  $\mu$ l of 12 mg/kg (body weight) of LRBA antibody or control normal rabbit IgG suspended in saline three times. LPS at 7.5 mg/kg in 0.2 ml PBS i.p was followed. About 100  $\mu$ l of blood was collected by submandibular venipuncture after 2 hours of LPS injection. Plasma samples were obtained by centrifugation at 3000 rpm for 15 min and used for cytokine assay. The TNF $\alpha$  and IL-6 concentrations were detected using the mouse CBA Th1/Th2/Th17 cytokine kit. The Phosflow Starter Kit contains Cytofix Fixation Buffer, Phosflow Perm Buffer III and Stain Buffer BSA.

#### Polynomial Fitting and Slope Calculation:

Polynomial fitting was used to represent nonlinear dataset in this study. High  $R^2$  values ( $R^2 \geq 0.9$ ) were used to describe the fitting accuracy and a polynomial trend line equation were used to represent the dataset. The slopes at each time point were calculated by  $n \cdot k \cdot x^{(n-1)}$  calculus method.

#### Statistics Analysis:

Comparisons of sample means was done using two-sample t test, assuming equal variance, and p value was calculated based on two-tailed test. Significance was taken as  $p < 0.05$ . Data are expressed as mean  $\pm$  standard deviation (SD) and are representative of two to three independent experiments. P value indications:  $< 0.001$  Extremely significant \*\*\*, 0.001 to 0.01 Very significant \*\* 0.01 to 0.05 Significant \*  $> 0.05$  Not significant ns  $\# > 0.05$ .

#### LRBA is Involved in the LPS/TLR4 Pathway:

The Toll-like receptor 4 (TLR4) pathway is one of the most important immune pathways to eliminate bacteria, fungi and viral infections. TLR4-mutated mice respond less to Gram-negative bacteria and are highly susceptible to infection (Cook, et al., Toll-like receptors in the pathogenesis of human disease. 2004. *Nature immunology* 5: 975-979). LRBA is upregulated in vitro by LPS (Wang, et al., Identification of a novel lipopolysaccharide-inducible gene with key features of both A kinase anchor proteins and chs1/beige proteins. 2001. *J Immunol* 166: 4586-4595; Kerr, et al., Analysis of lipopolysaccharide-response genes in B-lineage cells demonstrates that they can have differentiation stage-restricted expression and contain SH2 domains. 1996. *Proceedings of the National Academy of Sciences of the United States of America* 93: 3947-3952), which activates NF- $\kappa$ B. Agreeably LRBA gene has multiple NF- $\kappa$ B binding sites in or around the promoter range (Supplemental Table 1). Its paralogue (Lyst) deficient cells exhibit defective TLR signaling, specifically in TLR4 pathways (Cheng, et al., 2012. Novel functions of a regulator of lysosomal trafficking, LYST in TLR4 signal transduction. 2012. *Immunology* 137: 299-300). Vesicle-mediated localization and trafficking of TLR4 are required for its activation (Cheng, et al., 2012. Novel functions of a regulator of lysosomal trafficking, LYST in TLR4 signal transduction. 2012. *Immunology* 137: 299-300; Latz, et al., Lipopolysaccharide rapidly traffics to and from the Golgi apparatus with the toll-like receptor 4-MD-2-CD14 complex in a process that is distinct from the initiation of signal transduction. 2002. *The Journal of biological chemistry* 277: 47834-47843; Thieblemont & Wright, Transport of bacterial lipopolysaccharide to the golgi apparatus. 1999. *The Journal of experimental medicine* 190: 523-534). Recurrent bacterial infections in LRBA-deficient patients indicate an impaired TLR4/LPS pathway. These data suggest that LRBA is involved in the TLR4/LPS pathway.

Supplemental table 1  
Mouse CVID genes have multiple NF $\kappa$ B sites\*

Gene	NF $\kappa$ B site (GGGRNYYYCC, N: any base, R: purine, W: A or T, Y: T or C) and the surrounding sequences			
TACI	CTTCCTGG GTTTCCCC CTTCG (-, promoter)	CAGTAGGGCA TCCCCATCTT (+, exon)	TAGTTGGGAC GTCCCCTTTG (+, exon)	
BAFFR	CCCTCTGG CATTCCCC AGGC (+, promoter)	GGGACAGGG AGGTCCCTTG C (+, promoter)	CCTGTGGGCA TTCCCCATGGG (+, promoter)	
ICOS	GTGGTGGG AAATGCCT TTAA (+, 1st intron)	TGTTAGGGCA TTCCCCAAGT (+, exon)	CTGCTGGGGA TGTCCTTTTG (+, exon)	GCTGCTGGGATT CCATGCT (+, exon)

-continued

Supplemental table 1				
Mouse CVID genes have multiple NFkB sites*				
Gene	NFkB site (GGGRNWWYCC, N: any base, R: purine, W: A or T, Y: T or C) and the surrounding sequences			
CD19	<u>GGGCTGGG</u> <u>GCTCCCCCT</u> TTTC (1st intron)	<u>CCACTGGGAC</u> <u>TATCCATCCA</u> (-, exon)	<u>AATGCGTGGA</u> <u>TTCCATAGG</u> (-, exon)	<u>AGAATGGGGACT</u> <u>CACCCTGGGA</u> (-, exon)
CD20	<u>ACAGAGAG</u> <u>ACTTTCCC</u> TGTT (+, 1st intron)	<u>TGTGTTGGGA</u> <u>ATATCCATCC</u> (-, 1st intron)		
CD21	<u>TGGTTTGG</u> <u>AGATTCCCT</u> CAAC (-, promoter)			
CD81	<u>CCTCCGGG</u> <u>AAAGTCCA</u> AGGC (+, promoter)	<u>CCTTTGGGGA</u> <u>GCCCCACCCC</u> (+, 1st intron)		
LRBA	<u>GCGCGGGA</u> <u>CTACCCCT</u> ATGC (-, promoter)	<u>GACCAAGGAC</u> <u>TTCCCTGCTT</u> (+, exon)	<u>AAGCCGGGGC</u> <u>TCCCCATCAG</u> (+, exon)	

□□B sites are in bold and underlined in the promoter, intron or exon on the positive/negative (+/-) DNA strand.

To explore whether this gene is involved in inflammation induced by LPS and other stimuli in vivo, LRBA levels were examined in inflammatory mouse models and human asthmatic subjects. LRBA levels are significantly increased in plasma from mice stimulated with LPS, as seen in FIG. 32(A) or ovalbumin (OVA), seen in FIG. 32(B), in the culture supernatants of human mononuclear leukocytes stimulated with LPS, as seen in FIG. 32(C), and in plasma from asthmatic subjects undergoing an exacerbation of the disease, seen in seen in FIG. 32(D) and FIGS. 33(A)-(C). The presence of LRBA in human plasma also was confirmed by Western blots. 1 ml of human plasma was ultracentrifuged at 1200000 g then 20 µl of supernatant and all precipitation were used to load the PAGE gel. Cell extracts were prepared using radioimmunoprecipitation assay buffer (RIPA) buffer supplemented with protease and phosphatase inhibitors and Western blot detection/densitometry used to quantitate protein levels of specific gene products using a ChemiDoc XRS (Bio-Rad, Richmond, Calif.) imager and Quantity One software (Bio-Rad, Richmond, Calif.). Testing indicated that LRBA was indeed in the plasma, seen in FIG. 32(D, inset) and is supported by the fact that LRBA is detected in the plasma from trauma patients or subjects stimulated with LPS (Qian, et al., Inflammation, and P. the Host Response to Injury Large Scale Collaborative Research. Quantitative proteome analysis of human plasma following in vivo lipopolysaccharide administration using

16O/18O labeling and the accurate mass and time tag approach. 2005. *Molecular & cellular proteomics: MCP 4*: 700-709; Liu, et al., Inflammation, and P. the Host Response to Injury Large Scale Collaborative Research. High dynamic range characterization of the trauma patient plasma proteome. 2006. *Molecular & cellular proteomics: MCP 5*: 1899-1913).

CVID Receptor Genes are Involved in the LPS/TLR4 Pathway:

Similar to LRBA, deficiency of any CVID gene is associated with immunodeficiency, e.g. recurrent bacterial infections. Moreover, CVID genes have multiple NF-κB binding sites in or around the promoter range (Supplemental Table 1). These data suggest that these CVID genes may be involved in the TLR4/LPS pathway.

To investigate whether CVID genes also respond to LPS, mice were injected intraperitoneally with LPS. Twenty-four hours later the spleen and bone marrow cells were harvested and subjected to cytometry assay. The levels of B220, CD19 and TACI are significantly upregulated in both tissues while the levels of BAFFR, CD21 and TLR4 are significantly downregulated, as seen in Table 6 and FIGS. 34 and 35 and 37. The splenocytes and bone marrow cells were also subjected to ex vivo cell culture study with 24 h LPS stimulation, as seen in FIGS. 34 and 35. TACI is significantly upregulated by LPS on splenocytes and bone marrow cells. Interestingly, with LPS stimulation, the percentage of BAFFR is significantly decreased in the spleen and increased in the bone marrow in vivo, but is slightly increased in the splenocytes and decreased in the bone marrow cells, while the intensity of BAFFR is increased in cells from both tissues in ex vivo.

TABLE 6

LPS regulates CVID receptors, B220 and TLR4 in vivo.									
Percentage (%)						Median Intensity (arbitrary fluorescence intensity units)			
		PBS	LPS	fold	P value	PBS	LPS	fold	P value
Bone Marrow	B220	15.8 ± 1.2	15.5 ± 5.1	1.02	0.443	1672.3 ± 124.1	2423 ± 396.6	0.69↑	0.09
	CD19	14.9 ± 0.9	17.9 ± 5.5	0.83	0.88	1829.646.5	1951105	0.94	0.32
	CD21	26.9 ± 0.49	24.5 ± 1.23	1.1	0.07↓	<b>764.7 ± 35.0</b>	<b>378 ± 53.8</b>	<b>2.02↓</b>	<b>0.0006</b>
	BAFFR	35.2 ± 2.3	43.7 ± 4.9	0.81	0.14	<b>1094.3 ± 55.4</b>	<b>693.3 ± 84.1</b>	<b>1.58↓</b>	<b>0.012</b>
	TACI	3.1 ± 1.3	1.4 ± 0.35	2.16	0.22	637.730.7	617.719.7	1.03	0.39
Spleen	TLR4	57.4 ± 2.0	50.9 ± 3.3	1.13↓	0.08	576.3 ± 12.6	592 ± 28.8	0.97	0.85
	B220	<b>47.0 ± 3.2</b>	<b>58.7 ± 4.5</b>	<b>0.8↑</b>	<b>0.021</b>	4015.3 ± 89.3	4031.3 ± 153.2	1	0.88
	CD19	<b>49.3 ± 3.8</b>	<b>59 ± 4.1</b>	<b>0.8↑</b>	<b>0.04</b>	1928.362.4	1792237	1.07	0.39
	CD21	88.8 ± 1.8	80.9 ± 9.7	1.1	0.24	<b>846 ± 29.5</b>	<b>580.71 ± 56.5</b>	<b>1.45↓</b>	<b>0.04</b>
	BAFFR	93.1 ± 2.6	94.7 ± 0.92	0.98	0.36	<b>1002 ± 19.5</b>	<b>842.7 ± 73.1</b>	<b>1.19↓</b>	<b>0.022</b>
	TACI	<b>2.7 ± 0.40</b>	<b>7.9 ± 2.70</b>	<b>0.35↑</b>	<b>0.03</b>	479.3 ± 30.0	560.7 ± 60.1	1.1	0.85
	TLR4	<b>64.6 ± 2.3</b>	<b>55.7 ± 4.0</b>	<b>1.16↓</b>	<b>0.03</b>	511.3 ± 17.0	502.7 ± 3.1	1.02	0.43

Numbers in bold indicate significant change, numbers underlined indicate near significant change.

20

The regulation of NFκB on the BAFFR, CD19 and TACI was further investigated in LRBA WT and LRBA KD Raji cells using two proteasome inhibitors, MG132 and PS341, with three different doses for 4 and 14 hours to inhibit NFκB by blocking proteasome-mediated IκB degradation. As expected, the levels of BAFFR and CD19 are decreased by NFκB inhibitors in a dose-dependent manner, but the levels of TACI are increased in Raji cells. The levels of the receptor change significantly from 4 to 24 h but less significantly among different doses. However, there are significant changes among the different doses in the levels of for CD19 and TACI at 24 h in the LRBA WT cells. Interestingly, TACI in LRBA KD cells is not affected by either of the two inhibitors, as seen in FIGS. 36(A)-(C) and 37(A)-(C), indicating that LRBA may regulate TACI by proteasome degradation.

25

30

35

40

45

50

55

60

65

#### LRBA Regulates CVID Receptors In Vitro:

LRBA is an important vesicle trafficking regulator (Wang, et al., Identification of a novel lipopolysaccharide-inducible gene with key features of both A kinase anchor proteins and chs1/beige proteins. 2001. *J Immunol* 166: 4586-4595; Cullinane, et al., The BEACH Is Hot: A LYST of Emerging Roles for BEACH-Domain Containing Proteins in Human Disease. 2013. *Traffic*) and may function as a master regulator of multiple CVID receptors. To test this, LRBA WT and LRBA KD Raji cells were stimulated with LPS, and the cell surface levels of CVID receptors and TLR4 were analyzed by flow cytometry. BD FACSelect Multicolor Panel Designer was used to search antibodies and build up the panel for multiple color cytometry for LSRII FACS machine. Fluorophores directly conjugated antibodies against cell surface CVID proteins were used: CD19-PerCP-Cy5.5, CD20-PE-Cy7, CD21-V450, BAFFR-PE, TACI-APC, and CD81-APC-H7. Two panels were used when use live/dead discrimination with DAPI (overlap with PerCP-Cy5.5) or 7AAD (overlap with V450). The standard staining procedures were followed and 20,000 to half million cells were acquired. Data acquisition was performed using FACS LSRII flow cytometers and analyzed using FACSDiva version 6.1.2.

The results demonstrate that the knockdown of LRBA significantly decreases the cell surface levels of TACI, CD19 and CD20 but increases the cell surface levels of CD21 and

BAFFR. The LRBA knockdown also significantly decreases TACI and TLR4 positive cell numbers by four fold and two fold, respectively, but increases CD21 positive cell numbers by two fold, seen in FIGS. 38 and 39 and Table 7.

TABLE 7

Influence of LRBA knockdown on the cell surface levels of CVID and TLR4 receptors.				
	Wild type	Knockdown	fold	p value
Percentage (%)				
CD19	98.93 ± 0.50	98.57 ± 0.28	1.00	0.15
CD20	99.32 ± 0.95	99.18 ± 0.04	1.00	0.74
CD21	27.25 ± 3.54	55.08 ± 5.00	<b>0.49↑</b>	6E-07
BAFFR	87.30 ± 1.24	90.83 ± 0.93	<b>0.96↑</b>	0.0002
TACI	30.06 ± 3.41	7.38 ± 1.49	<b>4.07↓</b>	8E-07
TLR4	56.88 ± 6.21	31.27 ± 11.42	<b>1.82↓</b>	0.0007
Median Intensity (arbitrary fluorescence intensity units)				
CD19	7167.33 ± 215.86	5830.17 ± 159.95	<b>1.23↓</b>	<b>3E-07</b>
CD20	35802.00 ± 4300.52	29541.25 ± 332.06	<b>1.21↓</b>	<b>0.03</b>
CD21	1591.00 ± 41.19	1659.50 ± 72.48	<b>0.96↑</b>	<b>0.002</b>
BAFFR	3391.50 ± 312.08	4198.00 ± 496.75	<b>0.81↑</b>	<b>0.007</b>
TACI	2411.83 ± 114.57	1813.50 ± 412.89	<b>1.33↓</b>	<b>0.01</b>
TLR4	11664.40 ± 3828.47	11204.60 ± 2171.10	1.04	0.81

Numbers in bold indicate significant change.

As seen in FIGS. 38 and 39, each experimental data was represented by a marker on the figure, while each set of the experimental data obtained from LRBA WT or LRBA KD Raji cells stimulated with LPS over a series of time points was fitted to a polynomial trend line. High R<sup>2</sup> values (R<sup>2</sup>=1) were obtained, demonstrating that each set of data can be represented by a polynomial trend line equation. Then, the slope at each time point can be used to measure the rate of CVID receptor level change in response to LPS. The results, seen in Table 8, demonstrate that the slopes of the response curves at most points from LRBA KD cells are less than the curves from LRBA WT cells. This indicates that CVID receptors in the LRBA WT cells are more responsive to stimulators, as seen in FIG. 36(A)-(C) and 37(A)-(C). In addition to response speed change, the response phase of the CVID receptor response curves from WT and KD also are different with most are opposite or out of phase, seen in Table 8.

TABLE 8

Comparison of the change rate of the gene expression levels in response to stimulators in cells with LRBA knock down or overexpression (Fold change ratio)*.											
Fold	Gene	Time point								Fluctuation phase	FIG. #
		1	2	3	4	5	6	7	8		
LRBA KD LPS or EGF (WT/KD)	CD19	0.91	2.08	1.00	0.50	7.06	5.99			Opposite phase	40, 41
	CD20	7.63	8.84	85.84	4.73	42.97	3.24			Out of phase	40, 41
	BAFFR	1.16	2.01	1.56	2.18	1.26	0.52			Opposite phase	40, 41
	TACI	0.01	1.39	5.75	3.69	2.76	2.50			Opposite phase	40, 41
KD protease inhibitor (WT/KD)	CD19	0.91	1.80	0.10	9.81	1.18	0.86	0.60	1.09	Opposite phase	38, 39
	BAFFR	145.3	3.33	1.15	2.08	1.51	6.26	5.01	3.68	In phase	38, 39
	TACI	1.41	0.84	5.94	0.53	4.39	5.79	5.14	2.04	Opposite phase	38, 39
LRBA <sup>+++</sup> LPS LRBA <sup>+++</sup> /WT	B220	0.90	1.18	0.06	0.20	1.37	1.31	1.07	0.29	Opposite phase	7
	CD69	1.36	0.88	1.97	1.12	0.90	0.83	0.81	0.77	In phase	7
	BAFFR	1.30	5.19	4.95	1.43	0.60	17.88	4.50	20.40	Opposite phase	7
	TACI	1.52	1.99	0.14	2.35	0.52	1.26	0.32	1.13	In phase	7

KD/WT.

KD = knockdown,

WT = wild-type,

LRBA<sup>+++</sup> = LRBA Overexpression.

CD19 is based on percentage others are Median Intensity (arbitrary fluorescence intensity units).

To confirm these results, four LRBA potential dominant negative mutants (DNM) fused with green fluorescent protein (GFP) were constructed from BEACH (Beige and Chediak-Higashi), VHS-LIR [VPS (vacuolar protein sorting), Hrs (hepatocyte growth factor-regulated tyrosine kinase substrate) and STAM (signal transducing adaptor molecule), LC3 (light chain 3) Interacting Region], VHS and LIR domains and transfected into Raji cells. CVID and TLR4 receptors were analyzed in the GFP positive and negative populations. All LRBA DNMs significantly decrease cell surface CVID receptor positive cell numbers and cell surface intensity, as seen in FIGS. 40 and 41. VHS-LIR DNM decreases CD21, BAFFR and TACI by 2 to 3 times. The MFI downregulation of CD19 and CD20 by the LIR was further confirmed in several clones stably transfected with the GFP-LIR DNM constructs, as seen in FIGS. 42-44. The percentage of these receptors in wild type cells remains consistent indicating that the changes of these receptors in GFP positive cells (transfected) were induced specifically by LRBA DNMs.

#### LRBA Regulates CVID Receptors In Vivo:

The knockdown of LRBA downregulates CVID receptors, while the overexpression of LRBA may upregulate CVID receptors. The miR-150 knockout (KO) mice were used to test this possibility. There is one miR-150 potential site conserved in the LRBA coding region of the human and mouse LRBA genes, as seen in FIG. 42. Overexpression of miR-150 down-regulates LRBA, while in the miR-150 ko mice, LRBA is overexpressed, as seen in FIGS. 43 and 44. The B cell surface levels of BAFFR, TACI, CD69 (B cell activation marker), B220 and LRBA are increased in the splenocytes and bone marrow cells from the wild type C57BL/6J and the miR-150 KO mice after LPS stimulation, and are higher in the miR-150 KO mice in most cases. B220 and CD69 were increased over the entire stimulation time in both splenocytes and bone marrow cells. TACI increased dramatically after 24 h LPS stimulation. In the KO spleen, CD69, BAFFR and LRBA are higher, while TACI is lower

at the beginning of the stimulation (0 to 2 h), and higher later (3 to 24 h). BAFFR, TLR4 and TACI are lower on bone marrow cells in KO mice, as seen in FIGS. 43 and 44. The results from these different methods confirm each other and demonstrate that LRBA regulates multiple cell membrane receptors, including CVID and TLR4.

To understand the underlying molecular mechanism by which LRBA deficiency causes CVID and autoimmunity, first we examined the involvement of CVID receptors and LRBA in the LPS/TLR4/NFκB pathway, which is one of most important signal pathways in immune response, and is closely related to immunodeficiency and autoimmunity. Toll is an essential receptor for host defense against fungal and Gram-positive bacterial infections in *Drosophila* (Lemaitre, et al., The dorsoventral regulatory gene cassette spatzle/Toll/cactus controls the potent antifungal response in *Drosophila* adults. 1996. *Cell* 86: 973-983). The mammal TLR4 recognizes LPS from Gram-negative bacteria, fibrinogen cleaved by proteases from fungi and Gram-positive bacteria, and viral proteins (F protein from respiratory syncytial virus, vesicular stomatitis virus glycoprotein G, poxviral protein A46) (Stack & Bowie, Poxviral protein A46 antagonizes Toll-like receptor 4 signaling by targeting BB loop motifs in Toll-IL-1 receptor adaptor proteins to disrupt receptor:adaptor interactions. 2012. *The Journal of biological chemistry* 287: 22672-22682; Bezemer, et al., Dual role of Toll-like receptors in asthma and chronic obstructive pulmonary disease. 2012. *Pharmacological reviews* 64: 337-358). LPS is a crucial structural component of Gram-negative bacteria and a potent immunostimulators. Excessive LPS stimulation can result in systemic inflammation and death (Beutler & Rietschel, Innate immune sensing and its roots: the story of endotoxin. 2003. *Nature reviews. Immunology* 3: 169-176). It interacts with TLR4, activating the downstream transcription factors of the nuclear factor κB (NF-κB) family to produce several hundred inflammatory genes (Beutler & Rietschel, Innate immune sensing and its roots: the story of endotoxin. 2003. *Nature reviews. Immunology* 3: 169-176;

Poltorak, et al., Defective LPS signaling in C3H/HeJ and C57BL/10ScCr mice: mutations in Tlr4 gene. 1998. *Science* 282: 2085-2088; Akira, et al., Pathogen recognition and innate immunity. 2006. *Cell* 124: 783-801). NF- $\kappa$ B plays a pivotal role in inflammation and immune responses including inflammatory and immune responses (Baltimore, NF- $\kappa$ B is 25. 2011. *Nat Immunol* 12: 683-685; Hayden & Ghosh, NF- $\kappa$ B, the first quarter-century: remarkable progress and outstanding questions. 2012. *Genes & development* 26: 203-234), and is a hub transcription factor downstream of many proteins, defects of which cause immunodeficiency (Cunningham-Rundles, Human B cell defects in perspective. 2012. *Immunologic research* 54: 227-232). Therefore, LPS/TLR4 is one of most important signal pathways in immune response. It is important to defend against Gram-negative and some Gram-positive bacteria (Koppe, et al., Recognition of *Streptococcus pneumoniae* by the innate immune system. 2012. *Cellular microbiology* 14: 460-466), fungi (Millien, et al., Cleavage of fibrinogen by proteinases elicits allergic responses through Toll-like receptor 4. 2013. *Science* 341: 792-796) and viruses (Shinya, et al., The TLR4-TRIF pathway protects against H5N1 influenza virus infection. 2012. *Journal of virology* 86: 19-24). LRBA is involved in the signal transduction pathway initiated by LPS (Wang, et al., Identification of a novel lipopolysaccharide-inducible gene with key features of both A kinase anchor proteins and chs1/beige proteins. 2001. *J Immunol* 166: 4586-4595). Its deficiency is hypothesized to impair the TLR4 pathway. Other CVID genes are critical immune regulators, involved in the stimulation, survival and development of B cells. However, their involvements in LPS/TLR4 pathway have not been explored yet. Levels of LRBA and the CVID receptors are shown responsive to LPS stimulation, suggesting that they are involved in LPS/TLR4 signal pathways, agreeing with their critical roles in the immune system.

The data from proteasome inhibitors, which inhibit NF $\kappa$ B by blocking proteasome-mediated I $\kappa$ B degradation, suggests that LPS may regulate CVID receptors through NF $\kappa$ B. Intriguingly, TACI levels cannot be increased in Raji9 cells treated with proteasome inhibitors: 250 nM of MG-132 or 50 nM of PS-341 for 24 hr as in Raji cells, as seen in FIG. 42, suggesting that the deactivation of NF $\kappa$ B may be blocked by LRBA knockdown and thus the expression of TACI may be continually inhibited. In contrast, BAFFR and CD19 are decreased by the two NF- $\kappa$ B inhibitors in a dose-dependent manner, suggesting that the two genes are positively regulated by NF- $\kappa$ B.

LRBA was tested to determine if it is a master regulator for CVID receptors. LRBA is a unique CVID gene extraordinarily different from other CVID genes. First, it is a large gene encoding a 319 kD protein composed of multiple domains (Wang, et al., Identification of a novel lipopolysaccharide-inducible gene with key features of both A kinase anchor proteins and chs1/beige proteins. 2001. *J Immunol* 166: 4586-4595; Kerr, et al., Analysis of lipopolysaccharide-response genes in B-lineage cells demonstrates that they can have differentiation stage-restricted expression and contain SH2 domains. 1996. *Proceedings of the National Academy of Sciences of the United States of America* 93: 3947-3952), and could serve as a scaffold to interact with multiple proteins. Other CVID proteins are relative small: ICOS is 27 kD; TACI, 32 kD; BAFFR, 19 kD; CD81, 26 kD; CD21, 145 kD; CD20, 35 kD; and CD19, 61 kD. Second, CVID proteins are plasma membrane receptors on B cells except for ICOS which is on T cells. LRBA is expressed in every kind of cells and locates to almost everywhere in the cell and

is a regulator for vesicle trafficking. Vesicle trafficking is required for homeostasis and activation of plasma membrane receptors (Wang, et al., Identification of a novel lipopolysaccharide-inducible gene with key features of both A kinase anchor proteins and chs1/beige proteins. 2001. *J Immunol* 166: 4586-4595; Cullinane, et al., The BEACH Is Hot: A LYST of Emerging Roles for BEACH-Domain Containing Proteins in Human Disease. 2013. *Traffic*). Third, LRBA deficiency causes both immunodeficiency and autoimmunity in LRBA deficient patient, a phenomenon not seen with other CVID genes. TACI mutations also are associated with autoimmunity but to a much lesser extent (Salzer, et al., Relevance of biallelic versus monoallelic TNFRSF13B mutations in distinguishing disease-causing from risk-increasing TNFRSF13B variants in antibody deficiency syndromes. 2009. *Blood* 113: 1967-1976). Fourth, LRBA is the only CVID protein that is a protein kinase A anchor and can regulate protein activity by phosphorylation. Agreeably, LRBA deficiency causes more severe diseases, and in addition to immunodeficiency and autoimmunity, other medical conditions such as severe retarded growth and failure to thrive, growth hormone deficiency, asthma, monoarthritis, seizures, granulomatous infiltration, finger clubbing, hepatosplenomegaly, allergic dermatitis, and nephrotic syndrome are also observed in LRBA deficient patients. LRBA was shown to extensively associated with the endomembrane system including the Golgi complex, endosomes, lysosomes, plasma membrane, nucleus, pseudopodia and microtubules, and vesicle trafficking, which is responsive to LPS stimulation, suggesting that LRBA plays a regulatory but not a structural role in vesicle trafficking, which is essential for signal transduction of immune effectors. These results suggest that LRBA plays a role in vesicle trafficking and signal transduction essential for the immune system, deficiency of which caused by LRBA deficiency may cause the aforementioned diseases. Our previous study shows that LRBA regulate EGFR activation. Neurobeachin (Nbea) is required for the disposition of surface levels of glutamate and GABA,  $\gamma$ -aminobutyric acid (GABA) receptors at synapses (Nair, et al., Neurobeachin regulates neurotransmitter receptor trafficking to synapses. 2013. *The Journal of cell biology* 200: 61-80). Thus, LRBA may regulate other CVID genes, for example, CD19, CD20 and BAFFR, because their levels are low when LRBA is absent.

Therefore, the cell surface receptors (CVID receptors and TLR4) were examined for LRBA regulation. LRBA repression by multiple methods downregulates the levels of CD19, CD20, TACI and TLR4, seen in Table 6. In contrast, overexpression of LRBA in a mouse model has opposite effects, i.e., upregulation of these B cell markers, seen in FIGS. 36 and 37. The response speed for all genes, except for BAFFR, is decreased in the LRBA repressed cells but increased in LRBA overexpressed cells. The response phase for most genes in LRBA deregulated cells is out of phase or opposite to that of wild type (WT) cells, seen in Table 6 and FIGS. 36 and 37. The results demonstrate that the deregulated LRBA deregulates the four parameters (protein levels/activity, response speed and response phase) of these critical effectors, and subsequently may result in deregulated immune response, which requires high coordination among genes involved.

Interestingly, survival genes, BAFFR is increased, while anti-survival genes, e.g. TACI(18, 19), TLR4(54), and other CVID receptors (CD19, CD20 and CD21) are decreased with LRBA repression, seen in Table 6, which appears to result in enhanced survival signaling and more cells. This is supported by the findings that LRBA deficient patients have

more peripheral T cells, more CD20 positive B cells, lymphocyte infiltration and respond to anti-CD20 therapy. The effects of miR-150 on CVID receptors are mediated by LRBA. In another word, miR-150 K/O mice represent LRBA overexpression model in terms of CVID receptor regulation.

LRBA's presence in plasma and cell membranes may provide an easy way to modulate LRBA levels. Antibodies to LRBA also decrease the proinflammatory cytokines, IL-6 and TNF $\alpha$  in vivo, as seen in FIG. 41. Thus, LRBA, a critical regulator for multiple inflammatory diseases, may be an ideal therapeutic target to treat chronic inflammatory diseases.

The mammal Toll-like receptor 4 (TLR4) recognizes LPS from Gram-negative bacteria, fibrinogen cleaved by proteases from fungi and Gram-positive bacteria, and viral proteins (F protein from respiratory syncytial virus, vesicular stomatitis virus glycoprotein G, poxviral protein A46) (38, 39). Therefore, this receptor is important to defend against Gram-negative and some Gram-positive bacteria(46), fungi (47) and viruses(48). LRBA is involved in the signal transduction pathway initiated by LPS(5), which is a crucial structural component of Gram-negative bacteria and a potent immunostimulator. Excessive LPS stimulation can result in systemic inflammation and death(40). It interacts with TLR4, activating the downstream transcription factors of the nuclear factor  $\kappa$ B (NF- $\kappa$ B) family, to produce proinflammatory cytokines, IL-6 and TNF $\alpha$ . NF- $\kappa$ B plays a pivotal role in inflammation and immune responses. In signal transduction, it is downstream of many proteins, defects of which cause immunodeficiency and autoimmunity. LRBA deficiency impairs the TLR4 pathway by deregulating hub proteins such as NF- $\kappa$ B and mitogen-activated protein kinases (MAPKs), which, in turn, deregulate multiple critical immune genes such as CVID receptors, resulting in immunodeficiency and autoimmunity.

#### Example 10

Lipopolysaccharide (LPS)-responsive beige-like anchor (LRBA) deficiency causes both immunodeficiency (CVID) and autoimmunity with manifestations of antibody deficiency (1-3), indicating that it plays a fundamental role in the immune system. CVID is the most common late-onset primary immunodeficiency disease (PID). Transmembrane activator and calcium modulator and cyclophilin ligand interactor (TACI)(4) and B cell-activating factor receptor (BAFFR)(5), CD20(6), inducible costimulator (ICOS)(7) and members of the B cell coreceptor complex (CD19(8), CD21(9) and CD81(10)), also are associated with or cause CVID(11). About two-third of CVID patients have autoimmune problems (12, 13). As opposed to other CVID genes, the immunodeficiency caused by LRBA deficiency is highly associated with autoimmunity. To date, the 11 identified LRBA-deficient CVID patients had autoimmunity(1, 2, 14). TACI mutations also are associated with autoimmunity but to a lesser degree (36% vs. 23% of patients with wild-type TACI) (15). The association of immunodeficiency with autoimmunity is paradoxical, since immunodeficiency is lacking immunity, while autoimmunity is overactivation of the immunity to the body. LRBA deficient patients have markedly reduced T-cell proliferation in response to phytohaemagglutinin (PHA) and anti-CD3 mAb stimulations(3), and reduced B cell survival(1). On another hand, LRBA deficient patients have more CD20 positive B cells, lym-

phocyte infiltration and respond to anti-CD20 therapy(1-3), suggesting that overactivation of B cells may contribute to the autoimmunity.

LRBA was initially identified as an LPS-upregulated gene in B cells (16, 17). It belongs to the WDL-BEACH-WD40 (WBW) gene family containing the WBW super domain. LRBA and other WBW proteins appear to function as scaffolding proteins in vesicle trafficking(1, 16, 18, 19) and are important for human disease(18). Vesicle trafficking is required for homeostasis of inflammatory receptors and cytokines through cell membrane deposition, oligomerization, phosphorylation, internalization, recycling and degradation(20). To explain the paradoxical association of immunodeficiency and autoimmunity, it is hypothesized that LRBA deficient patients have defective vesicle trafficking, resulting in attenuation of both activation and deactivation of immune mediators. The attenuation of activation of immune mediators may lead to immunodeficiency, while the attenuation of deactivation of immune mediators may result in prolonged activation of the immunity and then autoimmunity. To test this hypothesis, LRBA was stably knocked down in Raji cells by the short hairpin (sh) RNA technique to study the effects of LRBA repression on NF $\kappa$ B activity. The results demonstrate that repression of LRBA attenuates both NF $\kappa$ B activation and deactivation, which may result in insufficient NF $\kappa$ B activity and prolonged NF $\kappa$ B activation, leading to immunodeficiency and autoimmunity.

LRBA Regulates NF $\kappa$ B in a Dual Mode:

NF- $\kappa$ B is the central regulator of the immune system and plays a pivotal role in inflammation and immune responses. Disturbed NF- $\kappa$ B signaling is implicated in the pathogenesis of human immunodeficiency and chronic autoimmune inflammatory diseases(21). Defects of several genes upstream of NF $\kappa$ B cause immunodeficiency(22). Therefore, deregulation of NF- $\kappa$ B signaling may be involved in LRBA deficiency associated immunodeficiency and autoimmunity. In another word, LRBA may be a regulator of NF- $\kappa$ B. To test this hypothesis, LRBA was knocked down in Raji cells by the short hairpin (sh) RNA technique as previously described(23). Several stable clones were obtained and named Raji9 cells. Raji cells were stimulated with LPS for different times from zero to several hours, and the NF- $\kappa$ B activity was measured by NF- $\kappa$ B luciferase reporter. The average levels of the NF- $\kappa$ B activity are higher in Raji cells with LRBA knockdown, as seen in FIG. 45(A). This is also confirmed by the flow cytometry measurements of the phospho-NF $\kappa$ B (pS529) levels, as seen in FIG. 45(B). The phosphorylation of 5529 in the activation domain stimulates NF- $\kappa$ B transcriptional activity, and thus may be used to reflect NF- $\kappa$ B activation(24). The results also show that the NF- $\kappa$ B activity is not stable but fluctuates over the time period of the stimulation. Without stimulation, the NF- $\kappa$ B activity is higher in Raji9 cells (LRBA KD) but declines and is lower with stimulation at 15 min and 30 min, then goes up and is higher. On the other hand, the NF- $\kappa$ B activity in Raji cells is the opposite of its activity in Raji9 cells, as seen in FIG. 46(B). The observed fluctuation of the NF- $\kappa$ B activity agrees with the finding that NF- $\kappa$ B activity oscillates during stimulation. Therefore, the levels of the NF- $\kappa$ B activity can be both lower and higher in Raji or Raji9 cells depending on the time when the activity is observed.

These results demonstrate that NF- $\kappa$ B activity is regulated by LRBA. To test if the regulation is dose-dependent, A549 cells were transfected with the LRBA shRNA plasmid DNA to knockdown LRBA. Three stable clones that have different levels of GFP expression were obtained, as seen in FIG. 45(D). The GFP expression levels may be used to indicate



LRBA shRNA levels, which should be inversely related to the levels of LRBA. The results show that the luciferase activity corresponds to the GFP levels and is inversely related to the levels of LRBA, as seen in FIG. 45(C), suggesting that knockdown of LRBA increases NF- $\kappa$ B activity in a dose-dependent manner in A549 cells.

As the NF- $\kappa$ B activity oscillates during stimulation, to measure the speed of the NF- $\kappa$ B activity change in response to stimulation, a trend line for each dataset was obtained by polynomial fitting, as seen in FIG. 46(B). The  $R^2$  value is 1, suggesting a perfect fitting, and the trend line can be used to represent the corresponding dataset. In another word, the dataset can be described by the trend line equation. Then the slope of the curve at each time point can be calculated and used for the speed of the NF- $\kappa$ B activity change at that time point. The results show that the speed of the NF- $\kappa$ B activity change in the wild type cells at most time point is higher than LRBA knockdown cells in Raji cells, as seen in Table 9,

To this end, we measured cytokines. The secreted levels of TNF $\alpha$  and IL-10 measured by the cytometric bead array (CBA) are significantly increased by knocking down LRBA, as seen in FIG. 48. The levels of TNF $\alpha$  are the highest at 1 hr stimulation, IL-10 is the highest at 4 hr stimulation. Interestingly, the speed of the TNF $\alpha$  or IL-10 levels change in the wild type cells at all-time points is lower than LRBA knockdown cells in Raji cells, seen in Table 9, suggesting that LRBA knockdown speed up level change of TNF $\alpha$  or IL-10. The level of IFN $\gamma$  is the highest at 30 min stimulation, IL-4 is the highest at 2 hr. IL-2 is lower in LRBA KD cells at 15 and 30 min. At other time point the difference is not obvious. The ELISA assays of intracellular and extracellular TNF $\alpha$  also confirm the CBA TNF $\alpha$  are higher when LRBA is knocked down. Similar to the above data, increased secretion of carboxypeptidase Y were observed in *Saccharomyces cerevisiae* with the deletion of LRBA orthologue, BPH1(29). Agreeably, the LRBA isoform, neurobeachin (NBEA) is a negative regulator of vesicle secretion(30).

TABLE 9

Comparison of the change rate of the gene expression levels or activity in response to stimulators in cells with LRBA knock down or overexpression (Fold change ratio)*											
Fold	Gene	Time point								Fluctuation phase	FIG.
		1	2	3	4	5	6	7	8		
LRBA KD LPS or EGF (WT/KD)	NF- $\kappa$ B	1.24	0.82	0.85	0.13	3.08	1.17	0.93		Opposite and out of phase	1A
	TNF $\alpha$	<b>2.33</b>	<b>4.04</b>	<b>3.03</b>	<b>3.31</b>	<b>2.23</b>				In phase	2D
	IL-10	<b>19.28</b>	<b>1.73</b>	<b>4.17</b>	<b>5.75</b>	<b>1.68</b>				Opposite phase	2D

\*Numbers in bold and italic are reversed ratios, i.e. KD/WT.  
 KD = knockdown,  
 WT = wild-type.

suggesting that LRBA knockdown attenuates both activation and deactivation of NF- $\kappa$ B activity. It also shows that the oscillation curve for Raji control cells is more regular than Raji9 cells, suggesting that NF- $\kappa$ B activity is deregulated by LRBA knockdown. These data also show that the NF- $\kappa$ B activity is lower at the beginning of the stimulation but is higher after prolonged stimulation.

#### LRBA Regulates MAPKs:

Like NF- $\kappa$ B, the mitogen-activated protein kinases (MAPKs) act as funnels to collect many stress-activated signals but function as bottle necks to filter and process these signals, and then have many diverse targets(26). Specifically, MAPKs are critical downstream hubs of the TLR4/LPS signal transduction(27) and may be affected by LRBA deficiency. The expression and activation of the three major MAPKs [p42/44, p38 and Jun N-terminal kinase (JNK)] were examined in Raji cells. The results suggest that the p42/44 kinase activity is reduced, while the JNK and p38 kinase activities are increased, as seen in FIG. 47, in LRBA KD cells. The phospho-p42/44 measured by flow cytometry intracellular staining also is decreased (data not shown). Similar results were observed in *Drosophila* where MAPK (p42/44 orthologue) is downregulated but JNK is increased when rugose (rg, LRBA orthologue) is mutated(28). The *Drosophila* MAPK and JNK have 82% and 78% identities with their human orthologues, respectively.

#### LRBA Regulates Cytokines:

The results show that LRBA regulates NF- $\kappa$ B and signal transduction kinase hubs, which suggests that cytokines regulated by these proteins also may be regulated by LRBA.

#### LRBA Immunodeficiency In Vitro Model.

In order for pathogens to efficiently spread to neighboring cells and evade the immune cells, and/or gain nutrients, one prominent strategy of many bacterial pathogens is to cause host cell death (31). On another hand, the host cell, first will try to kill the evaded pathogens. As such, cell death may be used as a hallmark of immunodeficiency. This study demonstrates that repression of LRBA deregulates multiple critical immune genes and can explain why LRBA deficiency causes immunodeficiency. It is hypothesized that Raji cells with LRBA knockdown can serve as an immunodeficiency in vitro model, i.e. they cannot fight pathogens efficiently when compared to wild type cells, manifested as more cell death. To test this assumption, Raji and Raji9 cells were infected separately with adenoviruses and Gram-negative bacteria and the annexin V apoptosis assay was conducted after 24 hrs, as seen in FIGS. 49(A) and (B). The results show that there are more dead cells or apoptotic cells when LRBA is knocked down, as seen in FIGS. 49(C) and (D).

Despite the tremendous progress in understanding the regulation of NF- $\kappa$ B, there is much that remains to be understood(32). Therapeutic strategies based on specifically targeting the NF- $\kappa$ B pathway have failed to show efficacy in human disease, although NF- $\kappa$ B is implicated to be critical in a host of human diseases(33). This study identified a new category of NF- $\kappa$ B regulator, LRBA, a vesicle trafficking regulator. LRBA is the first vesicle trafficking regulator that regulates NF- $\kappa$ B. Vesicle trafficking is required for both

activation and deactivation of many immune effectors. Agreeably, LRBA regulates both NF- $\kappa$ B activation and deactivation.

Based on these results, a dual regulation model of immune mediators is proposed for LRBA's regulating NF- $\kappa$ B and other genes, and in turn, regulating the immune system, as seen in FIG. 50. According to this model, at first, the activation of NF- $\kappa$ B is attenuated with LRBA repression, resulting in low transcription activity due to attenuated nuclear translocation of NF- $\kappa$ B, as seen in FIGS. 45(E) & (F) (First phase, before 30 min). The deactivation of NF- $\kappa$ B, however, also is attenuated with LRBA repression, resulting in higher transcription activity, due to the attenuated cytoplasmic translocation of NF- $\kappa$ B, as seen in FIGS. 45(A)-(D) and 46(A) & (B) (Second phase, after 30 min). The insufficient NF- $\kappa$ B activity at beginning may result in immunodeficiency, while prolonged NF- $\kappa$ B activity at a later phase, may result in autoimmunity due to increased production of proinflammatory cytokines, especially TNF $\alpha$ , as seen in FIG. 48. The fact that the response speed and levels of proinflammatory cytokines (TNF $\alpha$  and IL-10) are increased, seen in Table 9, may partially explain how LRBA deficiency causes autoimmunity. TNF $\alpha$  and IL-10 are implicated in the pathogenesis of Crohn's disease. TNF $\alpha$  levels are high in the gastrointestinal (GI) tract of IBD and may play a role in the inflammatory pathology of the disease(26). IL-10 has both immunoregulatory and immunostimulatory properties. It can facilitate B-cell proliferation, differentiation, and antibody production and CD8<sup>+</sup> T cell activation. TNF $\alpha$  is overexpressed in rheumatoid arthritis (RA) and other inflammatory diseases (27). IBD and RA are associated with LRBA deficiency (1-3), which suggest overexpression of these cytokines caused by LRBA deficiency may be responsible for the autoimmunity. Thus, LRBA may regulate both NF- $\kappa$ B activation and deactivation through regulating the levels, response speed and response phase of activity. Repression of LRBA may attenuate both the activation and deactivation of NF- $\kappa$ B and other genes.

Several fundamental implications can be obtained from this model: First, the immune system requires a rapid response, and the insufficient activation of immune effectors may cause immunodeficiency (phase 1); Second, the delayed and prolonged activation of immune effectors may cause autoimmunity (phase 2); Third, although autoimmunity and normal immunity may involve the same genes, they may be different, as autoimmunity results from the four deregulated parameters (protein levels, activation levels, response speed and response phase) of the immune effectors; Fourth, autoimmunity (phase 2) occurs following immunodeficiency (phase 1) and may be as a result of the immunodeficiency.

The members of NF- $\kappa$ B and MAPK protein families act as funnels to collect a great number of stress-activated signals but function as bottle necks to filter and process these signals, and then to participate in the regulation of hundreds of genes (26). They were examined in this study for LRBA regulation to investigate the molecular mechanism by which LRBA deficiency causes immunodeficiency and autoimmunity. LRBA knockdown upregulates NF- $\kappa$ B activity, TNF $\alpha$  and IL-10 levels. It also increases the phosphorylation levels (activity) of p38 and JNK but decreases that of p42/44, as seen in FIG. 45. The response speed for NF- $\kappa$ B and proinflammatory cytokines (TNF $\alpha$  and IL-10) is increased in the LRBA repressed cells but decreased in LRBA overexpressed cells. The response phase for most genes in LRBA deregulated cells is out of phase or opposite to that of wild type (WT) cells (Table 9 and FIG. 48. The results demonstrate

that the deregulated LRBA deregulates the four parameters (protein levels/activity, response speed and response phase) of these critical effectors, and subsequently may result in deregulated immune response, which requires high coordination among genes involved.

NF- $\kappa$ B is the master gene regulator in the immune response and plays a pivotal role in the immune system, including inflammatory and immune responses, and is a hub transcription factor downstream of many proteins, defects of which cause immunodeficiency(22). Other genes in this study also encode critical immune effectors closely associated with PIDs and autoimmunity, and may be controlled by NF- $\kappa$ B directly such as those genes that are known or potential NF- $\kappa$ B target genes (TNF $\alpha$ ), or indirectly, e.g. NF- $\kappa$ B activates TNF $\alpha$  which can activate JNK and p38(34, 35). Thus, LRBA may exert its effects on immunodeficiency and autoimmunity via its regulation of these genes through NF- $\kappa$ B.

Survival genes, i.e. NF- $\kappa$ B, AKT, TNF $\alpha$  and IL-10, or stress genes, i.e. p38 and JNK, are increased, while anti-survival genes, e.g. proliferation gene (p42/44)(36, 37) are decreased with LRBA repression (Table 9). This may result in enhanced survival signaling and more cells, which is supported by the findings that LRBA knockdown significantly increases cell survival, and that LRBA deficient patients have more peripheral T cells, more CD20 positive B cells, lymphocyte infiltration and respond to anti-CD20 therapy(1-3). These data suggest that the autoimmunity caused by LRBA deficiency may be associated with deregulated cell survival. Self-reactive T and B cells are deleted by apoptosis during the development of T and B cells in the thymus and bone marrow, respectively. The increased survival may enable self-reactive B or T cells to escape from destined apoptosis and to enter the blood stream and cause autoimmunity. However, when these cells are infected with Gram-negative bacteria or adenoviruses, more Raji9 cells die and become apoptotic. This suggests that Raji9 cells cannot efficiently fight infection and could be used as an in vitro immunodeficiency model.

Finally, current therapeutic strategies to treat inflammatory diseases are based on single cytokines. The cytokine cascade is highly redundant, and chronic inflammatory diseases, more often than not, are complex involving multiple cytokines(38). Therefore, inhibition of a single cytokine may not be sufficient to treat the disease and blocking a variety of different cytokines with multiple agents is theoretically impractical. Targeting a gene such as LRBA, that regulates multiple cytokines and other immune effectors, may be desirable. This gene is crucial in the regulation of multiple immune effectors, including various cytokines. LRBA's presence in plasma and cell membranes may provide an easy way to modulate LRBA levels. Antibodies to LRBA also decrease the proinflammatory cytokines, IL-6 and TNF $\alpha$  in vivo, as seen in FIG. 50. Thus, LRBA, a critical regulator for multiple inflammatory diseases, may be an ideal therapeutic target to treat chronic inflammatory diseases.

Although in contrast with most other cell types, NF- $\kappa$ B is constitutively activated in primary B cells and B cell lines, much of the NF- $\kappa$ B is still sequestered in the cytoplasm hence can be activated upon stimulation as shown in this study. In non immune cells, such as HeLa and NIH3T3 cells, the NF- $\kappa$ B nuclear translocation oscillates upon stimulation as a results of negative feedback loop of the NF- $\kappa$ B sequester I $\kappa$ B $\alpha$ , which is produced by NF- $\kappa$ B activation. In this study, it seems that NF- $\kappa$ B activity also oscillate in Raji B cells in response to stimulation, as seen in FIG. 45(E).

NF $\kappa$ B is constitutively active in Raji cells due to the EBV onco-protein, the latent membrane protein 1 (LMP1), which functions as a constitutively activated member of the tumor necrosis factor receptor (TNFR) superfamily activating a number of signaling pathways in a ligand-independent manner (39, 40). As the NF $\kappa$ B activity oscillates, i.e. the activation and deactivation of NF $\kappa$ B activity, in cells that NF $\kappa$ B is constitutively activated, it is able to study LRBA knockdown effects on attenuation for both activation and deactivation of NF $\kappa$ B activity in such cells as in this study.

To prove that these in vitro studies are clinically relevant. We explored if Raji cells can be used as a in vitro model of immunodeficiency. The results demonstrate that Raji LRBA KD cells can be used as a novel LRBA immunodeficiency in vitro model, which can be used to study at least apoptosis caused by pathogens. Due to the convenience of in vitro study, it will greatly facilitate studies on immunodeficiency.

Chronic inflammation leads to many chronic diseases, affecting almost half of American population. Overactivation of inflammatory mediators, e.g. NF- $\kappa$ B, TNF $\alpha$  and IL-6 plays a critical role in chronic inflammation. However, the regulation of CI is largely unknown. NF $\kappa$ B overactivation is central to the pathogenesis of atherosclerosis, its blockage even interferes with resolution of inflammation. (41)

In summary, LRBA regulates the bottleneck immune genes, NF- $\kappa$ B and MAPKs (p42/44, p38 and JNK), and critical immune effectors, IL-10 and TNF $\alpha$  at protein levels/activity, response speed and response phase. The proposed dual model of LRBA's regulating immune mediators, for the first time, provides a united way to explain the paradoxical association of immunodeficiency with autoimmunity at molecular levels. In LRBA deficient patients, in response to pathogens, the attenuated activation of immune effectors at phase 1 may result in insufficient immunity and thus immunodeficiency, while attenuated deactivation of immune effectors at phase 2 may lead to overactivated immunity and thus autoimmunity.

#### Reagents:

Monoclonal antibodies against the following proteins were purchased from BD Biosciences (San Jose, Calif., USA): Phosflow Starter Kit, Erk1/2 (pT202/pY204) PE-CF594, JNK (PT183/PY185) Alexa 647, NF-K $\kappa$ B p65 (pS529) PE-Cy7 and p38 MAPK (pT180/pY182) PerCP-Cy5.5. The LRBA Prestige antibodies (NBP1-90764 and NBP1-90765) were purchased from Novus Biologicals (Littleton, Colo., USA). The Alexa Fluor Conjugated secondary antibodies: Anti-mouse IgG-Alexa Fluor $\text{\textcircled{R}}$  555 and anti-rabbit IgG-Alexa Fluor $\text{\textcircled{R}}$  488 were purchased from Life Technologies (Grand Island, N.Y., USA). Phospho-MAPK Family Antibody Sampler Kit (9910S), MAPK Family Antibody Sampler (9926S), NF- $\kappa$ B Family Member Antibody Sampler Kit (#4766) were from Cell Signaling Technology (Danvers, Mass., USA).

#### Cell Culture and Stimulation:

HEK293 cell line were purchased from the American Type Culture Collection (Manassas, Va., USA) and maintained according to the company's instructions. Raji B cell line (Burkitt's lymphoma) was kindly provided by Dr. George Blanck (University of South Florida Morsani College of Medicine). These cells were cultured in RPMI1640 supplemented with 10% FBS and penicillin-streptomycin (5,000 IU/ml penicillin and 5,000  $\mu$ g/ml streptomycin). Raji cells were stimulated with LPS (1  $\mu$ g/ml).

#### Multiparametric Flow Cytometry:

BD FACSelect Multicolor Panel Designer was used to search antibodies and build up the panel for multiple color cytometry for LSRII FACS machine. Two panels were used

when use live/dead discrimination with DAPI (overlap with PerCP-Cy5.5) or 7AAD (overlap with V450). The standard staining procedures were followed and 20,000 to half million cells were acquired. Data acquisition was performed using FACS LSRII flow cytometers and analyzed using FACSDiva version 6.1.2.

Cytometric Bead Array (CBA) and ELISA Cytokine Assay:

Cell culture supernatants were directly used to detect human Th1 and Th2 cytokines (IL-2, IL-4, IL-5, IL-6, IL-10, TNF $\alpha$  and IFN- $\gamma$ ) using the human Th1/Th2 cytokine bead-array kit (BD Biosciences, San Jose, Calif.) according to the manufacturer's instructions. The TNF $\alpha$  concentrations were also measured by Human TNF $\alpha$  DuoSet ELISA kit (R&D, Catalog #DY210).

#### Western Blots:

Cell extracts were prepared using radioimmunoprecipitation assay buffer (RIPA) buffer supplemented with protease inhibitor cocktail set III, EDTA-free (Millipore, Cat. No. 539134) and phosphatase inhibitor cocktail set II (Millipore, Cat. No. 524625). PVDF transfer membranes (Thermo, Rockford, Ill.) were used for Western blotting. Blots were imaged and protein levels of specific gene products quantitated by a ChemiDoc XRS (Bio-Rad, Richmond, Calif.) imager and Quantity One software (Bio-Rad, Richmond, Calif.).

#### Luciferase Assay:

Ready-To-Glow $\text{\textsuperscript{TM}}$  NF- $\kappa$ B Secreted Luciferase Reporter System (Clontech) and Firefly Luciferase Assay Kit (Biotium, Calif., USA) were used following the manufacture's instruction.

#### Polynomial Fitting and Slope Calculation:

Polynomial fitting in Microsoft Excel was used to represent nonlinear dataset in this study. High  $R^2$  values ( $R^2 > 0.9$ ) were used to describe the fitting accuracy and a polynomial trend line equation were used to represent the dataset. The slopes at each time point were calculated by  $n \cdot k \cdot x^{(n-1)}$  calculus method.

#### Statistics Analysis:

Comparisons of sample means was done using two-sample t test, assuming equal variance, and p value was calculated based on two-tailed test. Significance was taken as  $p < 0.05$ . Data are expressed as mean  $\pm$  standard deviation (SD) and are representative of two to three independent experiments. P value indications:  $< 0.001$  Extremely significant \*\*\*, 0.001 to 0.01 Very significant \*\*, 0.01 to 0.05 Significant \*,  $> 0.05$  Not significant ns #  $\geq 0.05$ .

## REFERENCES

1. Lopez-Herrera, G., G. Tampella, Q. Pan-Hammarstrom, P. Herholz, C. M. Trujillo-Vargas, K. Phadwal, A. K. Simon, M. Moutschen, A. Etzioni, A. Mory, I. Srugo, D. Melamed, K. Hultenby, C. Liu, M. Baronio, M. Vitali, P. Philippet, V. Dideberg, A. Aghamohammadi, N. Rezaei, V. Enright, L. Du, U. Salzer, H. Eibel, D. Pfeifer, H. Veelken, H. Stauss, V. Lougaris, A. Plebani, E. M. Gertz, A. A. Schaffer, L. Hammarstrom, and B. Grimbacher. 2012. Deleterious Mutations in LRBA Are Associated with a Syndrome of Immune Deficiency and Autoimmunity. *American journal of human genetics* 90: 986-1001.
2. Burns, S. O., H. L. Zenner, V. Plagnol, J. Curtis, K. Mok, M. Eisenhut, D. Kumararatne, R. Doffinger, A. J. Thrasher, and S. Nejentsev. 2012. LRBA gene deletion in a patient presenting with autoimmunity without hypogammaglobulinemia. *The Journal of allergy and clinical immunology* 130: 1428-1432.

3. Alangari, A., A. Alsultan, N. Adly, M. J. Massaad, I. S. Kiani, A. Aljebreen, E. Raddaoui, A. K. Almomen, S. Al-Muhsen, R. S. Geha, and F. S. Alkuraya. 2012. LPS-responsive beige-like anchor (LRBA) gene mutation in a family with inflammatory bowel disease and combined immunodeficiency. *The Journal of allergy and clinical immunology* 130: 481-488 e482.
4. Salzer, U., H. M. Chapel, A. D. Webster, Q. Pan-Hammarstrom, A. Schmitt-Graeff, M. Schlesier, H. H. Peter, J. K. Rockstroh, P. Schneider, A. A. Schaffer, L. Hammarstrom, and B. Grimbacher. 2005. Mutations in TNFRSF13B encoding TACI are associated with common variable immunodeficiency in humans. *Nat Genet* 37: 820-828.
5. Warnatz, K., U. Salzer, M. Rizzi, B. Fischer, S. Gutenberger, J. Bohm, A. K. Kienzler, Q. Pan-Hammarstrom, L. Hammarstrom, M. Rakhmanov, M. Schlesier, B. Grimbacher, H. H. Peter, and H. Eibel. 2009. B-cell activating factor receptor deficiency is associated with an adult-onset antibody deficiency syndrome in humans. *Proceedings of the National Academy of Sciences of the United States of America* 106: 13945-13950.
6. Kuijpers, T. W., R. J. Bende, P. A. Baars, A. Grummels, I. A. M. Derks, K. M. Dolman, T. Beaumont, T. F. Tedder, C. J. M. van Noesel, E. Eldering, and R. A. W. van Lier. 2010. CD20 deficiency in humans results in impaired T cell-independent antibody responses. *Journal of Clinical Investigation* 120: 214-222.
7. Grimbacher, B., A. Hutloff, M. Schlesier, E. Glocker, K. Warnatz, R. Drager, H. Eibel, B. Fischer, A. A. Schaffer, H. W. Mages, R. A. Kroczeck, and H. H. Peter. 2003. Homozygous loss of ICOS is associated with adult-onset common variable immunodeficiency. *Nat Immunol* 4: 261-268.
8. van Zelm, M. C., I. Reisli, M. van der Burg, D. Castano, C. J. M. van Noesel, M. J. D. van Tol, C. Woellner, B. Grimbacher, P. J. Patino, J. J. M. van Dongen, and J. L. Franco. 2006. An antibody-deficiency syndrome due to mutations in the CD19 gene. *New England Journal of Medicine* 354: 1901-1912.
9. Thiel, J., L. Kimmig, U. Salzer, M. Grudzien, D. Lebrecht, T. Hagena, R. Draeger, N. Volxen, A. Bergbreiter, S. Jennings, S. Gutenberger, A. Aichem, H. Illges, J. P. Hannan, A. K. Kienzler, M. Rizzi, H. Eibel, H. H. Peter, K. Warnatz, B. Grimbacher, J. A. Rump, and M. Schlesier. 2012. Genetic CD21 deficiency is associated with hypogammaglobulinemia. *The Journal of allergy and clinical immunology* 129: 801-810 e806.
10. van Zelm, M. C., J. Smet, B. Adams, F. Mascart, L. Schandene, F. Janssen, A. Ferster, C.-C. Kuo, S. Levy, J. J. M. van Dongen, and M. van der Burg. 2010. CD81 gene defect in humans disrupts CD19 complex formation and leads to antibody deficiency. *Journal of Clinical Investigation* 120: 1265-1274.
11. Eibel, H., U. Salzer, and K. Warnatz. 2010. Common variable immunodeficiency at the end of a prospering decade: towards novel gene defects and beyond. *Current opinion in allergy and clinical immunology* 10: 526-533.
12. Podjasek, J. C., and R. S. Abraham. 2012. Autoimmune cytopenias in common variable immunodeficiency. *Frontiers in immunology* 3: 189.
13. Cunningham-Rundles, C., and C. Bodian. 1999. Common variable immunodeficiency: clinical and immunological features of 248 patients. *Clinical immunology* 92: 34-48.

14. Parvaneh, N., J. L. Casanova, L. D. Notarangelo, and M. E. Conley. 2013. Primary immunodeficiencies: a rapidly evolving story. *The Journal of allergy and clinical immunology* 131: 314-323.
15. Salzer, U., C. Bacchelli, S. Buckridge, Q. Pan-Hammarstrom, S. Jennings, V. Lougaris, A. Bergbreiter, T. Hagena, J. Birmelin, A. Plebani, A. D. Webster, H. H. Peter, D. Suez, H. Chapel, A. McLean-Tooke, G. P. Spickett, S. Anover-Sombke, H. D. Ochs, S. Urschel, B. H. Belohradsky, S. Ugrinovic, D. S. Kumararatne, T. C. Lawrence, A. M. Holm, J. L. Franco, I. Schulze, P. Schneider, E. M. Gertz, A. A. Schaffer, L. Hammarstrom, A. J. Thrasher, H. B. Gaspar, and B. Grimbacher. 2009. Relevance of biallelic versus monoallelic TNFRSF13B mutations in distinguishing disease-causing from risk-increasing TNFRSF13B variants in antibody deficiency syndromes. *Blood* 113: 1967-1976.
16. Wang, J. W., J. Howson, E. Haller, and W. G. Kerr. 2001. Identification of a novel lipopolysaccharide-inducible gene with key features of both A kinase anchor proteins and chs1/beige proteins. *J Immunol* 166: 4586-4595.
17. Kerr, W. G., M. Heller, and L. A. Herzenberg. 1996. Analysis of lipopolysaccharide-response genes in B-lineage cells demonstrates that they can have differentiation stage-restricted expression and contain SH2 domains. *Proceedings of the National Academy of Sciences of the United States of America* 93: 3947-3952.
18. Cullinane, A. R., A. A. Schaffer, and M. Huizing. 2013. The BEACH Is Hot: A LYST of Emerging Roles for BEACH-Domain Containing Proteins in Human Disease. *Traffic*.
19. Wang, J. W., J. J. Gamsby, S. L. Highfill, L. B. Mora, G. C. Bloom, T. J. Yeatman, T. C. Pan, A. L. Ramne, L. A. Chodosh, W. D. Cress, J. Chen, and W. G. Kerr. 2004. Deregulated expression of LRBA facilitates cancer cell growth. *Oncogene* 23: 4089-4097.
20. Wiley, H. S. 2003. Trafficking of the ErbB receptors and its influence on signaling. *Experimental cell research* 284: 78-88.
21. Kurylowicz, A., and J. Nauman. 2008. The role of nuclear factor-kappaB in the development of autoimmune diseases: a link between genes and environment. *Acta biochimica Polonica* 55: 629-647.
22. Cunningham-Rundles, C. 2012. Human B cell defects in perspective. *Immunologic research* 54: 227-232.
23. Wang, J. W., J. J. Gamsby, S. L. Highfill, L. B. Mora, G. C. Bloom, T. J. Yeatman, T. C. Pan, A. L. Ramne, L. A. Chodosh, W. D. Cress, J. D. Chen, and W. G. Kerr. 2004. Deregulated expression of LRBA facilitates cancer cell growth. *Oncogene* 23: 4089-4097.
24. Hoesel, B., and J. A. Schmid. 2013. The complexity of NF-kappaB signaling in inflammation and cancer. *Mol Cancer* 12: 86.
25. Nelson, D. E., A. E. Ihekweaba, M. Elliott, J. R. Johnson, C. A. Gibney, B. E. Foreman, G. Nelson, V. See, C. A. Horton, D. G. Spiller, S. W. Edwards, H. P. McDowell, J. F. Unitt, E. Sullivan, R. Grimley, N. Benson, D. Broomhead, D. B. Kell, and M. R. White. 2004. Oscillations in NF-kappaB signaling control the dynamics of gene expression. *Science* 306: 704-708.
26. Boring, L., J. Gosling, M. Cleary, and I. F. Charo. 1998. Decreased lesion formation in CCR2<sup>-/-</sup> mice reveals a role for chemokines in the initiation of atherosclerosis. *Nature* 394: 894-897.
27. Oeckinghaus, A., M. S. Hayden, and S. Ghosh. 2011. Crosstalk in NF-kappaB signaling pathways. *Nature immunology* 12: 695-708.

28. Wech, I., and A. C. Nagel. 2005. Mutations in rugose promote cell type-specific apoptosis in the *Drosophila* eye. *Cell death and differentiation* 12: 145-152.
29. Shiflett, S. L., M. B. Vaughn, D. Huynh, J. Kaplan, and D. M. Ward. 2004. Bph1p, the *Saccharomyces cerevisiae* 5 homologue of CHS1/Beige, functions in cell wall formation and protein sorting. *Traffic* 5: 700-710.
30. Volders, K., K. Nuytens, and J. W. M. Creemers. 2011. The Autism Candidate Gene Neurobeachin Encodes a Scaffolding Protein Implicated in Membrane Trafficking and Signaling. *Current Molecular Medicine* 11: 204-217.
31. Ashida, H., H. Mimuro, M. Ogawa, T. Kobayashi, T. Sanada, M. Kim, and C. Sasakawa. 2011. Cell death and infection: a double-edged sword for host and pathogen survival. *The Journal of cell biology* 195: 931-942.
32. Baltimore, D. 2011. NF-kappaB is 25. *Nat Immunol* 12: 683-685.
33. Hayden, M. S., and S. Ghosh. 2012. NF-kappaB, the first quarter-century: remarkable progress and outstanding questions. *Genes & development* 26: 203-234.
34. Han, J., J. D. Lee, L. Bibbs, and R. J. Ulevitch. 1994. A MAP kinase targeted by endotoxin and hyperosmolarity in mammalian cells. *Science* 265: 808-811.
35. Huang, G., L. Z. Shi, and H. Chi. 2009. Regulation of JNK and p38 MAPK in the immune system: signal integration, propagation and termination. *Cytokine* 48: 161-169.
36. Schrofelbauer, B., and A. Hoffmann. 2011. How do pleiotropic kinase hubs mediate specific signaling by TNFR superfamily members? *Immunological reviews* 244: 29-43.
37. DeSilva, D. R., E. A. Jones, M. F. Favata, B. D. Jaffee, R. L. Magolda, J. M. Trzaskos, and P. A. Scherle. 1998.

- Inhibition of mitogen-activated protein kinase kinase blocks T cell proliferation but does not induce or prevent anergy. *Journal of immunology* (Baltimore, Md.: 1950) 160: 4175-4181.
38. Holgate, S. T. 2009. Novel targets of therapy in asthma. *Curr Opin Pulm Med* 15: 63-71.
39. Gires, O., U. Zimmer-Strobl, R. Gonnella, M. Ueffing, G. Marschall, R. Zeidler, D. Pich, and W. Hammerschmidt. 1997. Latent membrane protein 1 of Epstein-Barr virus mimics a constitutively active receptor molecule. *The EMBO journal* 16: 6131-6140.
40. Kilger, E., A. Kieser, M. Baumann, and W. Hammerschmidt. 1998. Epstein-Barr virus-mediated B-cell proliferation is dependent upon latent membrane protein 1, which simulates an activated CD40 receptor. *The EMBO journal* 17: 1700-1709.
41. Monaco, C., and E. Paleolog. 2004. Nuclear factor kappaB: a potential therapeutic target in atherosclerosis and thrombosis. *Cardiovasc Res* 61: 671-682.
- 20 In the preceding specification, all documents, acts, or information disclosed do not constitute an admission that the document, act, or information of any combination thereof was publicly available, known to the public, part of the general knowledge in the art, or was known to be relevant to solve any problem at the time of priority.
- 25 The disclosures of all publications cited above are expressly incorporated herein by reference, each in its entirety, to the same extent as if each were incorporated by reference individually.
- 30 It is also to be understood that the following claims are intended to cover all of the generic and specific features of the invention herein described, and all statements of the scope of the invention which, as a matter of language, might be said to fall there between.

## SEQUENCE LISTING

<160> NUMBER OF SEQ ID NOS: 44

<210> SEQ ID NO 1

<211> LENGTH: 2863

<212> TYPE: PRT

<213> ORGANISM: Homo sapiens

<400> SEQUENCE: 1

```

Met Ala Ser Glu Asp Asn Arg Val Pro Ser Pro Pro Pro Thr Gly Asp
1          5          10         15
Asp Gly Gly Gly Gly Gly Arg Glu Glu Thr Pro Thr Glu Gly Gly Ala
20         25         30
Leu Ser Leu Lys Pro Gly Leu Pro Ile Arg Gly Ile Arg Met Lys Phe
35         40         45
Ala Val Leu Thr Gly Leu Val Glu Val Gly Glu Val Ser Asn Arg Asp
50         55         60
Ile Val Glu Thr Val Phe Asn Leu Leu Val Gly Gly Gln Phe Asp Leu
65         70         75         80
Glu Met Asn Phe Ile Ile Gln Glu Gly Glu Ser Ile Asn Cys Met Val
85         90         95
Asp Leu Leu Glu Lys Cys Asp Ile Thr Cys Gln Ala Glu Val Trp Ser
100        105        110
Met Phe Thr Ala Ile Leu Lys Lys Ser Ile Arg Asn Leu Gln Val Cys
115        120        125
Thr Glu Val Gly Leu Val Glu Lys Val Leu Gly Lys Ile Glu Lys Val
130        135        140

```

-continued

---

Asp	Asn	Met	Ile	Ala	Asp	Leu	Leu	Val	Asp	Met	Leu	Gly	Val	Leu	Ala
145					150					155					160
Ser	Tyr	Asn	Leu	Thr	Val	Arg	Glu	Leu	Lys	Leu	Phe	Phe	Ser	Lys	Leu
			165						170					175	
Gln	Gly	Asp	Lys	Gly	Arg	Trp	Pro	Pro	His	Ala	Gly	Lys	Leu	Leu	Ser
			180					185					190		
Val	Leu	Lys	His	Met	Pro	Gln	Lys	Tyr	Gly	Pro	Asp	Ala	Phe	Phe	Asn
	195						200					205			
Phe	Pro	Gly	Lys	Ser	Ala	Ala	Ala	Ile	Ala	Leu	Pro	Pro	Ile	Ala	Lys
	210					215					220				
Trp	Pro	Tyr	Gln	Asn	Gly	Phe	Thr	Phe	His	Thr	Trp	Leu	Arg	Met	Asp
225					230					235					240
Pro	Val	Asn	Asn	Ile	Asn	Val	Asp	Lys	Asp	Lys	Pro	Tyr	Leu	Tyr	Cys
			245						250					255	
Phe	Arg	Thr	Ser	Lys	Gly	Leu	Gly	Tyr	Ser	Ala	His	Phe	Val	Gly	Gly
			260					265					270		
Cys	Leu	Ile	Val	Thr	Ser	Ile	Lys	Ser	Lys	Gly	Lys	Gly	Phe	Gln	His
	275						280					285			
Cys	Val	Lys	Phe	Asp	Phe	Lys	Pro	Gln	Lys	Trp	Tyr	Met	Val	Thr	Ile
	290					295					300				
Val	His	Ile	Tyr	Asn	Arg	Trp	Lys	Asn	Ser	Glu	Leu	Arg	Cys	Tyr	Val
305					310					315					320
Asn	Gly	Glu	Leu	Ala	Ser	Tyr	Gly	Glu	Ile	Thr	Trp	Phe	Val	Asn	Thr
			325					330						335	
Ser	Asp	Thr	Phe	Asp	Lys	Cys	Phe	Leu	Gly	Ser	Ser	Glu	Thr	Ala	Asp
			340					345					350		
Ala	Asn	Arg	Val	Phe	Cys	Gly	Gln	Met	Thr	Ala	Val	Tyr	Leu	Phe	Ser
	355						360					365			
Glu	Ala	Leu	Asn	Ala	Ala	Gln	Ile	Phe	Ala	Ile	Tyr	Gln	Leu	Gly	Leu
	370					375					380				
Gly	Tyr	Lys	Gly	Thr	Phe	Lys	Phe	Lys	Ala	Glu	Ser	Asp	Leu	Phe	Leu
385					390					395					400
Ala	Glu	His	His	Lys	Leu	Leu	Leu	Tyr	Asp	Gly	Lys	Leu	Ser	Ser	Ala
			405						410					415	
Ile	Ala	Phe	Thr	Tyr	Asn	Pro	Arg	Ala	Thr	Asp	Ala	Gln	Leu	Cys	Leu
			420					425					430		
Glu	Ser	Ser	Pro	Lys	Asp	Asn	Pro	Ser	Ile	Phe	Val	His	Ser	Pro	His
	435					440						445			
Ala	Leu	Met	Leu	Gln	Asp	Val	Lys	Ala	Val	Leu	Thr	His	Ser	Ile	Gln
	450					455					460				
Ser	Ala	Met	His	Ser	Ile	Gly	Gly	Val	Gln	Val	Leu	Phe	Pro	Leu	Phe
465					470					475					480
Ala	Gln	Leu	Asp	Tyr	Arg	Gln	Tyr	Leu	Ser	Asp	Glu	Ile	Asp	Leu	Thr
			485					490						495	
Ile	Cys	Ser	Thr	Leu	Leu	Ala	Phe	Ile	Met	Glu	Leu	Leu	Lys	Asn	Ser
			500					505					510		
Ile	Ala	Met	Gln	Glu	Gln	Met	Leu	Ala	Cys	Lys	Gly	Phe	Leu	Val	Ile
		515					520					525			
Gly	Tyr	Ser	Leu	Glu	Lys	Ser	Ser	Lys	Ser	His	Val	Ser	Arg	Ala	Val
	530					535						540			
Leu	Glu	Leu	Cys	Leu	Ala	Phe	Ser	Lys	Tyr	Leu	Ser	Asn	Leu	Gln	Asn
545					550					555					560

Gly 565	Met	Pro	Leu	Leu 565	Lys	Gln	Leu	Cys	Asp 570	His	Val	Leu	Leu	Asn 575	Pro
Ala 580	Ile	Trp	Ile 580	His	Thr	Pro	Ala	Lys 585	Val	Gln	Leu	Met	Leu 590	Tyr	Thr
Tyr 595	Leu	Ser	Thr 595	Glu	Phe	Ile	Gly 600	Thr	Val	Asn	Ile	Tyr 605	Asn	Thr	Ile
Arg 610	Arg	Val	Gly 610	Thr	Val	Leu 615	Leu	Ile	Met	His	Thr 620	Leu	Lys	Tyr	Tyr
Tyr 625	Trp	Ala	Val 625	Asn	Pro 630	Gln	Asp	Arg	Ser	Gly 635	Ile	Thr	Pro	Lys	Gly 640
Leu 645	Asp	Gly	Pro 645	Arg	Pro	Asn	Gln	Lys 650	Glu	Met	Leu	Ser	Leu 655	Arg	Ala
Phe 660	Leu	Leu	Met 660	Phe	Ile	Lys	Gln	Leu 665	Val	Met	Lys	Asp	Ser 670	Gly	Val
Lys 675	Glu	Asp	Glu 675	Leu	Gln	Ala	Ile 680	Leu	Asn	Tyr	Leu	Leu 685	Thr	Met	His
Glu 690	Asp	Asp	Asn 690	Leu	Met	Asp 695	Val	Leu	Gln	Leu	Leu 700	Val	Ala	Leu	Met
Ser 705	Glu	His	Pro 705	Asn	Ser 710	Met	Ile	Pro	Ala	Phe 715	Asp	Gln	Arg	Asn	Gly 720
Leu 725	Arg	Val	Ile 725	Tyr	Lys	Leu	Leu	Ala	Ser 730	Lys	Ser	Glu	Gly 735	Ile	Arg
Val 740	Gln	Ala	Leu 740	Lys	Ala	Met	Gly 745	Tyr	Phe	Leu	Lys	His	Leu 750	Ala	Pro
Lys 755	Arg	Lys	Ala 755	Glu	Val	Met	Leu 760	Gly	His	Gly	Leu	Phe 765	Ser	Leu	Leu
Ala 770	Glu	Arg	Leu 770	Met	Leu	Gln 775	Thr	Asn	Leu	Ile	Thr 780	Met	Thr	Thr	Tyr
Asn 785	Val	Leu	Phe 785	Glu	Ile 790	Leu	Ile	Glu	Gln	Ile 795	Gly	Thr	Gln	Val	Ile 800
His 805	Lys	Gln	His 805	Pro	Asp	Pro	Asp	Ser 810	Ser	Val	Lys	Ile	Gln	Asn 815	Pro
Gln 820	Ile	Leu	Lys 820	Val	Ile	Ala	Thr	Leu 825	Leu	Arg	Asn	Ser	Pro 830	Gln	Cys
Pro 835	Glu	Ser	Met 835	Glu	Val	Arg	Arg 840	Ala	Phe	Leu	Ser	Asp 845	Met	Ile	Lys
Leu 850	Phe	Asn	Asn 850	Ser	Arg	Glu 855	Asn	Arg	Arg	Ser	Leu 860	Leu	Gln	Cys	Ser
Val 865	Trp	Gln	Glu 865	Trp	Met 870	Leu	Ser	Leu	Cys	Tyr 875	Phe	Asn	Pro	Lys	Asn 880
Ser 885	Asp	Glu	Gln 885	Lys	Ile	Thr	Glu	Met	Val 890	Tyr	Ala	Ile	Phe	Arg 895	Ile
Leu 900	Leu	Tyr	His 900	Ala	Val	Lys	Tyr	Glu 905	Trp	Gly	Gly	Trp 910	Arg	Val	Trp
Val 915	Asp	Thr	Leu 915	Ser	Ile	Thr	His 920	Ser	Lys	Val	Thr	Phe 925	Glu	Ile	His
Lys 930	Glu	Asn	Leu 930	Ala	Asn 935	Ile	Phe	Arg	Glu	Gln	Gln 940	Gly	Lys	Val	Asp
Glu 945	Glu	Ile	Gly 945	Leu	Cys 950	Ser	Ser	Thr	Ser	Val 955	Gln	Ala	Ala	Ser	Gly 960
Ile 965	Arg	Arg	Asp 965	Ile	Asn	Val	Ser	Val	Gly 970	Ser	Gln	Gln	Pro	Asp 975	Thr
Lys 980	Asp	Ser	Pro 980	Val	Cys	Pro	His	Phe	Thr	Thr	Asn	Gly	Asn	Glu	Asn

-continued

980						985					990				
Ser	Ser	Ile	Glu	Lys	Thr	Ser	Ser	Leu	Glu	Ser	Ala	Ser	Asn	Ile	Glu
995						1000					1005				
Leu	Gln	Thr	Thr	Asn	Thr	Ser	Tyr	Glu	Glu	Met	Lys	Ala	Glu	Gln	
1010						1015					1020				
Glu	Asn	Gln	Glu	Leu	Pro	Asp	Glu	Gly	Thr	Leu	Glu	Glu	Thr	Leu	
1025						1030					1035				
Thr	Asn	Glu	Thr	Arg	Asn	Ala	Asp	Asp	Leu	Glu	Val	Ser	Ser	Asp	
1040						1045					1050				
Ile	Ile	Glu	Ala	Val	Ala	Ile	Ser	Ser	Asn	Ser	Phe	Ile	Thr	Thr	
1055						1060					1065				
Gly	Lys	Asp	Ser	Met	Thr	Val	Ser	Glu	Val	Thr	Ala	Ser	Ile	Ser	
1070						1075					1080				
Ser	Pro	Ser	Glu	Glu	Asp	Ala	Ser	Glu	Met	Pro	Glu	Phe	Leu	Asp	
1085						1090					1095				
Lys	Ser	Ile	Val	Glu	Glu	Glu	Glu	Asp	Asp	Asp	Tyr	Val	Glu	Leu	
1100						1105					1110				
Lys	Val	Glu	Gly	Ser	Pro	Thr	Glu	Glu	Ala	Asn	Leu	Pro	Thr	Glu	
1115						1120					1125				
Leu	Gln	Asp	Asn	Ser	Leu	Ser	Pro	Ala	Ala	Ser	Glu	Ala	Gly	Glu	
1130						1135					1140				
Lys	Leu	Asp	Met	Phe	Gly	Asn	Asp	Asp	Lys	Leu	Ile	Phe	Gln	Glu	
1145						1150					1155				
Gly	Lys	Pro	Val	Thr	Glu	Lys	Gln	Thr	Asp	Thr	Glu	Thr	Gln	Asp	
1160						1165					1170				
Ser	Lys	Asp	Ser	Gly	Ile	Gln	Thr	Met	Thr	Ala	Ser	Gly	Ser	Ser	
1175						1180					1185				
Ala	Met	Ser	Pro	Glu	Thr	Thr	Val	Ser	Gln	Ile	Ala	Val	Glu	Ser	
1190						1195					1200				
Asp	Leu	Gly	Gln	Met	Leu	Glu	Glu	Gly	Lys	Lys	Ala	Thr	Asn	Leu	
1205						1210					1215				
Thr	Arg	Glu	Thr	Lys	Leu	Ile	Asn	Asp	Cys	His	Gly	Ser	Val	Ser	
1220						1225					1230				
Glu	Ala	Ser	Ser	Glu	Gln	Lys	Ile	Ala	Lys	Leu	Asp	Val	Ser	Asn	
1235						1240					1245				
Val	Ala	Thr	Asp	Thr	Glu	Arg	Leu	Glu	Leu	Lys	Ala	Ser	Pro	Asn	
1250						1255					1260				
Val	Glu	Ala	Pro	Gln	Pro	His	Arg	His	Val	Leu	Glu	Ile	Ser	Arg	
1265						1270					1275				
Gln	His	Glu	Gln	Pro	Gly	Gln	Gly	Ile	Ala	Pro	Asp	Ala	Val	Asn	
1280						1285					1290				
Gly	Gln	Arg	Arg	Asp	Ser	Arg	Ser	Thr	Val	Phe	Arg	Ile	Pro	Glu	
1295						1300					1305				
Phe	Asn	Trp	Ser	Gln	Met	His	Gln	Arg	Leu	Leu	Thr	Asp	Leu	Leu	
1310						1315					1320				
Phe	Ser	Ile	Glu	Thr	Asp	Ile	Gln	Met	Trp	Arg	Ser	His	Ser	Thr	
1325						1330					1335				
Lys	Thr	Val	Met	Asp	Phe	Val	Asn	Ser	Ser	Asp	Asn	Val	Ile	Phe	
1340						1345					1350				
Val	His	Asn	Thr	Ile	His	Leu	Ile	Ser	Gln	Val	Met	Asp	Asn	Met	
1355						1360					1365				
Val	Met	Ala	Cys	Gly	Gly	Ile	Leu	Pro	Leu	Leu	Ser	Ala	Ala	Thr	
1370						1375					1380				



-continued

---

Ser Ala	Thr His	Glu Leu	Glu	Asn Ile	Glu Pro	Thr	Gln Gly	Leu	
1385			1390			1395			
Ser Ile	Glu Ala	Ser Val	Thr	Phe Leu	Gln Arg	Leu	Ile Ser	Leu	
1400			1405			1410			
Val Asp	Val Leu	Ile Phe	Ala	Ser Ser	Leu Gly	Phe	Thr Glu	Ile	
1415			1420			1425			
Glu Ala	Glu Lys	Ser Met	Ser	Ser Gly	Gly Ile	Leu	Arg Gln	Cys	
1430			1435			1440			
Leu Arg	Leu Val	Cys Ala	Val	Ala Val	Arg Asn	Cys	Leu Glu	Cys	
1445			1450			1455			
Gln Gln	His Ser	Gln Leu	Lys	Thr Arg	Gly Asp	Lys	Ala Leu	Lys	
1460			1465			1470			
Pro Met	His Ser	Leu Ile	Pro	Leu Gly	Lys Ser	Ala	Ala Lys	Ser	
1475			1480			1485			
Pro Val	Asp Ile	Val Thr	Gly	Gly Ile	Ser Pro	Val	Arg Asp	Leu	
1490			1495			1500			
Asp Arg	Leu Leu	Gln Asp	Met	Asp Ile	Asn Arg	Leu	Arg Ala	Val	
1505			1510			1515			
Val Phe	Arg Asp	Ile Glu	Asp	Ser Lys	Gln Ala	Gln	Phe Leu	Ala	
1520			1525			1530			
Leu Ala	Val Val	Tyr Phe	Ile	Ser Val	Leu Met	Val	Ser Lys	Tyr	
1535			1540			1545			
Arg Asp	Ile Leu	Glu Pro	Gln	Asn Glu	Arg His	Ser	Gln Ser	Cys	
1550			1555			1560			
Thr Glu	Thr Gly	Ser Glu	Asn	Glu Asn	Val Ser	Leu	Ser Glu	Ile	
1565			1570			1575			
Thr Pro	Ala Ala	Phe Ser	Thr	Leu Thr	Thr Ala	Ser	Val Glu	Glu	
1580			1585			1590			
Ser Glu	Ser Thr	Ser Ser	Ala	Arg Arg	Arg Asp	Ser	Gly Ile	Gly	
1595			1600			1605			
Glu Glu	Thr Ala	Thr Gly	Leu	Gly Ser	His Val	Glu	Val Thr	Pro	
1610			1615			1620			
His Thr	Ala Pro	Pro Gly	Val	Ser Ala	Gly Pro	Asp	Ala Ile	Ser	
1625			1630			1635			
Glu Val	Leu Ser	Thr Leu	Ser	Leu Glu	Val Asn	Lys	Ser Pro	Glu	
1640			1645			1650			
Thr Lys	Asn Asp	Arg Gly	Asn	Asp Leu	Asp Thr	Lys	Ala Thr	Pro	
1655			1660			1665			
Ser Val	Ser Val	Ser Lys	Asn	Val Asn	Val Lys	Asp	Ile Leu	Arg	
1670			1675			1680			
Ser Leu	Val Asn	Ile Pro	Ala	Asp Gly	Val Thr	Val	Asp Pro	Ala	
1685			1690			1695			
Leu Leu	Pro Pro	Ala Cys	Leu	Gly Ala	Leu Gly	Asp	Leu Ser	Val	
1700			1705			1710			
Glu Gln	Pro Val	Gln Phe	Arg	Ser Phe	Asp Arg	Ser	Val Ile	Val	
1715			1720			1725			
Ala Ala	Lys Lys	Ser Ala	Val	Ser Pro	Ser Thr	Phe	Asn Thr	Ser	
1730			1735			1740			
Ile Pro	Thr Asn	Ala Val	Ser	Val Val	Ser Ser	Val	Asp Ser	Ala	
1745			1750			1755			
Gln Ala	Ser Asp	Met Gly	Gly	Glu Ser	Pro Gly	Ser	Arg Ser	Ser	
1760			1765			1770			

-continued

---

Asn	Ala	Lys	Leu	Pro	Ser	Val	Pro	Thr	Val	Asp	Ser	Val	Ser	Gln
1775						1780					1785			
Asp	Pro	Val	Ser	Asn	Met	Ser	Ile	Thr	Glu	Arg	Leu	Glu	His	Ala
1790						1795					1800			
Leu	Glu	Lys	Ala	Ala	Pro	Leu	Leu	Arg	Glu	Ile	Phe	Val	Asp	Phe
1805						1810					1815			
Ala	Pro	Phe	Leu	Ser	Arg	Thr	Leu	Leu	Gly	Ser	His	Gly	Gln	Glu
1820						1825					1830			
Leu	Leu	Ile	Glu	Gly	Thr	Ser	Leu	Val	Cys	Met	Lys	Ser	Ser	Ser
1835						1840					1845			
Ser	Val	Val	Glu	Leu	Val	Met	Leu	Leu	Cys	Ser	Gln	Glu	Trp	Gln
1850						1855					1860			
Asn	Ser	Ile	Gln	Lys	Asn	Ala	Gly	Leu	Ala	Phe	Ile	Glu	Leu	Val
1865						1870					1875			
Asn	Glu	Gly	Arg	Leu	Leu	Ser	Gln	Thr	Met	Lys	Asp	His	Leu	Val
1880						1885					1890			
Arg	Val	Ala	Asn	Glu	Ala	Glu	Phe	Ile	Leu	Ser	Arg	Gln	Arg	Ala
1895						1900					1905			
Glu	Asp	Ile	His	Arg	His	Ala	Glu	Phe	Glu	Ser	Leu	Cys	Ala	Gln
1910						1915					1920			
Tyr	Ser	Ala	Asp	Lys	Arg	Glu	Asp	Glu	Lys	Met	Cys	Asp	His	Leu
1925						1930					1935			
Ile	Arg	Ala	Ala	Lys	Tyr	Arg	Asp	His	Val	Thr	Ala	Thr	Gln	Leu
1940						1945					1950			
Ile	Gln	Lys	Ile	Ile	Asn	Ile	Leu	Thr	Asp	Lys	His	Gly	Ala	Trp
1955						1960					1965			
Gly	Asn	Ser	Ala	Val	Ser	Arg	Pro	Leu	Glu	Phe	Trp	Arg	Leu	Asp
1970						1975					1980			
Tyr	Trp	Glu	Asp	Asp	Leu	Arg	Arg	Arg	Arg	Arg	Phe	Val	Arg	Asn
1985						1990					1995			
Pro	Leu	Gly	Ser	Thr	His	Pro	Glu	Ala	Thr	Leu	Lys	Thr	Ala	Val
2000						2005					2010			
Glu	His	Val	Cys	Ile	Phe	Lys	Leu	Arg	Glu	Asn	Ser	Lys	Ala	Thr
2015						2020					2025			
Asp	Glu	Asp	Ile	Leu	Ala	Lys	Gly	Lys	Gln	Ser	Ile	Arg	Ser	Gln
2030						2035					2040			
Ala	Leu	Gly	Asn	Gln	Asn	Ser	Glu	Asn	Glu	Ile	Leu	Leu	Glu	Gly
2045						2050					2055			
Asp	Asp	Asp	Thr	Leu	Ser	Ser	Val	Asp	Glu	Lys	Asp	Leu	Glu	Asn
2060						2065					2070			
Leu	Ala	Gly	Pro	Val	Ser	Leu	Ser	Thr	Pro	Ala	Gln	Leu	Val	Ala
2075						2080					2085			
Pro	Ser	Val	Val	Val	Lys	Gly	Thr	Leu	Ser	Val	Thr	Ser	Ser	Glu
2090						2095					2100			
Leu	Tyr	Phe	Glu	Val	Asp	Glu	Glu	Asp	Pro	Asn	Phe	Lys	Lys	Ile
2105						2110					2115			
Asp	Pro	Lys	Ile	Leu	Ala	Tyr	Thr	Glu	Gly	Leu	His	Gly	Lys	Trp
2120						2125					2130			
Leu	Phe	Thr	Glu	Ile	Arg	Ser	Ile	Phe	Ser	Arg	Arg	Tyr	Leu	Leu
2135						2140					2145			
Gln	Asn	Thr	Ala	Leu	Glu	Ile	Phe	Met	Ala	Asn	Arg	Val	Ala	Val
2150						2155					2160			
Met	Phe	Asn	Phe	Pro	Asp	Pro	Ala	Thr	Val	Lys	Lys	Val	Val	Asn

-continued

---

2165	2170	2175
Tyr Leu Pro Arg Val Gly Val Gly Thr Ser Phe Gly Leu Pro Gln		
2180	2185	2190
Thr Arg Arg Ile Ser Leu Ala Ser Pro Arg Gln Leu Phe Lys Ala		
2195	2200	2205
Ser Asn Met Thr Gln Arg Trp Gln His Arg Glu Ile Ser Asn Phe		
2210	2215	2220
Glu Tyr Leu Met Phe Leu Asn Thr Ile Ala Gly Arg Ser Tyr Asn		
2225	2230	2235
Asp Leu Asn Gln Tyr Pro Val Phe Pro Trp Val Ile Thr Asn Tyr		
2240	2245	2250
Glu Ser Glu Glu Leu Asp Leu Thr Leu Pro Thr Asn Phe Arg Asp		
2255	2260	2265
Leu Ser Lys Pro Ile Gly Ala Leu Asn Pro Lys Arg Ala Ala Phe		
2270	2275	2280
Phe Ala Glu Arg Tyr Glu Ser Trp Glu Asp Asp Gln Val Pro Lys		
2285	2290	2295
Phe His Tyr Gly Thr His Tyr Ser Thr Ala Ser Phe Val Leu Ala		
2300	2305	2310
Trp Leu Leu Arg Ile Glu Pro Phe Thr Thr Tyr Phe Leu Asn Leu		
2315	2320	2325
Gln Gly Gly Lys Phe Asp His Ala Asp Arg Thr Phe Ser Ser Ile		
2330	2335	2340
Ser Arg Ala Trp Arg Asn Ser Gln Arg Asp Thr Ser Asp Ile Lys		
2345	2350	2355
Glu Leu Ile Pro Glu Phe Tyr Tyr Leu Pro Glu Met Phe Val Asn		
2360	2365	2370
Phe Asn Asn Tyr Asn Leu Gly Val Met Asp Asp Gly Thr Val Val		
2375	2380	2385
Ser Asp Val Glu Leu Pro Pro Trp Ala Lys Thr Ser Glu Glu Phe		
2390	2395	2400
Val His Ile Asn Arg Leu Ala Leu Glu Ser Glu Phe Val Ser Cys		
2405	2410	2415
Gln Leu His Gln Trp Ile Asp Leu Ile Phe Gly Tyr Lys Gln Gln		
2420	2425	2430
Gly Pro Glu Ala Val Arg Ala Leu Asn Val Phe Tyr Tyr Leu Thr		
2435	2440	2445
Tyr Glu Gly Ala Val Asn Leu Asn Ser Ile Thr Asp Pro Val Leu		
2450	2455	2460
Arg Glu Ala Val Glu Ala Gln Ile Arg Ser Phe Gly Gln Thr Pro		
2465	2470	2475
Ser Gln Leu Leu Ile Glu Pro His Pro Pro Arg Gly Ser Ala Met		
2480	2485	2490
Gln Val Ser Pro Leu Met Phe Thr Asp Lys Ala Gln Gln Asp Val		
2495	2500	2505
Ile Met Val Leu Lys Phe Pro Ser Asn Ser Pro Val Thr His Val		
2510	2515	2520
Ala Ala Asn Thr Gln Pro Gly Leu Ala Thr Pro Ala Val Ile Thr		
2525	2530	2535
Val Thr Ala Asn Arg Leu Phe Ala Val Asn Lys Trp His Asn Leu		
2540	2545	2550
Pro Ala His Gln Gly Ala Val Gln Asp Gln Pro Tyr Gln Leu Pro		
2555	2560	2565

-continued

---

Val Glu	Ile Asp	Pro Leu	Ile	Ala Ser	Asn Thr	Gly	Met His	Arg
2570			2575			2580		
Arg Gln	Ile Thr	Asp Leu	Leu	Asp Gln	Ser Ile	Gln	Val His	Ser
2585			2590			2595		
Gln Cys	Phe Val	Ile Thr	Ser	Asp Asn	Arg Tyr	Ile	Leu Val	Cys
2600			2605			2610		
Gly Phe	Trp Asp	Lys Ser	Phe	Arg Val	Tyr Ser	Thr	Asp Thr	Gly
2615			2620			2625		
Arg Leu	Ile Gln	Val Val	Phe	Gly His	Trp Asp	Val	Val Thr	Cys
2630			2635			2640		
Leu Ala	Arg Ser	Glu Ser	Tyr	Ile Gly	Gly Asn	Cys	Tyr Ile	Leu
2645			2650			2655		
Ser Gly	Ser Arg	Asp Ala	Thr	Leu Leu	Leu Trp	Tyr	Trp Asn	Gly
2660			2665			2670		
Lys Cys	Ser Gly	Ile Gly	Asp	Asn Pro	Gly Ser	Glu	Thr Ala	Ala
2675			2680			2685		
Pro Arg	Ala Ile	Leu Thr	Gly	His Asp	Tyr Glu	Val	Thr Cys	Ala
2690			2695			2700		
Ala Val	Cys Ala	Glu Leu	Gly	Leu Val	Leu Ser	Gly	Ser Gln	Glu
2705			2710			2715		
Gly Pro	Cys Leu	Ile His	Ser	Met Asn	Gly Asp	Leu	Leu Arg	Thr
2720			2725			2730		
Leu Glu	Gly Pro	Glu Asn	Cys	Leu Lys	Pro Lys	Leu	Ile Gln	Ala
2735			2740			2745		
Ser Arg	Glu Gly	His Cys	Val	Ile Phe	Tyr Glu	Asn	Gly Leu	Phe
2750			2755			2760		
Cys Thr	Phe Ser	Val Asn	Gly	Lys Leu	Gln Ala	Thr	Met Glu	Thr
2765			2770			2775		
Asp Asp	Asn Ile	Arg Ala	Ile	Gln Leu	Ser Arg	Asp	Gly Gln	Tyr
2780			2785			2790		
Leu Leu	Thr Gly	Gly Asp	Arg	Gly Val	Val Val	Val	Arg Gln	Val
2795			2800			2805		
Ser Asp	Leu Lys	Gln Leu	Phe	Ala Tyr	Pro Gly	Cys	Asp Ala	Gly
2810			2815			2820		
Ile Arg	Ala Met	Ala Leu	Ser	Tyr Asp	Gln Arg	Cys	Ile Ile	Ser
2825			2830			2835		
Gly Met	Ala Ser	Gly Ser	Ile	Val Leu	Phe Tyr	Asn	Asp Phe	Asn
2840			2845			2850		
Arg Trp	His His	Glu Tyr	Gln	Thr Arg	Tyr			
2855			2860					

<210> SEQ ID NO 2  
 <211> LENGTH: 13  
 <212> TYPE: PRT  
 <213> ORGANISM: Homo sapiens

<400> SEQUENCE: 2

Glu	Glu	Glu	Asp	Asp	Asp	Tyr	Val	Glu	Leu	Lys	Val	Glu
1				5						10		

<210> SEQ ID NO 3  
 <211> LENGTH: 7  
 <212> TYPE: PRT  
 <213> ORGANISM: Homo sapiens

<400> SEQUENCE: 3

-continued

Asp Asp Asp Tyr Val Glu Leu  
1 5

<210> SEQ ID NO 4  
<211> LENGTH: 13  
<212> TYPE: PRT  
<213> ORGANISM: Homo sapiens

<400> SEQUENCE: 4

Glu Lys Glu Asp Asp Glu Trp Ile Leu Val Asp Phe Ile  
1 5 10

<210> SEQ ID NO 5  
<211> LENGTH: 13  
<212> TYPE: PRT  
<213> ORGANISM: Homo sapiens

<400> SEQUENCE: 5

Glu Asp Glu Val Gly Asp Trp Leu Ile Ile Asp Leu Pro  
1 5 10

<210> SEQ ID NO 6  
<211> LENGTH: 10  
<212> TYPE: PRT  
<213> ORGANISM: Homo sapiens

<400> SEQUENCE: 6

Gly Gly Gly Arg Asn Asn Tyr Tyr Cys Cys  
1 5 10

<210> SEQ ID NO 7  
<211> LENGTH: 10  
<212> TYPE: PRT  
<213> ORGANISM: artificial  
<220> FEATURE:  
<223> OTHER INFORMATION: Mutated NFkB binding sequence from H sapiens

<400> SEQUENCE: 7

Gly Gly Thr Arg Asn Asn Tyr Tyr Ala Cys  
1 5 10

<210> SEQ ID NO 8  
<211> LENGTH: 387  
<212> TYPE: DNA  
<213> ORGANISM: artificial  
<220> FEATURE:  
<223> OTHER INFORMATION: Dominant negative DNA construct against LRBA

<400> SEQUENCE: 8

```
aggctcatgc ttcagacaaa tttaatcaca atgaccacat ataatgtgct gtttgagatt    60
cttatagaac agattggtac tcagggtgata cataaacagc atccagatcc tgattcttca    120
gtgaagatac aaaacctca gatactaaaa gtaattgcga ccctacttcg aaattctccc    180
cagtgtccag agagcatgga gggttcgcaga gcctttcttt ctgacatgat taaacttttt    240
aataacagta gagaaaacag gaggagcttg ctacaatgct ctgtgtggca agaattggatg    300
ctttctctct gctattttta tcctaagaat tcagatgagc aaaagataac agaaatggta    360
tacgccatat tcagaatcct gcttttac                                     387
```

<210> SEQ ID NO 9  
<211> LENGTH: 44  
<212> TYPE: DNA  
<213> ORGANISM: artificial

-continued

<220> FEATURE:  
<223> OTHER INFORMATION: Primer for cloning LRBA-GFP construct

<400> SEQUENCE: 9

tgtacaagta ctcagatcgg ctcatgcttc agacaaattt aatc 44

<210> SEQ ID NO 10  
<211> LENGTH: 40  
<212> TYPE: DNA  
<213> ORGANISM: artificial  
<220> FEATURE:  
<223> OTHER INFORMATION: Primer sequence 2 for LRBA-GFP construct

<400> SEQUENCE: 10

agttatctag atccggtggt aaagcaggat tctgaatatg 40

<210> SEQ ID NO 11  
<211> LENGTH: 123  
<212> TYPE: PRT  
<213> ORGANISM: Homo sapiens

<400> SEQUENCE: 11

Gln Thr Asn Leu Ile Thr Met Thr Thr Tyr Asn Val Leu Phe Glu Ile  
1 5 10 15

Leu Ile Glu Gln Ile Gly Thr Gln Val Ile His Lys Gln His Pro Asp  
20 25 30

Pro Asp Ser Ser Val Lys Ile Gln Asn Pro Gln Ile Leu Lys Val Ile  
35 40 45

Ala Thr Leu Leu Arg Asn Ser Pro Gln Cys Pro Glu Ser Met Glu Val  
50 55 60

Arg Arg Ala Phe Leu Ser Asp Met Ile Lys Leu Phe Asn Asn Ser Arg  
65 70 75 80

Glu Asn Arg Arg Ser Leu Leu Gln Cys Ser Val Trp Gln Glu Trp Met  
85 90 95

Leu Ser Leu Cys Tyr Phe Asn Pro Lys Asn Ser Asp Glu Gln Lys Ile  
100 105 110

Thr Glu Met Val Tyr Ala Ile Phe Arg Ile Leu  
115 120

<210> SEQ ID NO 12  
<211> LENGTH: 123  
<212> TYPE: PRT  
<213> ORGANISM: Homo sapiens

<400> SEQUENCE: 12

Gln Thr Asn Leu Ile Thr Met Thr Thr Tyr Asn Val Leu Phe Glu Ile  
1 5 10 15

Leu Ile Glu Gln Ile Gly Thr Gln Val Ile His Lys Gln His Pro Asp  
20 25 30

Pro Asp Ser Ser Val Lys Ile Gln Asn Pro Gln Ile Leu Lys Val Ile  
35 40 45

Ala Thr Leu Leu Arg Asn Ser Pro Gln Cys Pro Glu Ser Met Glu Val  
50 55 60

Arg Arg Ala Phe Leu Ser Asp Met Ile Lys Leu Phe Asn Asn Ser Arg  
65 70 75 80

Glu Asn Arg Arg Ser Leu Leu Gln Cys Ser Val Trp Gln Glu Trp Met  
85 90 95

Leu Ser Leu Cys Tyr Phe Asn Pro Lys Asn Ser Asp Glu Gln Lys Ile  
100 105 110

-continued

Thr Glu Met Val Tyr Ala Ile Phe Arg Ile Leu  
 115 120

<210> SEQ ID NO 13  
 <211> LENGTH: 221  
 <212> TYPE: PRT  
 <213> ORGANISM: Homo sapiens

<400> SEQUENCE: 13

Gly Trp Arg Val Trp Val Asp Thr Leu Ser Ile Thr His Ser Lys Val  
 1 5 10 15  
 Thr Phe Glu Ile His Lys Glu Asn Leu Ala Asn Ile Phe Arg Glu Gln  
 20 25 30  
 Gln Gly Lys Val Asp Glu Glu Ile Gly Leu Cys Ser Ser Thr Ser Val  
 35 40 45  
 Gln Ala Ala Ser Gly Ile Arg Arg Asp Ile Asn Val Ser Val Gly Ser  
 50 55 60  
 Gln Gln Pro Asp Thr Lys Asp Ser Pro Val Cys Pro His Phe Thr Thr  
 65 70 75 80  
 Asn Gly Asn Glu Asn Ser Ser Ile Glu Lys Thr Ser Ser Leu Glu Ser  
 85 90 95  
 Ala Ser Asn Ile Glu Leu Gln Thr Thr Asn Thr Ser Tyr Glu Glu Met  
 100 105 110  
 Lys Ala Glu Gln Glu Asn Gln Glu Leu Pro Asp Glu Gly Thr Leu Glu  
 115 120 125  
 Glu Thr Leu Thr Asn Glu Thr Arg Asn Ala Asp Asp Leu Glu Val Ser  
 130 135 140  
 Ser Asp Ile Ile Glu Ala Val Ala Ile Ser Ser Asn Ser Phe Ile Thr  
 145 150 155 160  
 Thr Gly Lys Asp Ser Met Thr Val Ser Glu Val Thr Ala Ser Ile Ser  
 165 170 175  
 Ser Pro Ser Glu Glu Asp Ala Ser Glu Met Pro Glu Phe Leu Asp Lys  
 180 185 190  
 Ser Ile Val Glu Glu Glu Glu Asp Asp Asp Tyr Val Glu Leu Lys Val  
 195 200 205  
 Glu Gly Ser Pro Thr Glu Glu Ala Asn Leu His Arg Ile  
 210 215 220

<210> SEQ ID NO 14  
 <211> LENGTH: 539  
 <212> TYPE: PRT  
 <213> ORGANISM: Homo sapiens

<400> SEQUENCE: 14

Arg Leu Met Leu Gln Thr Asn Leu Ile Thr Met Thr Thr Tyr Asn Val  
 1 5 10 15  
 Leu Phe Glu Ile Leu Ile Glu Gln Ile Gly Thr Gln Val Ile His Lys  
 20 25 30  
 Gln His Pro Asp Pro Asp Ser Ser Val Lys Ile Gln Asn Pro Gln Ile  
 35 40 45  
 Leu Lys Val Ile Ala Thr Leu Leu Arg Asn Ser Pro Gln Cys Pro Glu  
 50 55 60  
 Ser Met Glu Val Arg Arg Ala Phe Leu Ser Asp Met Ile Lys Leu Phe  
 65 70 75 80  
 Asn Asn Ser Arg Glu Asn Arg Arg Ser Leu Leu Gln Cys Ser Val Trp  
 85 90 95

Gln 100	Glu	Trp	Met	Leu	Ser	Leu	Cys	Tyr	Phe	Asn	Pro	Lys	Asn	Ser	Asp
Glu 115	Gln	Lys	Ile	Thr	Glu	Met	Val	Tyr	Ala	Ile	Phe	Arg	Ile	Leu	Leu
Tyr 130	His	Ala	Val	Lys	Tyr	Glu	Trp	Gly	Gly	Trp	Arg	Val	Trp	Val	Asp
Thr 145	Leu	Ser	Ile	Thr	His	Ser	Lys	Val	Thr	Phe	Glu	Ile	His	Lys	Glu
Asn 160	Leu	Ala	Asn	Ile	Phe	Arg	Glu	Gln	Gln	Gly	Lys	Val	Asp	Glu	Glu
Ile 175	Gly	Leu	Cys	Ser	Ser	Thr	Ser	Val	Gln	Ala	Ala	Ser	Gly	Ile	Arg
Arg 190	Asp	Ile	Asn	Val	Ser	Val	Gly	Ser	Gln	Gln	Pro	Asp	Thr	Lys	Asp
Ser 205	Pro	Val	Cys	Pro	His	Phe	Thr	Thr	Asn	Gly	Asn	Glu	Asn	Ser	Ser
Ile 220	Glu	Lys	Thr	Ser	Ser	Leu	Glu	Ser	Ala	Ser	Asn	Ile	Glu	Leu	Gln
Thr 235	Thr	Asn	Thr	Ser	Tyr	Glu	Glu	Met	Lys	Ala	Glu	Gln	Glu	Asn	Gln
Glu 250	Leu	Pro	Asp	Glu	Gly	Thr	Leu	Glu	Glu	Thr	Leu	Thr	Asn	Glu	Thr
Arg 265	Asn	Ala	Asp	Asp	Leu	Glu	Val	Ser	Ser	Asp	Ile	Ile	Glu	Ala	Val
Ala 280	Ile	Ser	Ser	Asn	Ser	Phe	Ile	Thr	Thr	Gly	Lys	Asp	Ser	Met	Thr
Val 295	Ser	Glu	Val	Thr	Ala	Ser	Ile	Ser	Ser	Pro	Ser	Glu	Glu	Asp	Ala
Ser 310	Glu	Met	Pro	Glu	Phe	Leu	Asp	Lys	Ser	Ile	Val	Glu	Glu	Glu	Glu
Asp 325	Asp	Asp	Tyr	Val	Glu	Leu	Lys	Val	Glu	Gly	Ser	Pro	Thr	Glu	Glu
Ala 340	Asn	Leu	Pro	Thr	Glu	Leu	Gln	Asp	Asn	Ser	Leu	Ser	Pro	Ala	Ala
Ser 355	Glu	Ala	Gly	Glu	Lys	Leu	Asp	Met	Phe	Gly	Asn	Asp	Asp	Lys	Leu
Ile 370	Phe	Gln	Glu	Gly	Lys	Pro	Val	Thr	Glu	Lys	Gln	Thr	Asp	Thr	Glu
Thr 385	Gln	Asp	Ser	Lys	Asp	Ser	Gly	Ile	Gln	Thr	Met	Thr	Ala	Ser	Gly
Ser 400	Ser	Ala	Met	Ser	Pro	Glu	Thr	Thr	Val	Ser	Gln	Ile	Ala	Val	Glu
Ser 415	Asp	Leu	Gly	Gln	Met	Leu	Glu	Glu	Gly	Lys	Lys	Ala	Thr	Asn	Leu
Thr 430	Arg	Glu	Thr	Lys	Leu	Ile	Asn	Asp	Cys	His	Gly	Ser	Val	Ser	Glu
Ala 445	Ser	Ser	Glu	Gln	Lys	Ile	Ala	Lys	Leu	Asp	Val	Ser	Asn	Val	Ala
Thr 460	Asp	Thr	Glu	Arg	Leu	Glu	Leu	Lys	Ala	Ser	Pro	Asn	Val	Glu	Ala
Pro 475	Gln	Pro	His	Arg	His	Val	Leu	Glu	Ile	Ser	Arg	Gln	His	Glu	Gln



-continued

---

Pro Gly Gln Gly Ile Ala Pro Asp Ala Val Asn Gly Gln Arg Arg Asp  
515 520 525

Ser Arg Ser Thr Val Phe Arg Ile Pro Glu Phe  
530 535

<210> SEQ ID NO 15  
<211> LENGTH: 23  
<212> TYPE: PRT  
<213> ORGANISM: Homo sapiens

<400> SEQUENCE: 15

Gly Gly Gly Ala Thr Ala Thr Thr Gly Thr Ala Gly Ala Ala Cys  
1 5 10 15

Thr Gly Thr Cys Thr Thr Thr  
20

<210> SEQ ID NO 16  
<211> LENGTH: 41  
<212> TYPE: DNA  
<213> ORGANISM: artificial  
<220> FEATURE:  
<223> OTHER INFORMATION: Primer for GFP-LRBA dominant negative construct

<400> SEQUENCE: 16

agttatctag atccggtgga actcaggaat acgaaacaca g 41

<210> SEQ ID NO 17  
<211> LENGTH: 39  
<212> TYPE: DNA  
<213> ORGANISM: artificial  
<220> FEATURE:  
<223> OTHER INFORMATION: Primer for GFPLIRF dominant negative LRBA construct

<400> SEQUENCE: 17

tgtacaagta ctcagatcgt ggcggcggtg tatgggtag 39

<210> SEQ ID NO 18  
<211> LENGTH: 38  
<212> TYPE: DNA  
<213> ORGANISM: artificial  
<220> FEATURE:  
<223> OTHER INFORMATION: Primer GFPLIRR for LRBA dominant negative construct

<400> SEQUENCE: 18

agttatctag atccggtgta gattagcttc ctcagtag 38

<210> SEQ ID NO 19  
<211> LENGTH: 554  
<212> TYPE: DNA  
<213> ORGANISM: Homo sapiens

<400> SEQUENCE: 19

agttatctag atccggtgta gattagcttc ctcagtaggg acctgccttc acccagaacc 60

cagctttttg agcccgaggag aagcgggtgg ctagtggggg gccttttagta acttacttga 120

ccgacaataa ctatttcctt cttgtcccct caaaacccta aaacaaaacc tagcctatatt 180

aacatatatt taatcttcca ataggggtttg gcgttggtgt cagcctcggg gagagagatt 240

ggacaaatat ctccaaggag aggagggcga cgccaaggac tttccacatc aactgctttg 300

gggtatctcc acaagttgga agagggaccc tttcgttttg cattgcgtgt gttgtgctca 360

ttaccagtgc agcgactgcc gtcccagggt gactctgagt tgctccttat cgtgagctag 420

-continued

---

caatggctag cgaagacatt cgtgtccctt ccccgccacc aacaggtgat gacgggggag	480
gtggagggag agaagaaacc cctactgaag ggggtgcatt gtctctgaaa ccagggtcc	540
ccatcagggg catc	554

<210> SEQ ID NO 20  
 <211> LENGTH: 22  
 <212> TYPE: DNA  
 <213> ORGANISM: Homo sapiens

<400> SEQUENCE: 20

ttttggttga catgttgga gt	22
-------------------------	----

<210> SEQ ID NO 21  
 <211> LENGTH: 22  
 <212> TYPE: DNA  
 <213> ORGANISM: Homo sapiens

<400> SEQUENCE: 21

gtgaccatgt tcccaacct ct	22
-------------------------	----

<210> SEQ ID NO 22  
 <211> LENGTH: 22  
 <212> TYPE: DNA  
 <213> ORGANISM: Mus musculus

<400> SEQUENCE: 22

atctcgttga catgttgga gt	22
-------------------------	----

<210> SEQ ID NO 23  
 <211> LENGTH: 23  
 <212> TYPE: RNA  
 <213> ORGANISM: Homo sapiens

<400> SEQUENCE: 23

cacaucugaa uguaacuuaa auu	23
---------------------------	----

<210> SEQ ID NO 24  
 <211> LENGTH: 23  
 <212> TYPE: RNA  
 <213> ORGANISM: Pan troglodytes

<400> SEQUENCE: 24

cacaucugaa uguaacuuaa auu	23
---------------------------	----

<210> SEQ ID NO 25  
 <211> LENGTH: 23  
 <212> TYPE: RNA  
 <213> ORGANISM: Macaca mulatta

<400> SEQUENCE: 25

cacaucugaa uguaacuuaa auu	23
---------------------------	----

<210> SEQ ID NO 26  
 <211> LENGTH: 23  
 <212> TYPE: RNA  
 <213> ORGANISM: Mus musculus

<400> SEQUENCE: 26

cacaucugaa uguaacuuaa auu	23
---------------------------	----

<210> SEQ ID NO 27

-continued

---

<211> LENGTH: 23  
 <212> TYPE: RNA  
 <213> ORGANISM: Rattus norvegicus

<400> SEQUENCE: 27

cacaucugaa uguaacuuaa auu 23

<210> SEQ ID NO 28  
 <211> LENGTH: 23  
 <212> TYPE: RNA  
 <213> ORGANISM: Oryctolagus cuniculus

<400> SEQUENCE: 28

cacaucugaa uguaacugaa auu 23

<210> SEQ ID NO 29  
 <211> LENGTH: 23  
 <212> TYPE: RNA  
 <213> ORGANISM: Sorex araneus

<400> SEQUENCE: 29

cccaucugaa uguaacuuaa agu 23

<210> SEQ ID NO 30  
 <211> LENGTH: 23  
 <212> TYPE: RNA  
 <213> ORGANISM: Erinaceus europaeus

<400> SEQUENCE: 30

cccaucugaa uguaacuuaa aug 23

<210> SEQ ID NO 31  
 <211> LENGTH: 23  
 <212> TYPE: RNA  
 <213> ORGANISM: Canis familiaris

<400> SEQUENCE: 31

cacaucugaa uguaacuuaa auu 23

<210> SEQ ID NO 32  
 <211> LENGTH: 23  
 <212> TYPE: RNA  
 <213> ORGANISM: Felis catus

<400> SEQUENCE: 32

cacaucugaa uguaacuuaa auu 23

<210> SEQ ID NO 33  
 <211> LENGTH: 23  
 <212> TYPE: RNA  
 <213> ORGANISM: Equus caballus

<400> SEQUENCE: 33

cacaucugaa uguaacuuaa auu 23

<210> SEQ ID NO 34  
 <211> LENGTH: 23  
 <212> TYPE: RNA  
 <213> ORGANISM: Bos taurus

<400> SEQUENCE: 34

cacauccgaa uguaacuuaa auu 23

-continued

---

<210> SEQ ID NO 35  
<211> LENGTH: 23  
<212> TYPE: RNA  
<213> ORGANISM: *Dasypus novemcinctus*  
  
<400> SEQUENCE: 35  
  
uacaucugaa uguaacuuag auu 23

<210> SEQ ID NO 36  
<211> LENGTH: 23  
<212> TYPE: RNA  
<213> ORGANISM: *Loxodonta africana*  
  
<400> SEQUENCE: 36  
  
uacaucugaa uguaacuuca auu 23

<210> SEQ ID NO 37  
<211> LENGTH: 23  
<212> TYPE: RNA  
<213> ORGANISM: *Echinops telfairi*  
  
<400> SEQUENCE: 37  
  
uacaucugaa uguaacuuua auu 23

<210> SEQ ID NO 38  
<211> LENGTH: 23  
<212> TYPE: RNA  
<213> ORGANISM: *Monodelphis domestica*  
  
<400> SEQUENCE: 38  
  
uacaccugaa uguaacuuua auu 23

<210> SEQ ID NO 39  
<211> LENGTH: 26  
<212> TYPE: RNA  
<213> ORGANISM: *Ornithorhynchus anatinus*  
  
<400> SEQUENCE: 39  
  
aaauacaucu gaaugaacu uaaaau 26

<210> SEQ ID NO 40  
<211> LENGTH: 23  
<212> TYPE: RNA  
<213> ORGANISM: *Anolis carolinensis*  
  
<400> SEQUENCE: 40  
  
aacaucugaa uguaacuuua acu 23

<210> SEQ ID NO 41  
<211> LENGTH: 23  
<212> TYPE: RNA  
<213> ORGANISM: *Gallus gallus*  
  
<400> SEQUENCE: 41  
  
ccuacugaa uguaacuuua auu 23

<210> SEQ ID NO 42  
<211> LENGTH: 23  
<212> TYPE: RNA  
<213> ORGANISM: *Xenopus tropicalis*  
  
<400> SEQUENCE: 42  
  
uacaucugaa uguaauuuua aug 23

-continued

---

```

<210> SEQ ID NO 43
<211> LENGTH: 61
<212> TYPE: DNA
<213> ORGANISM: artificial
<220> FEATURE:
<223> OTHER INFORMATION: top strand of shRNA based on human LRBA
sequence

<400> SEQUENCE: 43

gggatattgt agaaactgtc tttttcaaga gaaaagacag tttctacaat atcccttttt      60
t                                                                    61

<210> SEQ ID NO 44
<211> LENGTH: 61
<212> TYPE: DNA
<213> ORGANISM: artificial
<220> FEATURE:
<223> OTHER INFORMATION: bottom strand of shRNA based on human LRBA

<400> SEQUENCE: 44

ccctataaca tctttgacag aaaaagttct cttttctgtc aaagatgtta tagggaaaaa      60
a                                                                    61

```

---

What is claimed is:

1. A method of treating a disease based on lipopolysaccharide-responsive beige-like anchor (LRBA) up-regulation, comprising:

determining the cause of the disease based on LRBA up-regulation, wherein the cause is up-regulation of LRBA;

treating the disease based on LRBA up-regulation, wherein the treatment is:

down-regulating LRBA in the immune-based disease having LRBA up-regulation, further comprising:

administering a composition further comprising a dominant-negative LRBA composition, an anti-LRBA siRNA, an anti-LRBA shRNA, miRNA miR-150, miRNA miR-181, or a combination thereof;

wherein the dominant-negative LRBA composition is an LRBA-VHSLIR1 peptide of SEQ ID NO: 14 or an LRBA-VHS peptide of SEQ ID NO: 12;

wherein the disease based on LRBA up-regulation is asthma.

2. The method of claim 1, wherein the anti-LRBA shRNA targets an amino acid sequence shown in SEQ ID NO: 15.

3. The method of claim 2, wherein the anti-LRBA shRNA is shown in SEQ ID NO: 43, 44, or a combination thereof.

4. The method of claim 2, wherein the anti-LRBA shRNA is inserted into a plasmid construct.

5. The method of claim 4, wherein a vector for the plasmid construct is pLasiGFP or PhmsiGFP.

6. A method of treating a disease based on lipopolysaccharide-responsive beige-like anchor (LRBA) up-regulation, comprising:

determining the cause of the disease based on LRBA up-regulation, wherein the cause is up-regulation of LRBA;

treating the disease based on LRBA up-regulation, wherein the treatment is:

administering a composition further comprising a dominant-negative LRBA composition, an anti-LRBA siRNA, an anti-LRBA shRNA, miRNA miR-150, miRNA miR-181, or a combination thereof;

wherein the dominant-negative LRBA composition targets an amino acid sequence shown in SEQ ID NO: 2, 3, 4, 5, 6, 7, or 11;

wherein the anti-LRBA shRNA targets an amino acid sequence shown in SEQ ID NO: 15; and

wherein the dominant-negative LRBA composition is an LRBA-VHSLIR1 peptide having the sequence of SEQ ID NO: 14 or an LRBA-VHS peptide having the sequence of SEQ ID NO: 12;

wherein the disease based on LRBA up-regulation is asthma.

7. The method of claim 6, wherein the anti-LRBA siRNA is shown in SEQ ID NO: 43, 44, or a combination thereof.

\* \* \* \* \*